DOTTORATO DI RICERCA IN
SCIENZE CHIMICHE

CICLO XXXIV

COORDINATORE Prof. Baglioni Piero

MESSA A PUNTO E SCALAGGIO DI STRATEGIE SINTETICHE PER MACRO-CICLIZZAZIONI NON USUALI AL FINE DI MIGLIORARE LE PROPRIETÀ DI PEPTIDI QUALI INGREDIENTI FARMACEUTICI ATTIVI D'INTERESSE INDUSTRIALE

Settore Scientifico Disciplinare CHIM/06

Dottorando
Dott. D'Ercole Annunziata

_____
(firma)

Tutore
Prof. Papini Anna Maria

_____
(firma)

Coordinatore
Prof. Baglioni Piero

_____
(firma)

Anni 2018/2021

PhD in
CHEMICAL SCIENCES

CYCLE XXXIV

COORDINATOR Prof. Baglioni Piero

DEVELOPMENT AND SCALE-UP OF SYNTHETIC STRATEGIES FOR EXOTIC MACROCYCLISATION TO INCREASE DRUGGABILITY OF PEPTIDES AS ACTIVE PHARMACEUTICAL INGREDIENTS OF INDUSTRIAL INTEREST

Academic Discipline (SSD) CHIM/06

Doctoral Candidate	**Supervisor**
Dr. D'Ercole Annunziata	Prof. Papini Anna Maria
_____	_____
(signature)	*(signature)*

Coordinator
Prof. Baglioni Piero

_____
(signature)

Years 2018/2021

To me

«God, grant me the serenity to accept the things I cannot change,
courage to change the things I can,
and wisdom to know the difference.»

Unknown author
It was passed down orally as far as back A.D. 500

ABSTRACT

In the framework of the PhD project of industrial interest, I have been involved in the development and optimization of synthetic procedures to obtain peptides of pharmaceutical interest, both on the laboratory scale and for the industrial production, in the context of the University-Industry Joint Laboratory PeptFarm of the University of Florence.

This research develops through two parallel lines. The former is related to the development of a multigram, scalable cGMP-compliant MW-SP synthetic approach for the manufacture of the cyclic peptide Active Pharmaceutical Ingredient Eptifibatide acetate. Additionally, an alternative, patentable synthetic approach has been developed to overcome patent restrictions.

On the other hand, the development of an efficient synthetic strategy for the preparation of a library of stapled peptides of pre-clinical interest derived from relaxin hormone was performed, aiming to investigate their biological role. Moreover, the feasibility of an oral administration of serelaxin gastroprotected formulations was investigated.

According to the industrial perspective on research needs and opportunities in manufacturing, automation of as many steps as possible within an industrial production frame is pivotal to guarantee safety requirements. Solid-phase strategies are considered methods of election for medium-length peptide syntheses not only at the research scale but for large-scale production, as well. The possibility to use microwave-assisted technology on the large scale recently introduced, prompted us to evaluate the possibility to conveniently set-up a safe and fully cGMP-compliant pilot process to produce Eptifibatide acetate Active Pharmaceutical Ingredients (API), a generic hexapeptide, characterized by a single disulfide bridge. We investigated strategies based on the use of the microwave-assisted solid-phase peptide synthesis (MW-SPPS), by the use of a DIC/Oxyma Pure coupling protocol at 90 °C. This fully automated technology, previously accessible only at R&D level, has been recently made available also for the large-scale manufacturing of peptide APIs, taking constantly into account

the cost-effectiveness and dangerousness of each procedure. Accordingly, we developed an optimized process at the laboratory scale (1-5 mmol), which was subsequently successfully scaled-up to 70 mmol, obtaining all the information required by regulatory agencies to validate the process and qualify the pilot-scale plant. The process consists of 5 steps: 1) automated microwave-assisted solid-phase synthesis of Eptifibatide linear precursor; 2) cleavage from the resin with concomitant amino acid side-chains deprotection; 3) disulfide-bond formation in solution; 4) purification by flash column chromatography; 5) ion-exchange solid-phase extraction. Since the direct scale-up of a kg-scale, cGMP compliant peptide API production procedure is a challenge that requires an accurate understanding of each involved step, we preliminary performed a quality management risk assessment, which enabled a smooth and effective achievement of a successful final result. Moreover, in our optimization process, a reduction in time, solvents and waste have been obtained, ensuring compliance with the quality specifications, according to regulatory agencies requirements (FDA and EMA). Satisfactory results were obtained in terms of Eptifibatide acetate HPLC purity (99.6%) and Yield (22.1%).

Additionally, the investigation of an alternative on-resin cyclization strategy for therapeutic peptide industrial production of Eptifibatide acetate has been carried out in parallel with the aim to develop a robust and economically competitive production process avoiding intermediate steps of isolation to preserve the recovery guaranteeing a GMPs quality product, to overcome patent restrictions. A scalable, fully automated approach performed entirely in the same reactor has been developed. We explored and compared four solid-phase disulfide formation approaches (**A**, **B**, **C**, **D**) between the C-terminal Cys and the N-terminal 3-Mercaptopropionic acid (MPA). These mainly differ one from each other for the final cyclization step, obtained by direct formation of an S-S disulfide bridge (strategies **A**-**B**) or *via* side-chain-to-tail amide bond formation (strategies **C**-**D**). Strategy **D** resulted the best one, thanks to the concomitant reduction of the S-tert-butylthio (StBu) Cys protecting group (PG) and disulfide formation with the MPA reducing agent, enjoying the advantage of using an already qualified starting material. This strategy (**D**) represents an inventive (non-obvious)

6

strategy, (since we were the first to propose MPA to deprotect StBu on cysteine), which proposes for the first time to perform all the processes including disulfide bond formation in a single reactor (novelty), scalable on multigram-scale by Liberty Pro synthesizer (Industrial applicability). Therefore, according to the three patentability criteria required for a new production process: Novelty; inventive and industrial applicability, the present PhD work identifies a new patentable production process.[1]

In line with the synthesis of conformationally constraint relaxin derivatives, the present work describes the development of an innovative, efficient and reproducible MW-assisted Copper-Catalyzed Azide-Alkyne Cycloaddition (SP MW-CuAAC) performed on solid phase to prepare side-chain-to-side-chain clicked H_1-relaxin single B-chain analogues, overcoming the several synthetic drawbacks (aggregation tendency and poor solubility) which hamper relaxins syntheses.

All the relevant parameters, that are, resin (PEG-PS *vs* PS), solvent mixtures (H_2O:t-BuOH:DCM 1:1:1, DMSO:DMF 1:2), catalytic system (CuBr *vs* $CuSO_4$), microwave energy and reaction time were optimized using a systematic approach.[2] Two generations of H_1-relaxin single B-chain stapled analogues were obtained. First-generation (**VR** and **VIR**) and second-generation H_1-relaxin single B-chain peptides (**VII** and **VIIR**; **VIII** and **VIIIR**; **IX** and **IXR**) were characterized by different length and different position and orientation of the triazolyl ring, and were designed with the aim to stabilize the α-helix conformation and to expose the *binding cassette* motif. The α-helicity induced by the side-chain to side-chain stapling obtained was demonstrated by the circular dichroism (CD) performed both in phosphate buffer and in SDS micelle, thanks to the collaboration with Prof. A. Carotenuto (University of Naples Federico II). Moreover, in the frame of the collaboration with Prof. D. Bani (University of Florence) and Prof. A. Hossein (Institute of Neuroscience and Mental Health, University of Melbourne, Australia), H_1-relaxin analogues were biologically tested, to verify binding to cells expressing the receptor RXFP1 and activity

through cAMP signaling pathway in HEK-293T cells stably expressing the RXFP1 receptor.

Moreover, since the major challenge in the development of peptide drugs is to improve their oral bioavailability, we investigated the relative bio-potency of the intact serelaxin molecule (the recombinant form of human H2-relaxin) and the purified porcine one, in comparison with their proteolytic fragments obtained after treatment with Simulated Intestinal Digestion Fluid (SIF). Signalling events downstream receptor activation in THP-1 human monocytic cells were measured.

1. INTRODUCTION

1.1 BACKGROUND: CYCLIC PEPTIDES AS THERAPEUTICS

Peptides are involved in a wide range of biological processes. They engage catalytic reactions, inter-cellular and intracellular signal transfer, ribosomal synthesis of protein, etc. Their wide range of biological activities makes them excellent candidates as possible new therapeutic tools[3,4], since peptides are characterized by high selectivity and potency, biocompatibility, and limited immunogenicity.[5,6]

Nowadays, there are around 80 peptide drugs on the global market approved as drugs in the United States, Europe and Japan. Approvals have steadily increased over the last six decades, with a Compound Annual Growth Rate (CAGR) of ca. 7.7%. In fact, peptide drugs represent 5% of the global pharmaceutical market, with global sales exceeding US$ 50 billion in 2019. Moreover, a recent update shows that 150 peptides are in clinical development and others 400–600 peptides are undergoing preclinical studies. Moreover, according to the "Transparency Market Research" latest report, the global peptide therapeutics market is anticipated to expand till 2027 at a Compound Annual Growth Rate (CAGR) of 7.9%.[7]

Roughly half of these peptide drugs are manufactured by 9-fluorenylmethyloxycarbonyl/tert-butyl (Fmoc/tBu) solid-phase peptide synthesis (SPPS),[8] although, generally speaking, solid-phase strategies are commonly used to prepare small volumes of short peptides, whereas hybrid technologies (combining solid-phase and solution methods) are applied to produce longer peptide sequences and/or higher volumes.[9]

The large-scale manufacturing of peptides as APIs, requiring full compliance with cGMP regulations,[10] leads pharmaceutical companies to face many challenges related to the complexity of peptide synthesis in terms of size, modifications, conjugation methods, stability and purity.

The possibility of developing efficient and reliable scale-up processes is becoming more and more crucial for all pharmaceutical companies. Peptide manufacturers need to improve their processes both chemically and economically, *i.e.* in terms of profitability: such remarkable advancement can be achieved being able to optimize the solid-phase synthesis of an active peptide as pharmaceutical ingredient on a laboratory scale and then to perform the same synthesis on the larger scale, up to hundreds of times, with the same efficiency in terms of peptide quality and impurities profile.

An additional critical factor is the use of large quantities of non-aqueous hazardous organic solvents, such as dimethylformamide (DMF) and N-methyl-2-pyrrolidone (NMP), restricted under REACH (European Regulation on registration, evaluation, authorization, and restriction of chemicals). For this reason, there is a growing research interest in Green Solid-Phase Peptide Synthesis (GSPPS), looking for an alternative to DMF, commonly employed for washings, couplings, and Fmoc-removal steps.[11,12,13] In this context, SPPS in water is still a very demanding procedure.[14]

Moreover, to the best of our knowledge, among all the innovative synthetic technologies and approaches developed for peptides synthesis with the primary goal to identify greener solvents and procedures [15,16,17,18,19], MW irradiation is the unique one currently exploited in a commercially available synthesizer for multigram-scale production.

The advantages of the MW-technology applied to the large scale production were demonstrated by several experimental evidences (Jon Collins' personal communications from CEM U.S.A.).

CEM Corporation (Charlotte, NC, U.S.A.) provides three microwave-assisted solid-phase synthesizers allowing the scale-up of a MW-SPPS optimized process.

These instruments can perform respectively syntheses from 0.005 to 5 mmol scale (Liberty Prime and Liberty Blue systems) and from 5 to 800 mmol scale (Liberty Pro system). Last but not least, Liberty Pro system is qualifiable for peptide APIs cGMP large scale production, as required by medicines agencies specifications.

Therefore, once a synthetic protocol has been optimized at the laboratory scale (up to 5 mmol, Liberty Blue (CEM, Charlotte, NC, U.S.A.)), the same quality (indeed higher, usually) can be achieved directly on a much bigger scale. Therefore, intermediate-scale peptide synthesis is no longer required and the optimized synthetic strategy can be directly scaled up from grams to multigrams/kilograms solving both technical and economic issues linked to transfer the technology to an industrial kilogram-scale production plant.

Therefore, the advantage of a fully automated MW-assisted solid-phase synthesis coupled to a significant decreased production times and volume of wastes for cGMP-compliant peptide APIs production, become the primary focus of this work.

Moreover, if the synthetic target is a cyclopeptide, further difficulties arise. Cyclization is typically used as a method to constrain structures and stabilize the putative bioactive peptide folding, thus enhancing selectivity toward the target receptor. Last but not least, cyclic peptides are less degraded by proteases and therefore they display an in vivo higher stability. Indeed on average, one new cyclopeptide drug is approved each year.[20]

According to the type of bond between the two amino acids that furnishes the cycle, cyclic peptides can be classified in homodetic (containing only peptide bonds) and heterodetic (diverse functional groups are used to connect amino acids). Side-by-side of using homodetic and heterodetic, cyclic peptides cyclization can be introduced via isosteric and non-isosteric linkages.

Taking a look at natural conformational constrictions, intra or intermolecular disulfide bridges have a leading role in secondary structure stabilization and represent the main natural form of conformational constriction.

Among the different and sometime exotic cyclization strategies available in the tool-box of the peptide medicinal chemist, the first to be mentioned is the formation of disulfide bridge(s) by oxidation of suitably located cysteine and/or thiol-containing unnatural amino acid residues.

The most commonly used oxidation methods to form disulfide bridges are mediated by I_2, Tl(III) trifluoroacetate, potassium ferricyanide, dimethylsulfoxide (DMSO), both in acidic and basic conditions and/or simply in air in basic conditions or in the presence of activated charcoal.[21,22,23,24,25,26,27]

However, not all of these methods can be applied to the Kilogram-scale production. In developing a robust, large scale cGMPs-compliant chemical process, it is crucial to take into account critical factors such as reactants toxicity, raw materials costs, and optimization of the oxidative conditions (concentration, pH, etc.) to avoid uncontrolled intra- and inter-molecular disulfide formation frequently leading to oligomer/dimer undesired side products.[28]

1.2 EPTIFIBATIDE: A PROTOTYPICAL DISULFIDE-CONTAINING THERAPEUTIC PEPTIDE

1.2.1 Eptifibatide chemical structure and therapeutic functions

Eptifibatide is an heterodetic cyclic-heptapeptide characterized by the presence of the unnatural amino acid homoarginine (Har) and a single disulfide bridge between the C-terminal cysteinamide and the N-terminal deamino-cysteine residue, 3-mercaptopropionic acid (MPA), counting a molecular mass of 831.32 g/mol (Figure 1).

Figure 1. Eptifibatide: N^6-(Aminoiminomethyl)-N^2-(3-mercapto-1-oxopropyl)-L-lysylglycyl-L-α-aspartyl-L-tryptophyl-L-prolyl-L-cysteinamide, cyclic (1→6)-disulfide.

Eptifibatide (Integrilin®) belongs to the class of "disintegrins" which are a family of homologous peptide initially isolated and purified from viper venom, containing the RGD (arginine-glycine-aspartate) amino acid

sequence. These are among the most potent inhibitors of the adhesive proteins binding of platelet glycoprotein (GP) IIb-IIIa.[29,30] Eptifibatide binds Glycoprotein (GP) IIb/IIIa receptor in the pocket between its IIb and IIIa arms, with high affinity and specificity (Figure 2). In this way, it competes with fibrinogen and other adhesive ligands for their binding site, thereby preventing their ability to bind to the activated platelets. The low affinity (dissociation constant of 120 nM) allows a rapid dissociation from the receptor binding side. Therefore, it shows a reversible platelet aggregation inhibition after the end of the treatment.

Eptifibatide at higher concentrations may have the ability to interfere with vitronectin binding, the ligand for $\alpha v\beta 3$ in vascular cells, which may provide additional antithrombotic benefits. Thus, it is frequently used in combination with aspirin and unfractionated heparin.[31]
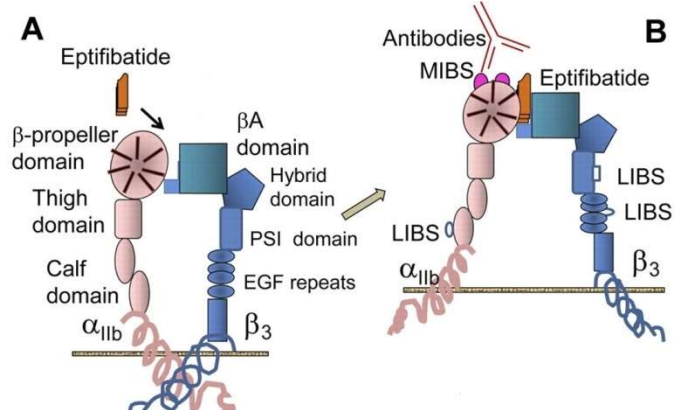
Figure 2. Eptifibatide mechanism of action.[32]

Integrilin® is indicated for acute myocardial infarction, thrombosis following angioplasty, unstable angina, atherosclerosis, transient ischemic attacks. Integrilin® is beneficial for those at high risk of developing myocardial infarction within 3-4 days of acute angina symptoms including for the patients who are likely to undergo percutaneous transluminal coronary angioplasty (PTCA). The commercial form Integrilin® is formulated as an Etifibatide acetate salt sterile solution for intravenous

injection in a single dose of 20 mg/ 10 ml vial, and as a sterile solution for four continuous infusion in a single dose of 75 mg/100 ml vial.[33]

1.2.2 Eptifibatide acetate generic cGMP-compliant industrial production requirements

Since many patents of peptide drugs are expiring, a large number of generic peptide drugs are also entering the market. Generics represent the easiest lucrative, low-cost alternative for Contract Manufacturing Organizations (CMOs) specialized in the production of peptides as Active Pharmaceutical Ingredients (APIs), that constantly strive to meet current Good Manufacturing Practice (cGMP) specification.[34]

In developing a robust, large scale cGMP-compliant chemical process, safety and coasts are crucial elements to take into account to be compliant with regulatory agencies requirements (*e. g.* FDA and EMA).[35]

Industries having to produce generic peptide drugs following cGMP requirements, shall submit an Abbreviated New Drug Application (ANDA), that is mandatory to demonstrate that the Active Pharmaceutical Ingredient (API) is the same as the Reference Listed Drug (RLD), to guarantee safety. Therefore, ANDA approval strictly depends on the impurity profile. In particular, a proposed generic synthetic peptide cannot contain more than 0.5% of each new specified peptide-related impurity that has to be characterized and demonstrated not affecting safety and effectiveness of the drug. [36,37,38] Therefore, optimization of the total production process, methods validation and facilities qualification become part and parcel of this demonstrative process, to assure and preserve the identity, quality, effectiveness and purity of the generic peptide drug candidate.

Interest toward peptide generics large scale manufacturing, and in particular Eptifibatide acetate, moved Fabbrica Italiana Sintetici (VI), a

world leading company in the production of APIs, to create a joint laboratory with PepLab research unit of the University of Florence with the aim to identify an alternative Eptifibatide production process characterized by "innovation" and "invention" (key requirements for a new patent submission), and to pioneering carried out a cGMP-compliant MW-assisted solid-phase peptide synthesis (MW-SPPS).

1.2.3 Eptifibatide acetate patent landscape

According to Eptifibatide production patents landscape the first patent, submitted by COR Therapeutics Inc., was approved by FDA in the late July 1999,[39] and in December 2008 Teva Pharmaceuticals submitted the first New Drug Application (ANDA). 51 patent documents can be counted up to now. An overall overview reveals that Eptifibatide is currently prepared on a large scale applying a hybrid strategy, based on solid-phase synthesis combined with in-solution strategies.[40,41,42,43]

The most relevant patented Eptifibatide production processes are summarized in Table 2.

Qin et al. disclosed the synthesis of a linear Eptifibatide precursor on Sieber resin. Acetamidomethyl (Acm) was used as orthogonal protecting group of thiol functions of both cysteine and mercaptopropionic acid (MPA). Contemporary Acm removal and disulfide formation led to desired cyclopeptide Eptifibatide.[44] Despite the method appears easy, the poor handling of the resin makes it less exploitable, with low yield as output. On the other hand, Wen et al. proposed the use of different solid supports, such as Rink Amide, Rink Amide AM, and Rink Amide MBHA resins. However, each strategy requires several intermediate steps before isolation of the desired cyclopeptide (Table 1).[45]

Table 1. Patent landscape of Eptifibatide industrial preparations

Proprietor	Year	Title	Description
Lonza AG, Basel (CH)	2006	Solid-phase peptide cyclization[46]	Sieber Resin; PBu3 mediated cleavage Cyclization on support.
Natco Pharma Limited	2009	Improved Process For Preparation Of Eptifibatide By Fmoc Solid Phase Synthesis[47]	Rink amide resin. Cysteine and mercaptopopionic acid protected by acm group. The linear peptide is oxidized by mild oxidation reagent iodine
Lonza AG, Basel (CH)	2011	Solid-phase peptide cyclization[48]	SPPS on Sieber resin using StBu protected cysteine, deprotection with Bu3P and cyclization in DIEA/ NMP
Millennium Pharmaceuticals, Inc. Cambridge, MA 02139 (US)	2011	Processes for preparing eptifibatide and pertinent intermediate compounds[49]	Convergent processes for preparing Eptifibatide. Mercaptopropionic acid residue was attached to the (2-7) Eptifibatide fragment through a disulfide linkage. Coupling of the N terminal Har and C-terminal Mpa was performed.
Laurus Labs Private Limited, Hviderabad (IN)	2014 2015	Process for preparing Eptifibatide[50,51]	Synthesis of fragments of different length on solid support and condensation with suitable building blocks, solid-phase or in solution. Coupling involves amino acids in (2+5), (4+3) and (3+4)
Chengdu Shengnuo BioTec Co., Ltd., Chengdu (CN)	2016	Eptifibatide preparation method[52]	Preparation of Eptifibatide by SPPS, oxidation of the crude linear peptide with different resins: Rink Amide resin, Rink Amide AM resin, and Rink Amide MBHA resin.

Moreover, all these procedures are generally designed to prevent the occurrence during the process of major side-reactions, such as racemization, deletion(s), Har deguanidylation, and oligomers/dimers sequences formation. In particular, the latter undermines formation of the disulfide bridge, which is often the crucial and final step of the synthesis. Most of the strategies used for disulfide bond formation in large scale are

reported in solution after cleavage of the corresponding linear precursor from the resin (Table 1). Strong oxidant reagents (such as H_2O_2, DMSO, I_2) are proposed for liquid-phase disulfide bond formation.[53] However, disulfide bridge formation in basic environment requires accurate reaction optimization conditions and in particular pH, concentration, and solvent mixture have to be carefully evaluated.

1.3.1 Human relaxin peptide family: H$_1$-, H$_2$-, H$_3$-relaxin structural similarities and their therapeutic applications

As mentioned above, the global pharmaceutical market sales for peptide APIs exceeded US$ 50 billion in 2019. In particular, Insulin and analogues are responsible for ca. 50% of peptide drug revenue ($25 billion).[54]

Therefore, the interest toward insulin-like peptides move scientist all over the word to investigate the biological role and the possible therapeutic functions of the members of this family.

The human relaxin peptide family consists of seven cystine-rich peptides (Figure 3).
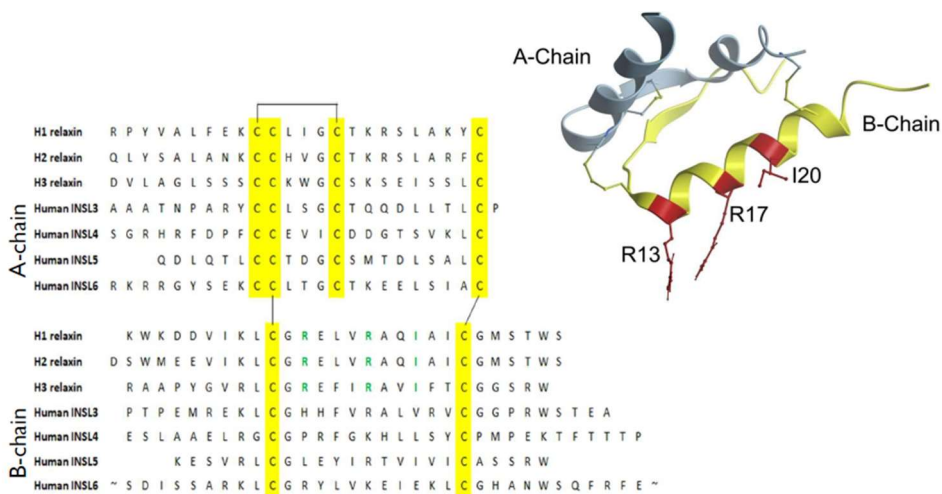
Figure 3. Comparison of primary structures among relaxin family peptides on the left side. Conserved cysteine residues are highlighted in yellow, and disulfide bridges are indicated by black lines. Three conserved residues R, R, I (in green) shared by H$_1$-, H$_2$-, and H$_3$-relaxin B chains define the *binding cassette*. 2-relaxin secondary structure reported on the right side.

Detailed structure-activity relationship (SAR) studies were performed to understand the role of important residues in each of these peptides

underlining similarities among them. They are heterodimeric peptide hormones composed, in their mature form, of an A chain, bearing an intramolecular disulfide bridge and a B chain linked *via* two disulfide bridges, which gave rise to the concept of the insulin superfamily. In particular, three amino acids on the B-chain *α-helix* (Arg ^{B13}, Arg ^{B17} and Ile^{B20}) are essential for the interaction with RXFP receptors and consequently for bioactivity. The conserved motif "RXXXRXXI", shared by H$_1$-, H$_2$- and H$_3$-relaxin, called "*binding cassette*" is recognized as a primary affinity binding site of RXFP1 receptor (Figure 4).[55]
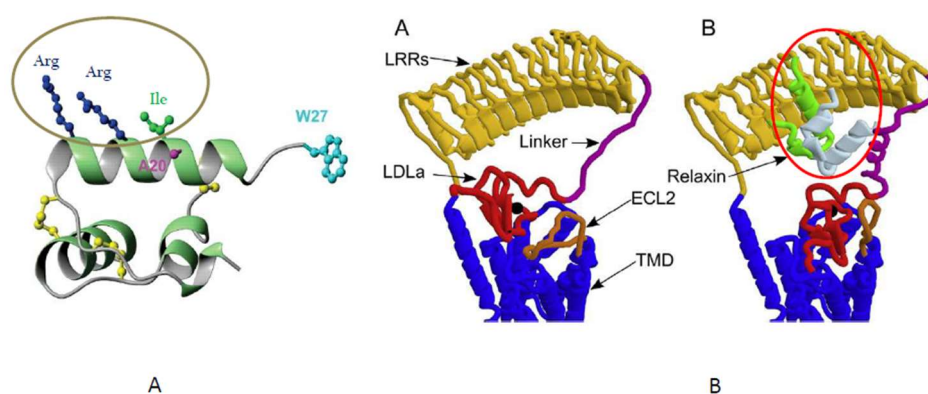
Figure 4. Panel A: H2-relaxin *binding cassette* golden circled, with residues Arg^{B13} and Arg^{B17} underlined in blue, and Ile^{B20} underlined in green. Panel B: transmembrane RXFP receptor general structure. *leucine-rich repeats* region (LRR) in yellow, linker in violet, H2-relaxin B-chain in green and H2-relaxin A-chain in grey.

Evolutionary studies revealed that insulin/relaxin-like peptides are ubiquitously found in vertebrates and non-vertebrates, as well.

Four of the seven peptide mentioned before (H$_1$-, H$_2$-, H$_3$-relaxin and INSL5) are known to signal through relaxin family peptide receptors, RXFP1-4, a family of transmembrane receptors (GPCRs) commonly referred to as LGRs (leucine-rich repeat-containing G-protein coupled receptors). Leucine-rich repeat region (LRR) is a structural protein domain

composed of 20-30 amino acid sequence rich in leucine and therefore highly hydrophobic.

Relaxins bind to the *leucine-rich repeats* region (LRR) via the B-chain, leaving the A-chain to potentially interact with a linker structure, promoting a conformational change which propagates back up the protein, favoring the activation of the receptor. In this trivalent binding mechanism, Ile^{B20} located three quarters to one turn toward the C-terminal end of the same helix, ensures that the hydrophobic side chain opposes the two Arg^{B13} and Arg^{B17}forming a nearly prehensile unit held together by the geometry of the same α-helix. The positively charged guanidine groups of the two arginines are chelated by two acidic residues Glu^{277} and Asp^{279} on LRR8 and Asp^{231} and Glu^{233} on LRR6, respectively, and are implicated in the formation of a network of hydrogen bonds. These bonds are stabilized by the interaction between Ile^{B20} and a cluster of hydrophobic amino acids, which include Trp^{180}, Ile^{182}, Leu^{204} and Val^{206}, the first two located on LRR4, while the others on LRR5.

Consequently, it seems that the A-chain, containing low affinity binding residues, acts as a scaffold for the B-chain, to help it present key residues to the receptor in the correct conformation (Figure 4).[56]

According to RXFPs distribution, RXFP1 was found in female and male reproductive tissues, in the brain, and in numerous other non-reproductive tissues such as the kidneys, heart, and lungs. While, RXFP2 is directly expressed on the same germ cells, kidneys cells and in the rat brain, associated with motor and limbic circuits.[57]

Also RXFP3 is primarily expressed in the brain: supraoptic and paraventricular nucleus, olfactory bulb, sensory cortex, amygdala, hippocampus, thalamus, and the superior and inferior colliculi.[58] It is also expressed in the adrenal gland, pancreas, salivary glands, thymus and testes.[55] On the contrary, RXFP4, is poorly expressed in the brain and is

strongly present in the gastrointestinal tract, mainly in the colon and rectum[59], and in other peripheral tissues, such as placenta, testis, kidney, thymus and prostate.[60]

Considering the wide distribution of RXFPs and their vital roles in physiology, insulin-like peptide ligands are studied for drug discovery and development. For example H_2-relaxin, one of the most studied due to its pleiotropic nature, is found to selectively bind and activate RXFP1. It was initially identified as "pregnancy hormone", with key roles in reproductive functions. Non-reproductive properties including anti-fibrotic and vasodilatory heart protective effects were later demonstrated.[61,62,63]

Premising results were collected from many preclinical and Phase III clinical trials with serelaxin, the recombinant form of human H_2-relaxin.[64,65,66,67,68]

On the other hand, H_3-relaxin activates the RXFP3 receptor mainly through the interaction with B chain, consequently showing to be involved in arousal, feeding, stress responses, cognition and drug addiction.[69]

Surprisingly, to the best of our knowledge, H_1-relaxin physiological role remain still unknown. However, structural similarities with H_2-relaxin and comparable preliminary biological results showing RXFP1 activation led to hypnotize H_2-relaxin analogue therapeutic uses.[70]

1.3.2 Synthetic drawbacks of relaxin-like peptides

The combination of the two chains, A and B, and the formation of the 3 disulfide bridges represented a significant synthetic challenge.

First attempts of relaxin synthesis reported in literature consist of the random combination of the two chains in oxidative conditions to form the 3 disulfide bridges. This approach, generally effective for native sequences, and highly dependent on the presence of an intact secondary

structure capable on directing the correct folding and disulfide formation, resulted unsuccessful.[71]

Subsequently, synthetic strategies focused on the use of orthogonal protecting groups for cysteine residues and sequential regioselective formation of 3 disulfide bridges.[72]

In particular, in 1965 Shanghai Institute of Biochemistry succeeded in completing the first synthesis of bovine insulin, although obtaining a yield of 0.001%. The two chains were synthesized independently by chemical synthesis in solution, cysteines were deprotected and then the free thiol were activated by S-sulfonation. Disulfide bridge were formed in basic environment (pH 10-12), at 4 °C for 24 hours, in presence of a reducing agent, DTT (dithiothreitol).[71]

In 1966 Marglin and Merrifield applied the SPPS strategy, taking advantage of the previously described combination method, to the two chains of bovine insulin increasing the synthetic yield of 3 orders of magnitude.[73] This represented the key work for the first chemical synthesis of human relaxin carried out with the same approach in 1984. The poor solubility of the B-chain hampered the combination of the two chains through the disulfide formation. However, several successful syntheses were obtained by SPPS of the two chains A and B with a Boc/Bzl strategy combined in solution at highly basic pH, including H_1-relaxin one performed in 1996.[74]

For the first time bombixin IV, an insulin-like neuropeptide present in the silkworm, was synthesized by Fmoc/tBu synthesis using orthogonal cysteine protecting groups approach, in 1990. Trityl (trt) protecting group on Cys^{A6}, Cys^{A11} and Cys^{B22}, *tert*-Butyl (tBu) on Cys^{A20} and Acetamidomethyl (Acm) on Cys^{A7} and Cys^{B10}, were used. Intramolecular disulfide bridge formation is achieved by oxidation with air. On the other hand, the first intermolecular bridge is obtained by activation of Cys^{A20}

with dipyridyldisulfide and subsequent thiolysis, while the second intermolecular bridge occurs with the contemporary Acm iodolysis.

Bŭllesbach and Schwabe completed the first synthesis of H$_2$-relaxin using Fmoc/tBu strategy for the A chain and Boc/Bzl for the B chain, with regioselective disulfide bridge formation after orthogonal deprotection (trt: Cys^{A10}, Cys^{A15} and Cys^{B22}; Methyl-Benzyl (MeBzl): Cys^{A24}; 3-Nitro-2-pyridinesulfenyl (NPys): Cys^{B23}, Acm: Cys^{A11} and Cys^{B11}), in 1991.[75] Nevertheless, this approach resulted in a modest yield. They performed a further synthesis of both the two chains A and B *via* Fmoc/tBu approach with the same ortogonal protections used in bombixin IV described above, obtaining an overall yield of 14%.[71]

An orthogonal poly-lysine *tag* linker was attached at the C-terminal end of the hydrophobic chains, removable after conventional purification by RP-HPLC by basic treatment of (NaOH), to overcome the poor solubility due to structural complexity and the prevalent hydrophobic nature of the two chains (A and B), and the consequent side reactions, such as aspartimide formation, associated with their synthesis followed by challenging characterization and purification.[76] This strategy was successfully applied to the synthesis of insulin glargine and returned a 20-fold higher yield.[71]

In order to reduce the complexity and low yield of the regioselective synthesis of relaxins, scientists have focused on short-length relaxins analogues of the native hormone able to maintain affinity for the receptor and/or show selectivity towards the receptor subtypes.

In this framework, Hossain et al. pioneering identified a "mini H$_2$-relaxin," consisting of two chains shorter in length than the native chains, H$_2$-(A4-24)(B7-24), showing 36 amino acids total *vs* 53 of the native hormone, in 2011.[77] The authors isolated and tested 24 analogues variously truncated at the N- and/or C-terminus. However, only H$_2$-(A4-24)(B7-24) showed comparable binding affinity to RXFP1 and nanomolar potency.

Hossain et al. reported the first synthesis of a single B-chain H_2-relaxin like peptide, in 2015. Since, the B-chain contains primary affinity residues (the so-called *binding cassette*), whereas the A-chain contains secondary affinity residues and helps to properly address the B-chain to the correct binding with the RXFP1, Hossein et al. chose B chain as reference sequence, synthesizing the analog B1-29. However, it resulted insoluble and poorly binding the RXFP1. Therefore, a second H_2-relaxin single B-chain like peptide was produced from the circulating isoform H_2-(A1-24)(B1-33) leading to the single chain analogue B7-33.

B7-33 exhibits the replacement of the Cys^{11} and Cys^{23} with isosteric serine residues to prevent possible dimerization/ aggregation and it shows N-terminal truncation and C-terminal elongation compared to the native H_2-relaxin B-chain.

B7-33 was the first single B-chain analogue of H_2-relaxin binding RXFP1, although with a significant decrease in affinity and potency. Surprisingly, B7-33 showed an equipotent activation of matrix metalloproteinase-2 (MMP-2) by ERK 1/2 phosphorylation, suggesting its potential use as therapeutic against fibrosis. Tests in 3 animal models were performed to confirm the strong activation of the cAMP pathway, without promoting the tumor growth generally associated with it.

Therefore, B7-33 represented an excellent *lead* for the development of synthetic analogues with higher stability, potency and *in vivo* efficacy.

1.3.3 Stapling approach as secondary structure stabilization

From a molecular point of view, peptides are generally flexible molecules, which tend to assume a specific conformation when bound to their cognate target. Therefore, the determination of the relationship between the conformation and the activity leads toward the design of more and more potent and selective synthetic derivatives that can be used as either

pharmacological probes or drug candidates. A wild variety of traditional and modern chemical strategies have been employed to increase the stability and reduce the flexibility of peptides.[78]

Since, H_2-relaxin B-chain is characterized by an α-helix conformation involving positions B^{11}-B^{24} necessary for the binding cassette interaction with the extracellular domain of RXFP1, secondary structure has to be preserved *via* structural reinforcement. In this frame, peptide stapling represents a successful strategy for constraining peptides typically in an α-helical conformation, obtained by covalently connecting the side-chains of two natural or non-natural amino acids depending on the chemical approach chosen.[79] The number of stapling bridges could be more than one, especially for long peptides. However, examples of more than two side stapling are not so common in literature. On the contrary, papers showing one and two-component stapling forming a single macrocycle on the peptide backbone are widely spread.

Selection of a constraining approach depends on several factors linked not only to the peptide structure to be stapled, but also to the biological aim. Examples of Hydrocarbon stapling, obtained by Ring Closing Metathesis (RCM) ruthenium catalyzed, are used to increase hydrophobicity. On the other hand, lactam and disulfide stapling are widely used to increase the α-helicity of the secondary structure.

Concerning relaxins structure stabilization, two significant works to stabilize the B single-chain of H_2- and H_3-relaxin, respectively, are reported in literature. The first related to dicarba dridge stabilization obtained *via* ring closure metathesis (RCM), and the second referred to either secondary structure stabilization *via* lactam bridge or disulfide bridge formation,[80] following the scheme *i, i+4*. Replacement of the intramolecular disulfide bridge with a non-reducible olefinic bridge demonstrated that the two isosteric analogs are equipotent to the native

27

hormone in binding and activating RXFP1, but exhibit decreased serum stability *in vitro*.[81,82]

On the other hand, disulfide bridges are associated with instability in basic conditions. To overcome these limitations many strategies have been developed, including the introduction of non-proteinogenic amino acid and backbone modifications.[83]

Interestingly, the amide bond may be mimicked by heterocycles such as triazoles, commonly introduced into the peptide backbone via Click Chemistry, an efficient and chemoselective synthetic method.

Copper(I)- and Ruthenium(II)-catalyzed azide alkyne cycloaddition are counted among the "Click reactions" most used to successfully stabilize α-helix conformation.

Since, this work deals with stapling obtained *via* Copper(I)- catalyzed azide alkyne cycloaddition an in-depth introduction to this subject is given in the following paragraph.

1.3.4 Triazole bridge as biocompatible modification for the synthesis of stapled analogues

Triazole linkage may be considered bioisostere of native amide bond. It is widely known that triazole ring reproduces very close amide properties in terms of dipole moment and the distance between two adjacent α-carbons separated by an amide bond. Moreover triazole has H-bond accepting and donating properties mimicking the peptide bond.[84,85] This led to consider triazole as an appropriate stabilizing moiety.

Starting from Rolf Huisgen's azide-alkyne cycloaddition, proceeding under thermal activation without regio-control, several cognate reactions were developed with the aim to improve selectivity and promote mild reaction conditions over time. The copper(I)-catalyzed azide alkyne cycloaddition (CuAAC) and Ruthenium(II)-catalyzed azide alkyne

cycloaddition (RuAAC) significantly improved reaction rate and led to regio-selective production of 1,4- and 1,5-[1, 2, 3]-triazoles, respectively.

The incorporation of 1,5- or 1,4- disubstituted triazoles into a peptide backbone provides access to both linear and bent peptide mimics. In fact, the 1,4-disubstituted 1,2,3-triazole regioisomer effectively mimics a trans amide bond[86, 87, 88, 89, 90, 91, 92], whereas the 1,5-disubstituted 1,2,3-triazole regioisomer, obtained by Ruthenium catalyzed azide alkyne cycloaddition (RuAAC), is a good model for a cis amide bond.[93, 94, 95]

For these reasons CuAAC is widely considered a prototypical click reaction to selectively obtain the 1,4-[1, 2, 3]-triazole derivative[96, 97], which represents a bioisostere of the *trans*-peptide bond.[98]

Moreover, position and orientation of [1, 2, 3]-triazolyl moiety within the bridge are key features to modulate the dipole moment and the exposure of sites containing hydrogen-bond acceptor. This may promote the interaction with the binding site of target proteins increasing affinity and/or selectivity.

Since, global conformational stability may be derived from the backbone conformational constraints, several works focused on the characterization of secondary structure formed after disulfide bridge replacement with triazole one.

A. M. Papini *et al.* demonstrated that the replacement of an *i-* to *i+5* disulfide bridge in Octreotide, an important bioactive peptide, with a [1, 2, 3]-triazolyl ring led to the stabilization of the β-turn bioactive conformation, [99] establishing a dynamic equilibrium between β-turn and 3_{10} helix-like conformations.[100] Chorev and colleagues report side-chain intramolecular triazole derivatives (*i* to *i+4*, *i* to *i+5*) cyclized free in solution after cleavage step [101], clarifying the relationship among the secondary structure motif and a specific cyclization pattern: α-helix

conformational folding obtained with "*i* to *i+4*" and the type I β-turn structurally related to "*i* to *i+5*"[1, 2, 3]-triazolyl bridge.[102]

The distance between the two azide and alkyne bearing residues resulted pivotal in a one- component CuAAC stapling. Chorev et al. reported the first instance of generating an α-helix secondary structure in which residues involved in CuAAC are placed in position *i, i+4* involving 7–8 atom chains into the brace between the two stereogenic carbon atoms.

Moreover, Scrima et al. carried out a copious work of synthesis and purification of *i, i+4*, 1,4-disubstituted-[1, 2, 3]triazolyl-containing analogues derived from human parathyroid hormone-related protein, underlining the importance of the ring-size bridge, location and the orientation of the [1, 2, 3]-triazolyl moiety within the bridge, with regard to the biological effect on the final stapled products.[103]

1.3.5 Copper(I)-catalyzed azide alkyne cycloaddition (CuAAC) mechanism

A brief summary of the CuAAC reaction mechanism is reported below. Figure 5 shows the most reliable mechanism in which a dicopper species are involved (**8**, **9**), and they may be responsible for the catalytic cycle. A source of Cu(I) is fundamental for the regioselectivity. The alkyne molecule (**2**) coordinates Cu(I) cation (**5**) in a n-coordinated metallic complex LnCu(I) (**6**). This dramatically decreases the acetylenic proton pKa, favoring the exothermic formation of acetylide (**7**). In aqueous systems this could happen without the use of a base, otherwise tertiary amine (TEA, DIPEA) and 2,6-lutidine are generally used respectively to increase reaction rate and to minimize the side-product formation. Afterwards, the azide (**1**) coordinates to the Cu(I)-acetylide complex *via* its negatively charged nitrogen atom, leading to a slightly bent allene-like structure (**8-9**), that rearranges into a copper-triazole species (**10**). The latter complex, *via* protonation or reaction with other electrophiles,

decomposes to give a 1,4 disubstituted-[1, 2, 3]-triazole (**3**) and the catalytic LnCu(I) (**5**), that can enter the next cycle.[104]
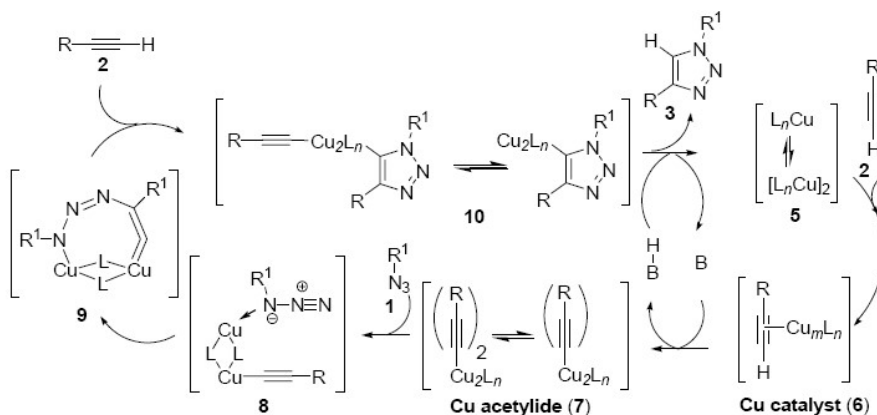
Figure 5. CuAAC reaction mechanism.

The robustness of this reaction has been demonstrated under a broad range of reaction conditions: catalytic system, solvents, and bases. Concerning the catalytic system, CuAAC can be performed with Cu in three different oxidation states: Cu(0), Cu(I), and Cu(II). However, it is well known that Cu(I) represents the active specie. Indeed, in the literature are reported different examples of Cu(I) *in situ* formation *via* reduction of Cu(II). This is usually reported using sulfate pentahydrate or copper acetate in presence of a sacrificial reducing agent typically sodium ascorbate.[105]

Moreover, copper catalyst can be used directly in its reduced form Cu(I) as copper salts like CuI or CuBr or, in presence of organic solvents, as coordination complexes such as $[Cu(PPh_3)_3]Br$[128], $[Cu(CH_3CN)4]PF_6$[89], $(EtO)_3P•CuI$.[106]

Concerning the solvent, different mixtures of aqueous alcohols (MeOH, EtOH, *t*-BuOH) have been used and an addition of DMSO in presence of less hydrophilic reagent led to maintain good reaction rates.[107]

2. AIM OF WORK

The present PhD project was developed through two parallel lines, the former of industrial interest and the latter of academic one.

Optimization on lab scale, scale-up and technology transfer to a pilot scale of an alternative cGMP compliant MW-assisted SPS of the disulfide-bridge containing cyclopeptide Eptifibatide acetate, were the goals of this PhD work unit, to validate a new production process and qualify the innovative pilot plan for peptide industrial production. In particular, the work would like to demonstrate the possibility to develop a safe, reproducible pilot production of a peptide API minimizing environmental and economic impact in compliance with the quality specification imposed by regulatory agencies (FDA, EMA).

Fmoc/tBu automated microwave-assisted solid-phase peptide synthesis (MW-SPPS) protocols, using the high-speed and high-efficiency CEM technology (Charlotte, NC, U.S.A.), widely used for R&D, available for both gram-scale (Liberty Prime and Liberty Blue systems) and more recently for Kilogram-scale synthesis thanks to the new developed cGMP compliant Liberty PRO were investigated.

Alongside, the second aim of industrial interest has been to develop an alternative, patentable production process entirely executable in the same reactor with the aims to minimize workers involvement for safety reasons and overcome patents manufacturing restrictions. In this frame, comparison among the thiol-free liquid-phase disulfide bond formation with four novel and different solid-phase approaches was performed.

On the other hand, the interest toward unknown biological functions of H_1-relaxin moved us to project a library of structurally simplified H_1-relaxin single B-chain analogues to overcome synthetic drawbacks characterizing Insulin-like peptides (poor solubility and aggregation tendency). Accordingly we planned a stapling strategy to stabilize α-helix

structure, since the lack of the A chain, and we needed to developed an easy and faster clicked approach able to performed synthesis and microwave-assisted copper-catalyzed azide-alkyne cycloaddition (MW-CuAAC) entirely on solid support.

In vitro tests were needed to demonstrate potential binding to RXFP1 receptor and biological pathways activation of stapled analogues.

Finally, with the aim to investigate a potential oral administration of H_2-relaxin to increase patients compliance overcoming the drawback of its short half-life (about 2 h[108]), we investigated if proteolytic serelaxin and porcin (pRLX) fragments generated by gut enzymes may retain the capability to bind to and activate the RXFP1 receptor.

3. RESULTS AND DISCUSSION

In order to attract pharmaceutical companies, manufacturers with the potential mission for forming a trusted relationship, to become suppliers of cGMP peptides, will have to demonstrate the Full Life Cycle peptide API Management. Therefore, to enter into the market with a cGMP scale-up facility for production, manufacturers have to take into considerations that GMP aims to build the quality into the peptide API.

During the development of the cGMP production process of peptide API Eptifibatide using microwave-assisted solid-phase synthesis (as proof-of-concept), in order to be ready performing regular audits, we had: 1) to get the facility design right from the start; 2) to validate processes; 3) to write good procedures and follow them; 4) to identify who does what; 5) to keep good records; 6) to train and develop staff; 7) to practice good hygiene; 8) to maintain facilities and equipment; 9) to build quality into the whole Eptifibatide acetate lifecycle. Therefore, a profound understanding of the "multidimensional workspace" was required to guarantee the robustness of that pilot scale production at the industrial level.

In this context, we report the laboratory process optimization (1-5 mmol) of the heterodetic cyclopeptide API Eptifibatide acetate (Figure 1) in 5 steps: a) automated MW-assisted solid-phase synthesis of on resin Eptifibatide linear precursor (Step 1); b) cleavage from the resin and amino acid side-chains deprotection (Step 2); c) in solution disulfide-bond formation (Step 3); d) purification by flash column chromatography (Step 4) followed by e) ion-exchange solid-phase extraction (Step 5); (Scheme 1).
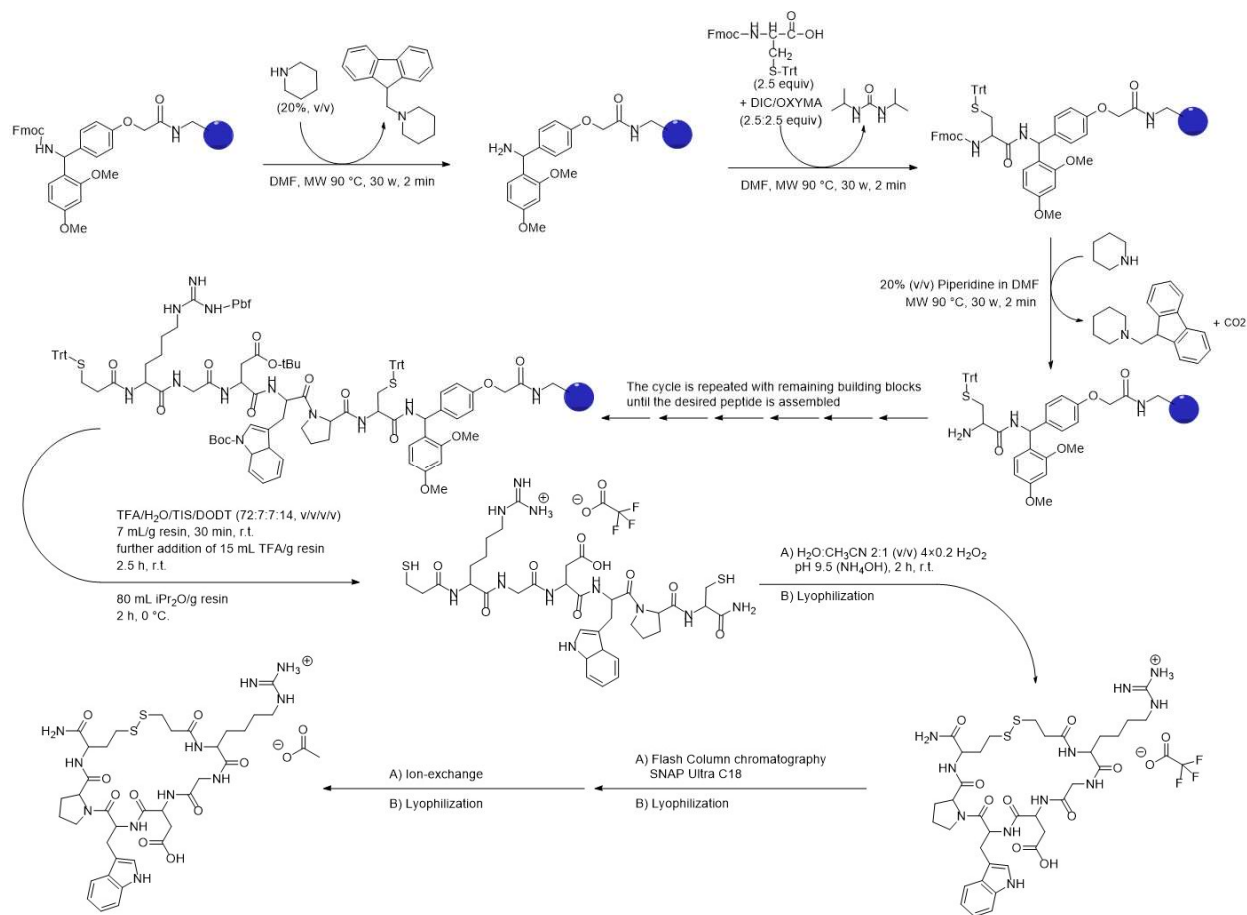
Scheme 1. Synthetic scheme of Eptifibatide acetate production.

In particular the in-solution disulfide bond formation critical step was carefully optimized. Therefore, we identified a scalable automated Eptifibatide acetate process production on lab scale (5 mmol), demonstrating the scalability of the industrial cGMP compliant manufacturing robust process for 70 mmol peptide API that we developed. We proved as Eptifibatide linear precursor can be produced in one day by automated MW-assisted process in the Liberty Pro synthesizer, dramatically decreasing the time for conventional room temperature solid-phase synthesis, usually requiring at least one week to obtain similar length peptides.

To the best of our knowledge, this is the first time that the automated MW-assisted solid-phase large scale peptide synthesizer Liberty Pro (CEM, Charlotte, NC, U.S.A) was used for cGMP production of a peptide API.

A detailed description of the investigation performed on each step is reported below.

3.1.1 Quality risk management: identification of Critical Quality Attributes and Critical Process Parameters

Abbreviated New Drug Application (ANDA) for Eptifibatide approval by regulatory agencies (as for any other peptide generic drug), required a systematic approach to preliminarily define critical quality attributes (CQAs) and understanding the process to follow, identifying critical material attributes (CMAs) and critical process parameters (CPPs). This allowed to establish the functional relationships linking CMAs/CPPs to CQAs. In this process, profound knowledge of peptide science and therefore of the organic chemistry of the molecule to be produced, is pivotal.

International conference of harmonization document Q8 (ICH Q8) defines CQAs as physical, chemical, biological or microbiological property or characteristic that should be within an appropriate limit, range or distribution to ensure desired product quality. On the other hand, ICH Q8 document identifies CPPs as process parameters which variability has an impact on CQAs. Therefore CPPs shall be monitored or controlled to ensure the required quality of the final product. The Ishikawa's diagram was selected to plot the list of the parameters to take into consideration for the herein described cGMP Eptifibatide acetate manufacturing process (Figure 6).
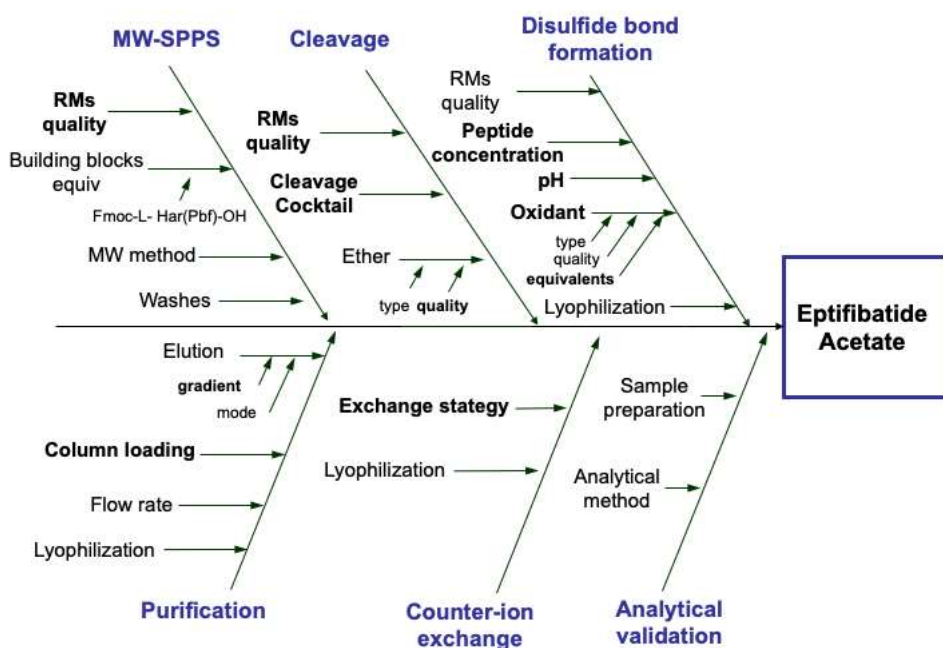
Figure 6. The Ishikawa's diagram for the development of the cGMP Eptifibatide acetate production process. Critical process parameters (CPPs) are reported in **bold**.

The identified CPPs were selected to design the set of experiments for process optimization. We followed the principles of the quality risk management to establish an appropriate controlled manufacturing process of cGMP Eptifibatide acetate pilot batch across the product life-cycle. In

particular, we evaluated the risk to quality (thanks to scientific knowledge of peptide chemistry) and we provided formalities and documentations of the performed experiments commensurate with the level of risk, integrated with facilities, equipment, and utilities qualification, materials management, laboratory control, and stability testing.[109]

As a matter of fact, GMP compliance requires documentation to ensure traceability of all process development, manufacturing, and testing activities. Manufacturers have to provide documentation to auditors who will assess the overall quality of operations within the company and of the final peptide API. In this context, Master Production Records (MPRs) are the most important documents to be defined before starting operations, listing all the required ingredients and necessary steps for the manufacturing process. MPRs have to be approved by quality control and never changed during the process, to ensure consistency, quality, and safety of the final API. Therefore, each production step will have to be performed according to MPRs and all the items (*e.g.* lot numbers, specific weights, equipment and facilities, personnel, etc.) recorded in Batch Production Records (BPRs).

Moreover, the identification of hazards and, the analysis and evaluation of risks associated with exposure to those hazards, is a relevant part of risk assessment (EUH019, hazard statement in Classification, Labelling & Packaging regulation).[110]

3.1.2 *STEP 1. Optimization of the automated MW- SPS of the fully protected Eptifibatide linear precursor, assisted by microwaves, decreasing process cost*

At the industrial level, costs flow in process costing require to evaluate direct material costs since the beginning of the process, i.e., reagents and solvents to use for peptide synthesis, isolation, purification including ion-

exchange solid-phase extraction. Solid-phase synthesis through stepwise assembly of building blocks on a solid support, usually requires large excesses of reagents essential to overcome limitations due to reactions in heterogeneous phase. However, this influences the cost of the final product.

In this framework, automation is fundamental to get continuous cycle manufacturing, minimizing intermediates isolation, preserving both safety and reproducibility. Moreover, production time is favourably decreased by MW technology thanks to a lower labour price, the most relevant cost for industrial manufacturers.

Solid-phase fully protected linear Eptifibatide precursor MPA(Trt)-Har(Pbf)-Gly-Asp(OtBu)-Trp(Boc)-Pro-Cys(Trt)-Rink Amide AM resin was built *via* standard Fmoc/tBu MW-SPPS strategy (Tables A1, A2, and A3). First of all, we optimised the microwave protocol up to 5 mmol scale. N,N′-diisopropylcarbodiimide (DIC) and Oxyma Pure were used as coupling system, that is non-explosive, compared to 1-hydroxybenzotriazole (HOBt), used for years for amide bond formation, but that is no more accepted at the industrial level.[111] Moreover, the coupling system based on DIC/Oxyma, in addition to being safe and low cost, does not require the use of a base unlike the most popular onium coupling methods, such as 3-[Bis(dimethylamino)methyliumyl]-3H-benzotriazol-1-oxide hexafluorophosphate (HBTU), requiring high base quantities (e.g *N,N*-diisopropylethylamine, DIPEA). Additionally, DIC is convenient in terms of time and solvent consumption since, it is stable at 90 °C (temperature reached in the microwave conditions) and requires lower DMF washing volumes because of its higher solubility compared to more classic coupling reagents.

3.1.2.1 *Evaluation of the minimal quantity of the high-cost building block Fmoc-L-Har(Pbf)-OH to limit Des-Har2-linear Eptifibatide formation*

As underlined above, a careful analysis of the purity profile is pivotal to produce a generic API compliant with cGMP requirements. The solid-phase synthesis of the linear Eptifibatide precursor requires the use of the high cost building block Fmoc-L-Har(Pbf)-OH. That prompted us to optimize its coupling conditions minimizing process cost. Moreover, the high hindrance of Pbf protecting group hampers successful coupling leading to Des-Har^2-linear precursor impurity formation. This issue is usually overcome by using large excesses of the activated building block and/or performing double couplings.

We optimized the synthetic process investigating: 1) single *vs* double coupling; 2) decreasing the excess of each coupling reaction; 3) increasing coupling time.

In particular, we demonstrated that the first coupling should not be performed decreasing equivalents of Fmoc-L-Har(Pbf)-OH less than 2.5 (Table 2, entries 1-3). On the other hand, a double coupling did not appear to be advantageous both in terms of Des-Har^2-linear precursor impurity formation, time consuming, and costs. Therefore, we identified one single coupling with 2.5 equivalents of Fmoc-L-Har(Pbf)-OH as the thoughtful compromise to obtain the highest crude purity and the minimum building block amount to use (Table 2, entries 4-5).

Table 2. Fmoc-L-Har(Pbf)-OH equivalents tested in coupling conditions to decrease production costs and limiting Des-Har^2-linear Eptifibatide impurity

Entry	Fmoc-L-Har(Pbf)-OH 1×/2× coupling(s) equiv	DIC/Oxyma pure equiv/equiv	Scale (mmol)	Time (min)	Des-Har^2-linear Eptifibatide (A/A %)**
1	2.5 + 2.5	2.5/2.5+2.5/2.5	1	10+10	0.7
2	2+ 0.5	2/2+0.5/0.5	1	10+10	0.7
3	1.5+1	1.5/1.5+1/1	1	10+10	1.1
4	2.5	2.5/2.5	1	10	1.0
5	2.5	2.5/2.5	5	15	0.6

**Loading of Rink Amide AM resin: 0.97 mmol/g.*
Coupling conditions of all other building-blocks: single coupling 1×2.5 equiv of building-block (0.4 M), 1×2.5 equiv DIC (3 M) and 1×2.5 equiv Oxyma pure (1 M). All reagents were dissolved in DMF. Final resin washing: 9.3 ml/g resin (IPA, 3×).
***Resin cleavage cocktail: TFA/H2O/TIS/DODT (92.5:2.5:2.5:2.5, v/v/v/v),20 mL/g resin, stirring 3 h at r.t. Method used to isolate Eptifibatide linear precursor crude: 80 mL solvent/g resin; 30 min stirring, r.t.; 150 min stirring 0 °C.*

3.1.2.2 *Scale-up activities: optimization of parameters of MW-SPPS and evaluation of critical material attributes*

Scaling-up the coupling step from 5 mmol on Liberty Blue to 70 mmol on Liberty PRO (characterized by an optimized dual-mode mixing with overhead mechanical agitation and N_2 bubbling, homogenously heating resin and diffusing solvents), required a proportional increase of MW power and reaction time to guarantee optimal performances of the synthesis. Increasing time of coupling was possible thanks to the stability and the efficiency of DIC/Oxyma pure coupling system under MW conditions. Reproducibility of the MW-SPPS to pilot-scale was unequivocally demonstrated (Tables A1, A2, and A3).

3.1.2.3 *Quality check of solvents and reagents in compliance with critical material attributes (CMAs)*

Industrial Raw Materials (RMs) are generally stored in large tanks in the manufacturer's warehouse department and they are withdrawn as

needed.[112],[113] The industrial grade material attributes have to be demonstrated compliant with the analytical ones.

Consequently, before starting the 70 mmol pilot scale production, industrial-grade DMF and Oxyma pure quality was tested (use test). First of all, we demonstrated that the reagents were compliant with suppliers certificate of analysis (CoA). Moreover, their performances were compared on a 5 mmol scale synthesis with a second synthesis performed in the same conditions using analytical-grade reagents. Since, UHPLC purity after cleavage of Eptifibatide linear precursor crude (DMF and Oxyma pure analytical-grade: 63.9%; DMF industrial-grade: 62.8%; Oxyma pure industrial-grade: 62.3%) and Des-Har^2-linear precursor impurity amount (DMF and Oxyma pure analytical-grade: 0.60%; DMF industrial-grade: 0.69%; Oxyma pure industrial-grade: 0.64%) resulted comparable, we considered acceptable to use industrial-grade DMF and Oxyma pure reagent decreasing process cost (Table 3).

Table 3. Use test for DMF and Oxyma Pure quality check

Entry	Reagents	Scale[*] (mmol)	UHPLC purity[**] (A/A %)	Des-Har^2-linear Eptifibatide precursor[**] (A/A %)
1	DMF and Oxyma Pure (analytical-grade)	5	63.9	0.60
2	DMF (industrial-grade)	5	62.8	0.69
3	Oxyma Pure (industrial-grade)	5	62.3	0.64

[*]*Loading of Rink Amide AM resin: 0.97 mmol/g.*
Coupling conditions: single coupling 1×2.5 equiv of building-block (0.4 M), 1×2.5 equiv DIC (3 M), and 1×2.5 equiv Oxyma pure (1 M). All reagents were dissolved in DMF. Final resin washing: 9.3 ml/g resin (IPA, 3×).
[**]*Resin cleavage cocktail: TFA/H$_2$O/TIS/DODT (92.5:2.5:2.5:2.5, v/v/v/v), 20 mL/g resin, stirring 3 h, r.t. Method used to isolate Eptifibatide linear precursor crude: 80 mL solvent/g resin, r.t., 30 min stirring, and 150 min stirring at 0 °C.*

3.1.3 STEP 2. Optimization of the amino-acid side-chain deprotections and cleavage from the resin to obtain the linear Eptifibatide precursor crude

The cleavage step, which consists in the contemporary cleavage of the peptide from the resin and side-chains deprotection, can potentially generate impurities to be precisely characterized to fulfil cGMP requirements for the final regulatory approval.

Identification of the Critical Quality Attributes (CQAs) of the API and Critical Processing Parameters (CPPs) are pivotal to release the final peptide batch.[114] Cleavage conditions have to be considered CPPs since their direct connection to the final purity profile (Figure 6, Table A4).

Deviations and Out Of Specification (OOS) from the expected behaviour may affect safety and efficacy of the final product, invalidating final approval for human use marketing. Consequently, further investigations to demonstrate the causes, followed by time consuming corrective actions would be required.

3.1.3.1 Investigation on the cleavage scavenger mixture effect on crude purity

The mixture TFA/TIS/DODT/H_2O (92.5:2.5:2.5:2.5, v/v/v/v) was tested first to cleave the Eptifibatide linear precursor from the resin. After cleavage, HPLC/ESI-MS analysis of the crude obtained after precipitation in ether, showed three main side-products: R_t 5.154 min, $[M + H]^+$ m/z = 890.39 (Imp a) and R_t 5.333 min, $[M + H]^+$ m/z = 890.39 (Imp b) both deviating +56 *m/z*; R_t 4.258 min, $[M + H]^+$ m/z = 878.32 (Imp c) deviating +44 *m/z*, from the calculated mass value $[M + H]^+$ m/z = 834.33 (R_t 4.333 min) of Eptifibatide linear precursor, respectively (Figures 7, A1, A2, and A3).
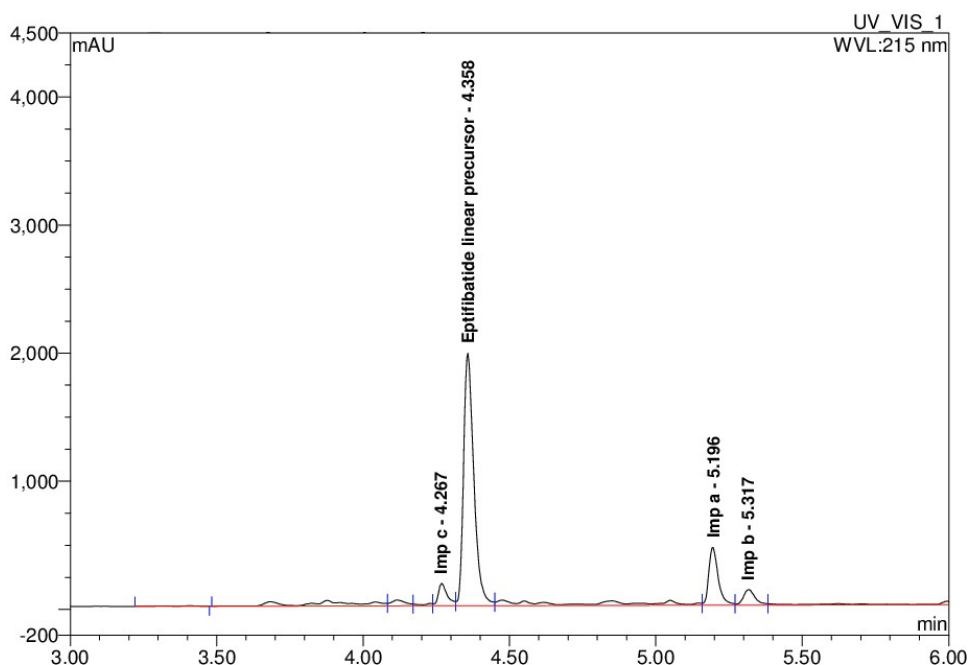
Figure 7. RP-UHPLC trace (zoom 3-6 min) of Eptifibatide linear precursor crude obtained using a mixture TFA/TIS/DODT/H$_2$O (92.5:2.5:2.5:2.5, v/v/v/v). C18 column Waters Acquity CSH (130Å, 1.7 µm, 2.1 × 100 mm); temperature 45°C; flow: 0.5 mL/min. Eluents: 0.1% (v/v) TFA in H$_2$O (A) and 0.1% (v/v) TFA in CH$_3$CN (B); λ 215 nm; gradient: 5-95% (v/v) B in A in 10 min. R$_t$ 4.27 min: Imp c, R$_t$ 4.36 min: linear Eptifibatide precursor. R$_t$ 5.2 min: Imp a, R$_t$ 5.32: Imp b.

Reactions to cleave tBoc and tBu protecting groups from Trp and Asp side-chains, respectively, generate tert-butyl carbocation species. This highly reactive electrophilic species shall be *in situ* entrapped by appropriate nucleophiles added to the TFA cleavage cocktail, i.e., scavengers, in order to prevent reattachment or modification of the deprotected nucleophilic side-chains, such as thiol function on cysteine.[115,116]

In the specific case of Eptifibatide linear precursor, cysteine and MPA thiol functions represent possible electrophilic attack acceptors. In this framework, MS/MS analysis of the peak at R$_t$ 5.154 min (Imp a) revealed the fragment [M+H]$^+$ m/z = 487.3 corresponding to b$_4$ fragment with tert-butyl carbocation reattachment on MPA thiol function (Figures A4 and

46

A5). Consequently, we can hypothesize that R_t 5.333 min (Imp b) corresponds to the impurity of tert-butyl derivative on cysteine thiol function.

Cysteine and MPA thiol functions in the crude could be both deprotected from the newly formed StBu-peptide side-product only using hazardous reagents, requiring expensive strong acid-resistant equipments. This was unnecessary because flash column chromatography allowed to obtain Eptifibatide final product in large scale, with percentages of impurities Imp a and Imp b, compliant with international regulatory standards (applicable to drug products) and guidance, regulatory authority research and assessment reports.

The best crude UHPLC purity was achieved performing the cleavage in two steps. In the first 30 minutes, two different cleavage cocktails were tested at 2 mmol scale: TFA/H_2O/TIS/DODT (72:7:7:14 v/v/v/v, 107 mL) and TFA/H_2O/TIS/DODT (60:10:10:20 v/v/v/v, 107 mL). In the second step, further 230 mL TFA were added and maintained under stirring for 2.5 h at r.t. to maximize Eptifibatide linear precursor crude recovery. Both cleavage conditions led to comparable impurities (Table 4). However, the best crude UHPLC-purity was achieved using the mixture TFA/H_2O/TIS/DODT (72:7:7:14 v/v/v/v, 107 mL). Therefore, we selected as cleavage mixture: TFA/H_2O/TIS/DODT (91:2.3:2.3:4.4 v/v/v/v) with scavenger concentrations: 0.11 M TIS, 0.33 M DODT, and 1.3 M H_2O.

Table 4. Cleavage cocktails tested to obtain the highest UHPLC crude purity

Entry	1st step cleavage mixture (volume ratio)	UHPLC crude purity[*] (A/A %)	Imp a[*] Imp b[*] (A/A %)
1	TFA/H$_2$O/TIS/DODT (72:7:7:14)	61.5	4.1 1.8
2	TFA/H$_2$O/TIS/DODT (60:10:10:20)	57.1	3.6 1.0

[*]*Method used to isolate Eptifibatide linear precursor crude: Et$_2$O (80 mL/g resin); r.t.; 30 min stirring, and 0 °C, 60 min stirring.*

Moreover, Imp c was hypothesized to correspond to the intermediate of Eptifibatide linear precursor containing Trp-carbamic acid ([M + H]$^+$ m/z = 878.32).[117, 118]

In fact, deprotection of tBoc protecting group from Trp indolyl side-chain occurs *via* a stepwise pattern consisting in tBu carbocation formation followed by acidolysis of Trp-carbamic acid intermediate derivative. Interestingly, slow decarboxylation kinetic is distinctly beneficial to avoid additional impurity formation by electrophilic attack of tBu carbocation to indolyl side chain, otherwise favoured in presence of unprotected Trp.

Our hypothesis was demonstrated monitoring disappearance of the peak at R$_t$ 4.258 (completed in 60 min) by additional treatment in acidic aqueous media of Eptifibatide linear precursor (Figure 8).
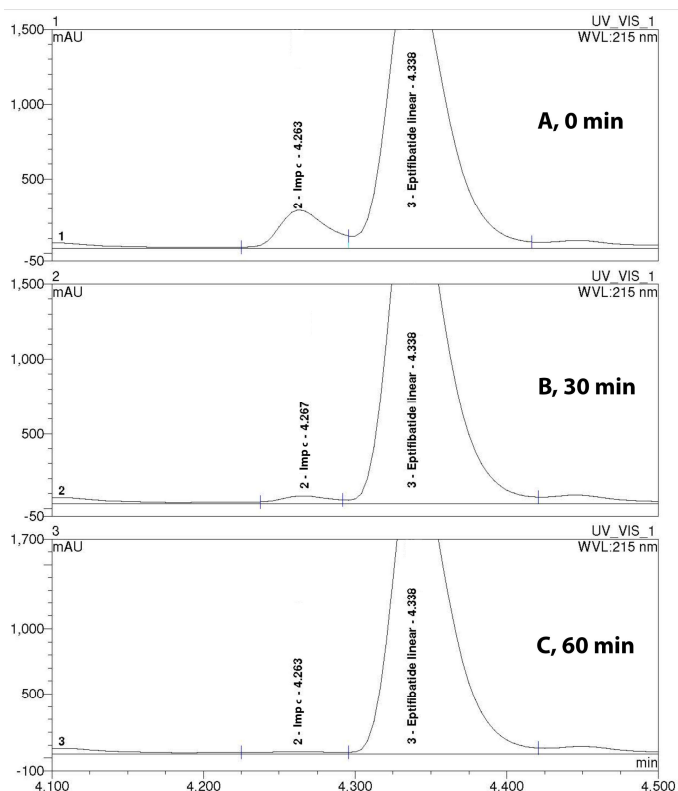
Figure 8. RP-UHPLC traces of Eptifibatide linear precursor crude monitoring Trp(Boc) deprotection at different reaction times (zoom 4.1-4.5 min.) Panel A: 0 min, Panel B: 30 min, Panel C: 60 min. C18 column Waters Acquity CSH™ (130Å, 1.7 μm, 2.1 × 100 mm); temperature 45°C; flow: 0.5 mL/min; eluent: 0.1% (v/v) TFA in H_2O (A) and 0.1% (v/v) TFA in CH_3CN (B), λ 215 nm, gradient: 12-45% B in 10 min. R_t 4.26 ± 0.015 min: Imp c, R_t 4.34 ± 0.01 min: linear Eptifibatide precursor.

3.1.3.2 *Evaluation of the optimal antisolvent to precipitate Eptifibatide linear precursor crude*

Eptifibatide linear precursor crude was precipitated after filtering off the resin from cleavage solution using an antisolvent. Diethyl ether (Et_2O), diisopropyl ether (iPr_2O), methyl-tert-butyl ether (MTBE), and cyclopentyl-methyl ether (CPME) were tested, considering also toxicity and safety (Table 5).

49

The high-cost CPME, recently introduced by Albericio and co-workers as "green alternative to the hazardous Et$_2$O and MTBE", did not fulfill industrial needs.[119,120]

Despite the good performances of MTBE (usually considered as an industrial alternative to Et$_2$O, typically used in lab-scale), in terms of cost (46-65 €/L), crude precipitate yield (73.9%) and UHPLC purity (55.4%), this antisolvent has the disadvantage to be classified in the list of Substances of Very High Concern (SVHC) drafted by the European Chemicals Agency (ECHA) as hazardous chemicals for human health and the environment.[121,122,123] On the other hand, iPr$_2$O was selected as antisolvent because of low volatility, facilitating large volumes management (crude yield 73.4% and UHPLC purity 58.8%) with a competitive cost (40-50 €/L). Moreover, the 10-fold scale-up of crude precipitation conditions maintained the same performances (Table 5, entries 2 and 5).

Table 5. UHPLC purity profile, yield, and cost of Eptifibatide linear precursor crude obtained after resin cleavage and precipitation using different solvents

Entry	Synthesis scale (mmol)	Ether	UHPLC crude purity[*] (A/A%)	Imp a[*] Imp b[*] (A/A %)	Yield[**] (%)	Cost[***] (€/L)
1		Et$_2$O	57.0	7.24 2.57	52.3	40-100
2	0.18	iPr$_2$O	58.8	6.85 2.57	73.4	40-50
3		MTBE	55.4	7.18 2.67	73.9	46-65
4		CPME	66.4	4.60 1.63	62.8	100-200
5	1.80	iPr$_2$O	60.7	6.45 1.05	73.5	40-50

*Resin cleavage cocktail: TFA/H2O/TIS/DODT (92.5:2.5:2.5:2.5, v/v/v/v),20 mL/g resin, stirring 3 h at r.t. Method used to isolate Eptifibatide linear precursor crude: 80 mL solvent/g resin; r.t.; 30 min stirring, and 0 °C, 150 min stirring.
** Yield % = [(g crude found) × (peptide content/100) / (g crude calcd)] × 100; average peptide content: 72% (UV detection).
*** Analytical-grade solvent costs for lab scale production.

3.1.3.3 STEP 1 + 2 scale-up activities

3.1.3.3.1 TFA quality check (use test)

Firstly, we minimized production costs through process optimization from 5 to 70 mmol scale to obtain Eptifibatide linear precursor crude. Industrial-grade TFA withdrawn from storage tank was tested in a cleavage reaction performed on a resin batch obtained at 5 mmol scale and compared with a second cleavage reaction performed in the same conditions using analytical-grade TFA. Since UHPLC purity of both Eptifibatide linear precursor crudes resulted comparable in terms of Eptifibatide linear crude purity (analytical-grade: 74.3%; industrial-grade:74.1%;) and Yield (analytical-grade: 84.2%; industrial-grade: 84.6%), we considered acceptable to use industrial-grade TFA decreasing process cost.

3.1.3.3.2 Scale up from 5 to 70 mmol scale

Additionally, a comparative analysis of both STEP 1 and STEP 2 processes among 5 and 70 mmol scale shows that the scale-up produced extremely comparable UHPLC crude purities (5 mmol: 74.1%; 70 mmol: 73.7%) and yields (5 mmol: 84.6%; 70 mmol: 82.2%). Moreover, both impurity profile of 5 mmol scale (Figure A6, Appendix) and 70 mmol scale (Figure A7, Appendix) show: Des-Har[2]-linear Eptifibatide precursor <0.1%, Imp a ca. 5%, and Imp b ca. 3% (Table 6). Interestingly, no new impurities were detected in 70 mmol scale crude analysis, demonstrating the successful direct scale-up process.

Table 6. Comparative analysis of 5 mmol *vs* 70 mmol scale process to obtain Eptifibatide linear precursor: UHPLC crude purity profile and yield

	STEP 1[*]+ 2[**] Output	70 mmol	5 mmol
Eptifibatide linear precursor crude	UHPLC purity (A/A%)	73.7	74.1
	Yield[***] (%)	82.2	84.6
Impurities	Des-Har^2-linear Eptifibatide precursor (A/A%)	<0.1	<0.1
	Imp a (A/A%)	5.5	5.3
	Imp b (A/A%)	3.5	2.1

Loading of Rink Amide AM resin: 0.97 mmol/g. Coupling conditions: single coupling 1×2.5 equiv building-block (0.4 M), 1×2.5 equiv DIC (3 M) and 1×2.5 equiv Oxyma pure (1 M). All reagents were dissolved in DMF. Final resin washing: 9.3 ml/g resin (3×iPrOH).
**Resin cleavage cocktail: TFA/H2O/TIS/DODT (72:7:7:14, v/v/v/v); 7 mL/g resin, stirring 30 min, r.t.; further addition of 15 mL TFA/g resin, stirring 2.5 h, r.t. Procedure used to isolate Eptifibatide linear precursor crude: 80 mL iPr2O/g resin, 2 h, 0 °C.*
$$***Yield(\%) = \frac{found\ weight \times (\frac{peptide\ content}{100})}{calcd\ weight} \times 100$$ *(UV average peptide content: 79.0%).*

3.1.3.3.3 *Evaluation of quality and risk assessment of resin cleavage materials: risk analysis associated with exposure to volatile ethers and peroxide content, exothermic hazard and TFA quality (use test)*

Volatility of ethers and their peroxide-forming tendency are directly related to inflammation and explosion propensity. Therefore, peroxide content in iPr$_2$O was identified as an hazard in risk assessment. [124] Moreover, peroxides can contribute to uncontrolled oxidation of amino acid side-chains (such as Cys, Trp) dramatically affecting purity outcomes. Three different industrial-grade iPr$_2$O with different peroxide content (0, 350, >1000 ppm), were compared with an analytical-grade peroxide-free iPr$_2$O (Merck KGaA, Darmstadt, Germany) (Table 7). Peroxide content >1000 ppm dramatically affected purity (32.5% *vs* >60%) of the crude displaying high retention time broad peaks in UHPLC profile (oligomer formation). A slight decrease in purity was obtained with iPr$_2$O containing 350 ppm peroxides. However, undoubtedly, careful

control of iPr$_2$O peroxide content (<350 ppm, ideally peroxide-free) has to be performed before precipitation of Eptifibatide linear precursor crude both for safety and purity.

Table 7. Influence of iPr$_2$O peroxide content on UHPLC crude purity

Entry	iPr$_2$O purity grade	Peroxide content[*] (ppm)	UHPLC purity[**] (A/A %)
1	Analytical	0	63.75
2		0	60.56
3	Industrial	350	56.79
4		>1000	32.5

[*]*Method used to measure peroxide content: peroxide test stripes (Quantofix, Macherey-Nagel, Germany, measurement range: 0-1000 ppm).*
[**]*Resin cleavage cocktail: TFA/H$_2$O/TIS/DODT (92.5:2.5:2.5:2.5, v/v/v/v), 20 mL/g resin, stirring 3 h at r.t. Method used to isolate Eptifibatide linear precursor crude: 80 mL solvent/g resin, 30 min stirring ant r.t., and 150 min stirring at 0°C.*

Precipitation of Eptifibatide linear precursor crude from TFA cleavage solution by adding iPr$_2$O was considered in the risk assessment management because of exothermic effect of ether addition. In particular, lab-scale preliminary tests for hazard evaluation to quantitatively assess heat development during the process is fundamental for the final scale-up.[45] Lab-scale precipitation from TFA cleavage solution was performed following the optimized conditions above described, controlling temperature <35 °C by ice-bath cooling.

In the 70 mmol pilot scale process, the temperature of the mixture was maintained <35 °C using a thermostated jacketed reactor under stirring to manage the temperature increase developed during the exothermic iPr$_2$O addition. This procedure allowed both to mitigate workplace safety risks and to guarantee Eptifibatide linear precursor crude quality.

3.1.3.3.4 *Identification of hold points in the scale-up process*

Our industrial production system was organized in batches. The adopted multi-step process would need to be stopped before the term to manage any technical unforeseen events or inspection and test plan process (hold points).

In particular, during the pilot-scale MW-SPPS (STEP 1), hold points were identified only after each coupling cycle (including washing and draining), before Fmoc-deprotection of the last building block on the resin. This is to avoid leaving reactive free amino functions on the resin in the reactor.

In addition, resin cleavage and side-chains deprotection in TFA harsh acidic conditions should be performed without delay to preserve purity and yield. The filtered solution containing the Eptifibatide linear precursor crude in TFA was held at r.t. for 24 hours. After that, the crude was precipitated in iPr$_2$O at 0 °C for 1 hour. UHPLC crude purity dramatically decreased (48%) compared with the one obtained after immediate precipitation (ca. 60%).

Therefore, the hold point to consider was the precipitation phase. A stability study of Eptifibatide linear precursor crude was performed maintaining the suspension after precipitation in iPr$_2$O at 0°C for 1, 3, and 24 h. UHPLC purities obtained, respectively 62.8%, 59.0% and 60.0%, resulted comparable demonstrating crude stability up to 24 hours (Table 8).

Table 8. Stability of Eptifibatide linear precursor crude in iPr$_2$O at different times

Entry	Time* (h)	UHPLC crude purity* (A/A %)
1	1	62.8
2	3	59.0
3	24	60.0

Scale: 5 mmol, resin cleavage cocktail: TFA/H2O/TIS/DODT (72:7:7:14, v/v/v/v), 7 mL/g resin stirring 30 min at r.t. Addition of 15 mL of TFA/g resin and further mixing for 2.5 h. Method used to isolate Eptifibatide linear precursor crude: 80 mL solvent/g resin at 0 °C at different times.

3.1.3.3.5 *cGMP equipment and facilities for 70 mmol scale MW-SPPS (STEP 1) and resin cleavage (STEP 2)*

cGMP peptide API production requires qualification of manufacturing equipment proving the suitability of the system. The qualification process consists of four main actions: design, installation, operational and performance qualifications. The design has to consider final product features, minimizing external contaminations, which could affect product quality. The plant was designed to include a walk-in fume hood (4 m^2) hosting the Liberty PRO MW-assisted synthesizer (CEM, Charlotte, NC, U.S.A) and to allow easy-cleaning procedures both before and after solid-phase peptide manufacturing (STEP 1).

The equipment to perform STEP 2 was designed to limit both air exposition and the operator's handling (Scheme 2).

After the drying session under N$_2$ inside Liberty PRO reaction vessel, the linear precursor-resin was transferred into the 5L jacketed glass filter reactor (RV1232), thermostated at 20 °C. The cleavage cocktail was added from the top of the reactor and the reaction was carried out under constant stirring.

Then, the peptide-cleavage cocktail solution was transferred into the 21L jacketed glass reactor (RV1233) through the filter on the bottom of the 5L reactor (RV1232). The driving force of this transfer was the difference of pressure during the vacuum application to the receiving reactor. Furthermore, the 5L reactor bottom was linked to the head of the 21L reactor (RV1233) by an inert Teflon tube.

21L Reactor (RV1233) was thermostated at 0°C and equipped with 2 thermometers (one inside the reactor, one immediately before the condenser) and 1 pHmeter (switched off during this step). The head of the 21 L reactor is linked to a 10 L glass reservoir by an inert Teflon tube and to a double-coil glass condenser (water-cooled) that is linked to a 5 L glass

collection flask. Ether addition to the peptide-cleavage cocktail solution was performed monitoring that temperature was maintained <35°C.

After crude precipitation, the suspension was transferred under vacuum to the 2L jacketed glass filter reactor (RV1231) by an inert Teflon tube connecting the bottom of the 21 L reactor (RV1233) to the head of the 2 L reactor (RV1231). Final crude filtration was performed at 0 °C. Both transfer of the suspension from the 21 L reactor (RV1233) and Eptifibatide linear precursor crude filtration were performed under vacuum. Finally, after a drying session under N_2, the filtering bottom was disassembled from the rest of the 2L reactor (RV1231) and the crude product was recovered.
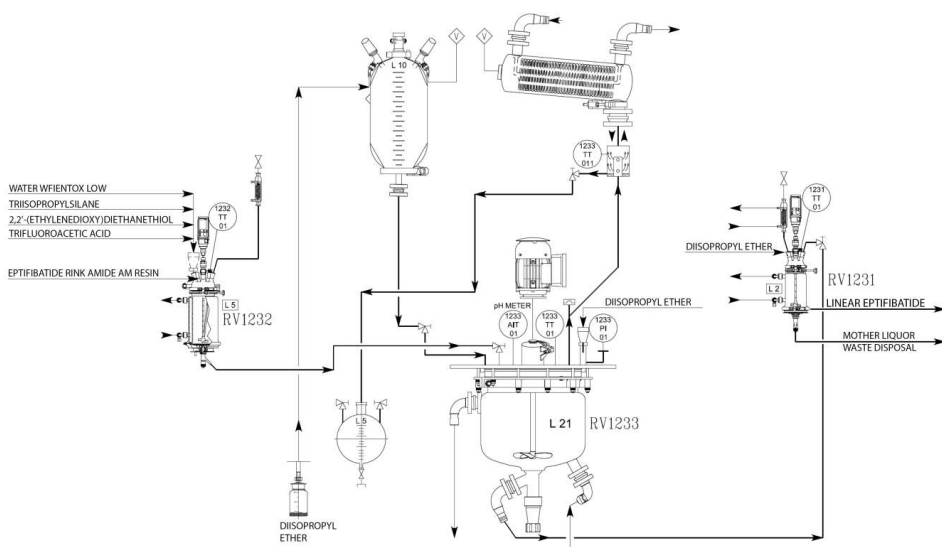
Scheme 2. Industrial plant scheme designed for resin cleavage, side-chain deprotections, and isolation of crude Eptifibatide linear precursor TFA salt (Table A5).

3.1.4 *STEP 3. Optimization of liquid-phase and solid-phase disulfide bond formation strategies to obtain crude Eptifibatide TFA salt*

According to the literature and patents above described (Table 1), several disulfide bridge approaches were possible to use [125,126,127,128]. These approaches can be grouped in two main sets: liquid-phase and solid-phase disulfide bond formation. In this work, a detailed investigation of all process parameters (PP) which can influence disulfide formation in liquid-phase approach was performed, to identify a reproducible and robust disulfide formation strategy. Moreover, the liquid-phase disulfide bond formation procedure optimized on 5 mmol scale was successfully scaled up to 70 mmol scale.

However, to overcome patent limitations, we further investigated 4 solid-phase different approaches (Strategies **A÷D**) in witch STE 1 and 3 can be performed in the same reactor.

3.1.4.1 *Optimization of liquid-phase disulfide bond formation to obtain crude Eptifibatide TFA salt*

In order to optimize the disulfide bond formation in solution, we firstly focused our attention on the mildest disulfide formation procedure based on the use of air. Air oxidation of unprotected linear peptides is accepted as the cleanest and safest strategy,[129] occurring in eco-friendly buffered aqueous solution.

Therefore, the disulfide bridge between MPA at position 1 and Cys at position 7 was formed in solution starting from the free thiol-containing linear precursor MPA-Har-Gly-Asp-Trp-Pro-Cys-NH$_2$ under very mild basic conditions in the presence of atmospheric oxygen. However, these basic reaction conditions could favour uncontrolled intermolecular disulfide arrangements. Therefore, high dilution conditions (0.1-1 mM) are generally used for selective air oxidation in 0.1 M NH$_4$HCO$_3$ aqueous solution at pH 7-8 in 24 hours. However, this led to use large solvent

volumes, dramatically increasing the final industrial process costs. Thus, a careful investigation of disulfide bond formation process parameters (pH, concentration, reaction time, and solvent mixture composition) that could affect the purity of the final product and the overall yield and costs was performed.

In particular, optimization of the air-oxidation conditions of the crude linear Eptifibatide precursor, was accomplished fine-tuning the following critical parameters: i) buffer (NH_4HCO_3 vs NH_4OH); ii) pH (7.5-9.5 range); iii) concentration (2.1-10.6 mM); iv) solvent (different ratio of H_2O/CH_3CN, considering the low solubility in water of both the linear precursor and Eptifibatide itself). Moreover, monitoring of the possible intermolecular disulfide bond side-products formation was an essential part of the study. Therefore, we used HPLC-ESI-MS to monitor the formation of Eptifibatide TFA salt (cyclic oxidized form) and the concomitant consumption of the Eptifibatide linear precursor (linear reduced form), in order to determine the conversion rate at different conditions, paying particular attention to the appearance of additional chromatographic peaks, attributed to dimers and oligomers formed by interchain disulfide bridge(s) (Figure A9, Appendix).

3.1.4.1.1 Evaluation pH and concentration effect at fixed reaction time 22 h, using air as oxidant

We initially tested the different conditions fixing the reaction time at 22 h, as summarized in Table 9. It is clear that simultaneously increasing the pH (from 7.5 to 9.5) and decreasing the concentration (from 10.6 to 2.1 mM) enabled us to obtain a complete conversion limiting inter-chain disulfide bridged side-products formation.

Table 9. Evaluation of reaction parameters 1. Effect of pH and concentration at fixed reaction time 22 h on liquid-phase disulfide bond formation in Eptifibatide

Entry	Concentration (mM)	pH	—SH to S—S Conversion (%)	Dimer (%)
1	10.6	7.5	12.0	4.7
2	5.5	8.0	40.2	8.0
3	3.2	8.5	57.5	4.9
4	2.1	9.5	85.0	4.6

At pH 7.5 the disulfide bond formation reaction was slow: only 12% Eptifibatide was formed after 22 h. On the other hand, an increase of pH from 8 to 9.5 allowed to obtain 85% of crude Eptifibatide at the same reaction time.

Therefore, efficiency of the disulfide bond formation reaction was tested at pH 9.5 focusing on the reaction rate and solution concentration (Figure 9).
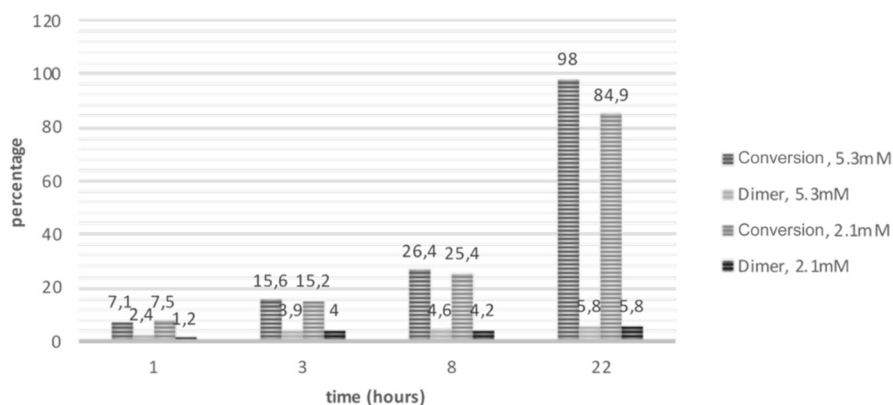
Figure 9. Evaluation of reaction parameters 2. Effect of reaction time and concentration at fixed pH 9.5 on liquid-phase disulfide bond formation in Eptifibatide.

In these pH conditions, disulfide bond formation occurred in 22 h. Moreover, we observed that decreasing the concentration (from 5.3 to 2.1 mM), the conversion at 22 h rate decreased without any advantage in terms of side-products formed. Generally speaking, the possibility to work

at higher concentration (5.3 mM) is preferred, since the volume to be handled is lower.

Moreover, no oxidation improvement was observed changing the composition of the solvent mixture H_2O/CH_3CN from 4:1 (v/v) to 2:1 (v/v) (Figure 10).
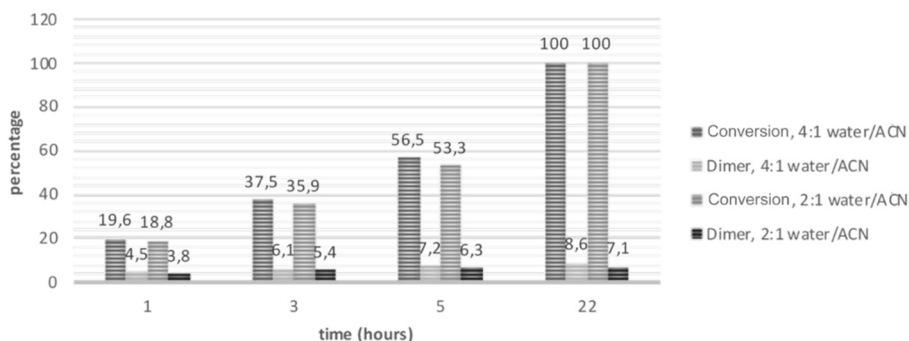
Figure 10. Evaluation of reaction parameters 3. Effect of solvent and reaction time at fixed pH 9.5 and concentration (5.3 mM) on liquid-phase disulfide bond formation in Eptifibatide.

However, selection of the less green and more expensive solvent mixture ratio H_2O/CH_3CN (2:1 (v/v)) compared to H_2O/CH_3CN (4:1 (v/v)) was forced by the lower dimer side-product formation in higher acetonitrile content mixture. In particular, in the higher water content mixture (4:1 (v/v)), a precipitate formation limited reaction monitoring and the putative side-product aggregate, sticking to the glass vessel, affected post-synthesis cleaning procedures.

In conclusion optimal air-oxidation conditions to obtain linear Eptifibatide precursor by liquid-phase disulfide formation were estimated to be: 5.3 mM concentration in H_2O/CH_3CN (2:1); pH 9.5; 22 h reaction time at room temperature. In these conditions 98% conversion of the linear precursor was obtained, leading to crude Eptifibatide with an HPLC purity 61% and dimer 6.6%, in 22h (Figure 11). [130]
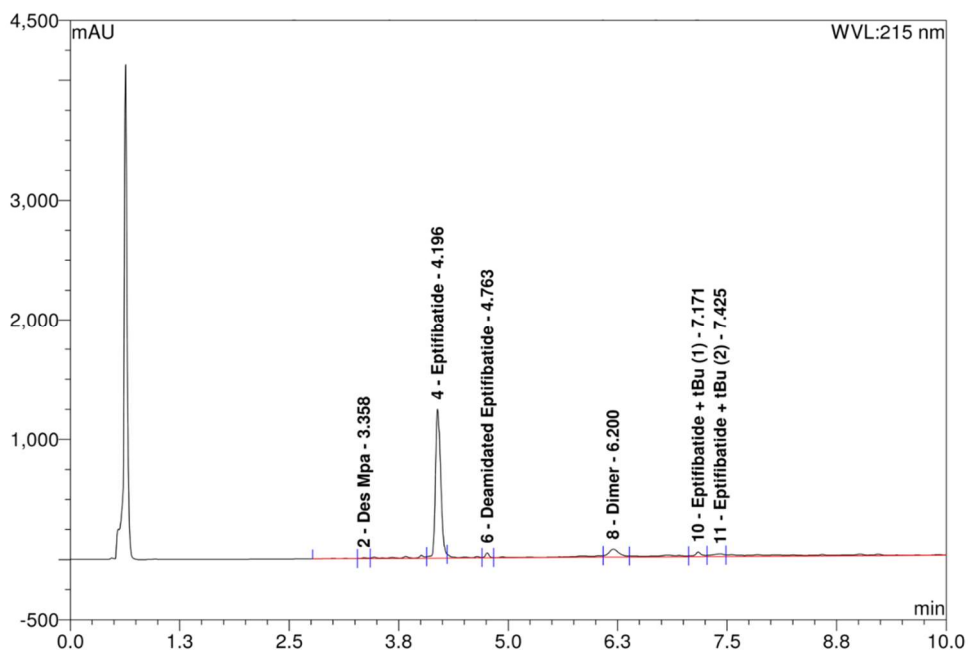
Figure 11. RP-UHPLC-ESI-MS traces of Eptifibatide crude obtained by liquid-pase disulfide bond formation reaction (5.3 mM Eptifibatide linear precursor in H_2O/CH_3CN, 2:1; r.t.; pH 9.5; 22h). RP-UHPLC-ESI-MS: C18 column Waters Acquity CSH (130Å, 1.7 μm, 2 × 100 mm); temperature 45°C; flow: 0.5 mL/min; eluent: 0.1% (v/v) TFA in H_2O (A) and 0.1% (v/v) TFA in CH_3CN (B), λ 215 nm, gradient: 12-45% (v/v) B in 10 min. Rt 4.196 min: Eptifibatide (Peak 1) and Rt 6.200 min: Dimer (Peak 2).

3.1.4.1.2 Evaluation H_2O_2 as oxidant. Investigation of the number of H_2O_2 additions and concentration effect

However, in order to speed up the disulfide bond formation reaction, we looked for an alternative oxidant, compatible with large scale production. Hydrogen peroxide aqueous solution was considered a balanced compromise in terms of efficacy, costs, sustainability, and cleaning procedure.[131,132,133,134]

Despite of a fast conversion (<15 min) of Eptifibatide linear precursor (5.3 mM in $H_2O:CH_3CN$ 2:1 v/v) at 0.5 mmol scale, after addition of 0.8 equiv H_2O_2 in one-shot at time 0 h, at pH 9.5 (NH4OH), a substantial formation of dimer impurity (>10%) occurred (Figure A10, Appendix).

Therefore, we investigated different reaction conditions to obtain complete conversion with the highest Eptifibatide TFA purity and lowest dimer impurity formation. In particular, the same equivalents of H_2O_2 (0.8 equiv) were added in 2 or 4 times (Table A6) and then the linear precursor concentration was decreased (Table A7).

Two additions of 0.44 equiv H_2O_2 (at 0 and 60 min, respectively) compared to 4×0.22 equiv (0, 30, 60, 90 min) did not influence either the Eptifibatide TFA yield or the dimer impurity formation. However, in a scale-up process, the possibility of 4 additions of a lower number of H_2O_2 equiv/time allows a more accurate in process control of the disulfide bond formation reaction (Figure 12).
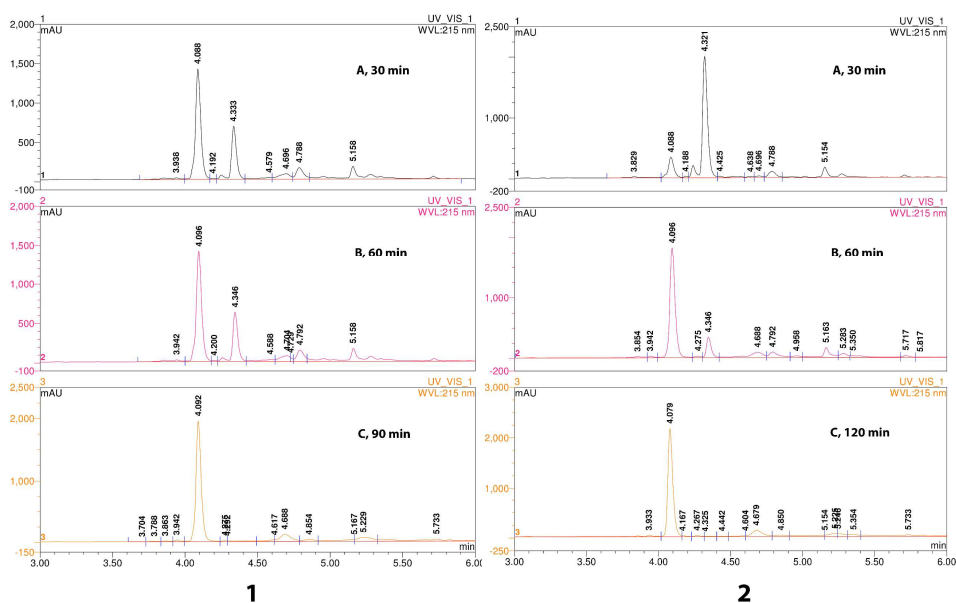
Figure 12. In process control of liquid-phase disulfide bond formation (0.5 mmol scale): RP-UHPLC traces of Eptifibatide crude obtained by Eptifibatide linear precursor crude in H_2O:CH_3CN 2:1 (v/v) (5.3 mM), with multiple additions of H_2O_2 at different times A-C (Table A6), pH 9.5, r.t. RP-UHPLC: C18 column Waters Acquity CSH (130Å, 1.7 μm, 2.1 × 100 mm); temperature 45°C; flow: 0.5 mL/min; eluent: 0.1% (v/v) TFA in H_2O (A) and 0.1% (v/v) TFA in CH_3CN (B), λ 215 nm, gradient: 5-95% (v/v) B in 10 min. R_t 4.085 ± 0.015 min: Eptifibatide TFA; R_t 4.33 ± 0.01 min: Eptifibatide linear precursor; R_t 4.77 ± 0.015 min: Dimer impurity.

In this framework, the concentration parameter was re-evaluated. Two different concentrations of linear Eptifibatide precursor crude (2.1 mM and 1.6 mM) with addition of 4×0.22 H_2O_2 were tested at 0.5 mmol scale (Figure 13). Lowering the linear precursor concentration from 5.3 mM (Entry 2, Table A6) to 1.6 mM (Entry 2, Table A7) led to a dramatic decrease of dimer impurity formation (from 8.0% to 3.9%) and an increase in UHPLC purity of Eptifibatide TFA (up to 67%).
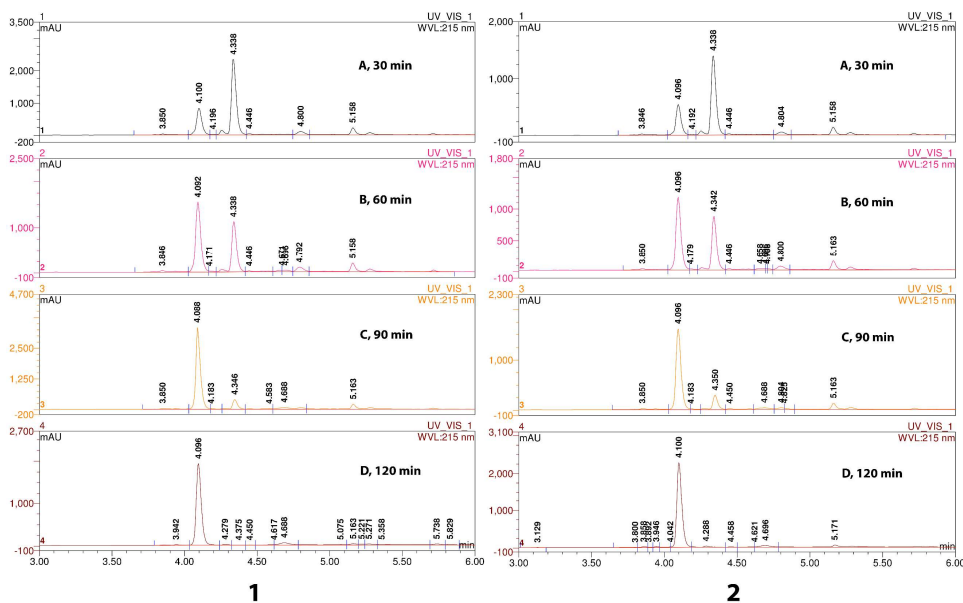
Figure 13. In process control of liquid-phase disulfide bond formation (0.5 mmol scale): RP-UHPLC traces of Eptifibatide crude obtained by Eptifibatide linear precursor crude in H_2O:CH_3CN 2:1 (v/v) at concentration 1 (2.1 mM) and 2 (1.6 mM), with 4×0.22 equiv H_2O_2 additions at 0, 30, 60, and 90 min (Table A7), pH 9.5, r.t. RP-UHPLC: C18 column Waters Acquity CSH (130Å, 1.7 μm, 2.1 × 100 mm); temperature 45°C; flow: 0.5 mL/min; eluent: 0.1% (v/v) TFA in H_2O (A) and 0.1% (v/v) TFA in CH_3CN (B), λ 215 nm, gradient: 5-95% (v/v) B in 10 min. R_t 4.09 ± 0.015 min: Eptifibatide TFA; R_t 4.33 ± 0.01 min: Eptifibatide linear precursor; R_t 4.79 ± 0.015: Dimer impurity.

In conclusion, the identified optimized conditions (Eptifibatide linear precursor crude 1.6 mM in H_2O:CH_3CN 2:1 (v/v), pH 9.5 (NH$_4$OH), 4×0.22 equiv H_2O_2 additions at 0, 30, 60, and 90 min) allowed to decrease reaction time from 22h to 2 h (Figures 12 and 13).

3.1.4.2 *STEP 3 scale-up activities*

The above described optimized conditions for disulfide bond formation, were tested at 10 mmol scale and repeated 5 times in cGMP compliant glassware.

In particular, comparative analysis of STEP 3 process (Table 10) shows that the scale-up produced extremely comparable UHPLC crude purities (5 mmol: 67.4%; 70 mmol: 66.4%) and increased yield (5 mmol: 90.7%; 70 mmol: 98.3%). Moreover, scale-up in process control demonstrates that dimer impurity formation was limited to <6% (Figures A11 and A12).

Table 10. Comparative analysis of 5 mmol *vs* 70 mmol scale process to obtain Eptifibatide TFA: UHPLC crude purity profile and yield

	STEP 3 Output[*]	70 mmol[***]	5 mmol
Eptifibatide crude	UHPLC purity (A/A%)	66.4	67.4
	Yield (%)[**]	98.3	90.7
Impurities	Dimer (A/A%)	5.3	5.9

Conditions for disulfide bond formation (70 and 5 mmol): Eptifibatide linear precursor crude (2.1 mM in H2O:CH3CN 2:1 v/v) was oxidized adding H2O2, pH 9.5 (NH4OH), 2 h, r.t.

$$**Yield\ (\%) = \frac{Eptifibatide\ crude\ weight\ \times\ (\frac{peptide\ content}{100})}{Eptifibatide\ linear\ crude\ weight\ \times\ (\frac{peptide\ content}{100})} \times 100$$

UV Eptifibatide crude average peptide content: 71.0 %, UV Eptifibatide linear precursor crude average peptide content: 79.0 %.
***The procedure was repeated 5 times at 10 mmol scale on cGMP compliant glassware.*

Concerning STEP 3 scale-up, a specific cGMP compliant industrial plant was designed both for liquid-phase disulfide bond formation and isolation of crude Eptifibatide TFA salt by freeze-drying (Scheme 3). In particular, a 21L jacketed glass reactor (RV1233) was thermostated at 20 °C. After loading from the top of the reactor, the Eptifibatide linear precursor crude (output from STEP 1+2) was solubilized in the mixture WFI/CH$_3$CN 2:1

(v/v) previously prepared in a 10L glass reservoir connected to the head of the reactor by an inert Teflon tube. The pH was adjusted to 9.5 adding dropwise NH_4OH (0.25 M in H_2O) and monitoring by a pHmeter inside the reactor (AIT1233).

The reaction mixture was recovered from the bottom of the reactor and transferred to steel plates into the freeze-dryer after monitoring the complete conversion by IPC *via* RP-UHPLC.

Lyophilization consisted of 3 phases: reaction mixture freezing (P atm, -60 °C), freeze-drying (0.9 mbar, -60 °C to r.t.), and room temperature drying (0.9 mbar, r.t.). The process continued till water content and residual solvents satisfied critical quality attributes (Table A4).
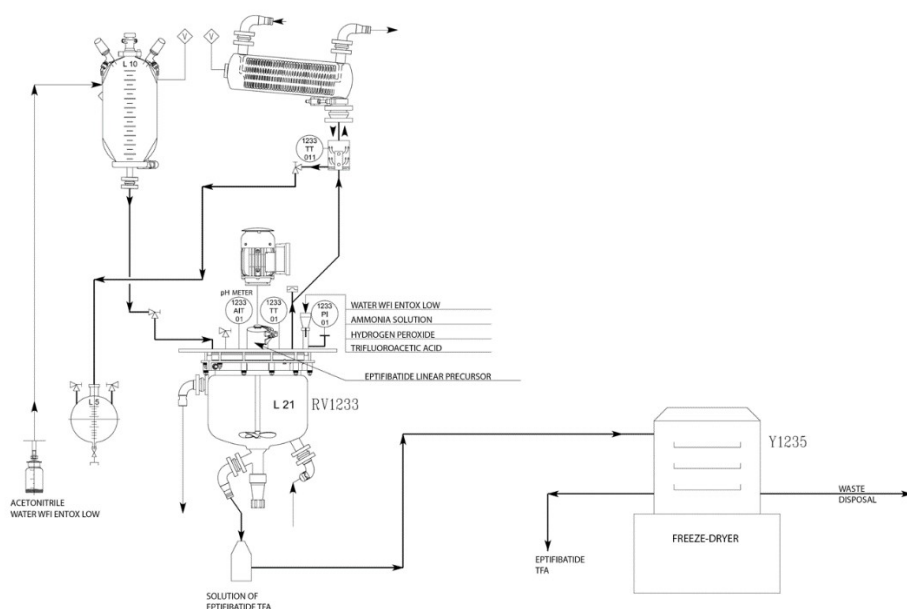
Scheme 3. Industrial plant scheme designed for liquid-phase disulfide bond formation to obtain crude Eptifibatide TFA salt (Table A5).

3.1.4.3 *Optimization of solid-phase disulfide bond formation to obtain crude Eptifibatide TFA salt*

As previously mentioned we investigate 4 solid-phase different approaches (Strategies **A÷D**, schemes 4 and 5) on lab scale by a Liberty Blue instrumentation without isolating linear Eptifibatide precursor, with the idea in mind of developing a completely automatic synthetic procedure to be scaled in the Liberty PRO solid-phase peptide synthesizer.

3.1.4.3.1 *Strategy A and B*
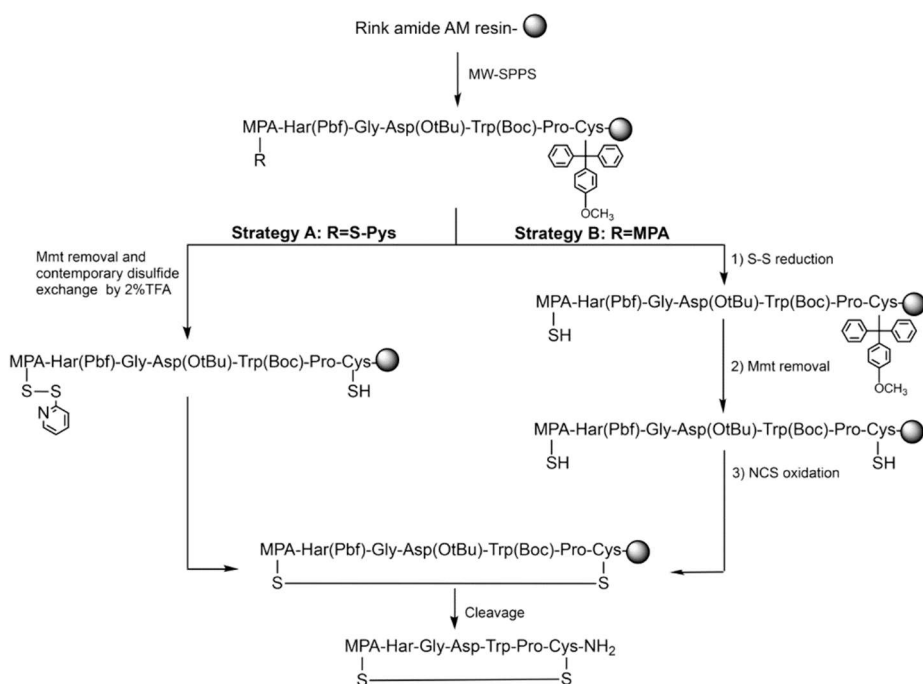
Scheme 4. Fully automated microwave-assisted synthesis of Eptifibatide performing solid-phase disulfide bond formation: Strategies A and B.

Strategy A

In particular in Strategy **A,** after coupling MPA(PyS) in the MW reactor to Har(Pbf)-Gly-Asp(OtBu)-Trp(Boc)-Pro-Cys(Mmt)-Rink Amide AM Resin, mild acidic conditions were used to cleave the Mmt protecting group on Cys and favouring the contemporary disulfide-exchange reaction

between free thiol on Cys side-chain and the pyridyne-2-thiol group (PyS) on MPA.[135,136,137] This reaction occurring in 25 min at r.t., led to the desired disulfide bond in crude Eptifibatide that, after resin cleavage, was recovered in 60% yield with 34.9% HPLC purity (Figure 14).
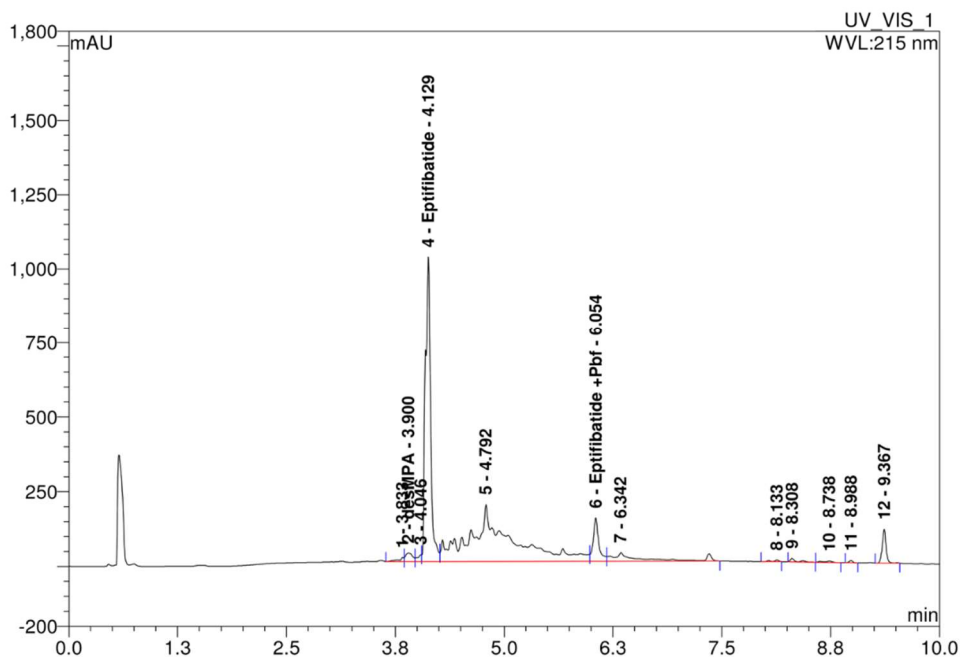
Figure 14. RP-UHPLC trace of Eptifibatide by solid-phase Strategy A. C18 column Waters Acquity CSH (130Å, 1.7 µm, 2.1 × 100 mm); temperature 45°C; flow: 0.5 mL/min. Eluents: 0.1% (v/v) TFA in H_2O (A) and 0.1% (v/v) TFA in CH_3CN (B); λ 215 nm; gradient: 5-95% (v/v) B in A in 10 min. R_t 4.1 min: Eptifibatide TFA; R_t 4.7 min: Dimer impurity; R_t 6.01 min: Eptifibatide (Pbf) TFA.

The main disadvantage of Strategy **A** is the high cost of the building blocks Fmoc-Cys(Mmt)-OH and MPA(PyS).

Strategy B

On the other hand in Strategy **B** after MW-assisted amide bond formation between DTDPA and the N-terminal amino function on Har(Pbf)-Gly-Asp(OtBu)-Trp(Boc)-Pro-Cys(Mmt)-Rink Amide AM Resin and DTT-

mediated reduction of the S-S bond in DTDPA linked to the peptide-resin, [138] we took advantage of N-chlorosuccinimide (NCS) oxidative properties, leading to the disulfide bond formation by the highly reactive sulfenyl chloride formation toward thiol in Cys after Mmt removal with a rapid, clean, and efficient reaction. As previously demonstrated by Albericio et al., this reaction was strongly affected in terms of final crude purity, by the possible use of NCS reagent excess.[139] A more important drawback of Strategy **B** is the use of the harmful NCS reagent requiring management of the resin out of the microwave reactor of the synthesizer to avoid dramatic and unsafe instrument contaminations, requiring cleaning procedures that will increase energy and water costs, a prime concern for manufacturers. On the other hand a big advantage (compared to the previous described strategy **A**) is the use of the harmless, inexpensive, and greener DTDPA that is essentially the MPA S-S bridged dimer, i.e. (MPA)$_2$ instead of the more expensive MPA(PyS) building block.

After resin cleavage, crude Eptifibatide was recovered in 82% yield with 42% HPLC purity (Figure 15).

Figure 15. RP-UHPLC trace of Eptifibatide by solid-phase Strategy B. C18 column Waters Acquity CSH (130Å, 1.7 μm, 2.1 × 100 mm); temperature 45°C; flow: 0.5 mL/min. Eluents: 0.1% (v/v) TFA in H_2O (A) and 0.1% (v/v) TFA in CH_3CN (B); λ 215 nm; gradient: 5-95% (v/v) B in A in 10 min. R_t 4.1 min: Eptifibatide TFA; R_t 6.01 min: Eptifibatide (Pbf) TFA.
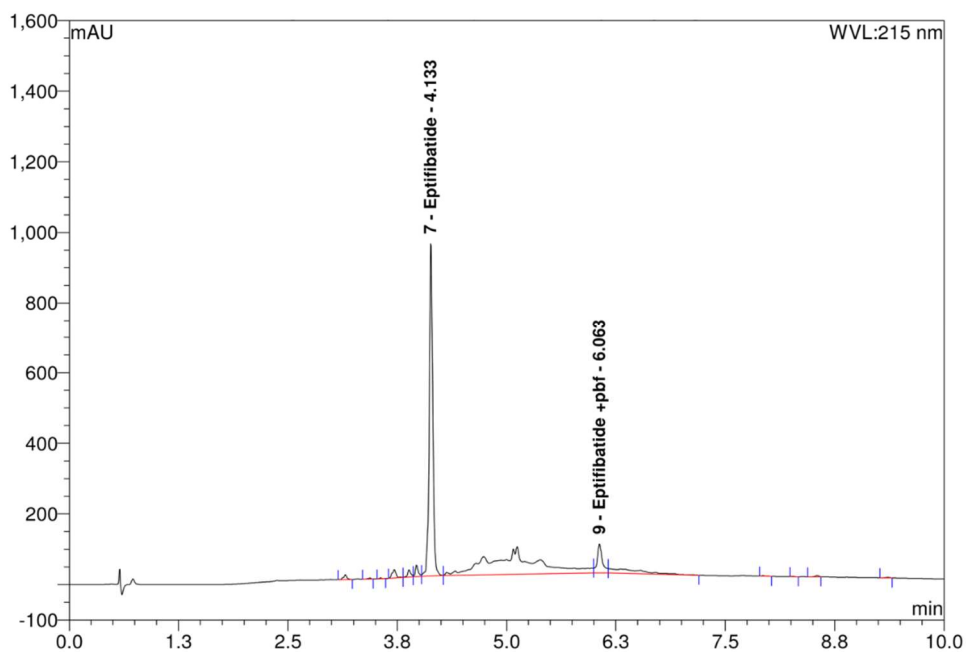
3.1.4.3.2 *Strategy C and D*
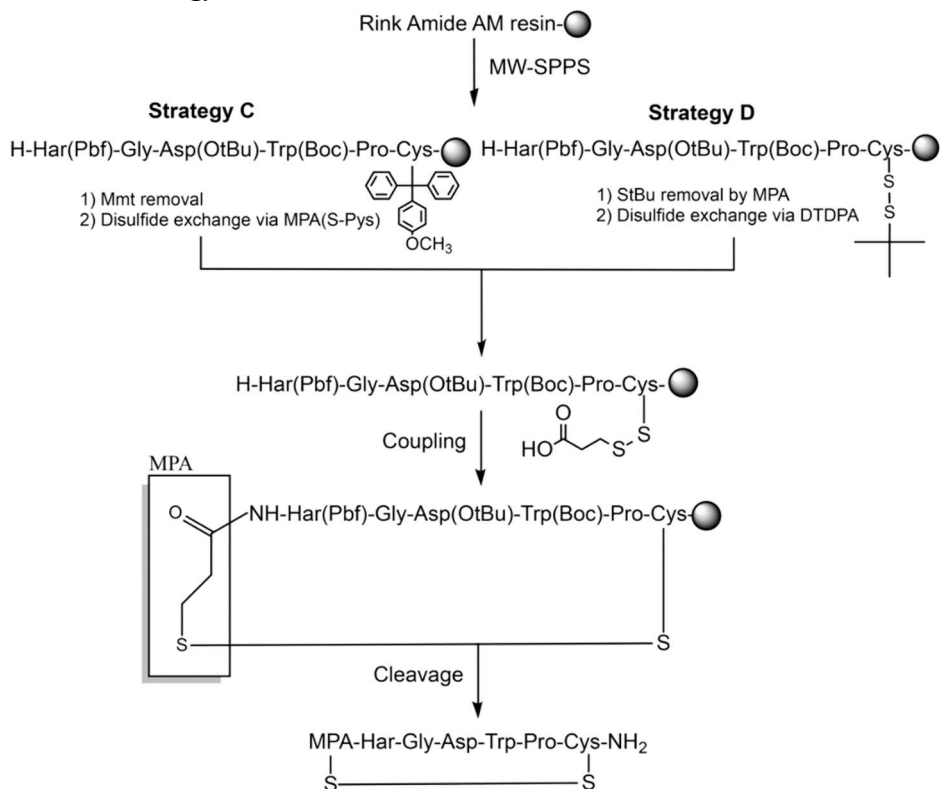
Scheme 5. Fully automated microwave-assisted synthesis of Eptifibatide performing solid-phase disulfide bond formation: Strategies C and D.

Strategy C

The Strategy **C** starts from the same peptide-resin fragment above described, i.e. Har(Pbf)-Gly-Asp(OtBu)-Trp(Boc)-Pro-Cys(Mmt)-Rink Amide AM Resin, used in Strategies **A** and **B**. After Mmt deprotection, S-S bond is formed on Cys7 free thiol function by MPA(PyS) mediated disulfide-exchange to obtain Cys(MPA). Then by PyBop/DIPEA activation (5:7 equiv) of the carboxylic function on Cys(MPA) at r.t. for 16h,[140] the head to MPA on Cysteine side-chain cyclization occurs by nucleophilic attack of the N-terminal Har on the peptide-resin (Scheme 5).

Optimization of Cys(MPA) formation on the resin was achieved performing the reaction directly in the MW reactor (90W, 50 °C, 30 min) as reported in Table A8, and as observed by IPC (Figure A13 in Appendix, IPC procedure in Material and Methods) of Har-Gly-Asp-Trp-Pro-Cys(MPA)-NH$_2$ cleaved from the resin.

After resin cleavage, crude Eptifibatide was recovered in 61% yield with 56.5% HPLC purity (Figure 16).
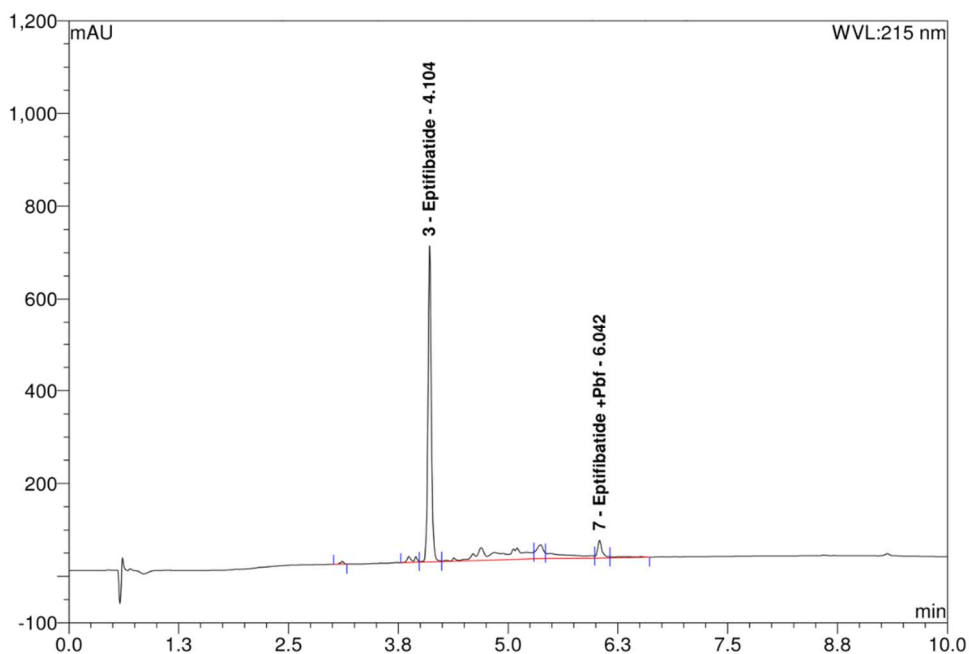
Figure 16. RP-UHPLC trace of Eptifibatide by solid-phase Strategy C. C18 column Waters Acquity CSH (130Å, 1.7 μm, 2.1 × 100 mm); temperature 45°C; flow: 0.5 mL/min. Eluents: 0.1% (v/v) TFA in H$_2$O (A) and 0.1% (v/v) TFA in CH$_3$CN (B); λ 215 nm; gradient: 5-95% (v/v) B in A in 10 min. R$_t$ 4.1 min: Eptifibatide TFA; R$_t$ 6.01 min: Eptifibatide (Pbf) TFA.

In conclusion, the peculiarity of Strategy **C** is the solid-phase formation of S-S bond by disulfide-exchange between MPA(PyS) and thiol function in Mmt-cleaved cysteine. Then, the carboxylic function on MPA linked on cysteine by S-S bridge, i.e. Cys(MPA), after appropriate activation could form the amide bond with the N-terminal amino function of Har(Pbf) on

the peptide-resin. This strategy has the advantage that in the peptide industry, the formation of the amide bond is pivotal and among the more important transformations in the design of synthetic plans. Moreover amide bond formation is optimized in solid-phase synthesis in particular in microwave-assisted peptide synthesizer.

Strategy D

The Strategy **D** (Scheme 5) takes advantage of the interesting step in strategy **C** above described (to form the disulfide bond directly on cysteine before closing the cyclopeptide by amide formation), using the less expensive building block Cys(StBu) compared to Cys(Mmt). Therefore, starting from the peptide-resin fragment Har(Pbf)-Gly-Asp(OtBu)-Trp(Boc)-Pro-Cys(StBu)-Rink Amide AM resin, the first issue of the strategy **D** is to propose a greener, safer and low cost reducing agent for orthogonal deprotection conditions of Cys(StBu) at position 7.

DTT was immediately excluded because of its high cost the industrialization process. Although DTT was widely reported in the literature as an efficient reducing agent also for functional groups in peptide sequences,[141,142] as well as demonstrated in the case on Strategy **B**. Several assays with different reagents were performed with the aim to deprotect Cys(StBu) and to provide a scalable fully automated solid-phase microwave-assisted cGMP-ready process of Eptifibatide (Optimization assays to perform Cys(StBu) deprotection, Material and Methods). In particular, 20% (v/v) β-mercaptoethanol (βME) in basic conditions (0.1 M NMM or 0.05 M DIPEA) in DMF[141,142] allowed to remove StBu at r.t., but in long time. In the case of the starting peptide-resin used in Strategy **D**, quantitative reduction was reached with the same reaction cocktail, in 15 min in microwave conditions (75 °C, 45 W).[141] However, the high toxicity and difficult cleaning procedures of the reaction vessel in the MW-

synthesizer, make βME inconvenient for a kilogram-scale solid-phase production.

Moreover, 10% (v/v) 2- (2-MEA) in DMF at r.t. allowed quantitative reduction in 16 h. An increase of 2-MEA reagent up to 20% (v/v) did not correspond to an improved reaction rate, but to the solid-phase formation of Har(Pbf)-Gly-Asp(OtBu)-Trp(Boc)-Pro-Cys(2-MEA)-Rink Amide AM resin as the result of a side-reaction involving the thiol functional group on Cys after StBu deprotection (IPC, Figure A14, Appendix). Considering that MPA is the moiety that in Eptifibatide is linked by an amide bond to Har and that in biological systems it has been reported to act as a reducing agent [142] we used MPA for our optimized fully single reactor solid-phase disulfide bond formation in Eptifibatide. To the best of our knowledge we were the first to propose MPA to deprotect StBu on cysteine in particular the peptide-resin Har(Pbf)-Gly-Asp(OtBu)-Trp(Boc)-Pro-Cys(StBu)-Rink Amide AM was treated with MPA/DIPEA (40:41 equiv) in DMF for 24 h at r.t. in the Liberty Blue instrument. We obtained an acceptable StBu deprotection with only 2.2 % residual Cys(StBu) containing peptide, but no disulfide-exchange on the free thiol on cysteine. Therefore, the desired disulfide-exchange to link MPA on cysteine was successfully achieved treating the resin directly in the reaction vessel into the instrument, with a DMF solution of the MPA dimer (DTDPA) and DIPEA (40:1.2 equiv) at r.t. for 21 h. Then, the peptide-resin was finally ready for head to MPA on Cysteine side-chain cyclization by amide bond formation between the carboxylic function of MPA on Cys and N-terminal Har, by MW-assisted coupling with DIC and Oxyma Pure (see Experimental section). After resin cleavage, crude Eptifibatide was recovered in 60% yield with 40.9% HPLC purity (Figure 17).
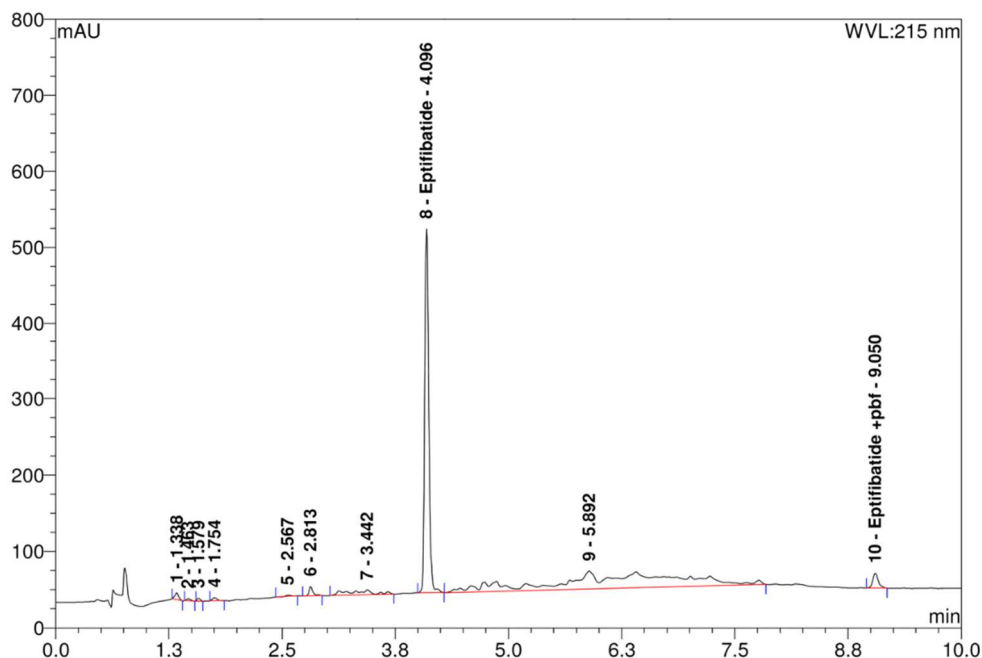
Figure 17. RP-UHPLC trace of Eptifibatide by solid-phase Strategy D. C18 column Waters Acquity CSH (130Å, 1.7 μm, 2.1 × 100 mm); temperature 45°C; flow: 0.5 mL/min. Eluents: 0.1% (v/v) TFA in H_2O (A) and 0.1% (v/v) TFA in CH_3CN (B); λ 215 nm; gradient: 12-45% (v/v) B in A in 10 min. R_t 4.1 min: Eptifibatide TFA; R_t 9.1 min: Eptifibatide (Pbf) TFA.

The relevance of Strategy **D** is essentially based on the selection of the StBu orthogonal protection on cysteine that is easily removed by MPA acting as a novel reducing agent for Cys(StBu) deprotection. Moreover, all Strategy **D** operations (amino acid couplings, orthogonal side-chain protecting groups removal, and final head to MPA on Cysteine side-chain cyclization) can be really carried out in a single reactor solid-phase condition. Easy washings of any reagent excesses that in any case corresponds to the common MPA and simple StBu compared to protecting groups and reagents used in the other strategies, is allowed by fully automated process in the instrumentation.

To the best of our knowledge, Strategy **D** represents an inventive (non-obvious) strategy, (since we were the first to propose MPA to deprotect StBu on cysteine), which proposes for the first time to perform all the

processes including disulfide bond formation in a single reactor (novelty) to prepare Eptifibatide acetate, scalable on multigram-scale by Liberty Pro synthesizer (Industrial applicability).

3.1.5 *STEP 4. Purification of crude Eptifibatide*

RP-UHPLC ESI-MS analysis of crude Eptifibatide TFA salt, obtained by liquid-phase disulfide bond formation in STEP 3, showed at both 5 mmol and 70 mmol scale that the main impurity (5.3% and 5.9%, respectively) was in agreement with the formation of dimers (Table 10, Figures A11 and A12, Appendix). A careful investigation of purification conditions by medium pressure chromatography was performed. In particular, flash Reverse Phase Chromatography (RPC) was selected as a versatile technology based on an automatic, low-cost, easy-handling purification equipment both for laboratory and pilot scale, such as Isolera One (Biotage, Uppsala, Sweden).[143,144]

The goal was to obtain Eptifibatide TFA purity >98.5% limiting both eluents consumption and the volume of eluted fractions to freeze-dry. Several parameters were considered: flow rate, eluents composition, column performance, and column cleaning procedure. Moreover, elution mode (linear or step gradient), column loading, and volume to be lyophilized after pooling homogeneous fractions were evaluated. Linear gradient is characterized by an automated gradual increase of strong solvent percentage over time, ensuring result reproducibility, minimizing the possibility of error. Compared to the step gradient method, no elution band broadening occurs. Consequently, fraction volumes to be lyophilized and related costs are decreased.

Starting from 5% Eptifibatide TFA crude column loading, two linear gradients were tested: 5-30% (v/v) B in A *vs* 10-37% (v/v) B in A, both eluted in 12 column volumes (A: 0.1% (v/v) TFA in H_2O, B: 0.1% (v/v)

TFA in CH$_3$CN). While 5-30% (v/v) B in A linear gradient required 0.8 L B and 2.4 L A (Figure A15, Appendix), the 10-37% (v/v) linear gradient required a slight lower amount of eluents (0.7 L B and 2.2 L A, Figure A16, Appendix). On the other hand, yield increased from 24.7% to 34.3% producing the same eluted volume (165 mL, Table 11). We demonstrated that crude loading should be maintained <5% to achieve the highest purity and recovery yield. Despite 8% loading required a lower number of purification batches, lower yield was observed (Table 11, 18.1% yield, Figure A17, Appendix). Fractions containing Eptifibatide TFA with 90-98.5% purity (recovery) could be collected for further purification to reach required purity, increasing final yield.

Table 11. Recovery, yield, and eluate volume from Flash Column Chromatography purification of Eptifibatide TFA

Entry	Gradient B in A[*] (%)	Column loading (%)	Purity (A/A%)	Recovery (g)	Yield[**] (%)	Eluate (mL)
1	5-30	5	>98.5	1.3	24.7	165
			95-98	1.0	-	180
			90-92	1.3	-	405
2	10-37	5	>98.5	1.8	34.3	165
			95-98	0.8	-	150
			90-92	0.523	-	300
3	10-37	8	>98.5	1.45	18.1	150
			95-98	1.23	-	195
			90-92	1.24	-	390

[*]*Flash Column chromatography conditions: Eptifibatide TFA crude was purified with Biotage Isolera One equipped with SNAP Ultra C18 120g column (volume 164 mL). Eluents: 0.1% (v/v) TFA in H$_2$O (A), 0.1% (v/v) TFA in CH$_3$CN (B); 12 column volumes linear gradients; flow rate: 50 mL/min; λ 215 nm.*

[**]$Yield(\%) = \dfrac{Eptifibatide\ purified\ weight\ \times\ (\frac{peptide\ content}{100})}{Eptifibatide\ crude\ weight\ \times\ (\frac{peptide\ content}{100})} \times 100$

UV Eptifibatide TFA average peptide content: 85%; UV Eptifibatide TFA crude average peptide.

3.1.5.1 *STEP 4 scale-up activities*

Purification experimental conditions of Eptifibatide TFA salt (linear gradient 10-37% (v/v) B in A in 12 column volumes, A: 0.1% (v/v) TFA in H_2O, B: 0.1% (v/v) TFA in CH_3CN, crude loading ≤5%) were successfully confirmed at 5 mmol and scaled-up to 10 mmol scale to be repeated 5 times on cGMP compliant equipment (HPLC purity 5 mmol: 99.2% and 70 mmol: 99.3%; yield 5 mmol: 40.5%; 70 mmol: 41.6%). All the impurities identified in previous steps were observed to be <0.5% after flash column chromatography purification (Table 12, Figures A18-S21, Appendix), in agreement with ANDA requirements for Eptifibatide, obtained following the cGMP process described herein.

Table 12. Comparative analysis of 5 mmol *vs* 70 mmol scale process to obtain purified Eptifibatide TFA: HPLC purity profile and yield

	STEP 4 Output[*]	70 mmol[***]	5 mmol
Eptifibatide TFA	HPLC purity (A/A%)	99.3	99.2
	Yield[**] (%)	41.6	40.5
Impurities	Imp a (A/A%)	<0.1	<0.1
	Imp b (A/A%)	<0.1	<0.1
	Des-Har^2-Eptifibatide (A/A%)	<0.1	<0.1
	Dimer (A/A%)	<0.1	<0.1
	Unknown (A/A%)	<0.5	<0.5

[*]*Flash Column chromatography conditions: Eptifibatide TFA crude was dissolved in H_2O: CH_3CN 1:1(v/v) (0.35M). Column loading 4% (5 mmol), 2.5% (70 mmol). Eluents: 0.1% (v/v) TFA in H_2O (A) and 0.1% (v/v) TFA in CH_3CN (B). Gradient: 10-37% (v/v) B linear gradient in 12 column volumes.*

$$^{**}Yield(\%) = \frac{Eptifibatide\ purified\ weight \times (\frac{peptide\ content}{100})}{Eptifibatide\ crude\ weight \times (\frac{peptide\ content}{100})} \times 100$$

UV peptide content of purified Eptifibatide: 85%; UV peptide content of Eptifibatide crude: 71%.
[***]*The procedure was repeated 5 times at 10 mmol scale on cGMP compliant equipment.*

3.1.6 *STEP 5. Counter-ion exchange to obtain Eptifibatide acetate salt*

Eptifibatide commercialized under the trade name Integrilin[®] has been approved by FDA as acetate salt.[145] Considering that resin cleavage, side-chains deprotection, quenching of the reaction to form disulfide bond, and final purification, performed in STEPs 2-4, required the use of harmful trifluoroacetic acid (pKa= 0), complete counter ion exchange of TFA with acetate anion (pKa= 4.5) was necessary. Therefore, we performed an SPE on the same equipment used for step 4 (Biotage Isolera, Uppsala, Sweden). In particular, Eptifibatide TFA salt presents a charge-to-charge interaction between the carboxylate in TFA and the cation on the homoarginine side-chain, the guanidinium group with a pKa ca. 12.5.

However, at pH >8, degradation of the disulfide bond in the drug was observed as previously described.[146] Therefore, the solution of purified Eptifibatide TFA salt (output of STEP 4) in pure H_2O (2.6 mM) at r.t. was adjusted at pH 8 adding an NH_4OH solution (1.5% (v/v) in H_2O). Under these conditions, the peptide was completely soluble and disulfide bond resulted stable. Thus, the mixture was loaded on a C18 column. Two isocratic elutions, consisting of a) 100% H_2O (3 column volumes) and b) 100% of 0.5% (v/v) AcOH in H_2O (3 column volumes), completely removed ammonium trifluoroacetate salt. Finally, the desired Eptifibatide acetate solution was eluted with 0.5% (v/v) AcOH in H_2O/CH_3CN 4:1 (v/v) (3 column volumes). The resulting homogenous fractions were pooled and freeze-dried to recover Eptifibatide acetate.

3.1.6.1 *STEP 5 scale-up activities*

The above described TFA/acetate counter-ion exchange strategy was successfully scaled-up from 5 mmol to 70 mmol scale (10 mmol scale repeated 5 times on cGMP compliant equipment) obtaining exactly the same 99.6% HPLC purity and slightly increased yield (5 mmol: 64.6%; 70

mmol: 65.8%, Table 13, Figures A22 and A23 in Appendix). Since TFA residual content is considered a Critical Quality Attribute (CQA) affecting safety of preclinical and clinical applications, the above described TFA/acetate exchange procedure was evaluated for its TFA residual content that was demonstrated to be significantly below the cGMP specification limit (5000 ppm). Moreover, acetate content resulted in 4-10% specification range (Table 13).

Table 13. Comparative analysis of 5 mmol *vs* 70 mmol scale process to obtain Eptifibatide acetate: HPLC crude purity profile and yield

	STEP 5[*] Output	70 mmol[***]	5 mmol
Eptifibatide	HPLC purity (A/A%)	99.6	99.6
	Yield[**](%)	65.8	64.6
Counter Ion	Acetate (w/w%)	3.9	4.6
	TFA (ppm)	230	335

[*]*Ion exchange conditions: purified Eptifibatide TFA was dissolved in H_2O (2.6mM), column loading 0.8%, pH 8.0 (NH_4OH). Eluents: 0.5% (v/v) AcOH in H_2O (A), 0.5% (v/v) AcOH in CH_3CN (B), H_2O (C), and CH_3CN (D). Elution: a) 100% C, 3 column volumes; b) 100% A, 3 column volumes; c) 20% B in A, 3 column volumes; d) 100% D, 2 column volumes.*

[**]$$Yield(\%) = \frac{Eptifibatide\ acetate\ weight \times (\frac{peptide\ content}{100})}{Eptifibatide\ purified\ TFA\ weight \times (\frac{peptide\ content}{100})} \times 100$$

UV Eptifibatide acetate peptide content: 87%; UV Eptifibatide purified TFA peptide content: 85%
[***]*The procedure was repeated 5 times at 10 mmol scale on cGMP compliant equipment.*

Considering the yield of each step (STEPs 1+2, 3, 4, and 5; Tables 6, 10, 12, and 13), the final total yield of the Eptifibatide acetate for the entire production process is 22.1%. All the listed quality attributes (Table 14) that are in agreement with the targets established in Module 3 of the Common Technical Document for the Registration of Pharmaceuticals for Human Use (ICH *M4: Common Technical Document*) demonstrate that

the above-described production process of Eptifibatide acetate allows the release of the final cGMP compliant batch.

Table 14. Eptifibatide acetate quality attributes for cGMP compliant batch release

Intermediate/ STEP	Quality attribute	Output found	Target
	Appearance	White powder	White to pink white powder
	HPLC identity[a]	Compliant	Standard-compliant R_t
	HPLC purity[a]	99.6%	$\geq$ 98.5%
	HPLC Assay[a]	91.2% w/w	n.a. reference value
	HPLC total impurities[a]	0.4%	<1.5%
	HPLC single largest impurity[a]	0.1%	<0.5%
	Weight	2 g	1-4 g
	Water content[b]	6.6%w/w	<10%
	Acetonitrile content[c]	105 ppm	<410 ppm
	TFA content[d]	230 ppm	5000 ppm
	Acetate content[d]	3.9%	<10%
	$[\alpha]_D^{20}$ [e]	-85.0 deg_angle	(-94.0)-(-79.0) deg_angle
	MS identification[f]	Compliant	$[M+H]^+$ 832.3[f]
	Bacterial endotoxins[g]	<1.25 EU/mg	<20 ppm
	Cd[h]	<0.25 ppm	<2 ppm
	Co[h]	<0.25 ppm	<2 ppm
	As[h]	<1 ppm	<10 ppm
	Sb[h]	<1 ppm	<20 ppm
	Ni[h]	<0.5%	<20 ppm
	Cu[h]	15 ppm	<20 ppm
	V[h]	<1 ppm	<10 ppm
	Li[h]	<0.25 ppm	<20 ppm
	Hg[h]	2 ppm	<2 ppm

(Intermediate/STEP column: Eptifibatide acetate — STEP 5)

[a]HPLC analytical methods are described in Materials and methods (Procedures A2, A3 and A5).
[b]Water content was quantified by Karl Fisher volumetric titration (USP 921, EP 2.5.12).
[c]Acetonitrile content was quantified by Headspace Gas-chromatography (HS-GC); analytical method is described in Materials and methods (Procedure A7).
[d]Ion exchange chromatography (IC); analytical method is described in Materials and methods (Procedure A8).
[e]Specific optical rotation $[\alpha]_D^{20}$ (USP 781, EP 2.2.7).
[f]Mass found detected by ESI-MS; analytical method is described in Materials and methods (Procedure A4).
[g]Bacterial endotoxins were quantified by microbiological tests (USP 85, EP 2.6.14).
[h]Heavy metals were quantified by Inductively Coupled Plasma Mass Spectroscopy (ICP-MS, ICH Q3D; USP232, 233, 730; EP 2.4.20).

Quality attributes of process intermediates and list of the equipment used to obtain cGMP compliant Eptifibatide are summarized in Table A4 and Table 14. This information is required by regulatory agencies to validate the process and qualify the pilot scale plant above described, to produce cGMP compliant Eptifibatide acetate. This is, to the best of our knowledge, the first proof-of-concept of a cGMP compliant generic peptide drug synthesized by a MW-assisted solid-phase synthesizer, at 70 mmol scale.

As mentioned above (see introduction, *Stapling approach as secondary structure stabilization)*, among the several classes of conformationally constrained peptides, the so-called stapled peptides which bear a side-chain-to-side-chain bridge are particularly interesting since they offer the possibility to stabilize specific conformational elements, such as α-helices or β-turns. Herein, we describe an efficient and reproducible microwave-assisted strategy to prepare side-chain-to-side-chain clicked peptides, performing the copper-catalysed azide-alkyne cycloaddition on solid phase, using as a model peptide the H$_1$-relaxin B single-chain (Peptide **1**, Figure I), which contains the binding cassette motif of this important bioactive peptide. Our aim is to synthesize a library of stapled, structurally simplified H$_1$-relaxin derivatives to investigate their biological properties.

From a synthetic point of view, starting from peptide **1** (Figure I), Cys^{10} and Cys^{22} were replaced with isosteric Ser residues, as previously done also by Hossain et al.[147] to avoid uncontrolled rearrangement of disulfide bridges that could lead to undesired products (Peptide **2**, Figure I).

Considering the need to insert a triazole bridge we planned the replacement of 2 natural residues with 2 not natural azide and alkyne bearing ones, with a putative 5 methylene ring size following the scheme *i, i+4* widely recognized correspond to an α-elix secondary structure stabilization motif.

A library of probable feasible replacement was hypothesized, taking into account the position involved in α-helix formation except Arg^{B12}, Arg^{B16} and Ile^{B19} engaged in receptor binding (Table I).

Table I. Library of Nle(εN₃) and Pra bearing H₁-relaxin single B-chain analogues

Substitution	Sequence
L⁹E¹³	KWKDDVIKPraSGRNle(εN₃)LVRAQIAISGMSTWS
	KWKDDVIKNle(εN₃)SGRPraLVRAQIAISGMSTWS
S¹⁰L¹⁴	KWKDDVIKLPraGRENle(εN₃)VRAQIAISGMSTWS
	KWKDDVIKLNle(εN₃)GREPraVRAQIAISGMSTWS
G¹¹V¹⁵	KWKDDVIKLSPraRELNle(εN₃)RAQIAISGMSTWS
	KWKDDVIKLSNle(εN₃)RELPraRAQIAISGMSTWS
E¹³A¹⁷	KWKDDVIKLSGRPraLVRNle(εN₃)QIAISGMSTWS
	KWKDDVIKLSGRNle(εN₃)LVRPraQIAISGMSTWS
L¹⁴Q¹⁸	**KWKDDVIKLSGREPraVRANle(εN₃)IAISGMSTWS**
	KWKDDVIKLSGRENle(εN₃)VRAPraIAISGMSTWS
A¹⁷I²¹	KWKDDVIKLSGRELVRPraQIANle(εN₃)SGMSTWS
	KWKDDVIKLSGRELVRNle(εN₃)QIAPraSGMSTWS
Q¹⁸S²²	KWKDDVIKLSGRELVRAPraIAINle(εN₃)GMSTWS
	KWKDDVIKLSGRELVRANle(εN₃)IAIPraGMSTWS

We initially fixed the use of positions 14 and 18 within the *binding cassette* which are not directly involved in receptor binding. Accordingly, our synthetic strategy continued with the replacement of Leu¹⁴ with L-Pra and Gln¹⁸ with L-Nle(εN₃) to build *i* to *i+4* side-chain-to-side-chain bridge, in order to introduce an α-helix conformation constriction inside the binding cassette (sequences in **bold**, Table I). Thus we planned sequence 14³,18⁶-(1H-1,2,3-triazole-4,1-diyl) derivative of [Ser¹⁰, Ala¹⁴, Nle¹⁸, Ser²²] H₁-relaxin B single-chain (Peptide **3**, Figure I), which has been the starting point to design the minimal-length 14³,18⁶-(1H-1,2,3-triazole-4,1-diyl) derivative of [Ser¹⁰, Ala¹⁴, Nle¹⁸] H₁-relaxin B single-chain analogue (10-21) (Peptide **4**, Figure I) containing the Relaxin Binding Cassette motif "RXXXRXXI" and two more residues on C- and

N-terminal sides that we used as a model sequence to develop the new on-resin MW-assisted CuAAC method.
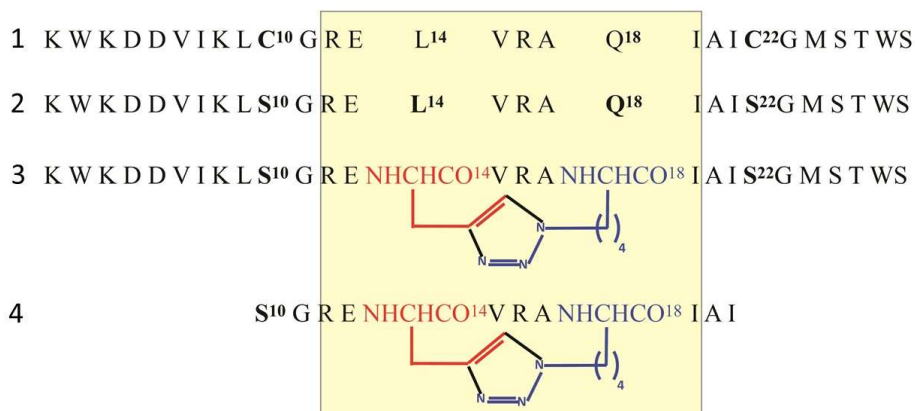
Figure I. 1: H$_1$-relaxin B single-chain analogue; **2**: [Ser^{10}, Ser^{22}] H$_1$-relaxin single B-chain analogues; **3**: 14^3,18^6-(1H-1,2,3-triazole-4,1-diyl) derivative of [Ser^{10}, Ala^{14}, Nle^{18}, Ser^{22}] H$_1$-relaxin B single-chain analogue; **4**: 14^3,18^6-(1H-1,2,3-triazole-4,1-diyl) derivative of [Ser^{10}, Ala^{14}, Nle^{18}] H$_1$-relaxin B single-chain analogue (10-21). *Relaxin binding cassett*e is underlined in yellow.

3.2.1 *Optimization of the on-resin MW-assisted copper-catalyzed azide-alkyne cycloaddition (MW-CuAAC)*

As widely known microwave irradiation in solution could radically increase the CuAAC reaction rate[148], improving the yield and reducing reaction time. However, the laborious and time-consuming in solution work-up required for the elimination of copper residues from the final product leads to the development of heterogeneous CuAAC reactions.[149] Click reaction on solid-phase represents the simplest strategy to perform an easy-cleanable CuAAC. To the best of our knowledge, literature reports CuAAC on solid-phase performed at r. t. for up to 24 h, which can be unsuitable in the presence of unstable residues and would hardly be scalable to large-scale production.[150]

Lietard *et al.* demonstrated that microwave-assisted CuAAC, both in solution and on a solid support, led to a high purity percentage in the synthesis of oligonucleotides.[151] Starting from this assumption, we aim to develop a robust synthetic strategy that enables the production of cyclic peptides by CuAAC assisted by microwave radiation on solid support, which could be particularly useful to overcome relaxins synthetic drawbacks mainly due to poor solubility and the propensity to aggregate, since to the disaggregation performances of microwave heating.

To perform the cyclisation, two different catalytic systems are herein described: Cu(I) *in situ* formation through $CuSO_4 \cdot 5H_2O$ reduction in the presence of sodium ascorbate in H_2O/alcohol[29], and the direct use of a Cu(I) salt, such as CuBr or CuI. This latter differs from the first due to the requirement of an excess of base (DIPEA, 2,6-lutidine) to deprotonate the alkyne moiety to form the Cu(I)-acetylide intermediate.[152]

3.2.1.1 Synthesis of the minimised stapled analogue $14^3,18^6$-(1H-1,2,3-triazole-4,1-diyl) derivative of [Ser^{10}, Ala^{14},Nle^{18}] H$_1$-relaxin B chain (10-21) (4)

To prevent side reactions, such as aggregation of hydrophobic fragments and intermolecular cyclization/dimerization, we selected a low loading PEG-PS-copolymer resin (Fmoc-Ile-NovaSyn TGA 0.2 mmol/g).

Working on a 0.1 mmol scale, the first three Fmoc-protected amino acids IAI were double coupled using standard MW-assisted method at 90 °C (Table RI), Fmoc-protected amino acids (5 equiv, 0.2 M in DMF) and DIC (5 equiv, 0.5 M in DMF)/OXYMA Pure (5 equiv, 1 M in DMF) coupling system.

The subsequent Fmoc-L-Nle(ϵN$_3$)-OH coupling carried out with conventional approach at r. t. using different reagents (HBTU, HATU, PyBop), bases (DIPEA and NMM) and solvents (TFE, DCM, DMF) failed, probably because of the steric hindrance of the triplet IAI. Therefore, since microwave energy is reported to have disaggregating properties (*e.g.* the ability to perturb α-helix secondary conformation affecting the large net dipole moment across the helix during peptide elongation [153]), we investigate a mild microwave-assisted coupling protocol, after an appropriate stability study of the azido moiety to MW-irradiation.

We simulated microwave-coupling cycle (deprotection and coupling) conditions, displaying a solution of Fmoc-L-Nle(ϵN$_3$)-OH (0.2 M in DMF) to four (A-C) mild microwave-assisted coupling cycles at 50 °C (Table RII, Appendix), following the Fmoc-L-Nle(ϵN$_3$)-OH percentage area at R_t 7.9 by RP-UHPLC (Figure II). We did not observe degradation of the azido group side-chain, since we did not observe R_t matching with the R_t of Fmoc-L-Lys-OH reference standard (D, Figure II).
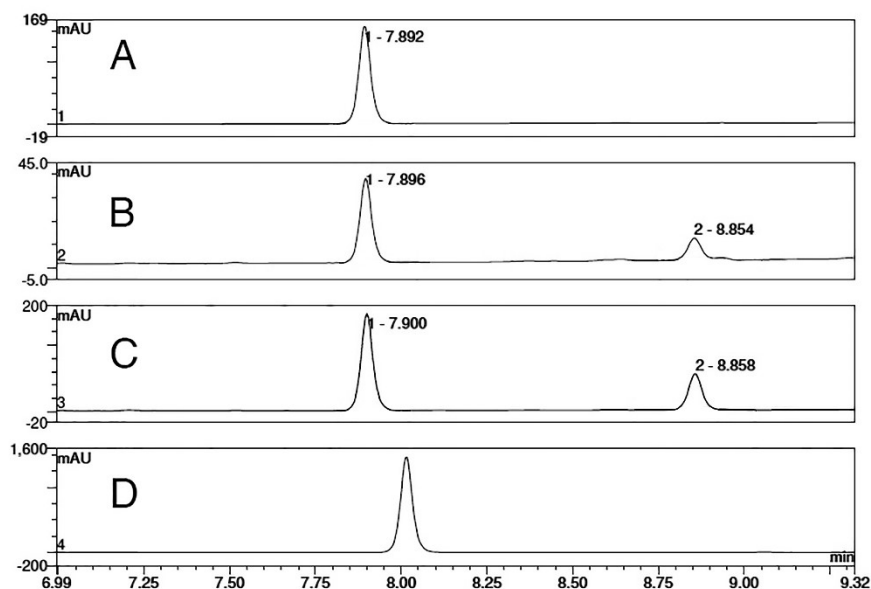
Figure II. RP-UHPLC traces for Fmoc-L-Nle(εN$_3$)-OH stability study at 50°C. C18 column Waters Acquity CSH (130Å, 1.7 μm, 2.1 × 100 mm); temperature 45°C; flow: 0.5 mL/min. Eluents: 0.1% (v/v) TFA in H$_2$O (A) and 0.1% (v/v) TFA in CH$_3$CN (B); λ 215 nm; gradient: 12-45% (v/v) B in A in 10 min. A: Fmoc-L-Nle(εN$_3$)-OH reference standard, R$_t$ 7.9 min; B: third coupling cycle (Table RII, Appendix); C: fourth coupling cycle (Table RII, Appendix); D: Fmoc-Lys-OH reference standard.

On the contrary, we observed an unknown peak at Rt 8.85 min, probably due to dibenzofulvene derived from the partial deprotection of Fmoc in DMF solution by microwave irradiation. Our hypothesis was supported by the formation of the same unknown peak at R$_t$ 8.85 min testing Fmoc-Gly-OH under the same MW-assisted coupling cycle conditions (Figure III). Thus, we checked the Fmoc-L-Nle(εN$_3$)-OH stability also to 90 °C MW-assisted standard coupling method (Table RI, Appendix), performing the synthesis of the linear precursor H-VRANle(εN$_3$)[18]IAI-OH by double coupling at 90°C for all the amino acids (MW-SPPS: general protocol), and we surprisingly demonstrated that any trace of H-VRANle(εNH$_2$)[18]IAI-OH derivative, which would have been present as [M+H]$^+$ 770,60 m/z (found) peak, was in ESI-MS spectrum (Figure III).
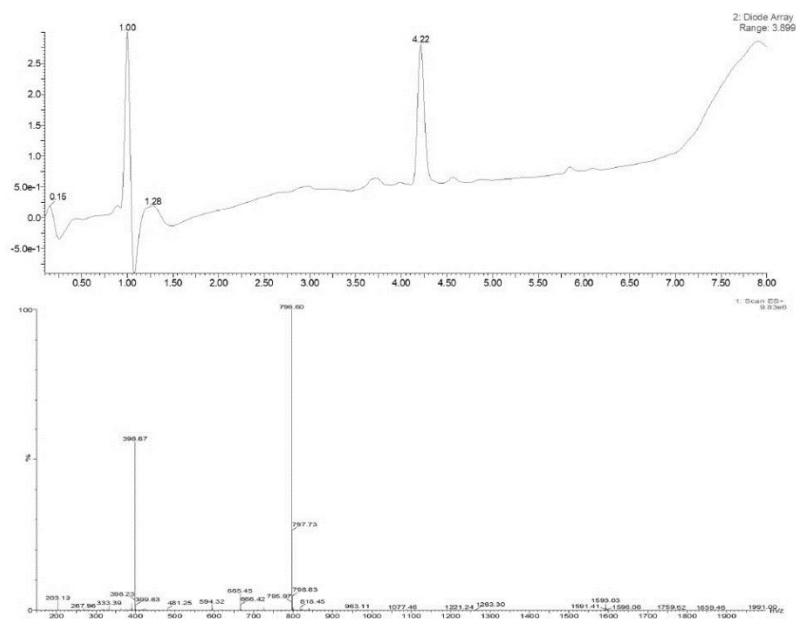
Figure III. RP-UHPLC trace of [L-Nle(εN$_3$)^{18}] H$_1$-relaxin B chain (13-21) obtained by solid-phase MW-SPPS at 90 °C. BIOshell C18 column (Å160, 2,7 μm 3,0 x 100 mm), temperature 45°C; flow: 0,6 mL/min; λ 215 nm. Eluents: 0.1% (v/v) TFA in H$_2$O (A) and 0.1% (v/v) TFA in CH$_3$CN (B); gradient: 20-60% (v/v) B in A in 5 min. R$_t$ 4.2 min: H-[L-Nle(εN$_3$)^{18}] H$_1$-relaxin B chain (13-21). ESI-MS (m/z): [M+H]$^+$ 796,60 (found), 796,84 (Calcd); [M+2H]$^{2+}$ 398,87 (found), 399,42 (calcd).

Therefore, single coupled the Fmoc-Pra-OH using the standard 90 °C MW-method (MW-SPPS: general protocol) to obtain the Fmoc-protected linear precursor [L-Pra^{14}, L-Nle(εN$_3$)^{18}] H$_1$-relaxin B chain (14-21), which has been the model sequence to subsequently optimize the MW-assisted CuAAC (Figure IV).
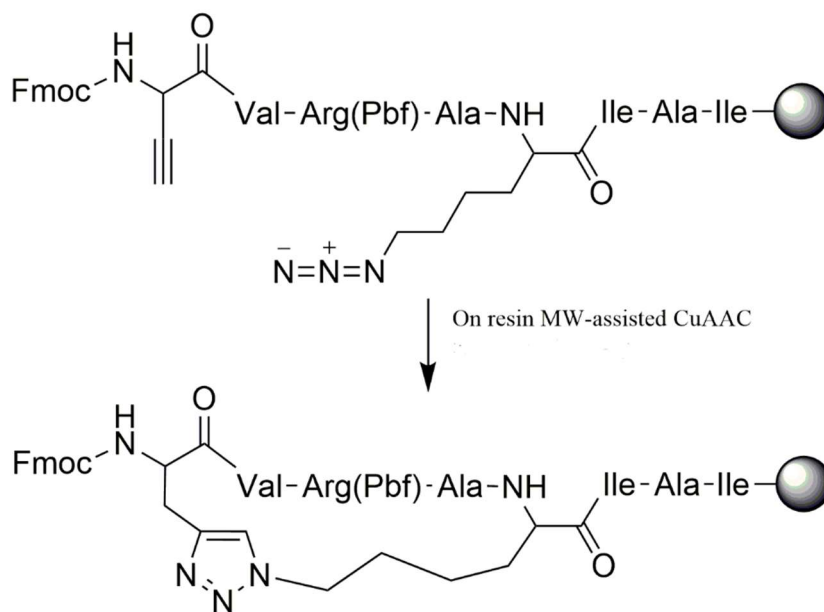
Figure IV. On-resin microwave CuAAC of the Fmoc-protected [L-Pra[14], L-Nle(εN$_3$)[18]] H$_1$-relaxin B chain (14-21).

We compared CuSO$_4$/NaAsc in H$_2$O/t-BuOH/DCM *vs* CuBr/ NaAsc in DMSO/DMF and a PEG-PS-copolymer resin *vs* a more commonly used and less expensive polystyrene resin (PS). Following a One-Factor-At-a-Time (OFAT) approach, we changed each critical factor at a time (resin, solvent, catalytic system, microwave energy and reaction time). Moreover, we modulated the microwave energy and the reaction time in order to increase the cyclization yield and concomitantly reduce the side reactions such as dimerization.

Firstly, we held constant the resin type (PEG-PS) and the catalytic system (CuSO$_4$/NaAsc) while we changed the temperature and the reaction time (Entry A-C, Table II). At 80 °C for 10 min (Table RIII, Appendix) we found the expected clicked product (37.7%) but we detected a side product, probably due to intermolecular dimerization (27.7%). Decreasing by half the microwave power(Table RIV, Appendix), we obtained 55 °C of final temperature which led to an increased clicked product (46.2%) and

decreased dimer (17.8%). Finally, reducing the reaction time to 5 min we found a high quantity of unreacted linear peptide (19.7%), while the dimer was still present (10%).

Replacing the catalytic system CuSO$_4$/NaAsc with CuBr/NaAsc, while maintaining the best temperature, reaction time and resin, we successfully obtained the clicked peptide in a good purity (64.1%, Entry D, Table II). Additionally, to assess also the role of the solid support, we fixed the best time of reaction and temperature (10 min at 55°C) and changed the resin (Entry E-F). The use of polystyrene (PS) resin confirmed that CuBr/NaAsc in DMSO/DMF (Entry F, Table II) is more efficient than CuSO$_4$/NaAsc in H$_2$O/t-BuOH/DCM with which we surprisingly did not obtain the clicked peptide Moreover, it was remarkable how using a high loading (0.7 mmol/g) PS resin we found a high quantity of unreacted linear peptide, instead of the expected increase of the dimer (Entry E, Table II, Figure V).

Table II. On-resin microwave-assisted CuAAC optimization study

Entry [a]	Solvent	Analogue	Resin [b]	Catalytic System	T.max (°C)	Time (min)	Cyclo (a/a%)	Linear (a/a%)	Dimer (a/a%)
A	A	**4** (14-21)	PEG-PS	CuSO$_4$ NaAsc	80	10	37.7	1.2	27.7
B	A	**4** (14-21)	PEG-PS	CuSO$_4$ NaAsc	55	10	46.2	2.6	17.8
C	A	**4** (14-21)	PEG-PS	CuSO$_4$ NaAsc	55	5	27.1	19.7	10.0
D	**B**	**4** (14-21)	**PEG-PS**	**CuBr NaAsc**	**55**	**10**	**64.1**	**0.9**	**5.5**
E	A	**4** (14-21)	PS	CuSO$_4$ NaAsc	55	10	-	68.3	1.0
F	B	**4** (14-21)	PS	CuBr NaAsc	55	10	19.7	21.4	6.8
G	B	**4**	PEG-PS*	CuBr NaAsc	55	10	55.8	5.8	3.7
H	**B**	**4**	**PEG-PS****	**CuBr NaAsc**	**55**	**10**	**69.1**	**-**	**6.5**

[a] *A-F: on-resin CuAAC of the Fmoc-protected fragment Pra^{14}VRA L-Nle(εN$_3$)^{18}IAI; G-H: on-resin CuAAC of the fragment S^{10}GREPra^{14}VRA L-Nle(εN$_3$)^{18}IAI.*
[b] *Resin PEG-PS: Fmoc-Ile-NovaSyn TGA 0.2 mmol/g; Resin PS Fmoc-Ile-Wang : 0.7 mmol/g; PEG-PS*: Fmoc-Ile-NovaSyn TGA 0.02 mmol/g; PEG-PS**: Fmoc-Ile-NovaSyn TGA 0.1 mmol/g.*
[c] *Solvent mixture A: H$_2$O:t-BuOH:DCM 1:1:1 v/v/v ; Solvent mixture B: DMSO:DMF 1:2 v/v.*
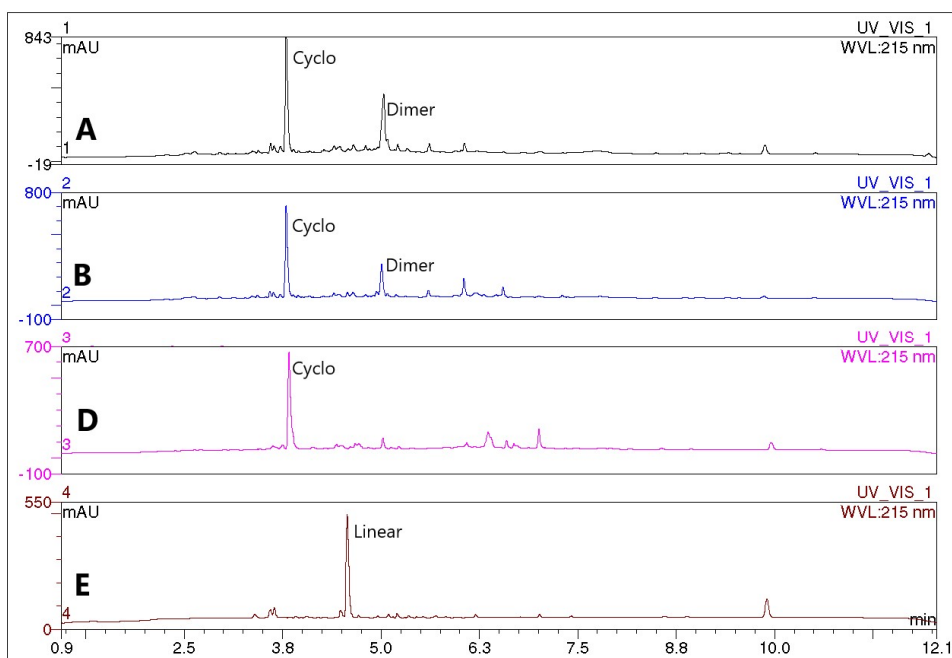
Figure V. Comparison among different MW-assisted CuAAC on Fmoc-protected [L-Pra[14], L-Nle(εN$_3$)[18]] H$_1$-relaxin B (14-21). Experiments **A, B, D** were performed with NovaSyn TGA resin 0.2 mmol/g. A: CuSO$_4$/sodium ascorbate, 80°C, 10 min; B: CuSO$_4$/sodium ascorbate, 55°C, 10 min; D: CuBr/sodium ascorbate 55°C, 10 min. Experiment **E** was performed with Wang polystyrene resin 0.7 mmol/g, CuSO$_4$/sodium ascorbate, 55°C, 10 min.

We can summarize that the dimer quantity depended both on the temperature/microwave energy and on the exposure time to microwave irradiation. Moreover, the use of the CuBr/NaAsc catalytic system increased the peak area % of the cyclic desired peptide in comparison with the use of CuSO$_4$/NaAsc one on solid support.

Therefore, thanks to the demonstrated Fmoc- L-Nle(εN$_3$)-OH stability to 90 °C MW-assisted coupling and the successfully developed on-resin MW-CuAAC, we synthesized the [L-Pra[14], L-Nle(εN$_3$)[18]] H$_1$-relaxin B (10-21) linear precursor (the so called Peptide **4** linear precursor) on Fmoc-Ile-NovaSyn TGA resin (0.19 mmol/g, 90µm beads) 0.02 mmol scale (Methods, H$_1$-relaxin) without any side reaction. Thus, we applied the on-resin MW-CuAAC conditions identified to obtain the stapled

Peptide **4**. The resin was treated with a TFA/TIS/water mixture (95:5:5, v/v/v, 1 mL mixture/100 mg of resin, (general cleavage protocol, Methods, H_1-relaxin) and Peptide **4** crude was obtained with an HPLC-purity of 55.8% in a short time (2 h total) and without isolation of intermediates (Entry G, Table II, Figure VI).
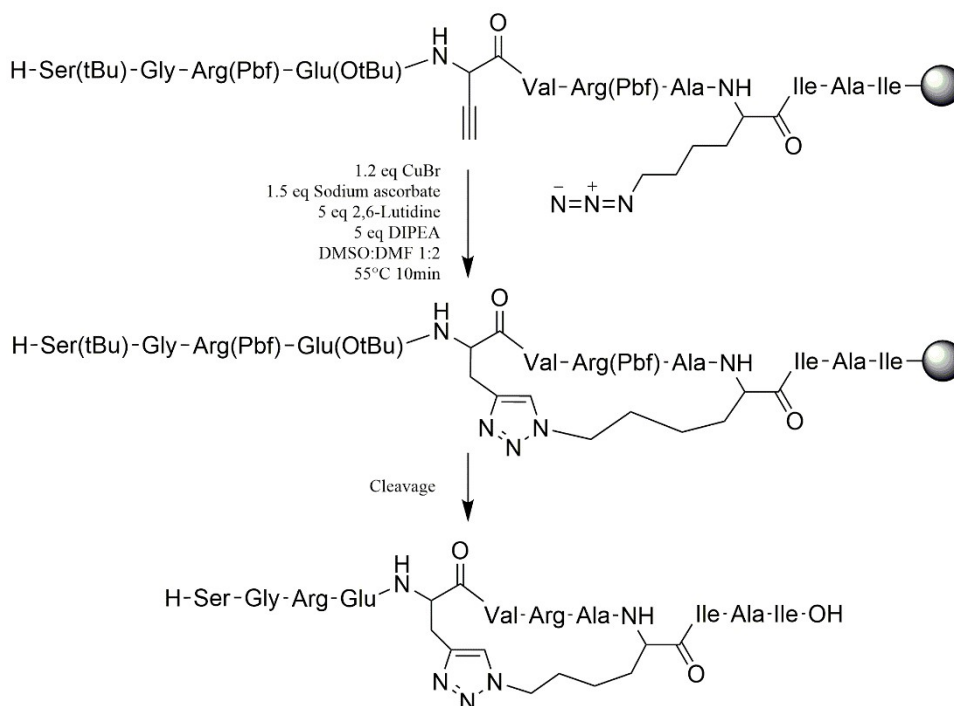
Figure VI. On-resin Microwave-assisted synthesis of $14^3,18^6$-(1H-1,2,3-triazole-4,1-diyl) derivative of [Ser^{10}, Ala^{14},Nle^{18}] H_1-relaxin B chain (10-21) (**4**).

To demonstrate the robustness and the reproducibility of the developed on-resin MW-assisted CuAAC, we repeated the Peptide **4** synthesis and cyclization on a five-fold larger scale (0.1 mmol, Entry H, Table II), with minor modifications to the microwave method because of the larger quantity of resin (Table RVI, Appendix), obtaining Peptide **4** crude 69.1% HPLC purity and 25.5% yield (Entry H, Table II, Figure VII).
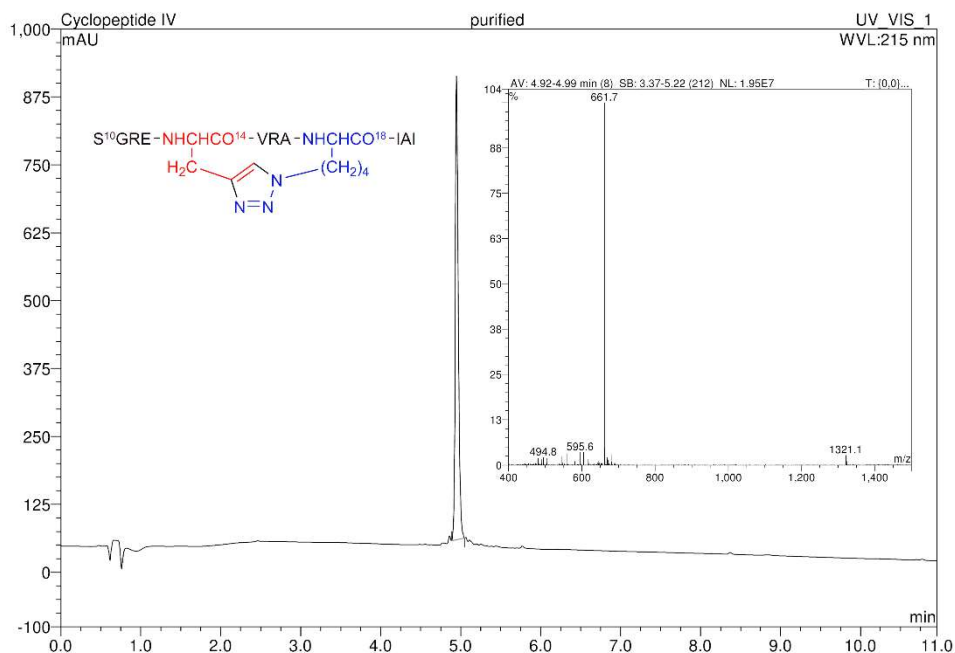
Figure VII. Analytical RP-UHPC-MS of the purified peptide $14^3,18^6$-(1H-1,2,3-triazole-4,1-diyl) derivative of [Ser^{10}, Ala^{14}, Nle^{18}] H$_1$-relaxin B chain (10-21) (**4**) (Entry G, Table II). UHPLC chromatogram of the expected peptide Rt = 4.95 min. Gradient 10–60% B in 10 min. Column Waters Acquity UHPLC CSH^{TM} C18 1.7 μm 2 X 100 mm at 0.5 mL/min. Solvent systems A (0.1% TFA in H$_2$O) and B (0.1% TFA in CH$_3$CN), λ 215. Inset: ESI-MS spectrum of the expected peptide [M+H]$^+$ 1321.1 (calcd 1321.5) [M+2H]$^{2+}$ 661.7 (calcd 661.2).

Therefore, this scale–up experiment provided a final crude purity profile comparable to the smaller scale (Entries H and G, Table II), clearly indicating the robustness of the developed strategy.

The chosen model Peptide **4** has been considered a suitable starting point for the preparation of longer H$_1$-relaxin single B-chain sequences.

3.2.2 *Selection criteria for the synthesis of H₁-relaxin single B-chain analogues library: sequence length, triazole position and orientation*

A library of linear standard references was synthesized in order to investigate the impact on biological properties of the α-helix conformational constriction mediated by triazole-bridge, comparing binding capacity and biological activity of both of the stapled peptides and their linear references. Sequence length, position and orientation of the side-chain to side-chain triazole stapling were investigated.

3.2.2.1 *Synthesis of the linear references library*

Firstly, we synthesized the so called B7-33 (Peptide **I**, Table III) as a positive control to verify RXFP1 binding ability, activation of cAMP mediated signaling.

We additionally synthesized three linear references of different lengths (Peptides **II**, **III**, and **IV)**, obtaining a total of four linear references (Table III).

Table III. H₁-relaxin single B-chain linear references

Ref.	Peptide sequence	Weight
I	VIKLSGRELVRAQIAISGMSTWSKRSL	2985.7
II*	SGRELVRAQIAI	1311.8
III	VIKLSGRELVRAQIAISG	1909.2
IV	KWKDDVIKLSGRELVRAQIAISG	2581.5

** Reference **II** corresponds to Peptide **4** in Figure VII. R, R, and I, in the Relaxing binding cassette, responsible for the interaction with RXFP1 are reported in orange. Serin isosteric residues replacing native cysteine ones are underlined in red.*

As reported above (paragraph *1.3.2*)*,* Hossein et al. identified the H₂-(A4-24)(B7-24) minimum active structure of H₂-relaxin performing truncation from both N- and C-terminal sides of the two chains A and B.[77]

Inspired by truncation performed by Hossein et al. on B-chain, we extended the length of the Peptide **4** (renamed "Reference **II**", Table III) until V^7 from the N-terminal side and G^{24} from C-terminal one (Peptide **III**, Table III).

Moreover, considering that H_1-relaxin x-ray diffraction spectrum is not still available, we relied on the structure-activity similarity between H_1- and H_2-relaxins to extend the sequence length toward the N-terminal side, to obtain a total length of 23 amino acids (Peptide **IV**, Table III) since the x-ray diffraction spectrum of human H_2-relaxin (Protein Data Bank) reveals that the secondary α-helix structure extends toward the N-terminal side.

More in detail, references **I**, **III** and **IV** were synthesized on a 0.05 mmol scale using low loading resins, respectively: Fmoc-Leu-TentaGel R PHB (loading: 0,22 mmol/g), Fmoc-Ile-TentaGel R PHB (loading 0,22 mmol/g), and Fmoc-Gly-TentaGel R PHB (loading 0,18 mmol/g). All Fmoc-protected amino acids were activated by DIC/Oxyma Pure coupling system and double coupled by the automated synthesizer Liberty Blue^{TM} (CEM, Charlotte, NC, U.S.A.). All couplings were performed at 90 °C (MW-SPPS general protocol).
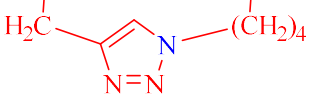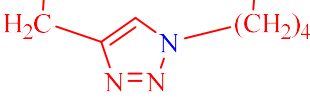
Reference **I**, **III** and **IV** crudes were cleaved and purified following the general cleavage and purification protocols (Materials and methods). After lyophilization, references were characterized by HPLC-ESI-MS (reference **I**: yield 22.1%, HPLC purity 89.6%, Figure R1; reference **III**: yield 20.2%, HPLC purity <98%, Figure R3; reference **IV**: yield 18.4 %, HPLC purity 95.5%, Figure R4, Appendix).

3.2.2.2 *Syntheses of first-generation H₁-relaxin single B-chain stapled analogues*

A first-generation H$_1$-relaxin single B-chain stapled analogues was synthesized.

Syntheses were performed on a 0,1 mmol scale using the Fmoc-Ile-TentaGel R PHB resin (loading 0,22 mmol/g) for Peptide **VR**, and the Fmoc-Gly-TentaGel R PHB resin (loading 0,18 mmol/g) for Peptide **VIR**. First-generation H$_1$-relaxin single B-chain stapled analogues were obtained starting from Reference **I** and **III** sequences and replacing amino acids in positions 14 and 18 with L-Pra and L-Nle(εN$_3$), following the scheme *i, i+4*. All Fmoc-protected amino acids were activated by DIC/Oxyma Pure coupling system and double coupled by the automated synthesizer Liberty Blue^{TM} (CEM, Charlotte, NC, U.S.A.), except for Fmoc-L-Pra and L-Nle(εN$_3$)-OH which were single coupled. All couplings were performed at 90 °C (MW-SPPS general protocol).The identified on-resin MW-CuAAC (CuBr/NaAsc in DMSO/DMF, at 55 °C for 10 min) was applied to staple linear precursors obtaining Peptides **VR** and **VIR** (Table IV). Peptides **VR** and **VIR** crudes were cleaved and purified following general protocols (Appendix). Purified stapled peptides were characterized by HPLC-ESI-MS (Peptide **VR**: yield 25.0%, HPLC purity >98.0%, Figure R5; Peptide **VIR**: yield 24.5%, HPLC purity 91.5%, Figure R6, Appendix).

Table IV. First-generation H_1-relaxin single B-chain stapled analogues

CODE	Peptide sequence	Weight
VR	H-SGRE-NHCHCO^{14} VRA·NHCHCO^{18}IAI-OH $\quad$ H$_2$C—[pyrazole/triazole ring N=N, N]—(CH$_2$)$_4$	1319.6
VIR	H-VIKLSGRE-NHCHCO^{14} VRA·NHCHCO^{18}IAISG-OH $\quad$ H$_2$C—[triazole ring N=N, N]—(CH$_2$)$_4$	1918.0

First-generation H_1-relaxin single B-chain stapled analogues were later *in vitro* tested, with the aim to investigate the biologically active minimal stapled length (2.3.3.2).
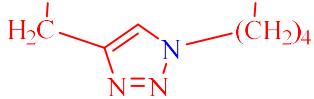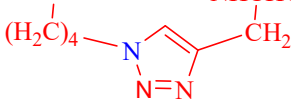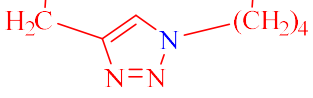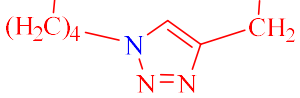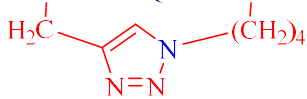
3.2.2.3 *Syntheses of second-generation H_1-relaxin single B-chain stapled analogues*

We started from Reference **IV** linear precursor characterized by 23 amino acids sequence to synthesize a library of second-generation H_1-relaxin single B-chain stapled analogues.

We investigated the effect of the triazole position and orientation along the backbone since several evidences in the literature demonstrated that an increased α-helicity and improved potency and selectivity may depend on these parameters.[96,98] In this frame, we synthesized six stapled analogues of 23 amino acids length. Therefore, we replaced the native amino acids with L-Pra-OH and L-Nle(εN$_3$)-OH, in both the two possible patterns to obtain C-term and N-term oriented triazole rings, following the scheme *i, i+4,* and we performed the on-resin MW-assisted CuAAC applying the experimental conditions identified for the stapling of Peptide **4**, obtaining: Peptides **VIIIR** and **VIII** (Stapling positions: 10, 14); Peptides **VIIR** and

Table V. Second-generation H_1-relaxin single B-chain stapled analogues

CODE	Peptide sequence	Weight
VIIR	H-KWKDDVIKLSGRE‑NHCHCO^{14} VRA·NHCHCO^{18}IAISG-OH (triazole staple: H_2C–...–N, $(CH_2)_4$, N=N)	2589.3
VII	H-KWKDDVIKLSGRE‑NHCHCO^{14} VRA NHCHCO^{18} IAISG-OH (triazole staple: $(H_2C)_4$–N, CH_2, N=N)	2589.3
VIIIR	H-KWKDDVIKL‑NHCHCO^{10} GRE‑NHCHCO^{14}VRAQIAISG-OH (triazole staple: H_2C–...–N, $(CH_2)_4$, N=N)	2630.4
VIII	H-KWKDDVIKL‑NHCHCO^{10} GRE‑NHCHCO^{14} VRAQIAISG-OH (triazole staple: $(H_2C)_4$–N, CH_2, N=N)	2630.4
IXR	H-KWKDDVIKLSGRELVR‑NHCHCO^{17}-QIA‑NHCHCO^{21}SG-OH (triazole staple: H_2C–...–N, $(CH_2)_4$, N=N)	2646.4
IX	H-KWKDDVIKLSGRELVR‑NHCHCO^{17}-QIA‑NHCHCO^{21}·SG-OH (triazole staple: $(H_2C)_4$–N, CH_2, N=N)	2646.4

Syntheses of X^3,Y^6-(1H-1,2,3-triazole-4,1-diyl) derivatives of [Ser^{10}, Ala^x, Nle(εN_3)^y, Ser^{22}] H_1-relaxin B chain, where "X" and "Y" are L-Pra and L-Nle(εN_3) positions (Table V), were carried out in a fully automated mode

by a suitable microwave-assisted peptide synthesizer (Liberty Blue (CEM, Charlotte, NC, U.S.A.)), and are based on five steps: 1) elongation of the C-terminal building block; 2) introduction of the unnatural amino acids Fmoc-L-Pra-OH and Fmoc-L-Nle(εN_3)-OH; 3) on-resin formation of the triazole ring; 4) elongation of the N-terminal building block; 5) final cleavage from the resin and contemporary deprotection (Figure VIII).
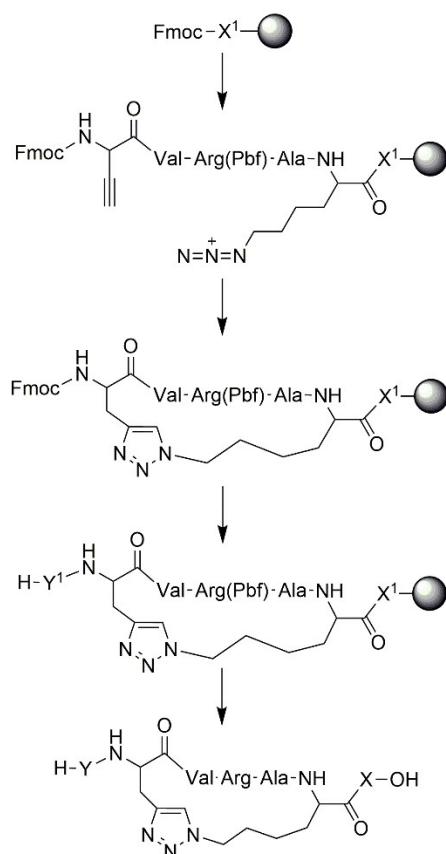
Figure VIII. On-resin MW-SPPS protocol to obtain second-generation H_1-relaxin single B-chain stapled analogues (Table V). X: C-term building block; Y: N-term building block; X^1: C-term protected building block; Y^1: N-term protected building block.

Syntheses of stapled peptides were performed on a 0,1 mmol scale using the Fmoc-Gly-TentaGel R PHB resin (loading 0,18 mmol/g).

The elongation of the C-terminal portion did not present particular criticalities. It was performed by MW-SPPS, using double coupling cycles for each Fmoc-protected amino acid (5 equivalents, 0.2 M in DMF), Oxyma pure (5 equiv, 1 M in DMF), and DIC (5 equiv, 0.5 M in DMF). Both deprotection and coupling reactions were performed at 90 °C except cysteine coupling carried out at 50 °C (MW-SPPS general protocol, Materials and methods).

The elongation of the central sequence flanked by L-Nle(εN_3) and L-Pra, was performed at 90°C (MW-SPPS general protocol, Materials and methods).

On-resin MW-CuAAC was performed by CuBr/NaAsc at 55°C for 10 min (see conditions Entry H, Table II). IPC was carried out to verify the occurred cyclization (IPC general protocol, Materials and methods). We reported HPLC-chromatograms of the Peptide **VIIIR** linear precursor and its stapled counterpart as examples, to show the R_t shift obtained after side-chain to side-chain cyclization (**VIIIR** Linear precursor: R_t: 4.32 min; Stapled peptide **VIIIR**: R_t: 3.78 min; top and middle chromatograms, Figure IX). 10% of the linear Peptide **VIIIR**, and ca. the same quantity of a by-product (hypnotized to be an interchain cyclized dimer) were detected. Thus, a second MW-assisted CuAAC was performed in the same conditions previously described and a 70% HPLC purity of the Peptide **VIIIR** crude was obtained.
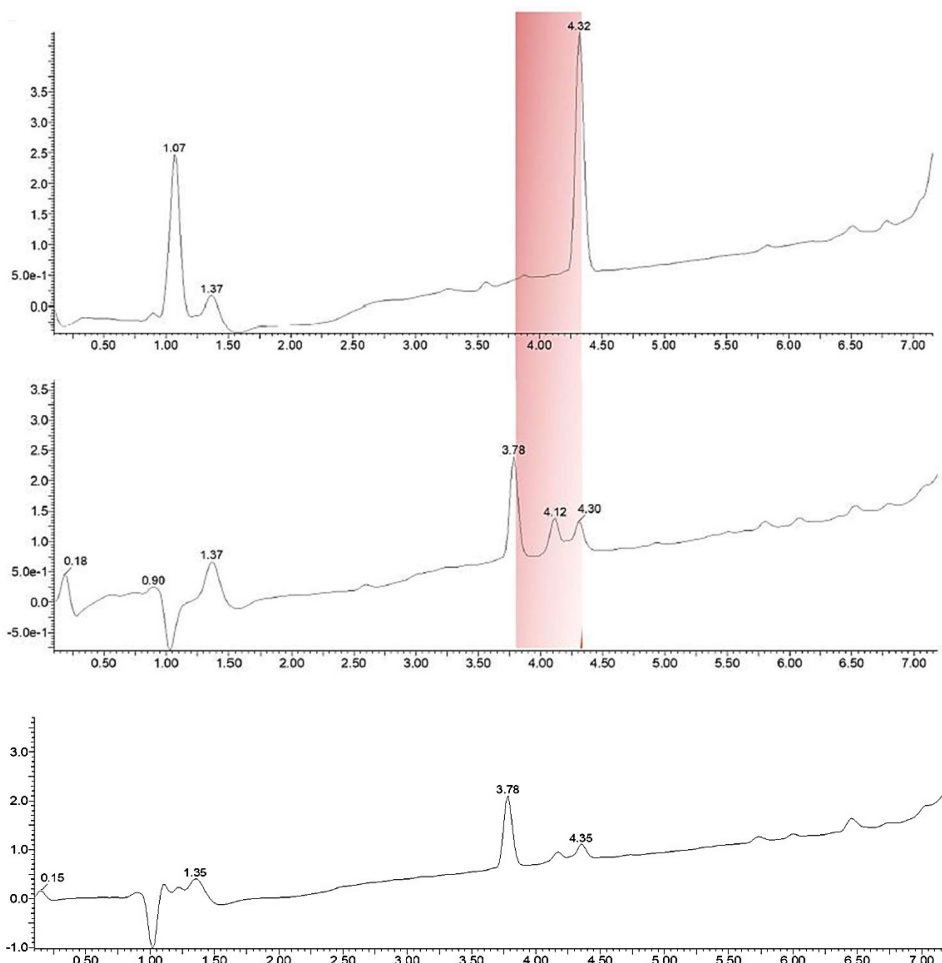
Figure IX. RP-HPLC traces of the **VIIIR** Linear precursor (Top), and the Stapled peptide **VIIIR** after the first MW-CuAAC (middle) and Stapled peptide **VIIIR** crude after the second MW-CuAAC(bottom). Red line: R_t shift. BIOshell C18 column (Å160, 2,7 μm 3,0 x 100 mm), temperature 35°C; flow: 0,6 mL/min; λ 215 nm. Eluents: 0.1% (v/v) TFA in H_2O (A) and 0.1% (v/v) TFA in CH_3CN (B); gradient: 20-55% (v/v) B in A in 5 min. R_t 4.3 min: **VIIIR** Linear precursor; R_t 3.8 min: Stapled peptide **VIIIR** (middle); R_t 3.8 min: Stapled peptide **VIIIR** crude (bottom).

The elongation of the N terminal building block was performed by a standard microwave-assisted protocol at 90 °C (MW-SPPS general protocol, Materials and methods).

Stapled peptide crudes were cleaved and purified as reported in the cleavage and purification general protocol (Materials and methods).

Purified stapled peptides were characterized by HPLC-ESI-MS (Peptide **VIIR**: yield 22.1%, HPLC purity 91.5%, Figure R7; Peptide **VII**: yield 22.4%, HPLC purity 91.0%, Figure R8; Peptide **VIIIR**: yield 21.3%, HPLC purity 90.0%, Figure R9; Peptide **VIII**: yield 19.9%, HPLC purity 93.0%, Figure R10; Peptide **IXR**: yield 17.5%, HPLC purity 93.0%, Figure R11; Peptide **IX**: yield 15.0%, HPLC purity 91.0%, Figure R12, Appendix).

We can conclude that the on-resin formation of the triazole ring *via* MW-CuAAC resulted in a fast and easy-manage approach to synthesize H_1-relaxin single B-chain stapled analogue, otherwise difficult to obtain due to the aggregation propensity and the low solubility.

Several advantages compared to the solution approach can be underlined: i) pseudo-dilution effect of the solid support; ii) the possibility to easily wash-out the copper catalyst by filtration; iii) reduction of synthetic steps number; iv) no isolation of the azido-intermediate linear peptide. Moreover, the use of microwaves decreases the aggregation tendency favouring the activated amino acid coupling, leading to the high percentage of crude purity.

3.2.3 *Circular dichroism of second-generation H₁-relaxin single B-chain stapled analogues and of the linear reference IV*

Evaluation of the secondary structure α-helicity of second-generation H_1-relaxin single B-chain stapled analogues induced by the side-chain to side-chain triazole stapling was explored by circular dichroism (CD) spectroscopy performed both in phosphate buffer (Figure X) and SDS micelles (FigureXI), within the collaboration with Prof. A. Carotenuto from the University of Naples, Federico II.

In agreement with our synthetic forecast, CD spectra of second-generation H_1-relaxin single B-chain stapled analogues showed a tendency to assume α-helical secondary conformation in contrast with their linear reference Peptide IV (green), in phosphate solution. Interestingly the 3 peptides of R series characterized by a C-term oriented triazole stapling (Peptide **VIIR**: blue; Peptide **VIIIR**: pale green and Peptide **IXR**: light blue) are slightly more helical than their N-term oriented triazole counterparts (Peptide **VII**: brown; Peptide **VIII**: pale blue and Peptide **IX**: light blue), with a minimum to 222 more intense.
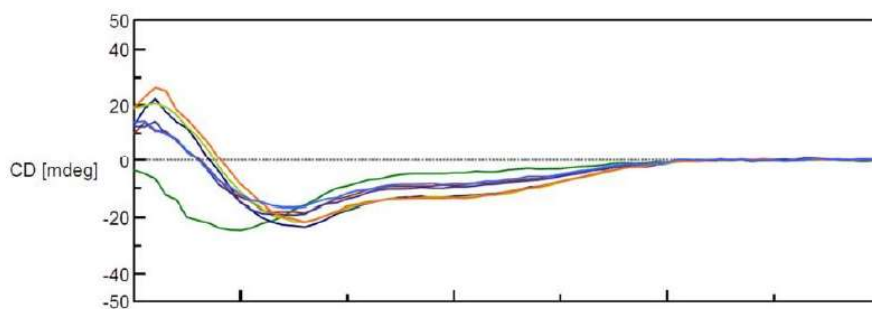
Figure X. CD spectra of the second-generation H_1-relaxin single B-chain stapled analogues and the linear reference IV in phosphate buffer. Reference IV: green; Peptide VIIR: blue; Peptide VII: brown; Peptide VIIIR: pale green; Peptide VIII: pale blue; Peptide IXR: orange; Peptide IX: light blue.

Moreover, since K^9, R^{13}, and R^{17} positively charged should be exposed on the same side of the α-helix leading to an amphipathic-like secondary

structure, and additionally, our stapled analogues should interact with a transmembrane GPCRs, CD spectroscopy in SDS micelles was performed, exploiting their transmembrane-mimetic features.[154]

Surprisingly, all peptides showed a pronounced helicity in SDS micelles, including the linear reference **IV** (green) although slightly less than the stapled ones. Among the stapled peptides, the Peptide **VIII** (pale blue) and the Peptide **VIIIR** (pale green) showed the highest degree of helicity (Figure XI).
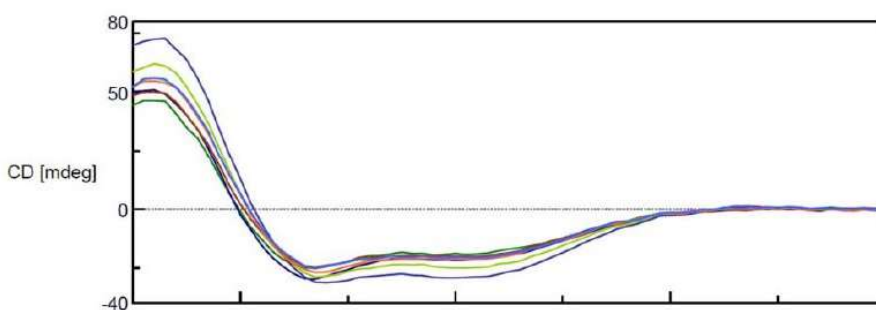
Figure XI. CD spectra of the second-generation H_1-relaxin single B-chain stapled analogues and the linear reference IV in SDS micelles. Reference IV: green; Peptide VIIR: blue; Peptide VII: brown; Peptide VIIIR: pale green; Peptide VIII: pale blue; Peptide IXR: orange; Peptide IX: light blue.

2.3.4 *In vitro evaluation of cAMP production in THP-1 cells treated with linear references, first- and second-generation H₁-relaxin B single-chain stapled analogues*

The activation of the RXFP1 receptor is complex. It requires the presence of the key feature "RXXXRXXI" relaxin binding cassette, involved in the interaction with the leucine-rich repeats ectodomain (LRR). However, this interaction alone is not sufficient to explain all of the activation events involved. In light of H_2-relaxin promising results showed in clinical trials for Acute Heart Failure (AHF) and the increased selectivity demonstrated for RXFP1 of H_2-relaxin truncated analogues on the C-terminus[155], Prof. A. Hossain and Prof. Ross Bathgate from the Florey Institute of Neuroscience and Mental Health (Australia), supported us testing the competition binding capacity of H_2-relaxin and B7-33 analogue (as positive references), H_1-relaxin B single-chain linear references and stapled analogues (both first- and second-generation) in HEK-293T cells, stably expressing the RXFP1 receptor, using Eu^{3+}-labelled H_2-relaxin as the competitive ligand (Figure XII). In particular, figure XII confirmed an equivalent ligand displacement capacity (% specific binding) of the minimal relaxin sequence B7-33 compared to the native ligand H_2-relaxin, although showing an active concentration one order of magnitude greater for the former, as previously reported by Hossein et al.[155] Our Peptide **I**, structurally identical to B7-33 resulted in ca. 25% less active than its twin (B7-33), probably due to the slightly decrease peptide content. Unfortunately, all the analogues synthesized, both the linear and the stapled once, did not show a significant displacement of the Eu^{3+}-labelled H_2-relaxin ligand. Among these, only Peptide **IX** seems to show a weak capacity (ca. 25%) to bind the RFPX1 receptor (Figure IX, bottom).
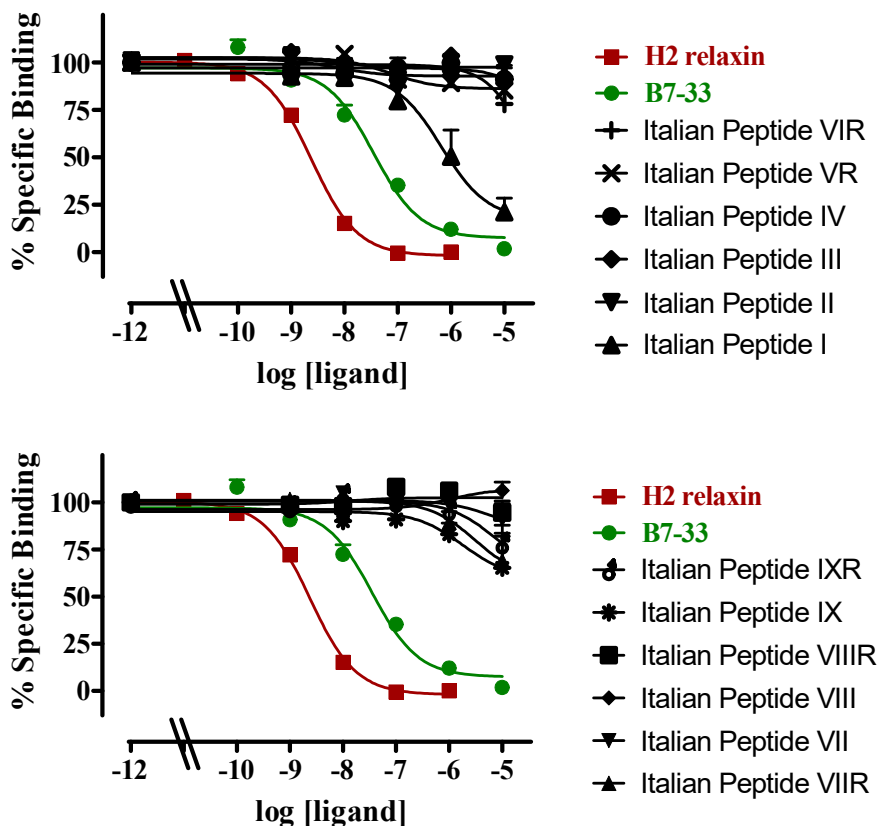
Figure XII. Competition binding results of H_2-relaxin, B7-33 analogue, H_1-relaxin B single-chain linear references and stapled analogues (first- and second-generation) in HEK-293T cells stably expressing the RXFP1 receptor using Eu^{3+}-labelled H_2-relaxin as the competitive ligand. Data are expressed as a percentage of specific binding.

All peptides previously tested for binding capacity have also been investigated for their biological properties. Specifically, linear references and stapled analogues were tested using a cAMP reporter gene assay, based on the activation of the cAMP signaling in HEK-293T cells co-transfected with RXFP1 and a pCRE-β-galactosidase reporter plasmid. Ligand-induced cAMP stimulation was expressed as a percentage of the maximum H_2-relaxin response for the RXFP1 receptor.[155]

As shown in figure XIII, the absence of binding reflects the deficiency of cAMP production for all the tested stapled analogues and the linear references, except for the Peptide I, in accordance with binding results.
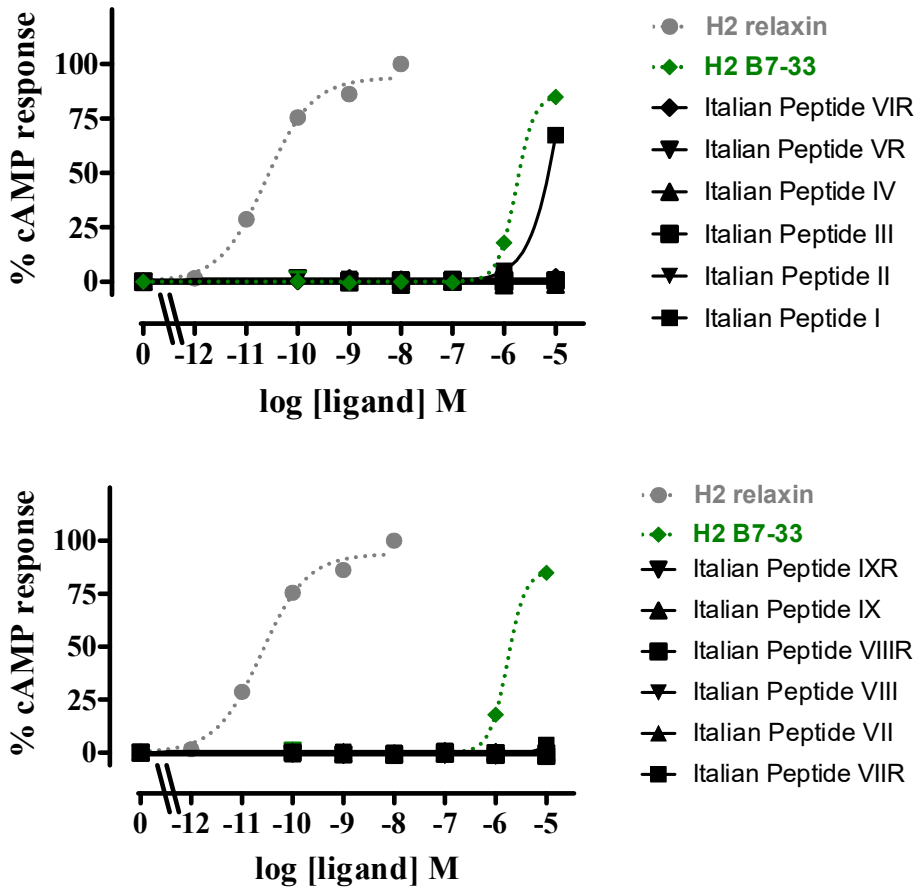
Figure XIII. cAMP activity of H_2-relaxin, B7-33 analogue, linear references and H_1-relaxin B single-chain stapled analogues (first- and second-generation) in HEK-293T cells expressing the RXFP1 receptor using a pCRE-galactosidase reporter gene system. Data are expressed as a percentage of maximum H_2-relaxin stimulated cAMP response and are pooled data from at least three experiments performed in triplicate.

2.3.5 *In vitro simulated intestinal digestion of serelaxin and porcine relaxin (pRLX)*

Despite favourable premises collected from many preclinical and clinical studies demonstrating serelaxin cardiovascular and anti-fibrotic effects, some key limitations of the treatment protocol have been identified as possible reasons for such failure: the most relevant is that serelaxin has a short half-life, about 2 h, and its in vivo effects are rapidly lost.[156]

Hence, to achieve steady therapeutic plasma levels, serelaxin has to be administered parenterally in repeated daily doses, with obvious drawbacks in terms of patients' compliance. This drawback highlights the need to explore alternative modes and routes of administration for serelaxin, enabling this peptide drug to achieve therapeutic levels. The development of pharmaceutical formulations of serelaxin suitable for oral delivery led us to investigate an *in silico* model to simulate the possible behaviour of gastroprotected formulations subjected to gut enzymatic digestion. The relative bio-potency of the intact molecule in comparison with its proteolytic fragments was assessed by measuring the signalling events downstream receptor activation in THP-1 human monocytic cells, in the framework of the collaboration with Prof. D. Bani of the University of Florence, Dept. Experimental & Clinical Medicine. Digestions were performed in our lab while digested mixtures were tested by Prof. Bani and co-workers. The current study was specifically designed to investigate this possibility on two similar RLX molecules suitable as protein therapeutics, serelaxin and purified porcine relaxin (pRLX), which both showed the ability to induce a marked, significant rise of cAMP in RXFP-1-expressing THP-1 cells at 100 ng/ml in their intact protein form.[157,158]

In detail, serelaxin and pRLX diluted solution (1.12 μM) were subjected to simulated gut digestion after the addition of Simulated Intestinal Fluid (SIF) at 37 °C. solution. Digestions were stopped adjusting pH from 6.8 to

4.0 by addition of HCl 0.1 M. Six digestion times were assayed (0, 10, 20, 30, 60 and 120 sec). Samples were centrifuged at 10000 rpm for 10', and the supernatant fluid was withdrawn and *in vitro* tested on THP-1 cells (Materials and Methods).

A 15-min stimulation of THP-1 cells with intact serelaxin (100 ng/ml) or pRLX (100 ng/ml) caused a statistically significant increase in intracellular cAMP as compared with the controls, which attained, respectively, 88.6% and 68.4% of the maximal cAMP rise induced by the adenylate cyclase activator forskolin (10^{-4} M). This higher efficacy of serelaxin in comparison with pRLX is in keeping with its higher affinity for the RXFP-1 receptor demonstrated in similar cellular models.[159] On the other hand, the digestion products of serelaxin showed a progressive decrease in cAMP generation which correlated with the time of exposure to SIF: this effect was already appreciable at 10, 20 and 30 s. and became prominent and statistically significant at 60 and 120 s: at this latter time point, the cAMP levels were similar to those detected in the unstimulated control cells. Conversely, the digestion products of pRLX did retain the capability to stimulate cAMP generation by THP-1 cells at levels comparable to those achieved by the intact peptide, at any SIF exposure times tested (Figure XIV).

cAMP production by THP-1 cells

a - p<0.001 vs. control
b - p<0.001 vs. control
c - p<0.001 vs. H2 RLX
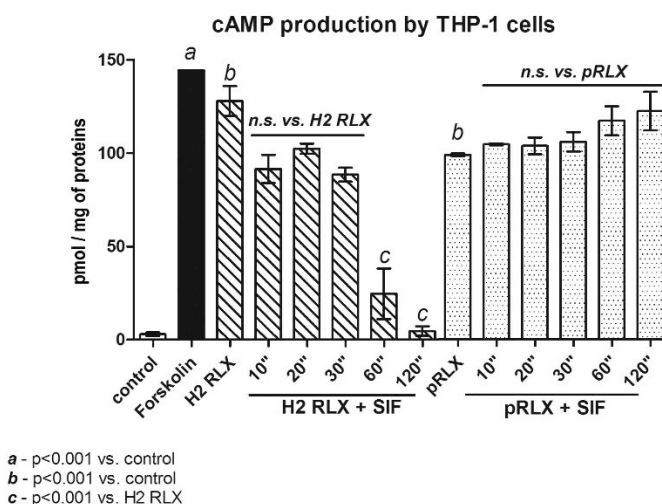
Figure XIV. cAMP production by THP-1 cells treated with pRLX and serelaxin digestive products.

4. MATERIALS AND METHODS

4.1 EPTIFIBATIDE ACETATE

Materials

Peptide grade *N,N*-dimethylformamide (DMF), all Fmoc protected amino acids (Fmoc-Gly-OH, Fmoc-Har(Pbf)-OH, Fmoc-Asp(OtBu)-OH, Fmoc-Cys(Trt)-OH, Fmoc-Cys(Mmt)-OH, Fmoc-Cys(StBu)-OH, Fmoc-Trp(Boc)-OH, Fmoc-Pro-OH), and the building blocks 3-mercaptopropionic acid (MPA) and 3,3′-dithiodipropionic acid (DTDPA) were purchased from Sigma Aldrich (Milan, Italy). Rink Amide AM resin was purchased from Sunresin New Materials Co. Ltd., Xi' AN (Shaanxi, China). 3-(2-Pyridinyldithio)propanoic acid MPA(PyS) was purchased from Carbosynth (Compton, UK).

Activators *N,N′*-diisopropylcarbodiimide (DIC) and Oxima pure and (benzotriazol-1-yloxy)tripyrrolidinophosphonium hexafluorophosphate (PyBOP) were purchased from Sigma Aldrich (Milan, Italy). N-Chlorosuccinimide (NCS), Trifluoroacetic acid (TFA), triisopropyl silane (TIS), and 2,2′-(ethylenedioxy)diethanethiol (DODT), *N,N*-diisopropylethylamine (DIPEA), diisopropyl ether (iPr$_2$O), diethylether (Et$_2$O), 2-Methoxy-2-methylpropane (MTBE), Methoxycyclopentane (CPME), 2-propanol, dichloromethane (DCM), Acetic acid (99-100%) and HPLC-grade H$_2$O were purchased from Sigma Aldrich (Milan, Italy). HPLC-grade acetonitrile (CH$_3$CN) was purchased from Carlo Erba (Milan, Italy).

Methods

Preparation of Eptifibatide linear precursor by Fmoc/tBu MW-SPPS (liquid-phase strategy)

The fully protected Eptifibatide linear precursor MPA(Trt)-Har(Pbf)-Gly-Asp(OtBu)-Trp(Boc)-Pro-Cys(Trt)-Rink Amide AM resin was obtained

starting from Rink Amide AM resin (loading 0.93 mmol/g, 5.4 g, 5 mmol). Sequence elongation was performed on a microwave-assisted solid-phase peptide synthesizer (Liberty Blue, CEM, Matthews, NC, U.S.A.) following the Fmoc/tBu strategy. Reaction temperatures were monitored by an internal fiber-optic sensor. Both deprotection and coupling reactions were performed in a Teflon vessel applying microwave energy under nitrogen bubbling. After the first Fmoc-deprotection, the following orthogonally protected amino acids were added from C- to N-terminal: Fmoc-Cys(Trt)-OH, Fmoc-Pro-OH, Fmoc-Trp(Boc)-OH, Fmoc-Asp(OtBu)-OH, Fmoc-Gly-OH, Fmoc-Har(Pbf)-OH and, MPA(Trt)-OH, in the presence of the coupling reagents DIC and Oxyma Pure. The Fmoc/tBu MW-SPPS cycle consisted in: 1) swelling in DMF (50 mL) for 30 min; 2) Fmoc-deprotection by 30% (v/v) piperidine/DMF (40 equiv, 66 mL); 3) washings with DMF (3 × 50 mL); 4) coupling of Fmoc-protected amino acids (2.5 equivalents, 0.4 M in DMF), Oxyma pure (2.5 equiv, 1 M in DMF), and DIC (2.5 equiv, 3 M in DMF); 5), washings with DMF (3 × 50 mL). Peptide elongation was performed by repeating the MW-SPS cycle for each amino acid. Both deprotection and coupling reactions were performed reaching 90 °C except 55 °C for cysteine coupling (Table A2). After all amino acids were coupled, the resin was filtered, washed with DMF (3 × 50 mL) and 2-propanol (3 × 50 mL), and dried under vacuum to obtain 15.2 g of MPA(Trt)-Har(Pbf)-Gly-Asp(OtBu)-Trp(Boc)-Pro-Cys(Trt)-Rink Amide AM resin.

Preparation of the peptide-resin precursor Har(Pbf)-Gly-Asp(OtBu)-Trp(Boc)-Pro-Cys(Mmt)-Rink Amide AM resin by Fmoc/tBu MW-SPPS (Strategies A, B, and C)

Preparation of the peptide-resin precursor Har(Pbf)-Gly-Asp(OtBu)-Trp(Boc)-Pro-Cys(Mmt)-Rink Amide AM resin by Fmoc/tBu MW-SPPS was performed in the above described synthetic conditions (coupling

system, amino acids equiv, MW-methods, equipment) on 5 mmol scale as reported in Table A2. After all amino acids were coupled, the resin was filtered, washed with DMF (3 × 50 mL) and with 2-propanol (3 × 50 mL), and dried under vacuum to obtain 12.3 g of peptide-resin. The linear Eptifibatide precursor on the resin was divided into three aliquots for subsequent solid-phase disulfide bond formation using strategies **A**, **B**, and **C**.

Preparation of the peptide-resin precursor Har(Pbf)-Gly-Asp(OtBu)-Trp(Boc)-Pro-Cys(StBu)-Rink Amide AM by Fmoc/tBu MW-SPPS (Strategy D)

The fully protected linear precursor Har(Pbf)-Gly-Asp(OtBu)-Trp(Boc)-Pro-Cys(StBu)-Rink Amide AM resin was obtained starting from the Rink Amide AM resin (loading 0.93 mmol/g, 1.1 g, 1 mmol). Sequence elongation was performed on the same equipment described above (Liberty Blue synthesizer, CEM, Matthews, NC, U.S.A.) following the Fmoc/tBu strategy. After the first Fmoc-deprotection, the following amino acids orthogonally protected, were added automatically from C- to N-terminal: Fmoc-Cys(StBu)-OH, Fmoc-Pro-OH, Fmoc-Trp(Boc)-OH, Fmoc-Asp(OtBu)-OH, Fmoc-Gly-OH, Fmoc-Har(Pbf)-OH, in the presence of the coupling reagents DIC and Oxyma Pure. The Fmoc/tBu MW-SPPS cycle consisted of: 1) swelling in DMF (15 mL) for 30 min; 2) Fmoc-deprotection by 30% (v/v) piperidine/DMF (20 mL, 60 equiv); 3) washings with DMF (3 × 15 mL); 4) coupling with the Fmoc-protected amino acids (5 equiv, 0.4 M in DMF), Oxyma Pure (5 equiv, 1 M in DMF), and DIC (5 equiv, 3 M in DMF); 5), washings with DMF (3 × 15 mL). Peptide elongation was performed by repeating the MW cycle for each amino acid coupling and deprotections as reported in Table A1. After all amino acids were coupled, the resin was filtered, washed with DMF (3

× 15 mL) and with 2-propanol (3 × 15 mL), and dried under vacuum to obtain 2.5 g of peptide-resin Har(Pbf)-Gly-Asp(OtBu)-Trp(Boc)-Pro-Cys(StBu)-Rink Amide AM. Disulfide bond formation was performed as described in strategy **D**.

Cleavage from the resin

The cleavage, with concomitant deprotection of acid-sensitive amino-acid side-chains was performed by treating MPA(Trt)-Har(Pbf)-Gly-Asp(OtBu)-Trp(Boc)-Pro-Cys(Trt)-Rink Amide AM resin (15.2 g, 5 mmol) with the cocktail TFA/TIS/ H_2O/ DODT (107 mL, 72:7:7:14, v/v/v/v) for 30 minutes at room temperature under mechanical stirring (150 rpm). Then the mixture was diluted with TFA (230 mL) and stirred mechanically for 2.5h. The resin was filtered and rinsed with fresh TFA (3 × 30 mL). The cleavage reaction mixture was transferred into a clean round bottom flask and the peptide was precipitated by addition the of ice-cold iPr$_2$O (1216 mL) in 30 minutes, keeping the temperature below 35°C. The suspension was stirred for 1h at 0°C. The solid crude was filtered, washed with ice-cold iPr$_2$O (4 × 150 mL), and dried under vacuum. Characterization of the filtered Eptifibatide TFA linear precursor crude was performed by analytical RP-HPLC-ESI-MS (Procedures A1, A2, A4). The Eptifibatide TFA linear precursor crude (5.137 g, 5 mmol) showed 74.1% RP-UHPLC purity (yield 84.6 %), R$_t$ 4.3 min, ESI-MS (m/z): [M+H]$^+$ 834.4 (found), 834.9 (calcd) (Figures A6 and A8).

Optimized procedure for liquid-phase disulfide bond formation

Eptifibatide TFA linear precursor crude (2.5 g, 2.44 mmol, UHPLC purity 74.1%) was introduced in a 2L round bottom flask, dissolved in H_2O/CH$_3$CN (1:1 (v/v), 750 mL) solution, and maintained under stirring. After 15 min, H_2O (500 mL) was added to the reaction mixture to obtain a

final concentration of 5.3 mM. The initial pH 2.5, was adjusted to 9.5, adding NH$_4$OH 7.5 % (v/v) (5.0 mL). The first aliquot of H$_2$O$_2$ (0.05 mL, 0.22 equiv) was added and the reaction mixture was stirred for 30 min at r.t. Then, HPLC In Process Control (IPC) was performed to monitor the disulfide bond formation (Procedure A6). This addition was repeated every 30 minutes until complete oxidation. A total of four addition in 2h was necessary to complete the disulfide bond formation. The reaction was quenched adding TFA 99.9% (v/v) (5 mL), adjusting pH to 2.5. Then the reaction mixture was lyophilized without further evaporation.

The recovered crude was characterized by analytical RP-UHPLC-ESI-MS (Procedures A2, A3, and A4). Crude Eptifibatide TFA salt (5.2 g, yield 90.7%) showed 67.4% UHPLC purity, R_t 4.1 min; ESI-MS (m/z): [M+H]$^+$ 832.5 (found); 831.96 (calcd) (Figure A11, Appendix).

Monitoring of the liquid-phase oxidation process

An aliquot of the reaction mixture (200 µL) in a test tube was added with TFA (100 µL) and water (200 µL). The solution was analyzed by RP-UHPLC-ESI-MS using the gradient 12-45% B in A. Eluents: 0.1% TFA in H$_2$O (A) and 0.1% TFA in CH$_3$CN (see IPC section above described for instrumentation details). IPC sample was analyzed by RP-UHPLC-MS on a Thermo Scientific Ultimate 3000 equipped with a variable wavelength detector and a Thermo Scientific-MSQ PLUS, using a C18 Waters Acquity CSH^{TM} (130Å, 1.7 µm, 2.1 × 100 mm); temperature 45°C; flow: 0.5 mL/min; eluents: 0.1% (v/v) TFA in H$_2$O (A) and 0.1% (v/v) TFA in CH$_3$CN (B), λ 215 nm.

Strategy A for solid-phase disulfide bond formation in Eptifibatide

MPA(PyS) (216 mg, 10 equiv) was coupled to the solid-phase protected linear peptide precursor Har(Pbf)-Gly-Asp(OtBu)-Trp(Boc)-Pro-

Cys(Mmt)-Rink Amide AM resin (230 mg, 0.1 mmol, 0.43 mmol/g) by a microwave-assisted protocol (75°C, 35W, 5 min) using DIC (0.154 mL, 10 equiv) and Oxyma Pure (142 mg, 10 equiv) as coupling reagents in DMF (5 mL). Then, the peptide-resin was filtered and washed with DMF (3 × 2 mL) and DCM (3 × 2 mL). 4-Methoxytriphenylmethyl (Mmt) cysteine deprotection and contemporary formation of the disulfide bridge via disulfide-exchange reaction with the head terminal MPA(PyS), was obtained by treating the resin with a mixture of TFA/DCM/TIS (10 mL, 3:92:5) for 25 min at r.t. Following the cleavage procedure described in the Supplementary Information, we performed the final cleavage with the cocktail TFA/H$_2$O/TIS (10 mL, 95:2.5:2.5).

Crude Eptifibatide (50 mg, 60% yield) was obtained with a 34.9% HPLC purity (Figure 14).

Strategy B for solid-phase disulfide bond formation in Eptifibatide

3,3′-Dithiodipropionic acid (DTDPA) (2.63 g, 5 equiv) was coupled to the peptide-resin Har(Pbf)-Gly-Asp(OtBu)-Trp(Boc)-Pro-Cys(Mmt)-Rink Amide AM resin (2.5 mmol, 7.3 g, 0.34 mmol/g) by a microwave-assisted protocol at 75°C (35 W, 5 min) using DIC (1.93 mL, 5 equiv) and Oxima Pure (1.77 g, 5 equiv) in DMF (40 mL). The coupling reaction was IPC monitored. The peptide-resin was filtered and washed with DMF (3 × 20 mL) and DCM (3 × 20 mL). DTDPA-Har(Pbf)-Gly-Asp(OtBu)-Trp(Boc)-Pro-Cys(Mmt)-Rink Amide AM resin was treated with dithiothreitol (DTT, 3 g, 19 mmol) and 0.1 M 4-methylmorpholine (NMM) in DMF (60 mL) to reduce the S-S bond in DTDPA forming MPA. After 12h IPC monitoring showed ca. 93% conversion (data not shown), the resin was washed with DMF (3 × 60 mL), Mmt deprotection was performed in a cocktail of TFA/TIS/DCM (8 × 20 mL, 2:5:93) until the yellow colour disappeared and the deprotection solution turned colourless. disulfide

bond formation was performed treating the supported protected linear peptide MPA-Har(Pbf)-Gly-Asp(OtBu)-Trp(Boc)-Pro-Cys-Rink Amide AM resin (2.1 g, 0.75 mmol) with a solution of N-chlorosuccinimide (120 mg, 1.2 equiv) in DMF (24 mL) for 10 min at r.t. After washing the resin with DCM (3 × 25 mL), the cleavage was performed following the procedure described in above (Cleavage from the resin) using a mixture of TFA/H$_2$O/TIS (40 mL, 95:2.5:2.5).

Crude Eptifibatide (590 mg, 82% yield) was obtained with a 42.4 % HPLC purity (Figure 15).

Strategy C for solid-phase disulfide bond formation in Eptifibatide

The peptide-resin Har(Pbf)-Gly-Asp(OtBu)-Trp(Boc)-Pro-Cys(Mmt)-Rink Amide AM resin (200 mg, 0.087 mmol) was treated with a cocktail of TFA/DCM/TIS (10 mL, 3:92:5) for 25 min at r.t. to deprotect the cysteine residue. Solid-phase disulfide-exchange between the activated MPA(PyS) (187 mg, 10 equiv) in DMF (5 mL) and DIPEA (45 µL, 3 equiv) and the free Cysteine thiol function on the peptide-resin was performed in the Microwave module of the Liberty Blue to form the disulfide bond (50 °C, 90W, 30 min). The resin was filtered, washed with DMF (3 × 3 mL) and DCM (3 × 3 mL) and dried under vacuum. The IPC showed 82 % of desired disulfide linear Eptifibatide derivative Har-Gly-Asp-Trp-Pro-Cys(MPA)-NH$_2$ (Figure A13, Appendix). The head to MPA on Cysteine side-chain cyclization (required to obtain Eptifibatide), was achieved by PyBop (226 mg, 5 equiv) and DIPEA (105µL, 7 equiv) in DMF (3 mL) at r.t. in 16h. The final cleavage from the resin was performed following the procedure described in the Supplementary Information using a cocktail of TFA/H$_2$O/TIS (5 mL, 95:2.5:2.5).

Crude Eptifibatide (50 mg, 61% yield) was obtained with a 56.5% HPLC purity (Figure 16).

Preparation of the peptide-resin precursor Har(Pbf)-Gly-Asp(OtBu)-Trp(Boc)-Pro-Cys(StBu)-Rink Amide AM by Fmoc/tBu MW-SPPS (Strategy D)

The fully protected linear precursor Har(Pbf)-Gly-Asp(OtBu)-Trp(Boc)-Pro-Cys(StBu)-Rink Amide AM resin was obtained starting from the Rink Amide AM resin (loading 0.93 mmol/g, 1.1 g, 1 mmol). Sequence elongation was performed on a microwave-assisted solid-phase peptide synthesizer Liberty Blue (CEM, Matthews, NC, U.S.A.) following the Fmoc/tBu strategy. Reaction temperatures were monitored by an internal fiber-optic sensor. Both deprotection and coupling reactions were performed in a Teflon vessel applying microwave energy under nitrogen bubbling. After the first Fmoc-deprotection, the following amino acids orthogonally protected, were added automatically from C- to N-terminal: Fmoc-Cys(StBu)-OH, Fmoc-Pro-OH, Fmoc-Trp(Boc)-OH, Fmoc-Asp(OtBu)-OH, Fmoc-Gly-OH, Fmoc-Har(Pbf)-OH, in the presence of the coupling reagents DIC and Oxyma Pure. The Fmoc/tBu MW-SPPS cycle consisted of: 1) swelling in DMF (15 mL) for 30 min; 2) Fmoc-deprotection by 30% (v/v) piperidine/DMF (20 mL, 60 equiv); 3) washings with DMF (3 × 15 mL); 4) coupling with the Fmoc-protected amino acids (5 equiv, 0.4 M in DMF), Oxyma Pure (5 equiv, 1 M in DMF), and DIC (5 equiv, 3 M in DMF); 5), washings with DMF (3 × 15 mL). Peptide elongation was performed by repeating the MW cycle for each amino acid coupling and deprotections as reported in Table A1. After all amino acids were coupled, the resin was filtered, washed with DMF (3 × 15 mL) and with 2-propanol (3 × 15 mL), and dried under vacuum to obtain 2.5 g of peptide-resin Har(Pbf)-Gly-Asp(OtBu)-Trp(Boc)-Pro-Cys(StBu)-Rink Amide AM.

Strategy D for optimized fully single reactor solid-phase disulfide bond formation in Eptifibatide

The StBu protecting group was removed from cysteine on the linear peptide-resin Har(Pbf)-Gly-Asp(OtBu)-Trp(Boc)-Pro-Cys(StBu)-Rink Amide AM (loading 0.43 mmol/g, 1.6 g, 0.7 mmol), treating the resin with a solution of MPA (2.44 mL, 40 equiv) and DIPEA (5 mL, 41 equiv) in DMF (25 mL). After 24 h at room temperature (without removing the resin from the Liberty Blue instrument), the IPC monitoring the reaction progress in solid-phase showed an almost complete cysteine deprotection. The resin was filtered, washed with DMF (3 × 25 mL) and DCM (3 × 25 mL), and added with a solution of DTDPA (5.9 g, 40 equiv) and DIPEA (146.3 µL, 1.2 equiv) in DMF (25 mL), and maintained for 21 h at r.t. under N_2 bubbling in the instrument. The IPC showed that Cys(MPA) was correctly formed on the peptide-resin by disulfide-exchange (data not shown). Therefore, after filtration and washings with DMF (3 × 25 mL), the peptide-resin was added with DIC (130 µL, 1.2 equiv) and Oxyma Pure (120 mg, 1.2 equiv) under two consecutive MW cycles, refreshing the reagents solution (70 °C, 150W in 30 sec and then 90 °C, 30W in 10 min) to form the head to MPA on Cysteine side-chain amide-bond cyclisation including the disulfide bridge of Eptifibatide (IPC, Figure A14, Appendix). Finally, the resin was filtered and washed with DMF (3 × 25 mL) and DCM (3 × 25 mL), then dried under vacuum. The final cleavage was performed following the procedure described in the Supplementary Information using the cocktail TFA/H_2O/TIS (20 mL, 95:2.5:2.5).

Crude Eptifibatide (400 mg, 60% yield) was obtained with a 40% HPLC purity (Figure 17).

Optimization assays to perform Cys(StBu) deprotection

Dithiothreitol-mediated reduction

Har(Pbf)-Gly-Asp(OtBu)-Trp(Boc)-Pro-Cys(StBu)-Rink Amide AM resin (loading 0.42 mmol/g, 0.47 g, 0.2 mmol) swelled in DMF (4 mL) for 30 min in a 20 mL round bottom flask, was filtered and added into a 20 mL round bottom flask with a solution of dithiothreitol (DTT) (1g, 6.5 mmol) and NMM (110 µL, 1 mmol) in DMF (10 mL). The reaction mixture was stirred for 3h at r.t. After StBu was almost completely removed (IPC above described), the reaction mixture was filtered and washed with DMF(3 × 5 mL), DCM (3 × 5 mL), and dried under vacuum.

β-Mercaptoethanol-mediated reduction with NMM or DIPEA

Har(Pbf)-Gly-Asp(OtBu)-Trp(Boc)-Pro-Cys(StBu)-Rink Amide AM resin (loading 0.42 mmol/g, 0.23 g, 0.1 mmol) was introduced into the Liberty Blue™ reactor and swelled in DMF (4 mL) for 30 min. The solvent was filtered off and a solution of β-mercaptoethanol (βME, 0.8 mL, 11.4 mmol) and NMM (44µL, 0.4 mmol, 0.1 M) in DMF (3.2 mL) was added. MW conditions were applied for 15 min (35W, 75°C) and after IPC to monitor the almost complete StBu deprotection, the resin was filtered, washed with DMF (3 × 2 mL), DCM (3 × 2 mL), and dried under vacuum. The procedure with DIPEA used the same procedure above described with the following reagent amounts: β-mercaptoethanol (βME, 1.8 mL, 25.6 mmol), DIPEA (100 µL, 0.57 mmol, 0.05 M) in DMF (7.2 mL).

2-Aminoethane-1-thiol-mediated reduction. Har(Pbf)-Gly-Asp(OtBu)-Trp(Boc)-Pro-Cys(StBu)-Rink Amide AM resin (0.12 g, 0.05 mmol, 0.42 mmol/g) was swelled with DMF (3 mL) for 30 min in a 10 mL round bottom flask. Then the resin was filtered and placed in a 10 mL round bottom flask. A solution of 2-aminoethane-1-thiol (2-MEA, 0.5 mL, 2

mmol) with NMM (22 µL, 0.2 mmol) in DMF (2.5 mL) was added to the resin that was stirred for 16h at r.t.. After IPC to evaluate the almost complete StBu deprotection, the resin was filtered, washed with DMF (3 × 5 mL) and DCM (3 × 5 mL), and dried under vacuum.

MPA-mediated reduction. Har(Pbf)-Gly-Asp(OtBu)-Trp(Boc)-Pro-Cys(StBu)-Rink Amide AM resin (loading 0.42 mmol/g, 0.12 g, 0.05 mmol) was swelled with DMF (3 mL) for 30 min in a 10 mL round bottom flask. The resin was filtered, placed in a 10 mL round bottom flask, and added with a solution of MPA (0.17 mL, 2 mmol) with DIPEA (360 µL, 2.1 mmol) in DMF (2.5 mL). The resin mixture was stirred for 16 h at r.t.. After IPC to evaluate the almost complete StBu deprotection, the reaction mixture was filtered, washed with DMF(3 × 5 mL) and DCM (3 × 5 mL), and dried under vacuum.

All the procedures above described lead to Har(Pbf)-Gly-Asp(OtBu)-Trp(Boc)-Pro-Cys(SH)-Rink Amide AM resin.

In Process Control (IPC) monitoring of the solid-phase reactions progress

A sample of peptide-resin (25 mg) was washed with DMF (3 × 3 mL) and DCM (3 × 3 mL) and dried under vacuum. Peptide cleavage from the resin and concomitant deprotection of the acid sensitive amino-acid side-chains were carried out with the cocktail TFA/TIS/H_2O (1 mL, 96:2:2). The mixture was maintained for 30 min at 38°C under magnetic stirring. The resin was washed with TFA (1 mL) and filtered. The crude product was precipitated with ice-cold Et_2O (4 mL), collected after centrifugation, dissolved in H_2O (1 mL), freeze-dried by a LIO5P DGT lyophilizer (5Pascal, Milan, Italy) and analyzed by RP-UHPLC-MS on a Thermo Scientific Ultimate 3000 equipped with a variable wavelength detector and a Thermo Scientific-MSQ PLUS, using a C18 Waters Acquity CSH^{TM}

(130Å, 1.7 μm, 2.1 × 100 mm); temperature 45°C; flow: 0.5 mL/min; eluents: 0.1% (v/v) TFA in H_2O (A) and 0.1% (v/v) TFA in CH_3CN (B), λ 215 nm.

Flash column chromatography purification procedure

Crude Eptifibatide TFA salt obtained (4.90 g, 5.2 mmol, UHPLC purity 67.4%), dissolved in H_2O/CH_3CN (1:1 (v/v), 15 mL) was loaded on SNAP Ultra C18 120g column (Biotage Isolera One, Uppsala, Sweden) Eluents: 0.1% (v/v) TFA H_2O (A), 0.1% (v/v) TFA CH_3CN (B). Flow rate: 25 mL/min. λ 215 nm. Elution method: a) 100% (v/v) A, 5 column volumes, b) 10-37% (v/v) B in A gradient, 12 column volumes, c) 100% (v/v) B, 2 column volumes. Fractions of 18 mL volume were collected and analyzed by RP-UHPLC-ESI-MS (Procedures A2, A3, and A4). Fractions corresponding to R_t 4.1 min and UHPLC purity <98.5% were collected obtaining a total volume of 198 mL that was lyophilized.

Eptifibatide TFA salt (1.69 g, yield 40.5%) was characterized by: 99.2% UHPLC purity, R_t 4.1 min (Figure A20, Appendix); ESI-MS (m/z): $[M+H]^+$ 832.5 (found); 831.96 (calcd).

Exchange strategy

Purified Eptifibatide TFA salt (4.74 g, 5.0 mmol, UHPLC purity 99.2%) was introduced into a 3L round bottom flask, dissolved with pure H_2O (1923 mL, 2.6 mM), and pH was adjusted to 8 with NH_4OH 1.5% (v/v) (9.6 mL) under mechanical stirring (150 rpm). The solution was loaded on SNAP Ultra C18 120 g column (Biotage Isolera One, Uppsala, Sweden). Eluents: 0.5% (v/v) AcOH H_2O (A), 0.5% (v/v) AcOH CH_3CN (B). Elution method: a) 100% (v/v) H_2O, 3 column volumes; b) 100% (v/v) A, 3 column volumes c) 20% (v/v) B in A 3 column volumes, d) 100% (v/v) CH_3CN, 2 column volumes. Flow rate: 50 mL/min. λ 215 nm. Fractions of

20 mL volume were collected and analyzed by RP-UHPLC-ESI-MS (Procedures A2, A3, and A4). Fractions corresponding to R_t 4.0 min and UHPLC purity <98.5% were collected obtaining a total volume of 60 mL that was lyophilized.

Obtained Eptifibatide acetate was analyzed by RP-UHPLC-ESI-MS (Procedure A2, A3, A4, and A5). TFA and acetate contents were quantified by Ion exchange chromatography (Procedure A8).

Eptifibatide acetate (2.99 g, yield 64.6%) characterized by: 99.6% UHPLC purity, R_t 4.0 min (Figure A22, Appendix); ESI-MS (m/z): [M+H]$^+$ 832.5 (found); 831.96 (calcd). TFA residual content: 335 ppm; acetate content: 4.6% w/w.

Overview of Eptifibatide acetate cGMP production at 70 mmol scale

The procedures optimized for each step at 5 mmol scale (Step 1+2, Step 3, Step 4, and Step 5) were scaled-up to the pilot scale (70 mmol). MPA(Trt)-Har(Pbf)-Gly-Asp(OtBu)-Trp(Boc)-Pro-Cys(Trt)-Rink Amide AM resin was produced in a large scale cGMP qualified MW-assisted solid-phase peptide synthesizer (Liberty Blue, CEM, Matthews, NC, U.S.A.), obtaining 196 g in a single batch. Cleavage from the resin was performed in a single batch obtaining 51 g of Eptifibatide TFA linear precursor crude showing 73.7% of HPLC purity (Yield 82.2%). The disulfide bond in Eptifibatide TFA linear precursor crude was formed in 5×10 g batch, obtaining 50 g total of Eptifibatide TFA crude with a purity of 66.4% (Yield 98.3%). Eptifibatide TFA crude was purified by flash chromatography in 5 batches. Fractions with HPLC purity >98.5% (R_t 23.0 min, Table A9) obtained after purification of each batch, were collected leading to 4 g/batch of pure Eptifibatide TFA (99.2% HPLC purity, Yield 41.6%). Each batch of pure Eptifibatide TFA salt (4 g) was treated as described in the above described "Exchange strategy" obtaining

2 g/batch of the Eptifibatide acetate active pharmaceutical ingredient (API) with a purity of 99.6% (Yield 65.8%). The total yield of the Eptifibatide acetate cGMP production process resulted in o prevent adhesion22.1%.

Glassware was cleaned following the standard operating procedures (SOP) before and after the manufacturing operations. Moreover, all the personnel involved in the cGMP process was adequately trained in technical operations, safety behavior, personal hygiene, and technical clothing in accordance with the cGMP requirements. The construction criteria of the pilot-scale facility followed the cGMP structural requirements (e.g., air-lock, system air shower, etc.). Monitoring of microbial contamination was duly scheduled as well as facility sanitizations.

H₁-RELAXIN

Materials

All Fmoc-protected amino acids, Fmoc-Ser-NovaSyn TGA resin (0.16 mmol/g, 90 μm beads), Fmoc-Ile-NovaSyn TGA (0.19 mmol/g, 90 μm beads), Fmoc-Ile-Wang resin (0.7 mmol/g, 100-200 μm beads), DIC, Oxyma, were purchased by Novabiochem (Merck KGaA, Darmstadt, Germany). DIPEA, 2, 6-lutidine, DMSO, DCM and trifluoroacetic acid (TFA) were purchased by Sigma Aldrich (Milano, Italy). 2-(1H-benzotriazol-1-yl)-1,1,3,3-tetramethyluronium hexafluorophosphaten (HBTU) and 1-[Bis(dimethylamino)methylene]-1H-1,2,3-triazolo[4,5-b]pyridinium 3-oxide hexafluorophosphate (HATU) were purchased from Iris Biotech GmbH (Marktredwitz, Germany).

Peptide-synthesis grade N,N-dimethylformamide (DMF) was purchased from Scharlau (Barcelona, Spain); acetonitrile from Carlo Erba (Milano, Italy). The scavengers for cleavage of peptides from resin, Triisopropyl silane (TIS) and 1,2-Ethanedithiol (EDT), were purchased from Sigma Aldrich (Milano, Italy). Diisopropyl ether (iPr₂O), diethyl ether (Et₂O), Click reagent copper (I) bromide (CuBr), copper (II) sulfate pentahydrate ($CuSO_4 \cdot 5H_2O$) and sodium L-ascorbate were purchased from Sigma Aldrich (Milano, Italy).

Serelaxin (batch B917056/1/1, prepared by Boehringer-Ingelheim Inc.) was kindly donated by the Relaxin RRCA Foundation, Florence, Italy. For comparison, parallel experiments were carried out with highly purified luteal porcine RLX (pRLX, ~3000 U/mg), kindly donated by Dr. Antonio L. Scarpa, formerly at IBSA Institut Biochimique, Lugano, CH. Stock aliquots of both peptides (500 μg/ml) were stored at -80° C and thawed immediately before further use. Throughout the experiments, silicon-coated test tubes were used to prevent the adhesion of the peptides to the walls.

Unless otherwise stated, all chemicals and reagents used in the experiments were from Sigma-Aldrich (Milan, Italy), while cell culture plastic ware was from VWR-Avantor (Milan, Italy).

Methods

MW-SPPS: general protocol

Peptides were synthesised with a Liberty Blue[TM] (CEM, Matthews, NC, U.S.A.) automated peptide synthesiser, equipped with a CEM Discovery® microwave reactor following the Fmoc/tBu strategy. Reaction temperatures were monitored by an internal fiberoptic sensor. The Fmoc deprotections were performed with 20% piperidine in DMF (2 M). Double couplings were performed by Fmoc-amino acids (5 equiv, 0.2 M), DIC (5 equiv, 0.5 M) and Oxyma Pure (5 equiv, 1 M) except for Fmoc-L-Pra and L-Nle(ϵN$_3$)-OH which were single coupled (Fmoc-Aa 2.5 equiv, 0.2 M; DIC 2.5 equiv, 0.5 M; and Oxyma Pure 2.5 equiv, 1 M). Both deprotection and coupling reactions were performed in a Teflon vessel with microwave energy (90 °C) and nitrogen bubbling (Standard MW-SPPS protocol (Table RI); Mild MW-SPPS protocol (Table RII).

Conventional SPPS: general protocol

Fmoc-Pra[14]VRALys(N$_3$)[18]IAI-Wang (Experiments **E** and **F**, Table II) was obtained starting from Fmoc-Ile-Wang resin (0.7 mmol/g, 100-200 mesh) using a manual Fmoc/tBu SPPS strategy (0.025 mmol scale). The resin was swollen for 40 min in DMF (1mL/100mg resin). Single couplings were carried out with Fmoc-protected amino acids (5 equiv, 0.35 M), HBTU, (5 equiv, 0.35M) and DIPEA, (6 equiv, 0.43 M) in DMF for 25 min, at r.t. aging with an automated batch synthesizer PLS 4×4, Advanced ChemTech (Louisville, KY, US). Single coupling of Fmoc- L-Nle(ϵN$_3$)-

OH and Fmoc-Pra-OH were performed with Fmoc-protected amino acids (2.5 equiv, 0.17 M), HATU (2.8 equiv, 0.2 M) and DIPEA (3.8 equiv, 0.3 M) in DMF for 25 min. After each coupling, the resin was washed with DMF (3 × 5 mL) and DCM (2 × 5 mL).

Small-scale Analytical Cleavage (In Process Control, IPC): general protocol

A sample of the resin (25 mg) bearing the clicked analogue has been washed as follows: 1) DMF (3 x 3 mL); 2) Fmoc-His-OH solution (to help the elimination of copper ions according to the well-known formation of Cu-Histidine complexes) in DMF:H_2O 1:1 (3 x 2 mL, 5 mM); 3) DCM (3 x 3 mL) and dry off. Peptide cleavage from the resin and deprotection of the amino acids side chains were carried out with TFA/TIS/H_2O (96:2:2: v/v/v/v, 1 mL) solution. The mixture was maintained for 30 minutes at 38°C under magnetic stirring. The resins were washed with TFA (1 mL) and then filtered. The crude product was precipitated with ice-cold Et_2O (4 mL), collected by centrifugation, dissolved in H_2O (1 mL) and lyophilized by a 5Pascal LIO5PDGT lyophilizer (Milan, Italy).

Cleavage: general protocol

Final cleavage from the resin with concomitant side-chains deprotection was achieved by treatment of resin-bound peptide with a TFA/TIS/water solution (95:5:5, 1 mL mixture/100 mg of resin). The cleavage was carried out for approximately 3 h at room temperature. The resin was filtered, rinsed TFA (3 × 3 mL). The peptide solution was added to the washes and the product was precipitated from this solution by the addition of ice-cold Et_2O (15 mL). The crude was washed with ice-cold Et_2O (3 x 3 mL) and dried under vacuum.

Purification: general protocol

Peptide crudes underwent a double step of purification: a Flash chromatography purification to obtain the first crude of 60-80% HPLC purity, and a following semi-preparative purification to obtain the final purified peptide with <90% HPLC purity.

Flash chromatography purification was performed by a Biotage Isolera One instrument (Uppsala, Sweden), equipped with a UV Detector and a 30 g SNAP Ultra C_{18} column (column volume (CV) 45 mL). Eluents: 0.1% (v/v) TFA in H_2O (A) and 0.1% % (v/v) TFA in CH_3CN (B), gradient 3 CV 100% A, 10 CV 10- 60% (v/v) B in A, 3CV 100% B, flow rate: 25 mL/min.

Fractions corresponding to the R_t of the desired peak with UHPLC purity 60-80% were collected and lyophilized by a LIO5P DGT lyophilizer (5Pascal, Milan, Italy).

The obtained crude peptides were further purified by RP-HPLC semi-preparative Waters 600 instrument (Milford, Massachusetts), equipped with a Waters UV Detector model 2487 (Milford, Massachusetts) and a C_{18} Bio-Sepax^{TM} column (200 Å, 5 µm 10 X 150 mm). Temperature 35°C; flow: 4.0 mL/min; eluents: 0.1% (v/v) TFA in H_2O (A) and 0.1% (v/v) TFA in CH_3CN (B), gradient: 20–55% (v/v) B in A in 20 min; λ 215 nm. Fractions corresponding to the R_t of the desired peak with UHPLC purity <90% were collected, lyophilized by a LIO5P DGT lyophilizer and analyzed by RP-UHPLC-ESI-MS on a Waters Alliance instrument (model 2695, Milford, Massachusetts) equipped with a UV Diode Array Detector (model 2996, Waters Corporation, Milford, Massachusetts), an ESI-MS Micromass ZQ^{TM} single quadrupole mass spectrometer (Waters, Milford, Massachusetts), and a C_{18} Waters Acquity UHPLC CSH^{TM} column (Å160, 1.7 µm, 2 × 100 mm). Temperature 35°C; flow: 0.6 mL/min; eluents:

0.1% (v/v) TFA in H_2O (A) and 0.1% (v/v) TFA in CH_3CN (B), gradient: 10–60% (v/v) B in A in 10 min; λ 215 nm.

Microwave-assisted SPPS of $14^3, 18^6$-(1H-1,2,3-triazole-4,1-diyl) derivative of [Ala^{14}, Nle^{18}] H_1-relaxin B chain (14-21).

[L-Pra^{14}, L-Nle(εN_3)^{18}] H_1-relaxin B chain (14-21) linear precursor was synthesised on a 0.1 mmol scale starting from Fmoc-Ile-NovaSyn TGA resin (0.19 mmol/g, 90 μm beads). All Fmoc-amino acids were coupled by double coupling (Fmoc-amino acids 5 equiv, 0.2 M, DIC 5 equiv, 0.5 M and Oxyma Pure 5 equiv, 1 M), exposed to the microwave cycle described in Table RI.

Subsequencially, the resin was divided into four portions (0.025 mmol each) to perform the experiments **A-D**.

Experiment **A**. Peptide-resin (0.025 mmol), $CuSO_4 \cdot 5H_2O$ (1.2 equiv), sodium ascorbate (1.5 equiv) in H_2O:t-BuOH:DCM 1:1:1 (3 mL), microwave-assisted CuAAC in **Errore. L'origine riferimento non è stata trovata.**.

Experiment **B**. Peptide-resin (0.025 mmol), $CuSO_4 \cdot 5H_2O$ (1.2 equiv), sodium ascorbate (1.5 equiv) in H_2O:t-BuOH:DCM 1:1:1 (3 mL), microwave-assisted CuAAC in Table RIV.

Experiment **C**. Peptide-resin (0.025 mmol), $CuSO_4 \cdot 5H_2O$ (1.2 equiv), sodium ascorbate (1.5 equiv) in H_2O:t-BuOH:DCM 1:1:1 (3 mL), microwave-assisted CuAAC in
Table.

Experiment **D**. Peptide-resin (0.025 mmol); CuBr (1.2 equiv) and sodium ascorbate (1.5 equiv) diluted into a mixture of DMSO (1 mL) and DMF (2 mL), DIPEA (5 equiv) and 2,6-Lutidine (5 equiv), microwave-assisted CuAAC in Table RIV.

Experiment **E**. H-Pra[14]VRALys(N₃)[18]IAI-Wang resin (0.02 mmol); CuSO₄·5H₂O (1.2 equiv), sodium ascorbate (1.5 equiv) in H₂O:t-BuOH:DCM 1:1:1 (3 mL), microwave-assisted CuAAC at 55°C for 10 min (Table RIV).

Experiment **F**. H-Pra[14]VRALys(N₃)[18]IAI-Wang resin (0.02 mmol), CuBr (1.2 equiv) and sodium ascorbate (1.5 equiv) diluted into a mixture of DMSO (1 mL) and DMF (2 mL), DIPEA (5 equiv) and 2,6-Lutidine (5 equiv), microwave-assisted CuAAC at 55°C for 10 min (Table RIV).

Each peptide was cleaved following the general cleavage protocol described above and analysed by RP UHPLC-MS. Column Waters Acquity UHPLC CSH^{TM} C18 (1.7 μm 2 × 100 mm). . Eluents: A (0.1% (v/v) TFA in H₂O) and B (0.1% (v/v) TFA in CH₃CN), gradient 10–80% (v/v) B in A in 10 min. Flow: 0.5 mL/min, temperature: 65°C, λ 215 nm. Clicked peptide, R_t 3.8 min. C₄₀H₇₀N₁₄O₉ ESI-MS (m/z): [M+H]⁺: 891.1 (calcd), 891.5 (found). Unreacted linear peptide, R_t 4.6 min. C₄₀H₇₀N₁₄O₉ ESI-MS (m/z): [M+H]⁺ 891.1 (calcd), 891.7 (found). Dimer peptide, R_t 5.0 min. C₈₀H₁₄₀N₂₈O₁₈ ESI-MS: ESI-MS (m/z): [M+H]⁺ 1782.2 (calcd); [M+2H]²⁺ 891.6 (calcd), 891.8 (found); [M+3H]³⁺ 594.7 (calcd), 595.1 (found).

Stability study of Fmoc-Lys(N₃)-OH

A Fmoc- L-Nle(εN₃)-OH (79 mg, 0.2 M) solution in DMF has been subjected to four microwave-assisted cycles described in Table RI. Standard microwave-assisted coupling cycle protocol at 90°C

Step	Temperature (°C)	Power (W)	Hold Time (s)	Delta T (°C)
Deprotection	80	200	30	2
	90	50	70	1
Coupling	75	170	15	2

90	30	100	1

Table The study was followed by RP-UHPLC MS, samples were analyzed with the gradient 5-95% B in 10 minutes, column at 45°C, at λ 254 nm, mass range 50-1000 m/z.

Microwave-assisted SPPS of $14^3,18^6$-($1H$-1,2,3-triazole-4,1-diyl) derivative of [Ser^{10}, Ala^{14}, Nle^{18}] H$_1$-relaxin B chain (10-21), Peptide 4.

$14^3,18^6$-($1H$-1,2,3-triazole-4,1-diyl) derivative of [Ser^{10}, Ala^{14}, Nle^{18}] H$_1$-relaxin B chain (10-21), the so called Peptide **4** was synthesized on Fmoc-Ile-NovaSyn TGA resin (0.19 mmol/g, 90µm beads) 0.02 mmol scale with the microwave-assisted method described in Table RI. The on-resin CuAAC was performed by CuBr (1.2 equiv) and sodium ascorbate (1.5 equiv) diluted into a mixture of DMSO (1 mL) and DMF (2 mL), DIPEA (5 equiv) and 2,6-Lutidine (5 equiv), microwave-assisted CuAAC at 55°C for 10 min (Table RIV). The peptide was cleaved following the general cleavage protocol and analyzed by RP-UHPLC-MS.

A microwave-assisted larger scale synthesis was performed on 0.1 mmol in the same experimental conditions. Triazole stapling was carried out by CuBr (1.2 equiv) and sodium ascorbate (1.5 equiv) diluted into a mixture of DMSO (6 mL) and DMF (12 mL), DIPEA (87 µL, 5 equiv) and 2,6-Lutidine (53 µL, 5 equiv), applying a microwave-assisted CuAAC at 55°C for 10 min (Table RVI).

The peptide was cleaved following the general cleavage protocol and analyzed by RP-UHPLC-MS. The crude peptide (148 mg) was purified by a Flash chromatography system (Biotage Isolera One, Sweden) with UV Detector, equipped with a 30 g SNAP Ultra C$_{18}$ column, column volume 45 mL. Eluents: 0.1% (v/v) TFA in H$_2$O (A) and 0.1% % (v/v) TFA in CH$_3$CN (B), gradient 3 CV 100% A, 10 CV 10- 60% (v/v) B in A, 3CV

100% B, flow rate: 25 mL/min. After lyophilisation we obtained 42.3 mg (yield 25.5%) of purified peptide **4**.

The peptide was characterised by Thermo Scientific MSQ Plus spectrophotometer (ESI-MS) with analytic Ultimate 3000 UHPLC (Thermo Scientific) on Acquity UPLC Column CSH C18 1.7 um 2.1 x 100 mm. Eluents: 0.1% (v/v) TFA in H_2O (A) and 0.1% (v/v) TFA in CH_3CN (B), gradient 10-60 % (v/v) B in A in 10 min, flow rate: 0.5 mL/min, temperature 45°C, λ 215 nm. R_t 4.9 min: Peptide **4**. Purity (HPLC): >95%. $C_{56}H_{97}N_{21}O_{16}$ ESI-MS (m/z): $[M+H]^+$: 1320.5 (calcd), 1321.1 (found), $[M+2H]^{2+}$: 661.3 (calcd), 661.7 (found).

Circular dichroism

CD spectra of second-generation H_1-relaxin single B-chain stapled analogues were recorded using quartz cells of 0.1 cm path length with a JASCO J-710 CD spectropolarimeter at 25 °C. All spectra were measured in the 260-190 nm spectral range, 1 nm bandwidth, 4 accumulations and 100 nm/min scanning speed. Each peptide was dissolved in water to prepare a 1 mM peptide stock solution. The CD spectra were performed in water, in PBS and in SDS (20 mM) using a peptide concentration of 100 μM

Simulated intestinal digestion

The effects of duodenal enzyme digestion on the noted serelaxin and pRLX preparations was tested by the addition of a simulated intestinal fluid (SIF). SIF was prepared according to USP specifications (Test Solutions, United States Pharmacopeia 35, NF 30, 2012). In detail, KH_2PO_4 (0.68 g) was dissolved in water (25 mL). pH was adjusted to 6.8 with 0.2 N NaOH (7.7 mL).

200 μL of the stock solution pRLX (0.084 mM, 5918 uma) were added to 14.8 mL of SIF in a 50 mL Falcon, mixing in a 37 °C bath (final pRLX solution 1.12 μM). On the other hand, 20 μL of the stock solution Human relaxin (0.84 mM, 5963 uma) were added to 14.8 mL of SIF in a 50 mL Falcon, mixing in a 37 °C bath (final Human relaxin solution 1.12 μM). For both the two relaxins (pRLX and Human) six digestion times were assayed (0, 10, 20, 30, 60 and 120 sec). Digestion was stopped by withdrawing an aliquot of 200 μL and quenching the reaction with HCl 0.1 M (17.5 μL) for each digestion time. Samples were centrifuged at 10000 rpm for 10', and the supernatant fluid was withdrawn and quickly frozen and stored at -80° C until further use. Digestion was performed in duplicate for both the two relaxins.

Cell culture and cAMP assay

Human monocytic THP-1 cells were purchased at the European Collection of Cell Cultures (ECACC, Salisbury, UK) and cultured in suspension in RPMI medium containing 10% foetal calf serum, 250 U/ml penicillin G and 250 μg/ml streptomycin, in a 5% CO_2 atmosphere at 37 °C. Aliquots containing $6x10^5$ THP-1 cells in 1 ml PBS were placed in a 24-well plate, added with IBMX (100 μM) to prevent cAMP catabolism and then incubated with intact serelaxin (100 ng/ml), pRLX (100 ng/ml) or equivalent solutions of their digestion by-products. The cAMP assay was carried out 15 min after addition of the stimuli, i.e. in the midst of the second, sustained cAMP surge upon RXFP1 stimulation. Measurements of cAMP were determined by the chemiluminescent HitHunterXP™ cAMP II assay (DiscoverX, Birmingham, UK). The standard curve was performed in duplicate and the experimental points in triplicate. Since the standard curve was sigmoidal, nonlinear regression was used to extrapolate unknown experimental cAMP values, expressed as nmol/l,

according to the manufacturer's instructions. Two independent experiments, each in duplicate, were performed. For positive control, the adenylate cyclase activator forskolin (10^{-4} M) was used. Finally, the values of cAMP in each experimental sample were normalized by the amount of proteins, measured by the micro-BCA^{TM} Protein Assay Kit (Pierce, IL, USA) method and expressed as mg/ml.

5. CONCLUSIONS

In the industrial synthesis of APIs, maximizing the yield and the final purity are mandatory goals. This task answers the need to have an efficient process in terms of product recovery, minimizing waste associated with each chemical reaction and cutting the overall cost of the process.

In this frame, to develop a process to be transferred at a large scale, a deep understanding of the reaction parameters, to better control of the whole reaction system, plays a crucial role.

Accordingly, herein we optimized and successfully transferred from the lab-scale process (5 mmol) to 70 mmol scale the Eptifibatide acetate API production protocol (Synthesis and contemporary cleavage from the resin and deprotection (STEP1+2), in solution disulfide formation (STEP3), Flash column chromatography purification (STEP4) and TFA/acetate counter ion exchange (STEP5)). The assessment of the quality risk management followed to establish an appropriate controlled manufacturing process of the cGMP Eptifibatide acetate pilot batch was carried out. Each critical factor was identified and optimized to obtain the best purity and yield. Eptifibatide acetate critical attributes that were within CQA limits allowed the batch release of cGMP-compliant Eptifibatide acetate to regulatory agencies approval (Table 14). The key benefits of the new automated large-scale microwave solid-phase peptide synthesizer resulted in rapid production times and ability to incorporate green chemistry protocols based on MW-SPPS improving peptide purity and minimizing excess reagents. The pilot plant equipped with this technology was qualified by F.I.S. - Fabbrica Italiana Sintetici S.p.A. for cGMP peptide production.

Moreover, our results definitely demonstrate that the strong collaboration between an academic facility and a contract development manufacturing organization, already recognized as a leader in Europe for small molecule

APIs & intermediates industrial GMP production, is a powerful example of joint-laboratory satisfying the needs of a market entry strategy into peptide API production.

Additionally, in order to develop an innovative, patentable Eptifibatide acetate production process, we focused our attention on the challenging step of the disulfide formation, which could be hampered by some drawbacks particularly relevant for the large-scale production, such as the formation of unwanted oxidation by-products, mainly dimers. Therefore we investigated two liquid phase oxidation respectively by air and H_2O_2 as oxidants, subsequently compared with four different solid-phase disulfide bridge formation strategies. Liquid-phase one performed by H_2O_2 led to the best final purity profile and Yield (HPLC purity 99.6 %, Yield 22.1%). Thus it was chosen as model Eptifibatide production process to perform the qualification plant.

However, the development of four solid-phase disulfide bridge formation strategies ($A \div D$), and in particular of the best one strategy **D** allowed to overcome patent exclusive rights, simplify the respect of cGMP compliances, cutting the financial and time costs related to multiple equipment qualification.

In particular, Strategy **D** was characterized by the concomitant reduction of the S-tert-butylthio (StBu) Cys protecting group (PG) and disulfide formation with the MPA reducing agent, enjoying the advantage of using an already qualified starting material. Therefore, unlike the others, Strategy **D** presents an inventive, non-obvious StBu deprotection from Cys mediated by MPA (first proposed), in which for the first time both MW-SPPS and disulfide bond formation occurs in the same reactor (novelty), and it can be potentially scalable on multigram-scale by Liberty Pro synthesizer (Industrial applicability). According to the three patentability criteria required for a new production process: Novelty; inventive and

industrial applicability, the present PhD work identified strategy **D** as a new patentable production process to obtain Eptifibatide acetate API.[160]

On the other hand, the growing interest toward insulin-like peptides as therapeutics fueled by the evidence of H_3-relaxin involvement in arousal, feeding, stress responses, cognition and drug addiction, and the H_2-relaxin clinical trials efficacy demonstrated to treat AHF and fibrosis, led to suppose a possible H_1-relaxin physiological role, still unknown.

This assumption is supported by the fact that relaxin peptides (H_1-, H_2- and H_3-relaxin) share a conserved motif "RXXXRXXI" called "binding cassette", recognized as a primary affinity binding site of RXFP1-4 receptors (Figure 4).

Interest toward H_1-Relaxin moved us to project a library of structurally simplified H_1-relaxin single B-chain analogues to overcome synthetic drawbacks characterizing Insulin-like peptides (poor solubility and aggregation tendency). Accordingly, we planned a stapling strategy to stabilize α-helix structure, since of the lack of the A chain. To the best of our knowledge, the triazole stapling technique has never been considered before to obtain structural constriction in the field of relaxin analogues syntheses, despite the widely known versatility of triazole side-chain to side-chain cyclization improving analogues solubility and modulating receptor subtype selectivity (position and orientation of the stapling). Therefore, an innovative, easy and faster Solid-phase microwave-assisted copper-catalyzed azide-alkyne Cycloaddition (SP MW-CuAAC) has been developed with the aim to decrease the cost and complexity of the relaxin derivatives syntheses, exploiting the disaggregation performances of microwave heating and the solid-phase advantages, like the copper easy washing out and the increased recovery due to any intermediate isolations.

All the relevant parameters (resin, solvent, catalytic system, microwave energy and reaction time) were optimized using a systematic one-factor-at-a-time approach. To demonstrate the robustness and the reproducibility of the SP MW-assisted CuAAC 0.1 mmol scale was performed.

We replaced 2 natural residues with 2 not natural azide and alkyne bearing ones (Fmoc-L-Pra-OH; Fmoc-L-Nle(εN_3)-OH), excluding Arg[B12], Arg[B16] and Ile[B19] engaged into receptor binding, with a putative 5 methylene ring size following the scheme *i, i+4* widely recognized correspond to an α-elix secondary structure stabilization motif.

Two generations of H_1-relaxin single B-chain stapled analogues were synthesized. First-generation (Peptides **VR** and **VIR**) and second-generation (Peptide **VII** and **VIIR**; Peptide **VIII** and **VIIIR**; Peptide **IX** and **IXR**).

First-generation H_1-relaxin single B-chain stapled analogues were obtained investigating different lengths (Peptides **VR**: 10-21; Peptides VIR: **6-23**) while looking for the minimum active length.

Second-generation H_1-relaxin single B-chain stapled analogues allowed to investigate the position and orientation of the triazole stapling with a maximum length of 23 amino acids.

Circular dichroism demonstrated an increased α-helicity for stapled analogues compared to their linear references as expected. Interestingly, 3 peptides of the R series characterized by a C-term oriented triazole stapling (Peptide **VIIR**; Peptide **VIIIR** and Peptide **IXR**) showed a slightly increased helicity than their N-term oriented triazole counterparts (Peptide **VII**; Peptide **VIII** and Peptide **IX**).

In vitro competition binding capacity of H_2-relaxin and B7-33 analogue (as positive references), H_1-relaxin single B-chain linear references and stapled analogues (both first- and second-generation) were performed in

HEK-293T cells, stably expressing the RXFP1 receptor, using Eu^{3+}-labelled H_2-relaxin as the competitive ligand.

Unfortunately, all analogues synthesized, both the linear and the stapled ones, did not show a significant displacement of the Eu^{3+}-labelled H_2-relaxin ligand except for Peptide **IX** that showed a weak capacity (ca. 25%) to bind RFPX1 receptor (Figure IX, bottom). The lack of binding reflected the absence of cAMP production for all the tested stapled analogues and their linear references, assessed by cAMP reporter gene assay carried out in HEK-293T.

Last but not least, herein we investigated the possibility of an oral administration of serelaxin using an *in silico* model to simulate the possible behaviour of gastroprotected formulations subjected to gut enzymatic digestion. The relative bio-potency of the intact molecule in comparison with its proteolytic fragments was assessed by measuring the signalling events downstream receptor activation in THP-1 human monocytic cells.

The reported findings showed that both the intact proteins at the known bioactive concentration of 100 ng/ml induced a marked, significant rise of cAMP in RXFP-1-expressing THP-1 cells. On the other hand, exposure of the serelaxin solution to SIF caused a substantial loss of bioactivity, in terms of detectable intracellular cAMP, already appreciable after the shortest 30 s. incubation and dropping down to the levels of the unstimulated control cells after 120 s. Conversely, and unexpectedly, the SIF-exposed pRLX samples retained full capability to stimulate cAMP generation by THP-1 cells, at any digestion time assayed. These results provide serious clues against the possibility to develop effective serelaxin preparations to be administered orally, since susceptibility of H_2-RLX to be rapidly decomposed by gut digestive enzymes. On the contrary, the promising results obtained from the digestion fragments of porcine relaxin

lead to the hypothesis of a possible oral administration. Therefore, possible future developments could concern the characterisation of pRLX digestion products with the aim to identify sequences of biologically active digestion derivatives, to be used as promising therapeutic lead compounds.

6.ABBREVIATIONS

Aa Amino Acid

Acm Acetamidomethyl

AcOH Acetic Acid

AHF Acute Heart Failure

ANDA Abbreviated New Drug Application

API Active Pharmaceutical Ingredient

Arg Arginine

Boc tert-butyoxycarbonyl

βME β-mercaptoethanol

CAGR Compound Annual Growth Rate

calcd calculated

cAMP: cyclic Adenosine Monophosphate

CDMO Contract development Manufacturing Organization

cGMP current Good Manufactoring Practices

CH_2Cl_2 Dichloromethane

CH_3CN, ACN acetonitrile

CH_3COONH_4 Ammonium Acetate

CLP Classification Labelling and Packaging

CMOs Contract Manufacturing Organizations

CPME Methoxycyclopentane

CPP Critical Processing Parameter

CQA Critical Quality Attribute

Cys Cysteine

DIC N,N'-Diisopropylcarbodiimide

Oxyma pure® Ethyl cyanohydroxyiminoacetate

DMF Dimethylformamide

DMSO Dimethyl Sulfoxide

DODT 2,2'-(Ethylenedioxy)diethanethiol

DTDPA or MPA_2 3,3′-Dithiodipropionic Acid

DTT 1,4-Dithiothreitol

ECACC European Collection of Cell Cultures

ECHA European Chemicals Agency

ELISA Enzyme Linked Immunosorbent Assay

EMA European Medicines Agency

ERK Extracellular signal-Regulated Kinase

ESI-MS Electrospray Ionisation Mass Spectrometry

Et_2O DEE Ethoxyethane

FA Formic Acid

FC Flash Chromatography

FD&C Federal Food, Drug and Cosmetic Act

FDA Food and Drug Administration

Fmoc Fluorenylmethyloxycarbonyl

FY Financial Year

HS-GC Headspace Gas Chromatography

GDUFA Generic Drug User Fee Act

GPCRs G Protein-Coupled Receptors

GVL 5-Methyloxolan-2-oneSPPS Solid Phase Peptide Synthesis

GSPPS Green Solid-Phase Peptide Synthesis

H_2O_2 Hydrogen Peroxide

Har Homoarginine

HBTU 3-[Bis(dimethylamino)methyliumyl]-3H-benzotriazol-1-oxide hexafluorophosphate

HCl Hydrochrloric Acid

HOBt 1-hydroxybenzotriazole

HP High Pressure/Performance

HPLC High Performance Liquid Chromatography

IBMX 3-IsoButyl-1-MethylXanthine

IC Ione Exchange Chromatography

ICP-MS Inductively Coupled Plasma Mass Spectroscopy

IEC Ion Exchange Chromatography

INSL Insuline-Like Peptide

iPr$_2$O 2-[(Propan-2-yl)oxy]propane

iPrOH Isopropyl Alcohol

KOH potassium hydroxide

LGR Leucine-rich repeat-containing G-protein coupled Receptors

Leu Leucine

LRR Leucine-Rich Repeat

LPPS Liquid Phase Peptide Synthesis

MBHA 4-Methylbenzhydrylamine

2-MEA 2-aminoethane-1-thiol

Met Methionine

MeTHF 2-Methyltetrahydrofuran

MMP Matrix Metalloproteinases

Mmt 4-methoxytrityl

Mpa 3-Mercaptopropionic acid

MPA(PyS) 3-(pyridyne-2-thiol)propanoic acid

MTBE 2-Methoxy-2-methylpropane

MW MicroWave

MW-CuAAC MW-Assisted Copper-Catalyzed Azide-Alkyne Cycloaddition

MW-SPS MicroWave Solid-Phase Synthesis

MW-SPPS MicroWave Solid-Phase Peptide Synthesis

NCS N-Chlorosuccinimide

NH$_4$HCO$_3$ Ammonium bicarbonate

NH$_4$OH Ammonium Hydroxide

NMM 4-methylmorpholine

NMP N-Methyl-2-pyrrolidone Dichloromethane

NPyS 3-nitro-2-pyridynesulfenyl

OOS Out Of Specification

Pbf 2,2,4,6,7-pentamethyldihydrobenzofuran-5-sulfonyl

PBS Phosphate Buffered Saline

PEG Polyethylene Glycol

pRLX porcine relaxin

PS-PEG Polystyrene-Polyethylene glycol

PyBOP (benzotriazol-1-yloxy) tripyrrolidinophosphonium hexafluorophosphate

PyS pyridine-2-thiol

REACH European Regulation on registration, evaluation, authorization and restriction of chemicals

R&D Research and Development

RLD Reference Listed Drug

RM Raw Material

RP-HPLC Reverse Phase High Performance Liquid Chromatography

RPC Reverse Phase Chromatography

RPMI Roswell Park Memorial Institute

R_t retention time

RXFP Relaxin-Family Peptide Receptor

SAR Structure Activity Relationship

SPE Solid Phase Extraction

SP MW-assisted CuAAC Solid Phase Microwave-Assisted Copper Catalyzed Azide-Alkyne Cycloaddition

StBu S-tert-Butylthio

SVHC Substances of Very High Concern

tBu tert-Butyl

TFA Trifluoroacetic acid

TIS Triisopropylsilane

Trp Triptofane

Trt Triphenylmethyl

USD United States Dollars

VBFR Variable Bed Flow Reactor

WFI Water For Injection

7. APPENDIX

EPTIFIBATIDE ACETATE

Table A1. 1 mmol scale MW-SPPS[*]: coupling cycle parameters

Step	T. max (°C)	Power (W)	Time (s)	Volume (mL)
Resin swelling (DMF)	r.t.	-	-	9.0
Fmoc deprotection (Piperidine in DMF 30% v/v)	90	180 80 40	15 15 120	13.0
Resin washing (5× DMF)	r.t.	-	-	9.0
Coupling Fmoc-L-Cys(Trt)-OH	55	6 10 13 14 14	120 60 60 60 600	9.4
Coupling Building-block	90	9 12 15 19 26	120 120 120 120 120	9.4
Resin washing (2× DMF)	r.t.	-	-	9.0

MW-SPPS was performed on Liberty Blue (Charlotte, NC, U.S.A.).

Table A2. 5 mmol scale MW-SPPS[*]: coupling cycle parameters

Step	T. max (°C)	Power (W)	Time (s)	Volume (mL)
Resin swelling (DMF)	r.t.	-	1800	47
Fmoc deprotection (Piperidine in DMF 30% v/v)	90	300 150 60	30 5 120	61
Resin washing (5× DMF)	r.t.	-	-	47
Coupling Fmoc-L-Cys(Trt)-OH	55	13 15 18 17 17	120 60 60 60 600	50
Coupling Building-block	90	17 22 24 27 26	120 60 60 60 600	50
Resin washing (2× DMF)	r.t.	-	-	47

[*]*MW-SPPS was performed on Liberty Blue (Charlotte, NC, U.S.A.).*

Table A3. 70 mmol scale MW-SPPS[*]: coupling cycle parameters

Step	T. max (°C)	Power (W)	Time (s)	Hold time (s)	Operation details	Volume (L)
Resin swelling DMF	r.t.	-	600	-	-	1.0
Fmoc deprotection (Piperidine in DMF 30% v/v)	90	1200	1200	5	DMF volume	0.7
	85	1000	1200	120	Piperidine volume	0.3
Line cleaning	-	-	-	-	Deprotection cleaning volume	0.2
					Drain washing volume	1.0
Resin washing (5× DMF)	r.t.	-	15	-	-	5.0
Coupling Fmoc-L-Cys(Trt)-OH	45	900	1200	5	DIC solution volume	0.1
	50	500	1200	600	Oxyma Pure solution volume	0.2
Coupling building-block	85	1800	1200	5	Building block solution volume	0.3
	90	800	1200	180	Flush volume	0.2
Line cleaning	-	-	-	-	Building block backflushvolume	0.3
Resin washing (2× DMF)	r.t.	-	15	-	-	2.0

[*]MW-SPPS was performed on Liberty PRO (Charlotte, NC, U.S.A.).

Table A4. Quality attributes of process intermediates to obtain cGMP compliant Eptifibatide

Intermediate/ STEP	Quality attribute	Output found	Target
On resin Eptifibatide linear protected precursor STEP 1	Weight loss on drying[*]	4% w/w	20% w/w
	Appearance	Brownish beads without lumps	White yellowish, orange, reddish, ochre to brownish beads with or without lumps
	Weight	196 g	150-210 g
Eptifibatide linear precursor crude STEP 2	Water content[**]	3%	<5%
	Weight loss on drying	7.4%	<10%
	Appearance	White powder without lumps	White to brownish powder with or without lumps
	HPLC Identity[***]	Compliant	Standard-compliant R_t
	HPLC Purity[***]	73.7%	n.a. reference value
	Weight	51 g	40-80 g
Eptifibatide crude TFA salt STEP 3	Conversion	99%	n.a. reference value
	Water content[**]	8.9%	<10%
	Acetonitrile content[****]	50 ppm	<410 ppm
	Appearance	Yellowish powder	White, off white, yellowish white to brownish powder
	HPLC identity[***]	Compliant	Standard-compliant R_t
	HPLC purity[***]	66.4%	n.a. reference value
	Weight	10 g	7-12 g
Purified Eptifibatide TFA salt STEP 4	HPLC purity[***]	99.3%	≥98.5%
	Water content[**]	5.3%	<10%
	Acetonitrile content[****]	293 ppm	<410 ppm
	HPLC identity[***]	Compliant	Standard-compliant R_t
	Weight	2 g	1-4 g

Weight loss on drying (LOD) was detected by thermogravimetric analysis (TGA, USP 891).

**Water content was quantified by Karl Fisher volumetric titration (USP 921, EP 2.5.12).*

***HPLC analytical methods are described below (Procedures A1, A2 and A3).*

****Acetonitrile content was quantified by Headspace Gas-chromatography (HS-GC). Analytical method is described below (Procedure A7).*

Table A5. List of equipment used for cGMP compliant Eptifibatide production process

Step	Description	Equipment Manufacturer	Scheme Code
1 **MW-SPPS**	Liberty Pro	CEM Corporation (Charlotte, NC, U.S.A.)	n.a.
2 **Resin cleavage and side-chains deprotection**	Jacketed glass filter reactor 2 L	Asahi Glassplant Inc (Omuta, Japan)	RV1231
	Jacketed glass filter reactor 5 L	Asahi Glassplant Inc (Omuta, Japan)	RV1232
	Jacketed glass reactor 21 L	Büchi AG (Uster, Switzerland)	RV1233
3 **Disulfide bond formation**	Jacketed glass reactor 21 L	Büchi AG (Uster, Switzerland)	RV1233
	Freeze Drying	Martin Christ G. GmbH (Osterode am Harz, Germany)	Y1235
4 **Flash Column Chromatography Purification**	Isolera LS (Flash chromatography)	Biotage (Uppsala, Sweden)	n.a.
	Freeze Drying	Martin Christ G. GmbH (Osterode am Harz, Germany)	Y1235
5 **Counter-ion exchange**	Jacketed glass filter reactor 2 L	Asahi Glassplant Inc (Omuta, Japan)	RV1231
	Isolera LS (Flash chromatography)	Biotage (Uppsala, Sweden)	n.a.
	Freeze Drying	Martin Christ G. GmbH (Osterode am Harz, Germany)	Y1235

Table A6. Effect of multiple additions of H_2O_2 at different times, in liquid-phase disulfide bond formation

Entry	Time (min)	H_2O_2 (equiv)	—SH to S—S conversion[*] (%)	Eptifibatide TFA UHPLC purity (A/A%)	Dimer impurity (A/A%)	Yield[**] (%)
1	0	0.44	0			
	30		68.4			
	60	0.44	70.0	64.1	8.1	86.3
	90		100			
2	0	0.22				
	30	0.22	15.6			
	60	0.22	-	64.2	8.0	84.5
	90	0.22	86.0			
	120		100			

[*]*Conditions for disulfide bond formation (0.5 mmol): Eptifibatide linear precursor crude (5.3 mM in H_2O:CH_3CN 2:1 v/v) was oxidized adding H_2O_2, pH 9.5 (NH_4OH), 2h, r.t.*

[**]$Yield(\%) = \frac{Eptifibatide\ crude\ weight\ \times\ (\frac{peptide\ content}{100})}{Eptifibatide\ linear\ crude\ weight\ \times\ (\frac{peptide\ content}{100})} \times 100$

UV Eptifibatide crude average peptide content: 71%; UV Eptifibatide linear precursor crude average peptide content: 79%.

Table A7. Effect of peptide concentration in liquid-phase disulfide bond formation

Entry	Conc. (mM)	Time (min)	H_2O_2 (equiv)	—SH to S—S conversion[*] (%)	Eptifibatide TFA UHPLC purity (A/A%)	Dimer impurity (A/A%)	Yield[**] (%)
1	2.1	0	0.22	-	67.2	4.8	86.3
		30	0.22	27.3			
		60	0.22	58.9			
		90	0.22	88.1			
		120	-	100			
2	1.6	0	0.22	-	67.9	3.9	84.5
		30	0.22	28.3			
		60	0.22	58.2			
		90	0.22	84.2			
		120	-	100			

[*]*Conditions for disulfide bond formation (0.5 mmol): Eptifibatide linear precursor crude (entry 1: 2.1 mM and entry 2: 1.6 mM in H_2O:CH_3CN 2:1 v/v) was oxidized adding H_2O_2, pH 9.5 (NH_4OH), 2h, r.t.*

[**]$Yield(\%) = \frac{Eptifibatide\ crude\ weight\ \times\ (\frac{peptide\ content}{100})}{Eptifibatide\ linear\ crude\ weight\ \times\ (\frac{peptide\ content}{100})} \times 100$

UV Eptifibatide crude average peptide content: 71%; UV Eptifibatide linear precursor crude average peptide content: 79%.

Table A8. IPC of effective disulfide-exchange reaction leading to Cys(MPA) in H-Har(Pbf)-Gly-Asp(OtBu)-Trp(Boc)-Pro-Cys(MPA)-Rink Amide AM resin: optimization of MW conditions (Strategy C)

Entry	Temp (°C)	Power (W)	Time (min)	Cys(MPA) containing peptide HPLC purity (%)
1	25	0	20	11.0
2	50	90	10	48.4
3	50	90	30	81.5

Table A9. Pilot scale flash purification in process control of eluted fractions

Fraction	UHPLC purity[*] (A/A%)	Limit
15	97.0%	
16	99.1%	
17	99.6%	
18	99.5%	
19	99.4%	
20	99.3%	
21	99.1%	$\geq 98.5\%$
22	98.9%	
23	99.3%	
24	98.9%	
25	98.9%	
26	99.5%	
Collected eluate	99.2%	

*Fractions were collected at R_t 23.0 min (Procedure A4).
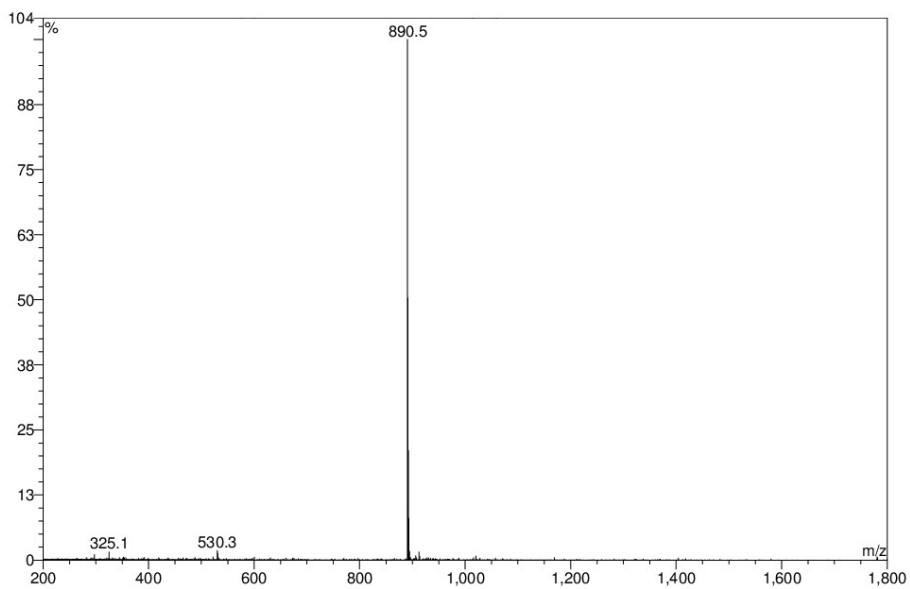
Figure A1. ESI-MS spectrum of Imp a. ESI-MS (m/z): [M+H]$^+$ 890.5 (found), 890.4 (calcd).
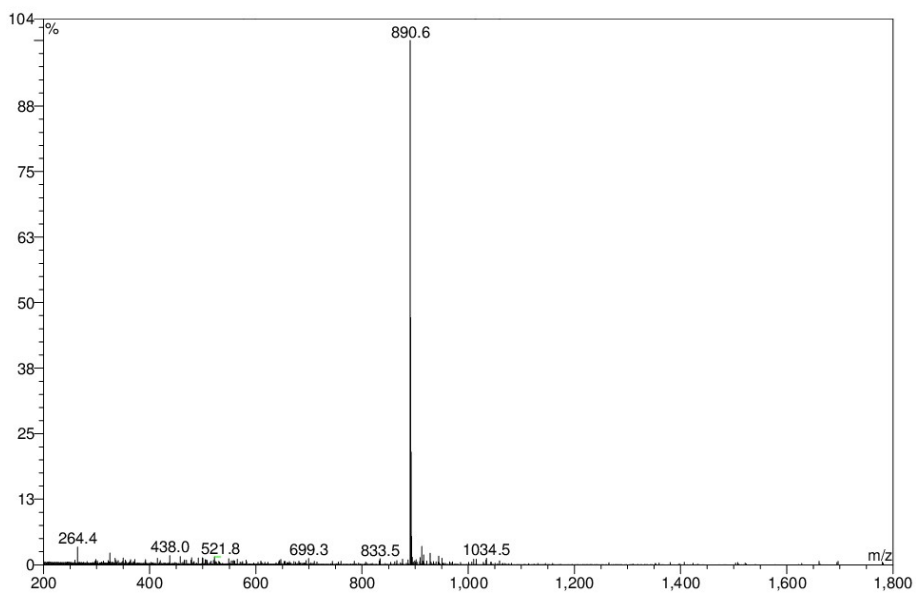
Figure A2. ESI-MS spectrum of Imp b. ESI-MS (m/z): [M+H]$^+$ 890.6 (found), 890.4 (calcd).
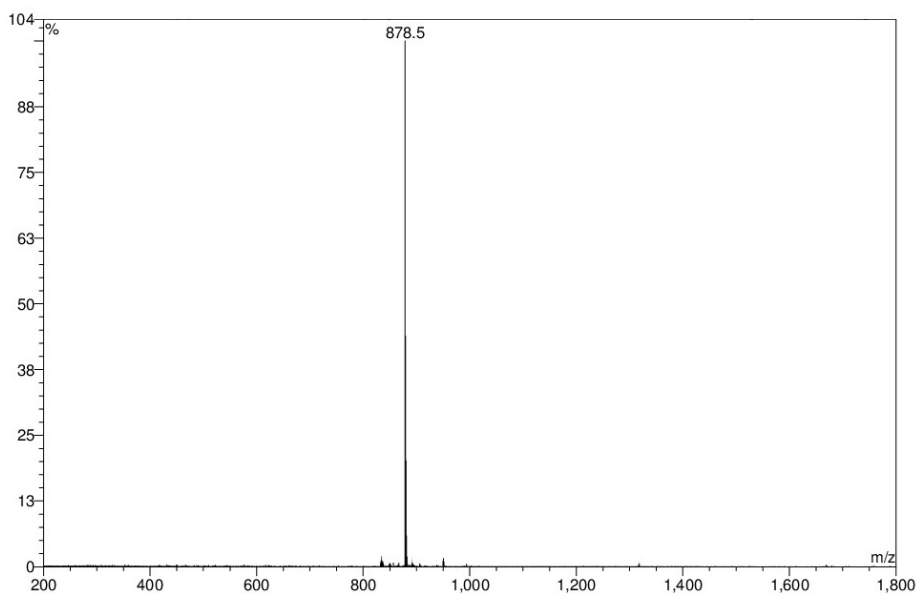
Figure A3. ESI-MS spectrum of Imp c. ESI-MS (m/z): $[M+H]^+$ 878.5 (found), 878.3 (calcd).
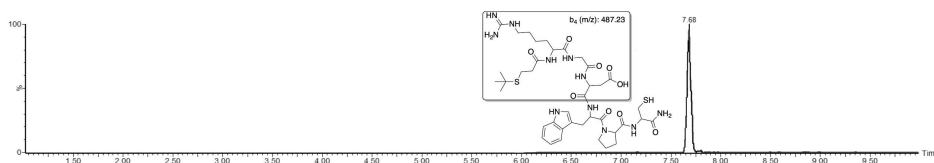
Figure A4. HPLC/ESI-MS/MS spectrum of the fragment b_4. ESI-MS/MS (m/z): $[M+H]^+$ 487.23 (found), 488.24 (calcd).
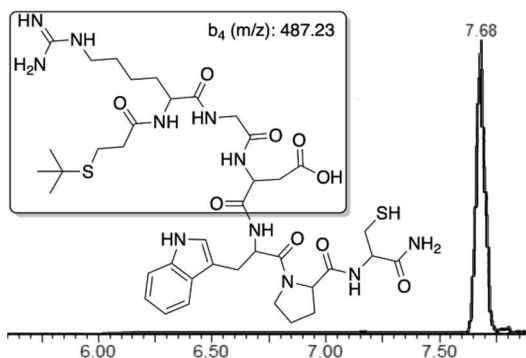
Figure A5 HPLC/ESI-MS/MS (zoom 5.60-7.54 min)spectrum of the fragment b_4. ESI-MS/MS (m/z): $[M+H]^+$ 487.23 (found), 488.24 (calcd).
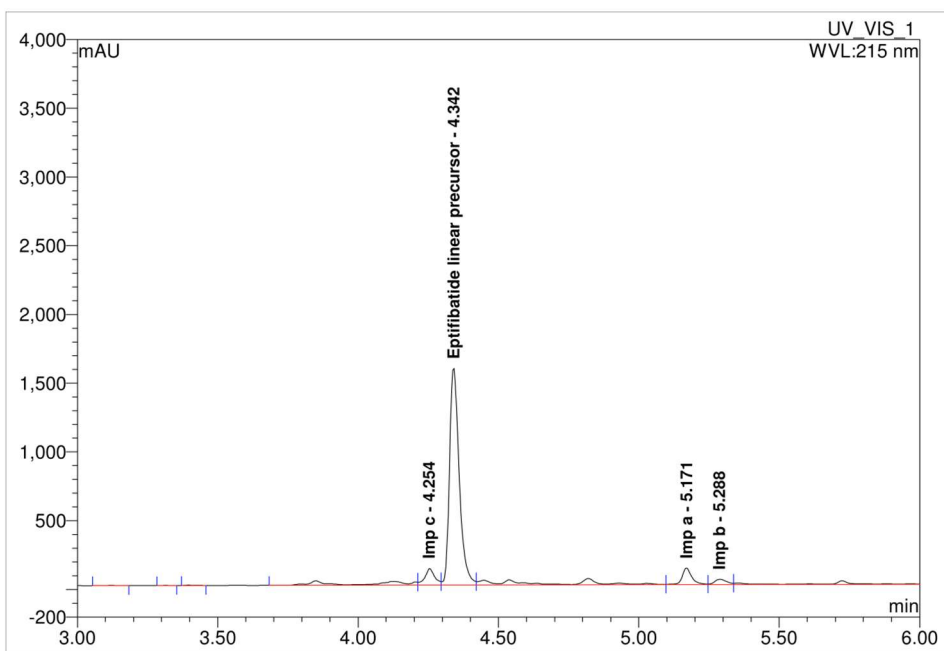
Figure A6. RP-UHPLC trace (zoom 3-6 min) of Eptifibatide linear precursor crude (STEP 1+2: 5 mmol scale). C18 column Waters Acquity CSH (130Å, 1.7 μm, 2.1 × 100 mm); temperature 45°C; flow: 0.5 mL/min. Eluents: 0.1% TFA in H_2O (A) and 0.1% TFA in CH_3CN (B); λ 215 nm; gradient: 5-95% B in A in 10 min. R_t 4.25 min: Imp c, R_t 4.34 min: Eptifibatide linear precursor. R_t 5.17 min: Imp a, R_t 5.29: Imp b.
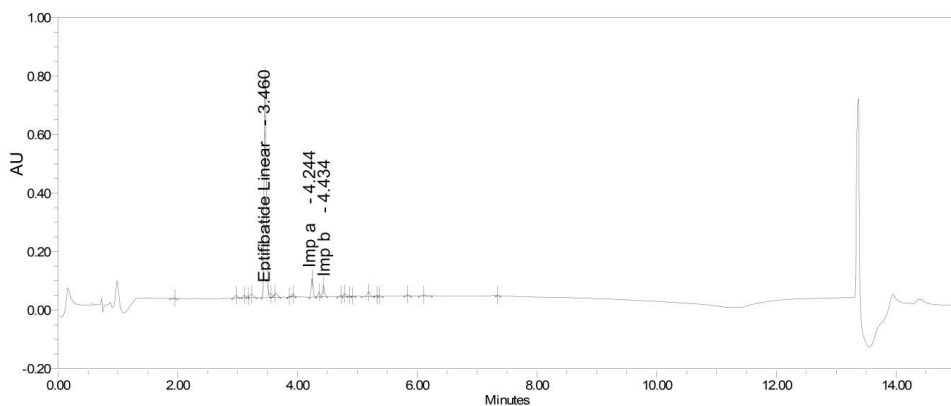
Figure A7. RP-HPLC trace of Eptifibatide linear precursor crude obtained following Procedure A1 (STEP 1+2, 70 mmol scale). Eptifibatide linear precursor. R_t 4.24 min: Imp a, R_t 4.43: Imp b.

160
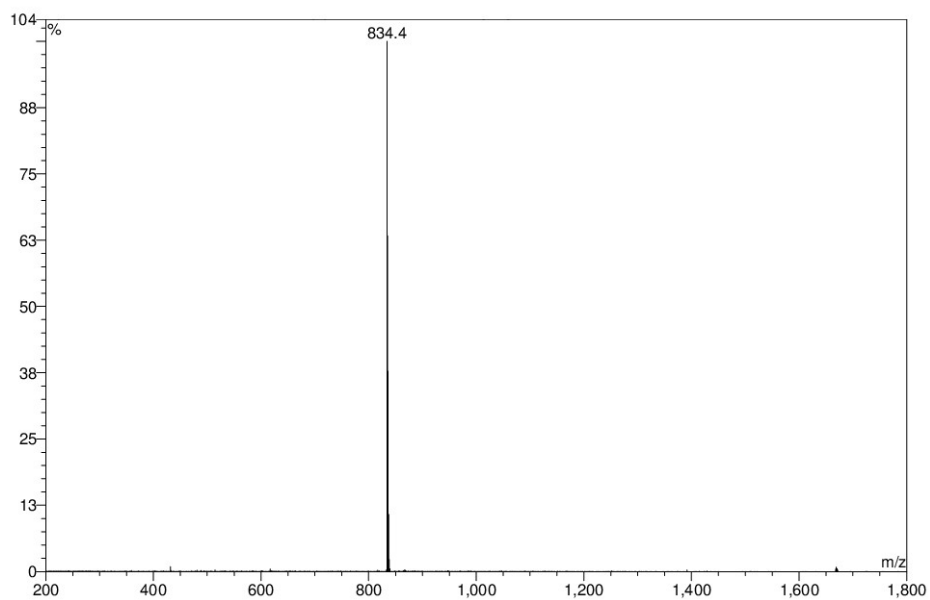
Figure A8. ESI-MS spectrum of Eptifibatide linear precursor. ESI-MS (m/z): [M+H]$^+$ 834.4 (found), 834.3 (calcd).
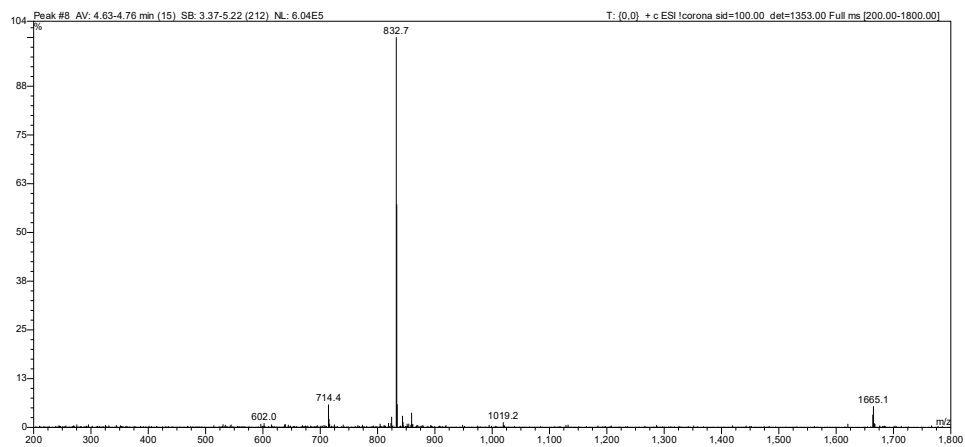
Figure A9. ESI-MS of impurity (Rt 4.67 min). ESI-MS (m/z): $[M+H]^+$ 1665.1 (found), $[M+H]^+$ 1665.9 (calcd), $[M+2H]^{2+}$ 832.7 (found); $[M+2H]^{2+}$ 833.4 (calcd).
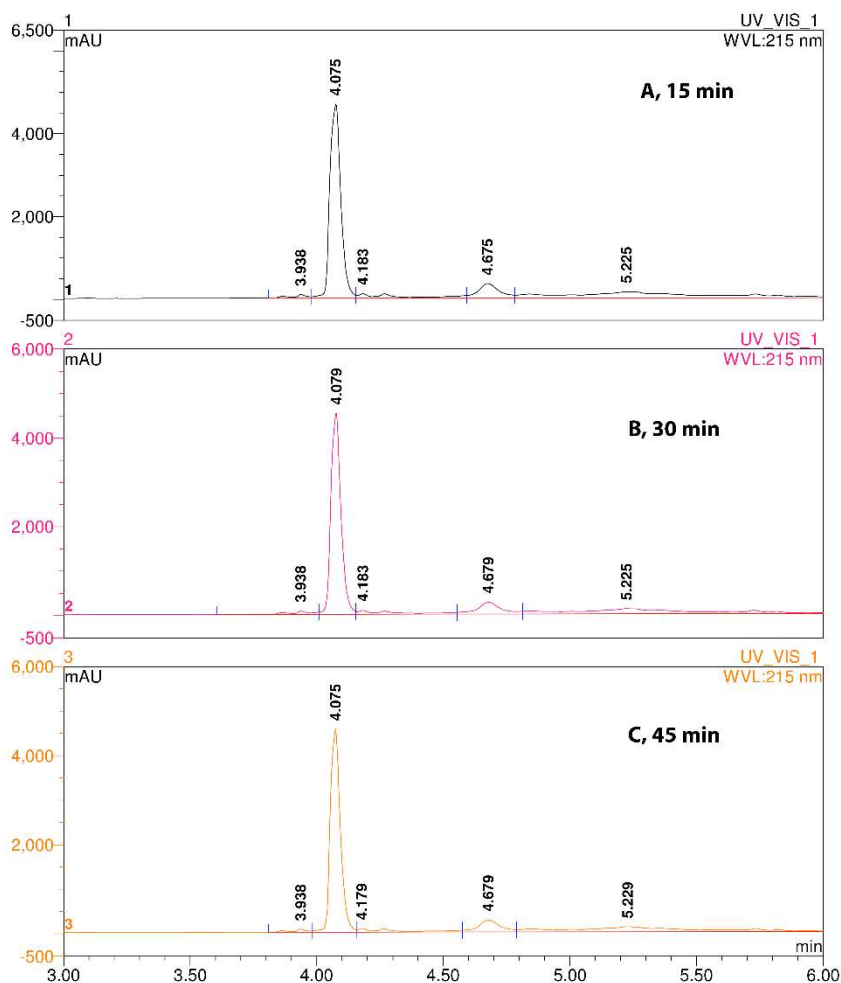
Figure A10. In process control of liquid-phase disulfide bond formation (0.5 mmol scale, 45 min): RP-UHPLC traces of Eptifibatide crude obtained by Eptifibatide linear precursor in H_2O:CH_3CN 2:1 (v/v) (5.3 mM), with addition of H_2O_2 in one-shot (0.8 equiv) at time 0, pH 9.5, r.t. RP-UHPLC: C18 column Waters Acquity CSH (130Å, 1.7 μm, 2.1 × 100 mm); temperature 45°C; flow: 0.5 mL/min. Eluents: 0.1% TFA in H_2O (A) and 0.1% TFA in CH_3CN (B); λ 215 nm; gradient: 5-95% B in A in 10 min. R_t 4.07 min: Eptifibatide TFA; R_t 4.67 min: Dimer impurity.
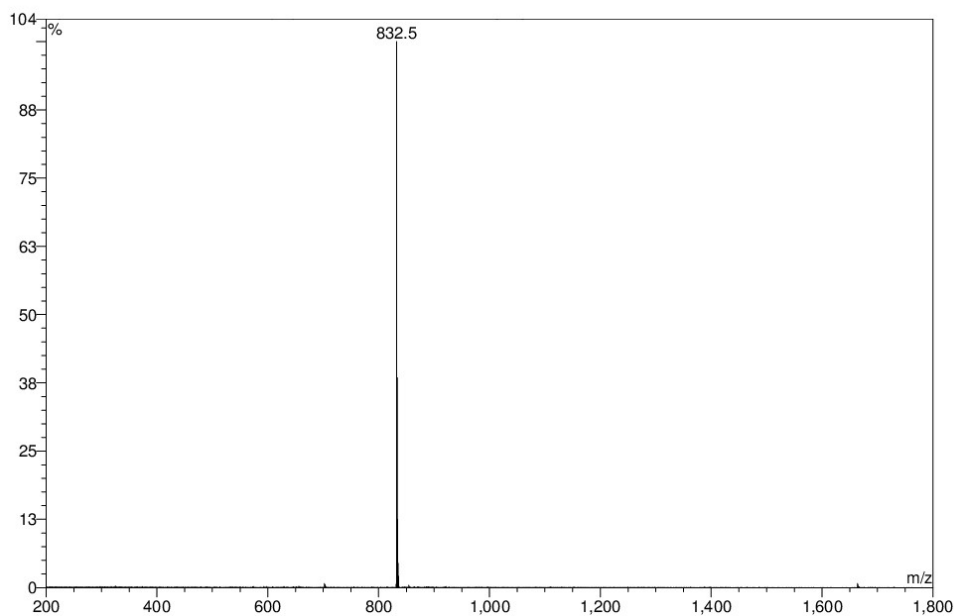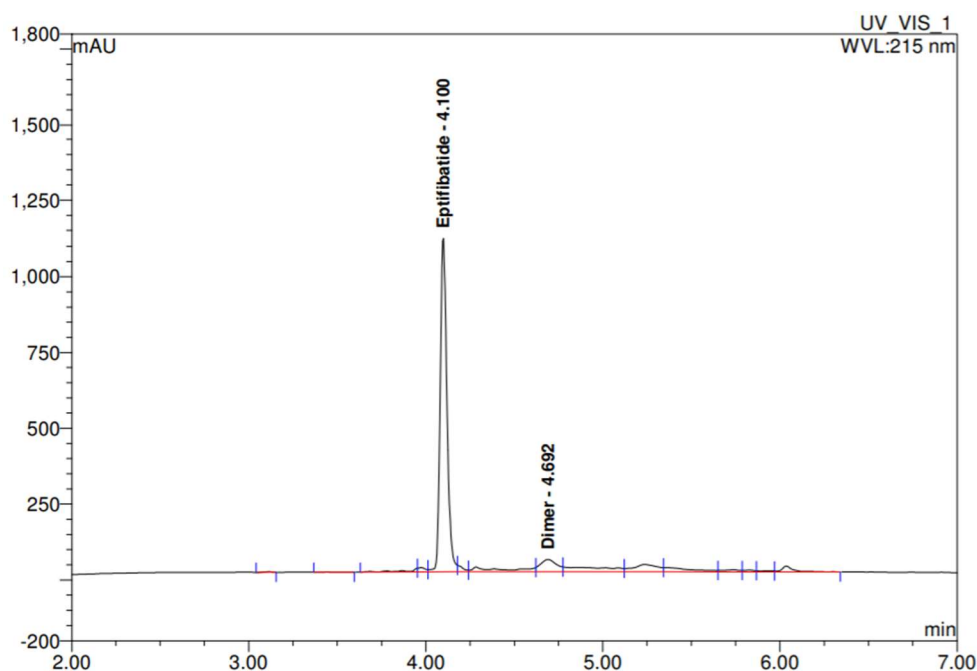
Figure A11. RP-UHPLC trace (zoom 2-7 min) of Eptifibatide TFA (STEP 3: 5 mmol scale). C18 column Waters Acquity CSH (130Å, 1.7 µm, 2.1 × 100 mm); temperature 45°C; flow: 0.5 mL/min. Eluents: 0.1% TFA in H_2O (A) and 0.1% TFA in CH_3CN (B); λ 215 nm; gradient: 5-95% B in A in 10 min. R_t 4.1 min: Eptifibatide TFA; R_t 4.7 min: Dimer impurity. ESI-MS spectrum of Eptifibatide TFA salt. ESI-MS (m/z): $[M+H]^+$ 832.5 (found), 832.3 (calcd).
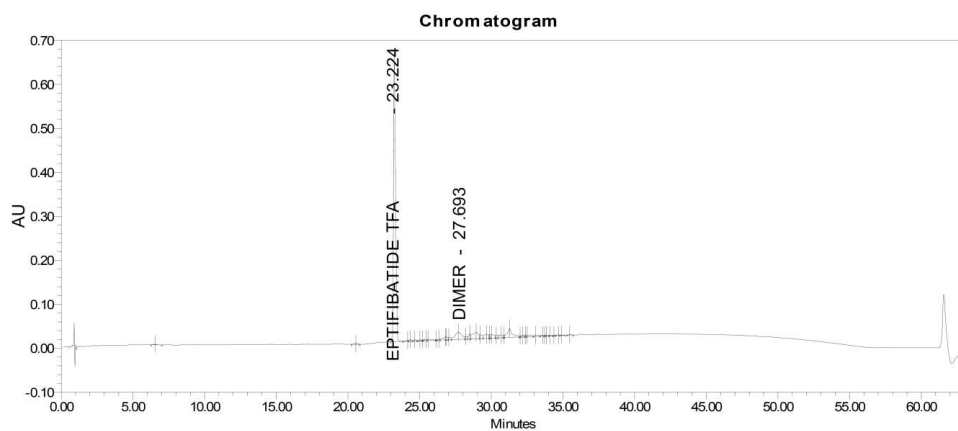
Figure A12. RP-UHPLC trace of Eptifibatide TFA obtained following Procedure A3 (STEP 3: 70 mmol scale). R_t 23.2 min: Eptifibatide TFA; R_t 27.7 min: Dimer impurity.

Figure A13. IPC trace by RP-UHPLC-ESI-MS of Har-Gly-Asp-Trp-Pro-Cys(MPA) obtained by solid-phase disulfide-exchange (50 °C, 90W, 30 min) in Strategy **C**. C18 column Waters Acquity CSH (130Å, 1.7 μm, 2.1 × 100 mm); temperature 45°C; flow: 0.5 mL/min. Eluents: 0.1% TFA in H_2O (A) and 0.1% TFA in CH_3CN (B); λ 215 nm; gradient: 5-95% B in A in 10 min.

Har-Gly-Asp-Trp-Pro-Cys-NH$_2$
[M+H]$^+$: 747.32

Har-Gly-Asp-Trp-Pro-Cys(2-MEA)-NH$_2$ (21.5 %)
[M+H]$^+$: 821.33
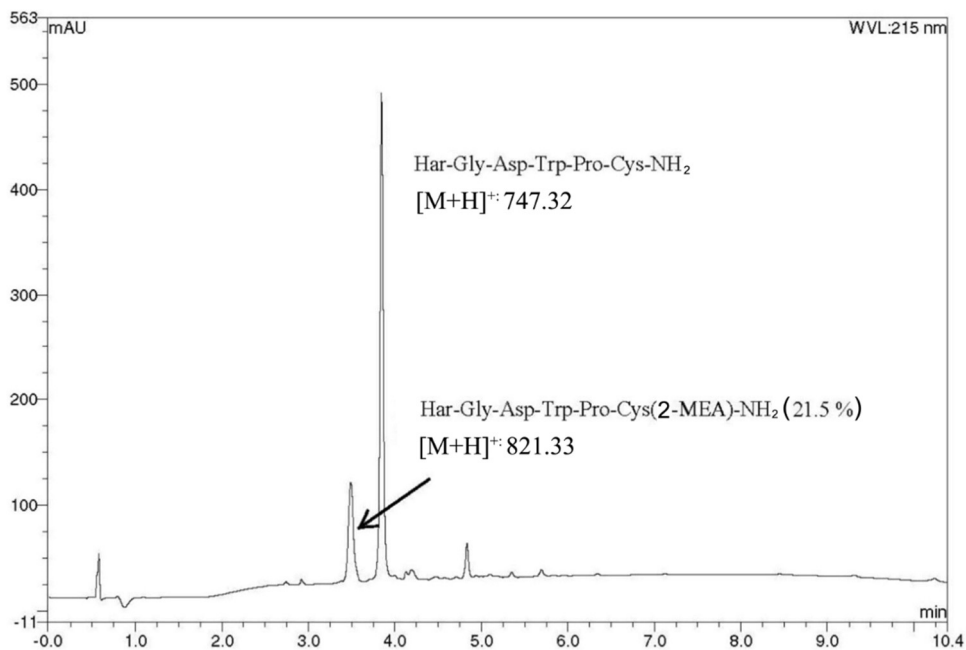
Figure A14. IPC trace by RP-UHPLC to monitor Cys deprotection in Har(Pbf)Gly-Asp(OtBu)-Trp(Boc)-Pro-Cys(StBu)-Rink Amide AM resin using 2-MEA 20% (v/v) in DMF: detection of Cys(2-MEA) in peptide-resin. C18 column Waters Acquity CSH (130Å, 1.7 μm, 2.1 × 100 mm); temperature 45°C; flow: 0.5 mL/min. Eluents: 0.1% TFA in H$_2$O (A) and 0.1% TFA in CH$_3$CN (B); λ 215 nm; gradient: 5-95% B in A in 10 min.
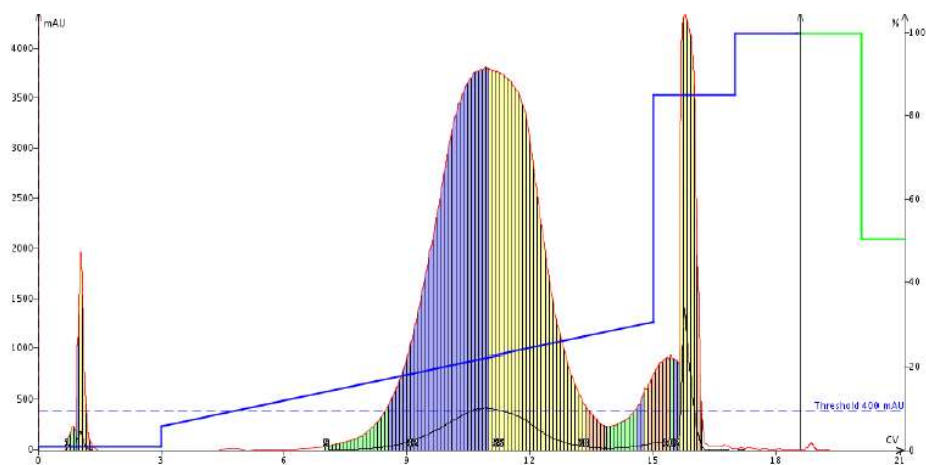
Figure A15. Chromatogram report of the different fractions obtained by Flash column chromatography (FCC) of Eptifibatide TFA (6.6 mmol crude). FCC equipment: Biotage Isolera One equipped with SNAP Ultra C18 120g column (volume 164 mL), crude loading 5%. Eluents: 0.1% TFA (v/v) in H_2O (A) and 0.1%TFA (v/v) in CH_3CN (B); linear gradient in 12 column volumes, 5-30% (v/v) B in A; flow rate: 50 mL/min; λ 215 nm.
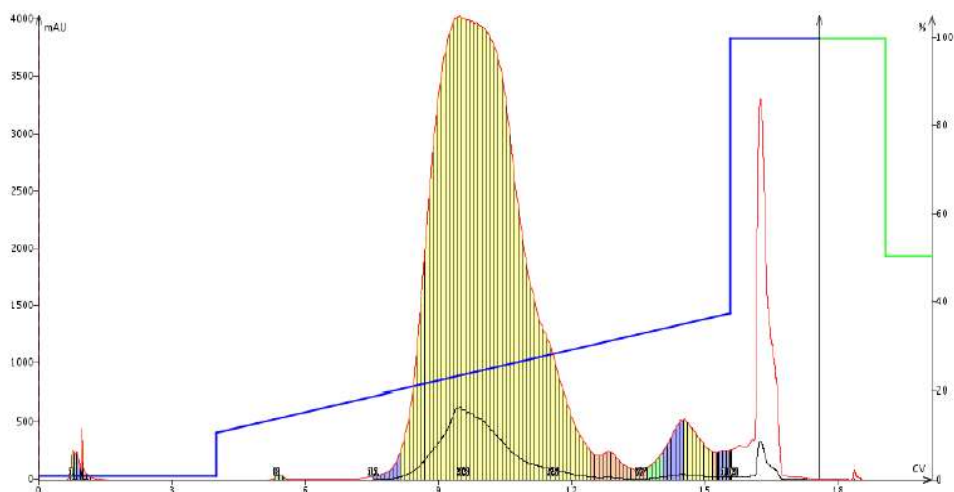
Figure A16. Chromatogram report of the different fractions obtained by Flash column chromatography (FCC) of Eptifibatide TFA (6.5 mmol crude). FCC equipment: Biotage Isolera One equipped with SNAP Ultra C18 120g column (volume 164 mL), crude loading 5%. Eluents: 0.1% TFA (v/v) in H_2O (A) and 0.1%TFA (v/v) in CH_3CN (B); linear gradient in 12 column volumes, 10-37% (v/v) B in A; flow rate: 50 mL/min; λ 215 nm.
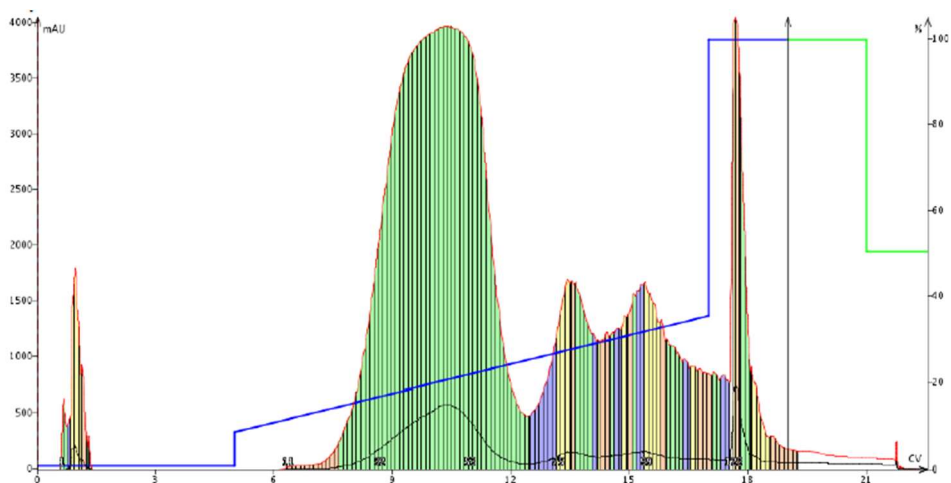
Figure A17. Chromatogram report of the different fractions obtained by Flash column chromatography (FCC) of Eptifibatide TFA (10.2 mmol crude). FCC equipment: Biotage Isolera One equipped with SNAP Ultra C18 120g column (volume 164 mL), crude loading 8%. Eluents: 0.1% TFA (v/v) in H_2O (A) and 0.1%TFA (v/v) in CH_3CN (B); linear gradient in 12 column volumes, 10-37% (v/v) B in A; flow rate: 50 mL/min; λ 215 nm.
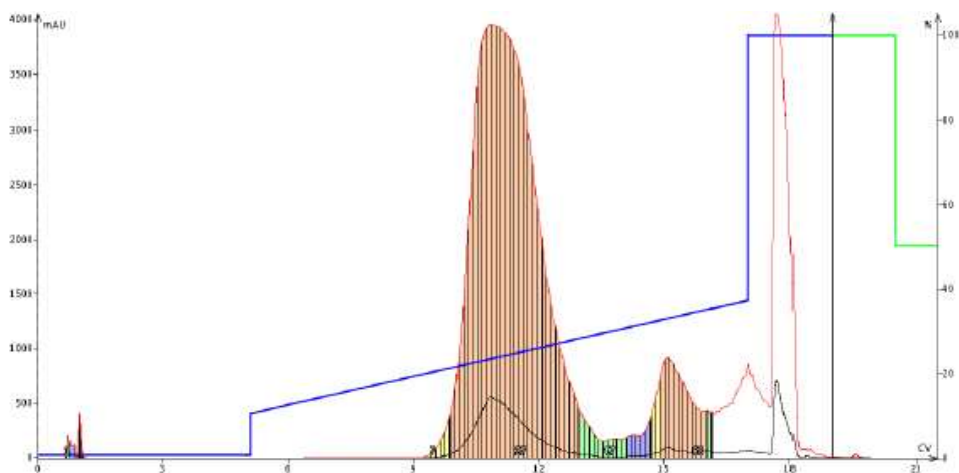
Figure A18. Chromatogram report of the different fractions obtained by Flash column chromatography (FCC) of Eptifibatide TFA (5 mmol crude). FCC equipment: Biotage Isolera One equipped with SNAP Ultra C18 120 g column (volume 164 mL), crude loading 4%. Eluents: 0.1% TFA (v/v) in H_2O (A) and 0.1%TFA (v/v) in CH_3CN (B); linear gradient in 12 column volumes, 10-37% (v/v) B in A; flow rate: 50 mL/min; λ 215 nm.
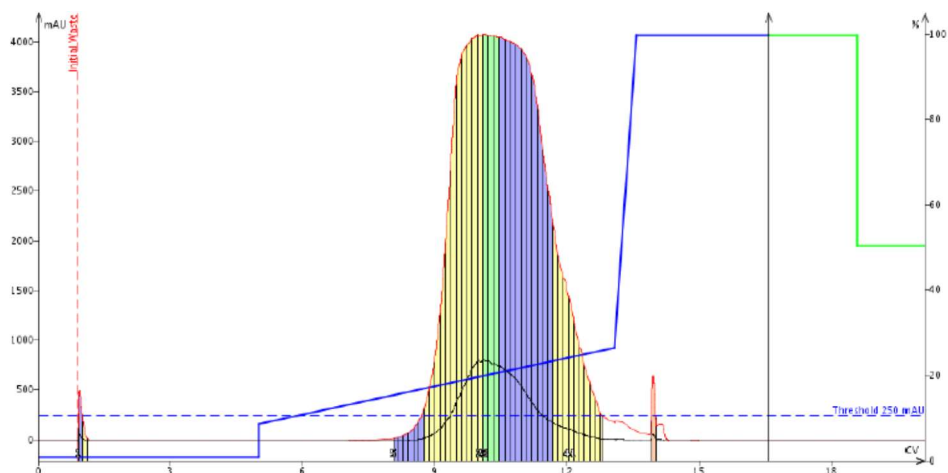
Figure A19. Chromatogram report of the different fractions obtained by Flash column chromatography (FCC) of Eptifibatide TFA (10.5 mmol crude). FCC equipment: Biotage Isolera One equipped with SNAP Ultra C18 400g column (volume 590 mL), crude loading 2.5%. Eluents: 0.1% TFA (v/v) in H_2O (A) and 0.1%TFA (v/v) in CH_3CN (B); linear gradient in 12 column volumes, 10-37% (v/v) B in A; flow rate: 100 mL/min; λ 215 nm.
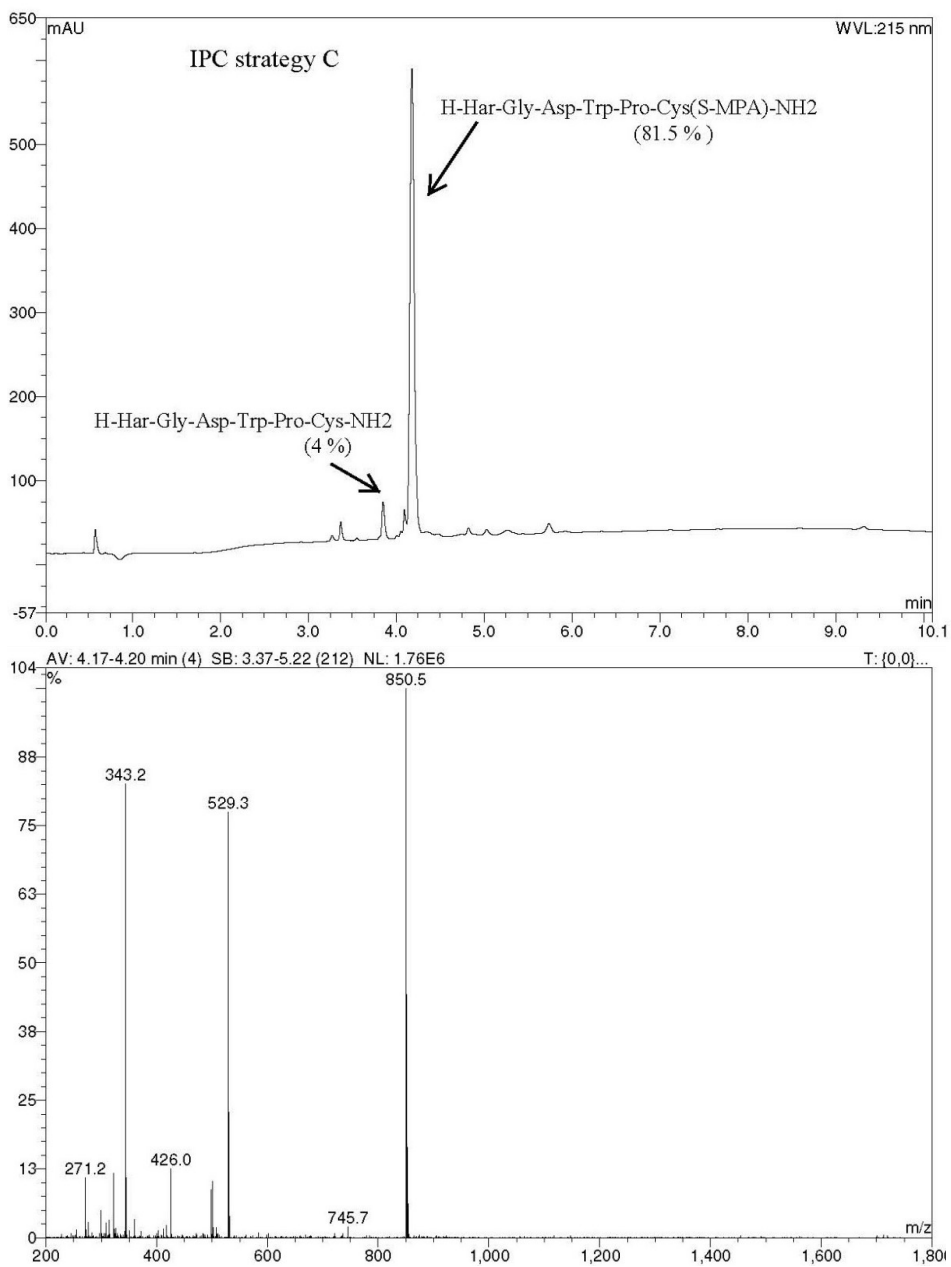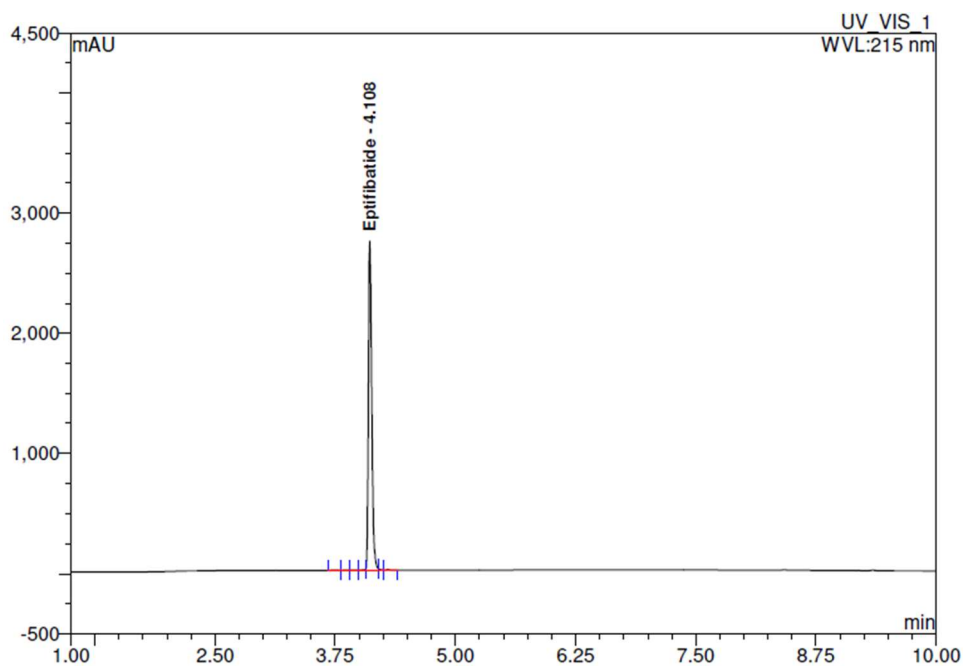

Figure A20. RP-HPLC trace (zoom 1-10 min) of Eptifibatide TFA purified (STEP 4: 5 mmol). C18 column Waters Acquity CSH (130Å, 1.7 μm, 2.1 × 100 mm); temperature 45°C; flow: 0.5 mL/min. Eluents: 0.1% TFA in H_2O (A) and 0.1% TFA in CH_3CN (B); λ 215 nm; gradient: 5-95% B in A in 10 min. R_t 4.1 min: Eptifibatide TFA purified.
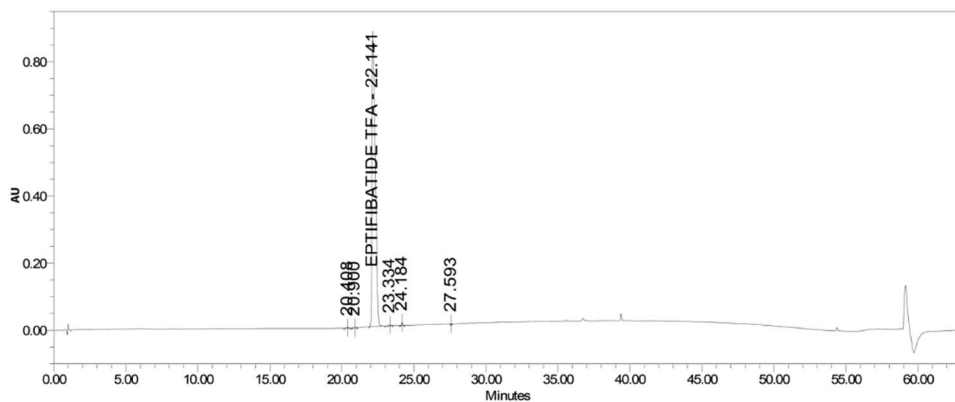
Figure A21. RP-HPLC trace of Eptifibatide TFA purified obtained following Procedure A3 (STEP 4: 70 mmol scale). R_t 22.1 min: pure Eptifibatide TFA.
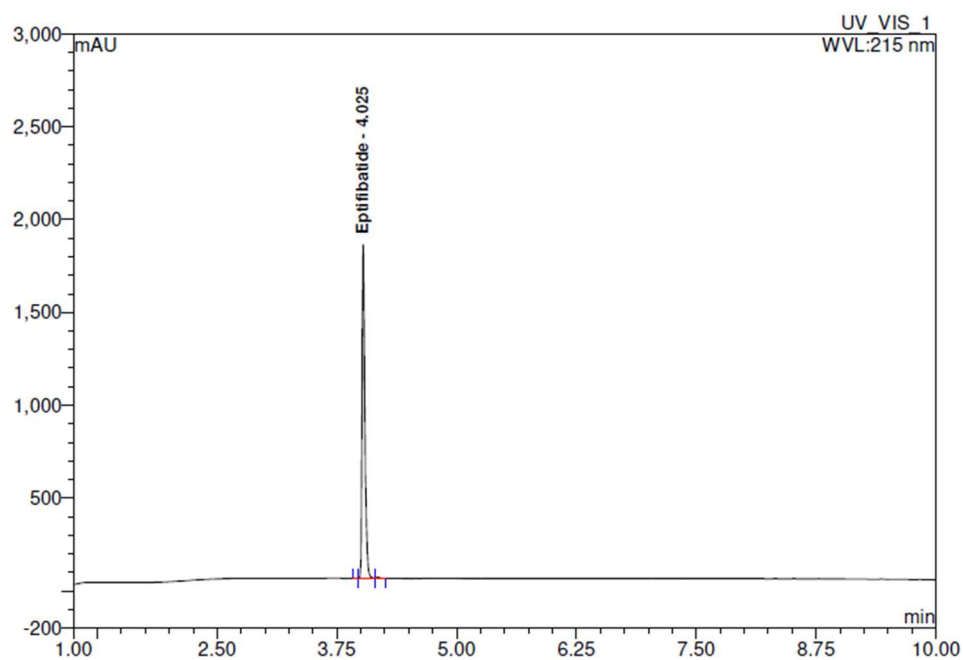
Figure A22. RP-HPLC trace (zoom 1-10 min) of Eptifibatide acetate (STEP 5: 5 mmol). C18 column Waters Acquity CSH (130Å, 1.7 μm, 2.1 × 100 mm); temperature 45°C; flow: 0.5 mL/min. Eluents: 0.1% (v/v) TFA in H_2O (A) and 0.1% (v/v) TFA in CH_3CN (B); λ 215 nm; gradient: 5-95% (v/v) B in A in 10 min. R_t 4.0 min: Eptifibatide acetate.
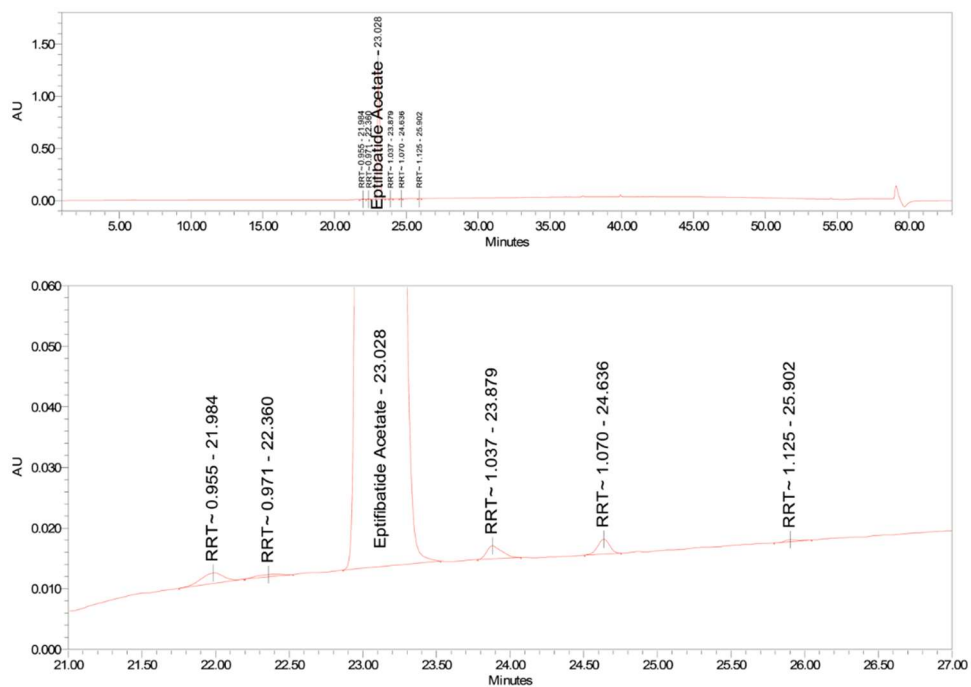
Figure A23. RP-HPLC trace of Eptifibatide acetate obtained following Procedure A3 (STEP 5: 70 mmol scale, above: full chromatogram, below: zoom 21-27 min). R_t 23.0 min: Eptifibatide acetate.

Analytical procedures

Procedure A1. HPLC analytical procedure to evaluate purity of Eptifibatide linear precursor crude (70 mmol scale)

C18 column Waters BEH (130Å, 1.7 μm, 2.1 × 100 mm); temperature 40 °C; flow: 0.5 mL/min. Eluents: 0.1% (v/v) TFA in MilliQ Water (A) and 0.1% (v/v)TFA in CH₃CN (B); λ 215 nm; gradient: 5-95% (v/v) B in A in 10 min.

Procedure A2. Procedure to calculate of Eptifibatide linear precursor crude identity (70 mmol scale)

$$\text{Diff R}_t = \frac{R_{t_s} - R_{t_{std}}}{R_{t_{std}}} \times 100$$

R_{t_s}: retention time of Eptifibatide acetate peak in the sample solution chromatogram

$R_{t_{std}}$: retention time of Eptifibatide acetate peak in the chromatogram of the first injection of the calibration standard solution

Diff R$_t$: ± 5%

Procedure A3. HPLC analytical procedure to evaluate the purity of: Eptifibatide TFA crude, purified Eptifibatide TFA salt, and Eptifibatide acetate salt (70 mmol scale).

C8 column Phenomenex Kinetex (100Å, 2.6 μm, 3.0 × 150 mm); temperature 20°C; flow: 0.8 mL/min. Eluents: 0.1% (v/v) TFA in H₂O (A) and 0.1% (v/v) TFA in CH₃CN (B); λ 215 nm; gradient: 07-99% (v/v) B in A in 58 min. R$_t$ 23.2 min: Eptifibatide TFA; R$_t$ 27.7 min: Dimer impurity (absent in STEP4 and STEP5).

Procedure A4. ESI-MS of: Eptifibatide TFA linear precursor, Eptifibatide TFA crude, purified Eptifibatide TFA salt, and purified Eptifibatide acetate salt

MS method: 300-1200 m/z; 0-18 min; ionization mode: ESI^+; data continuum; cone 40 V. MS tune conditions: capillary 1.20 kV; cone 40 V; source temperature 120 °C; probe temperature 500 °C.

Procedure A5. HPLC (relative) assay[161] against a reference standard of Eptifibatide acetate

$$\text{Eptifibatide \% w/w} = \frac{A_c}{A_{std}} \times \frac{C_{std}}{C_c} P_{std}$$

A_c: Eptifibatide acetate area count of the sample solution injection

A_{std}: Eptifibatide acetate average area count of the calibration standard solution (6 injections)

C_c: Eptifibatide acetate concentration of the sample solution (mg/mL)

C_{std}: Eptifibatide acetate reference standard concentration (mg/mL)

P_{std}: Eptifibatide acetate reference standard purity (%)

Procedure A6. HPLC analytical procedure for In Process Control (IPC) to monitor disulfide bond formation

200μL of the reaction mixture were added with 100μL TFA into 2mL glass vial to quench disulfide bond formation reaction. Then, 200μL H_2O were added. The solution was analyzed by RP-UHPLC ESI-MS using 5-95% (v/v) B in A in 10 min. A: 0.1% (v/v) TFA in H_2O, B: 0.1% (v/v) TFA in CH_3CN. Conversion % of Eptifibatide linear precursor crude in Eptifibatide TFA salt:

$$C(\%) = \frac{\text{Eptifibatide TFA (\% A/A)}}{\text{Eptifibatide TFA (\% A/A)} + \text{Eptifibatide linear precursor (\% A/A)}} \times 100$$

Procedure A7. Headspace Gas-chromatography (HS-GC) analytical procedure to evaluate CH_3CN content in Eptifibatide acetate

Gas-chromatography (GC) conditions: Silica capillary column Agilent DB-624 (1.8 µm, 0.32 mm × 30 m); split ratio 1:10; column gradient temperature: isotherm 40 °C for 4 min, from 40 °C to 60 °C at 8 °C/min, from 60 °C to 85 °C at 5 °C/min, isotherm 85 °C for 2 min, from 85 °C to 220 °C at 30 °C/min, isotherm 85 °C for 2 min. Helium (BOC Gases, ultrapure) as carrier gas at a flow rate of 1 mL/min. Detector: FID (Air 400 mL/min, Hydrogen 40 mL/min).

Headspace (HS) conditions: oven temperature: 110 °C; loop temperature: 130 °C; Transfer line temperature: 150°C; vial size: 10 mL filled with 1mL of sample solution; vial equilibration time: 15 min; pressurization time: 0.2 min; vial pressurization: 15 psi.

Calculation:

$$\text{Solvent ppm} = \frac{A_{\text{sample}}}{A_{\text{std cal}}} \times \frac{C_{\text{std cal}}}{C_{\text{sample}}} \times 10^6$$

A_{sample}: CH$_3$CN area count of the sample solution injection

$A_{\text{std cal}}$: CH$_3$CN average area count of calibration standard solution injections (6)

C_{sample}: CH$_3$CN concentration of the sample solution (mg/mL)

$C_{\text{std cal}}$: CH$_3$CN reference standard concentration (mg/mL)

Solvent ppm < 410 ppm

Procedure A8. Ion exchange chromatography (IC) to evaluate residual TFA and acetate content in Eptifibatide acetate

IC conditions: C8 column Dionex Ion-Pac AS11-HC, pre-column (13 µm, 4.0 × 50 mm); analytical column (2000Å, 70 nm, 4.0 × 250 mm); temperature 30°C; flow: 1.0 mL/min. Eluent: H$_2$O, eluent generator cartridge: KOH; λ 215 nm; gradient: 1-5 mM of KOH in 15 min, 5-55 mM of KOH in 25 min. Rt 21.00 ± 1 min: TFA

Calculation:

$$\text{Solvent ppm} = \frac{A_{\text{sample}}}{A_{\text{std cal}}} \times \frac{C_{\text{std cal}}}{C_{\text{sample}}} \times 10^6$$

A$_{\text{sample}}$: TFA area count of the sample solution injection

A$_{\text{std cal}}$: TFA average area count of calibration standard solution injections

(6)

C$_{\text{sample}}$: TFA concentration of the sample solution (mg/mL)

C$_{\text{std cal}}$: TFA reference standard concentration (mg/mL)

Calculation:

$$\text{A) cf} = \frac{\text{mw}_{\text{acetate}}}{\text{mw}_{\text{sodium acetate trihydrate}}} = 0.434$$

$$\text{B) } C_c = \frac{A_c}{A_{std}} \times C_{std} \times \text{cf}$$

$$\text{C) Acetate \% w/w} = \frac{C_c}{C_{API}} \times 100$$

cf: correction factor acetate/sodium acetate trihydrated

mw: molecular weight

C$_{\text{sample}}$: Acetate concentration of the sample solution (mg/mL)

C$_{\text{std cal}}$: Sodium acetate trihydrate reference standard concentration (mg/mL),

A$_{\text{sample}}$: Acetate area count of the sample solution injection

A$_{\text{std cal}}$: Acetate average area count of calibration standard solution (6 injections)

C$_{\text{API}}$: Eptifibatide acetate concentration of the sample solution injection (mg/mL)

H$_1$-RELAXIN

Table RI. Standard microwave-assisted coupling cycle protocol at 90°C

Step	Temperature (°C)	Power (W)	Hold Time (s)	Delta T (°C)
Deprotection	80	200	30	2
	90	50	70	1
Coupling	75	170	15	2
	90	30	100	1

Table RII. Mild microwave-assisted coupling cycle protocol at 50°C

Step	Temperature (°C)	Power (W)	Hold Time (s)	Delta T (°C)
Deprotection	50	90	240	2
	22	0	120	2
Coupling	25	50	10	2
	49	35	780	1

Table RIII. On-resin MW-assisted CuAAC at 80°C for 10 min, for 0.025 mmol scale

Temperature (°C)	Power (W)	Hold Time (s)	Delta T (°C)
75	100	30	2
80	60	600	1

Table RIV. On-resin MW-assisted CuAAC at 55°C, for 10 min for 0.025 mmol scale

Temperature (°C)	Power (W)	Hold Time (s)	Delta T (°C)
49	150	15	2
54	30	600	1

Table RV. On-resin MW-assisted CuAAC at 55°C for 5 min, for 0.025 mmol scale

Temperature (°C)	Power (W)	Hold Time (s)	Delta T (°C)
49	150	30	2
54	30	300	1

Table RVI. On-resin MW-assisted CuAAC at 55°C for 10 min, for 0.1 mmol scale

Temperature (°C)	Power (W)	Hold Time (s)	Delta T (°C)
51	150	30	2
54	40	600	1

HPLC-ESI-MS characterization of linear references
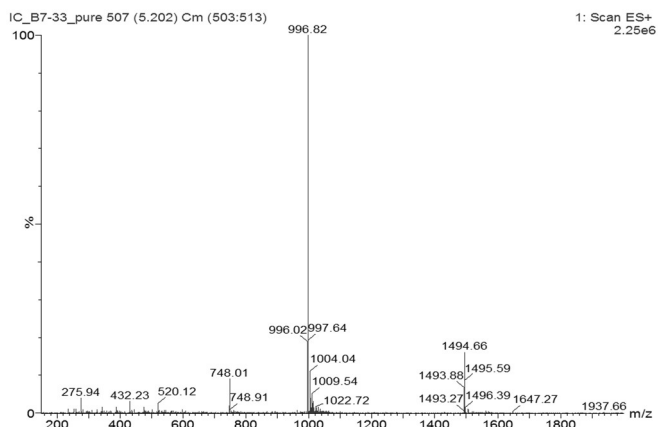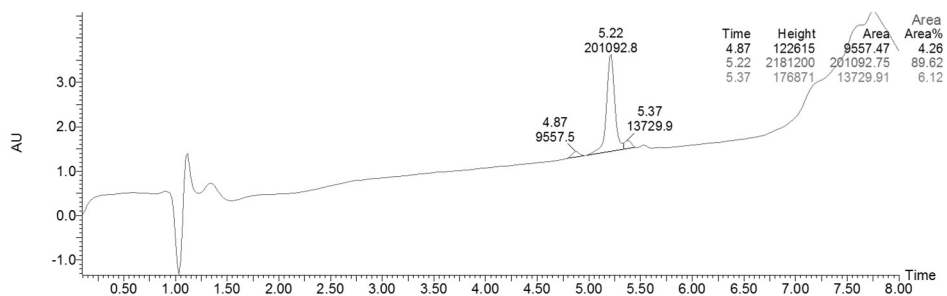
Figure R1. RP-HPLC trace of the Reference **I**. BIOshell C18 column (Å160, 2,7 μm 3,0 x 100 mm), temperature 20°C; flow: 0,6 mL/min; λ 215 nm. Eluents: 0.1% (v/v) TFA in H_2O (A) and 0.1% (v/v) TFA in CH_3CN (B); gradient: 10-60% (v/v) B in A in 5 min. R_t 5.2 min: Reference **I**. ESI-MS (m/z): $[M+H]^+$: 2986.7 (Calcd), $[M+2H]^{2+}$: (found), 1493.8(Calcd), $[M+3H]^{3+}$: 996.8 (found), 996.2 (Calcd).
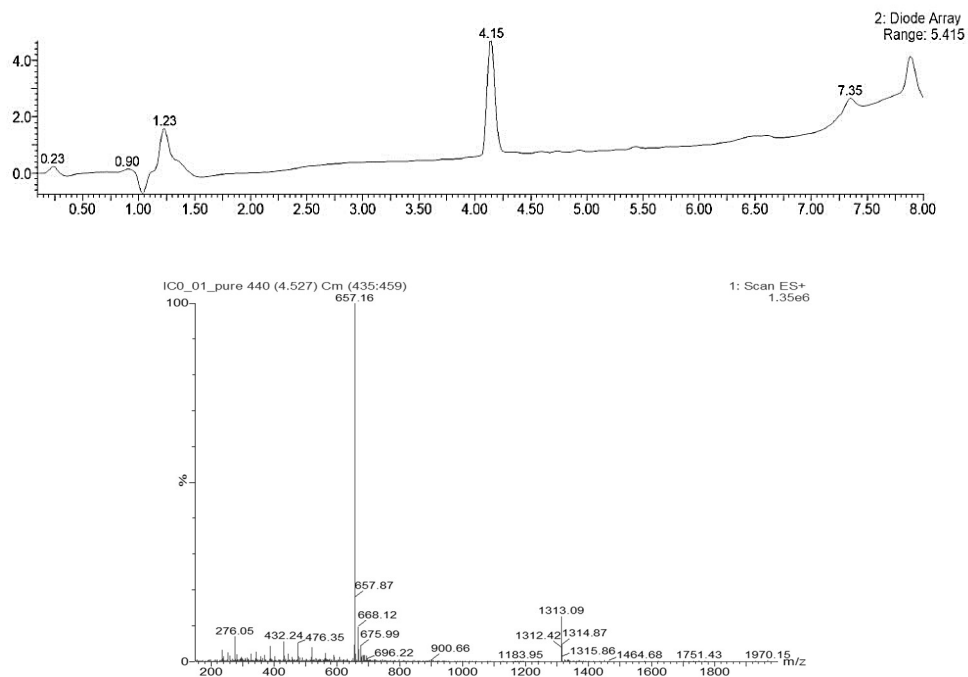
Figure R2. RP-HPLC trace of the Reference **II**. BIOshell C18 column (Å160, 2,7 µm 3,0 x 100 mm), temperature 20°C; flow: 0,6 mL/min; λ 215 nm. Eluents: 0.1% (v/v) TFA in H$_2$O (A) and 0.1% (v/v) TFA in CH$_3$CN (B); gradient: 10-60% (v/v) B in A in 5 min. R$_t$ 4.2 min: Reference **II**. ESI-MS (m/z): [M+H]$^+$: 1312.1 (found), 1312.8 (Calcd), [M+2H]$^{2+}$: 657.2 (found), 657.1 (Calcd).
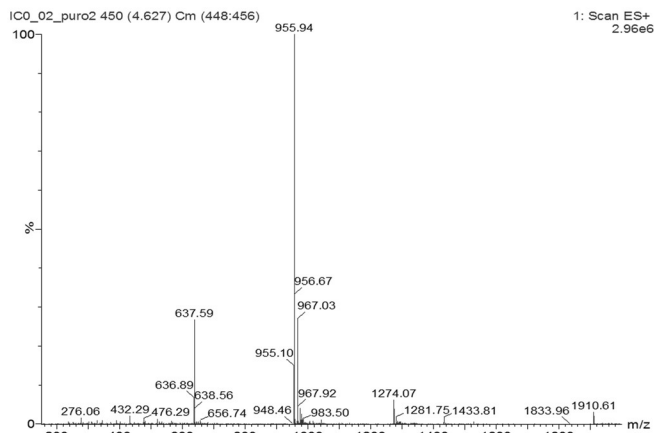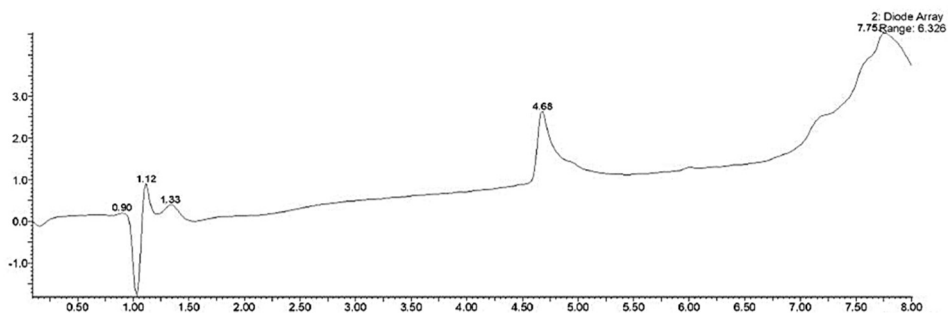
Figure R3. RP-HPLC trace of the Reference **III**. BIOshell C18 column (Å160, 2,7 μm 3,0 x 100 mm), temperature 20°C; flow: 0,6 mL/min; λ 215 nm. Eluents: 0.1% (v/v) TFA in H_2O (A) and 0.1% (v/v) TFA in CH_3CN (B); gradient: 10-60% (v/v) B in A in 5 min. R_t 4.7 min: Reference **III**. ESI-MS (m/z): [M+H]$^+$: 1910.6 (found), 1910.2 (Calcd), [M+2H]$^{2+}$: 955.4 (found), 956.1 (Calcd). [M+3H]$^+$: 637.6 (found), 637.5 (Calcd).
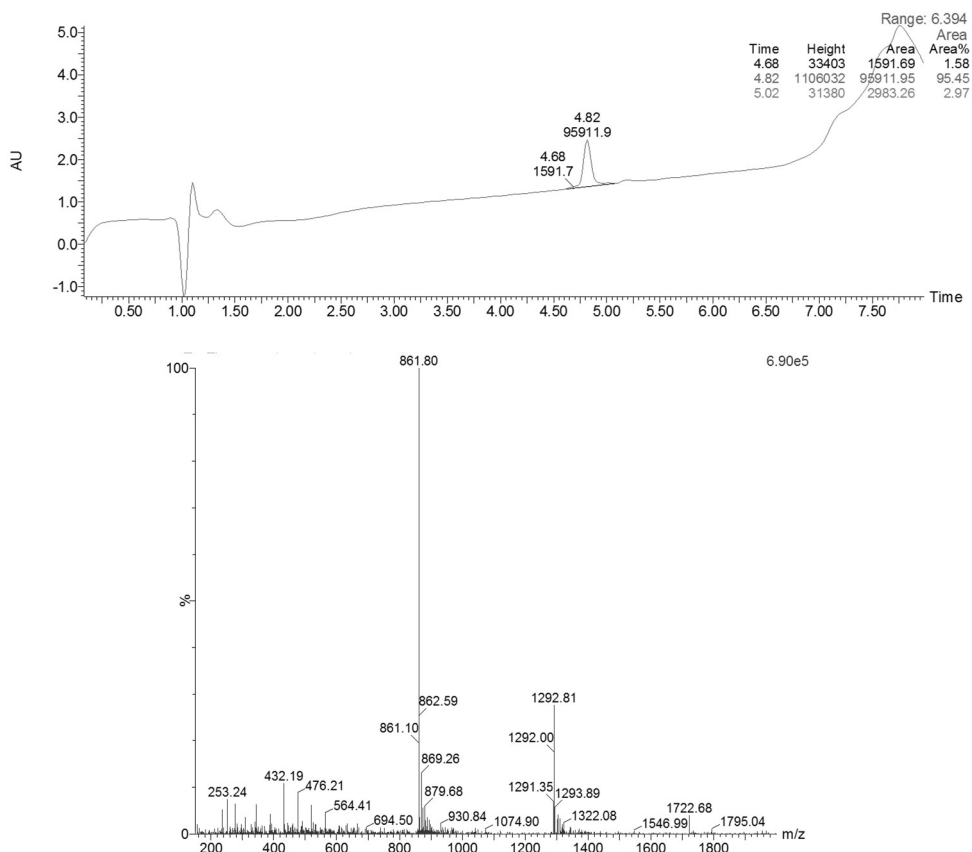
Figure R4. RP-HPLC trace of the Reference **IV**. BIOshell C18 column (Å160, 2,7 μm 3,0 x 100 mm), temperature 20°C; flow: 0,6 mL/min; λ 215 nm. Eluents: 0.1% (v/v) TFA in H$_2$O (A) and 0.1% (v/v) TFA in CH$_3$CN (B); gradient: 10-60% (v/v) B in A in 5 min. R$_t$ 4.8 min: Reference **IV**. ESI-MS (m/z): [M+H]$^+$: 2583.5 (Calcd), [M+2H]$^{2+}$: 1292.8 (found), 1292.3 (Calcd), [M+3H]$^+$: 861.8 (found), 861.8 (Calcd).

HPLC-ESI-MS characterization of stapled peptides
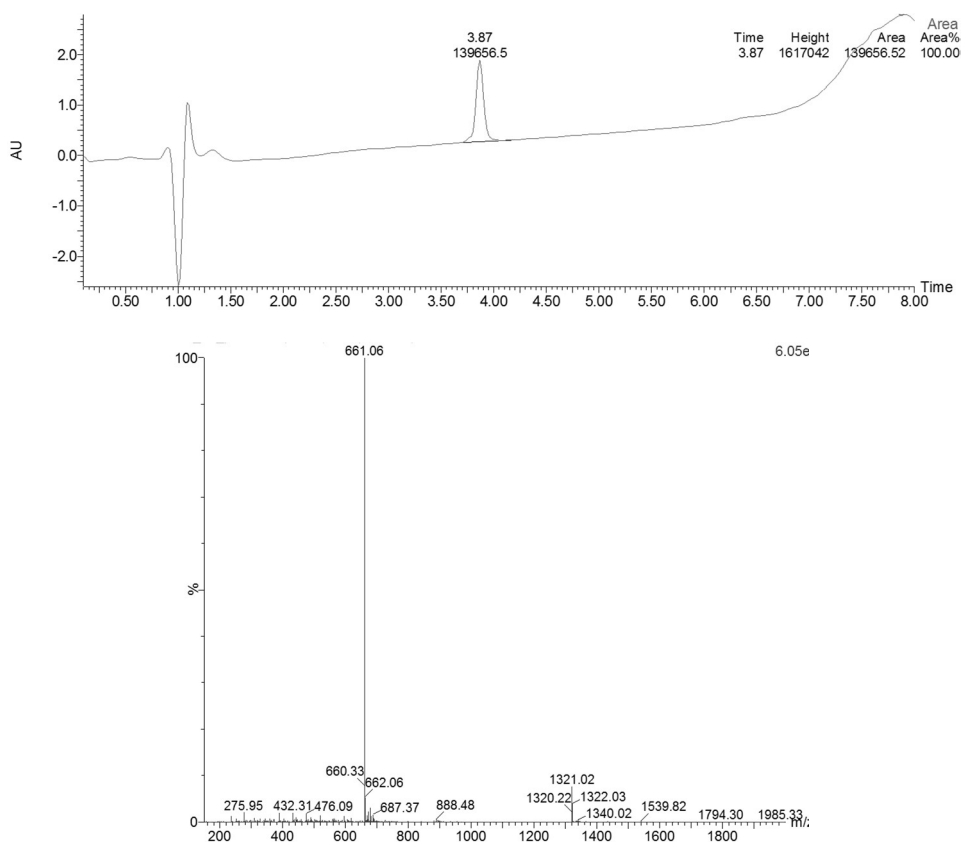
Figure R5. RP-HPLC trace of the Stapled peptide **VR**. BIOshell C18 column (Å160, 2,7 μm 3,0 x 100 mm), temperature 20°C; flow: 0,6 mL/min; λ 215 nm. Eluents: 0.1% (v/v) TFA in H_2O (A) and 0.1% (v/v) TFA in CH_3CN (B); gradient: 20-60% (v/v) B in A in 5 min. R_t 3.9 min: Stapled peptide **VR**. ESI-MS (m/z): $[M+H]^+$: 1321.0 (found), 1320.6 (Calcd), $[M+2H]^{2+}$: 661.1 (found), 660.8 (Calcd).
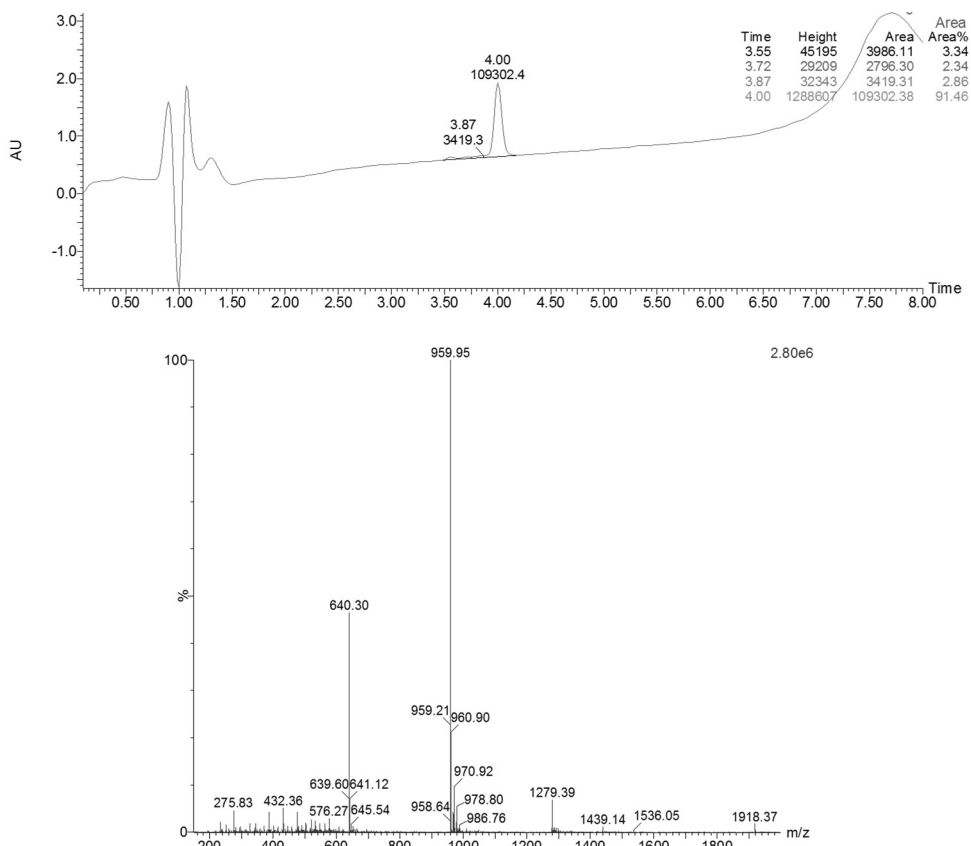
Figure R6. RP-HPLC trace of the Stapled peptide **VIR**. BIOshell C18 column (Å160, 2,7 μm 3,0 x 100 mm), temperature 35°C; flow: 0,6 mL/min; λ 215 nm. Eluents: 0.1% (v/v) TFA in H$_2$O (A) and 0.1% (v/v) TFA in CH$_3$CN (B); gradient: 20-60% (v/v) B in A in 5 min. R$_t$ 4.0 min: Stapled peptide **VIR**. ESI-MS (m/z): [M+H]$^+$: 1918.4 (found), 1919.0 (Calcd), [M+2H]$^{2+}$: 960.0 (found), 960.0 (Calcd), [M+3H]$^{3+}$: 640.3 (found), 640.3 (Calcd).
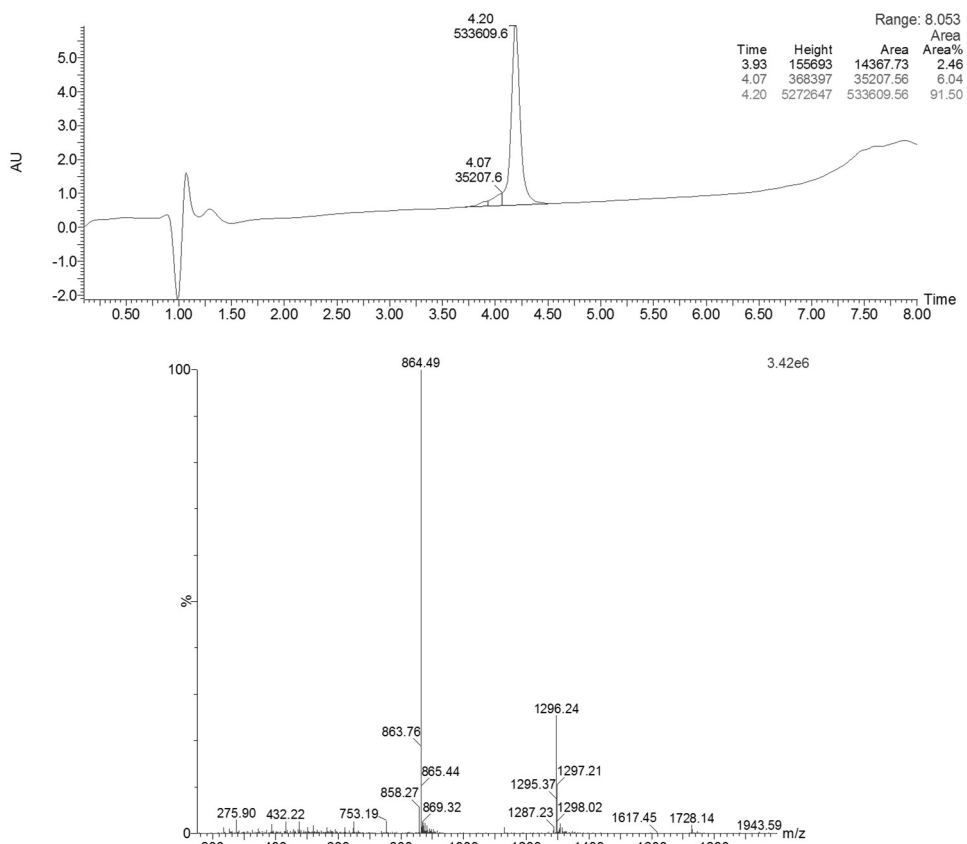
Figure R7. RP-HPLC trace of the Stapled peptide **VIIR**. BIOshell C18 column (Å160, 2,7 μm 3,0 x 100 mm), temperature 35°C; flow: 0,6 mL/min; λ 215 nm. Eluents: 0.1% (v/v) TFA in H_2O (A) and 0.1% (v/v) TFA in CH_3CN (B); gradient: 20-60% (v/v) B in A in 5 min. R_t 4.2 min: Stapled peptide **VIIR**. ESI-MS (m/z): [M+H]$^+$: 2590.3 (Calcd), [M+2H]$^{2+}$: 1296.2 (found), 1295.7 (Calcd), [M+3H]$^{3+}$: 864.5 (found), 865.1 (Calcd).
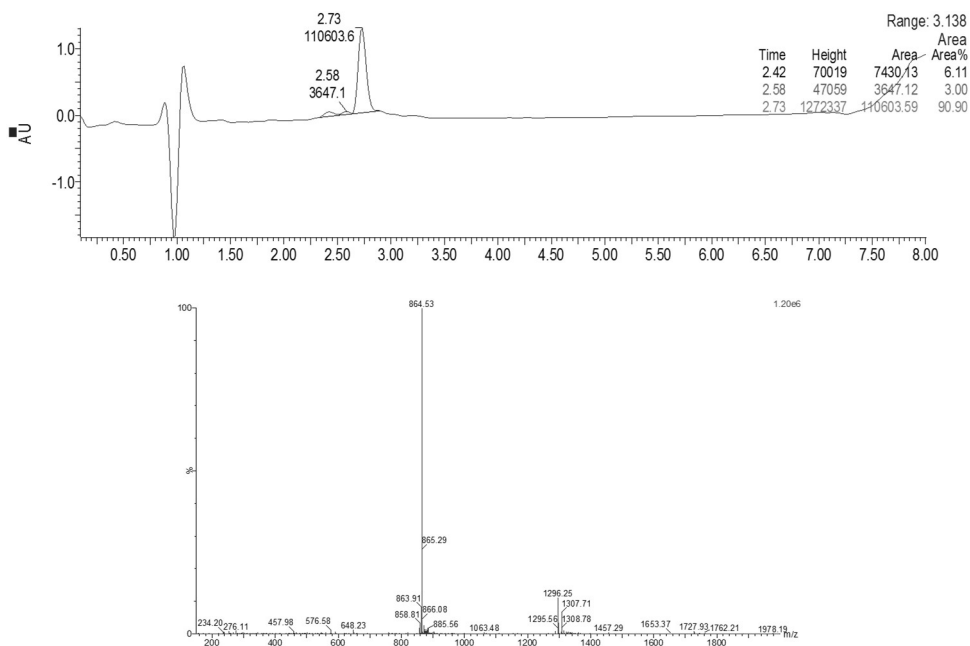
Figure R8. RP-HPLC trace of the Stapled peptide **VII**. BIOshell C18 column (Å160, 2,7 μm 3,0 x 100 mm), temperature 35°C; flow: 0,6 mL/min; λ 215 nm. Eluents: 0.1% (v/v) TFA in H$_2$O (A) and 0.1% (v/v) TFA in CH$_3$CN (B); gradient: 25-55% (v/v) B in A in 5 min. R$_t$ 2.7 min: Stapled peptide **VII**. ESI-MS (m/z): [M+H]$^+$: 2590.3 (Calcd), [M+2H]$^{2+}$: 1296.3 (found), 1295.7 (Calcd), [M+3H]$^{3+}$: 864.5 (found), 865.1 (Calcd).
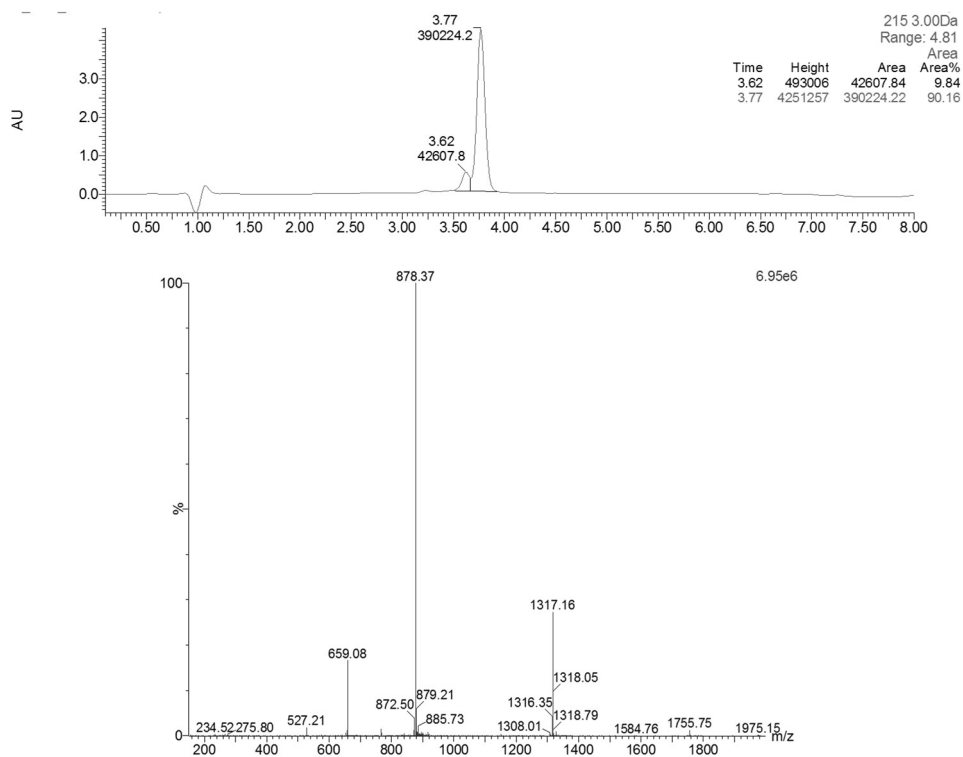
Figure R9. RP-HPLC trace of the Stapled peptide **VIIIR**. BIOshell C18 column (Å160, 2,7 μm 3,0 x 100 mm), temperature 35°C; flow: 0,6 mL/min; λ 215 nm. Eluents: 0.1% (v/v) TFA in H_2O (A) and 0.1% (v/v) TFA in CH_3CN (B); gradient: 20-55% (v/v) B in A in 5 min. R_t 3.8 min: Stapled peptide **VIIIR**. ESI-MS (m/z): $[M+H]^+$: 2631.4 (Calcd), $[M+2H]^{2+}$: 1317.2 (found), 1317.7 (Calcd), $[M+3H]^{3+}$: 878.4 (found), 877.8 (Calcd).
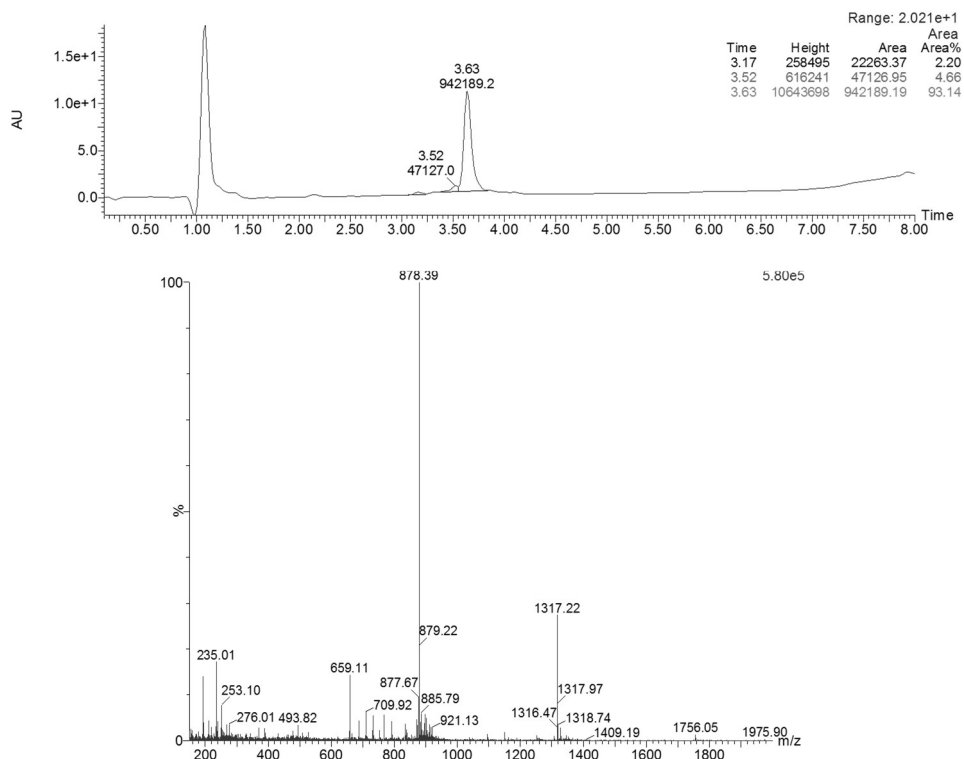
Figure R10. RP-HPLC trace of the Stapled peptide **VIII**. BIOshell C18 column (Å160, 2,7 μm 3,0 x 100 mm), temperature 35°C; flow: 0,6 mL/min; λ 215 nm. Eluents: 0.1% (v/v) TFA in H_2O (A) and 0.1% (v/v) TFA in CH_3CN (B); gradient: 25-55% (v/v) B in A in 5 min. R_t 3.6 min: Stapled peptide **VIII**. ESI-MS (m/z): $[M+H]^+$: 2631.4 (Calcd), $[M+2H]^{2+}$: 1317.2 (found), 1317.7 (Calcd), $[M+3H]^{3+}$: 878.4 (found), 877.8 (Calcd).
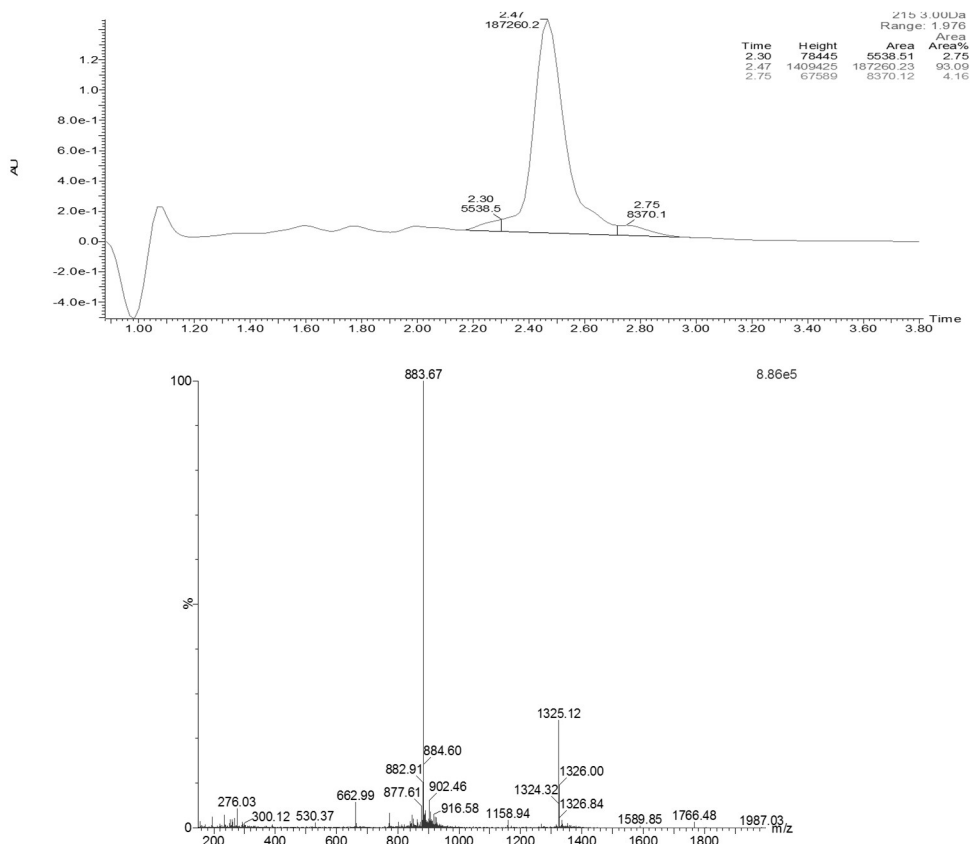
Figure R11. RP-HPLC trace of the Stapled peptide **IXR** (zoom 0-3.8 min). BIOshell C18 column (Å160, 2,7 μm 3,0 x 100 mm), temperature 35°C; flow: 0,6 mL/min; λ 215 nm. Eluents: 0.1% (v/v) TFA in H_2O (A) and 0.1% (v/v) TFA in CH_3CN (B); gradient: 25-55% (v/v) B in A in 5 min. R_t 2.5 min: Stapled peptide **IXR**. ESI-MS (m/z): [M+H]$^+$: 2647.4 (Calcd), [M+2H]$^{2+}$: 1325.1 (found), 1324.7 (Calcd), [M+3H]$^{3+}$: 833.7 (found), 833.1 (Calcd).
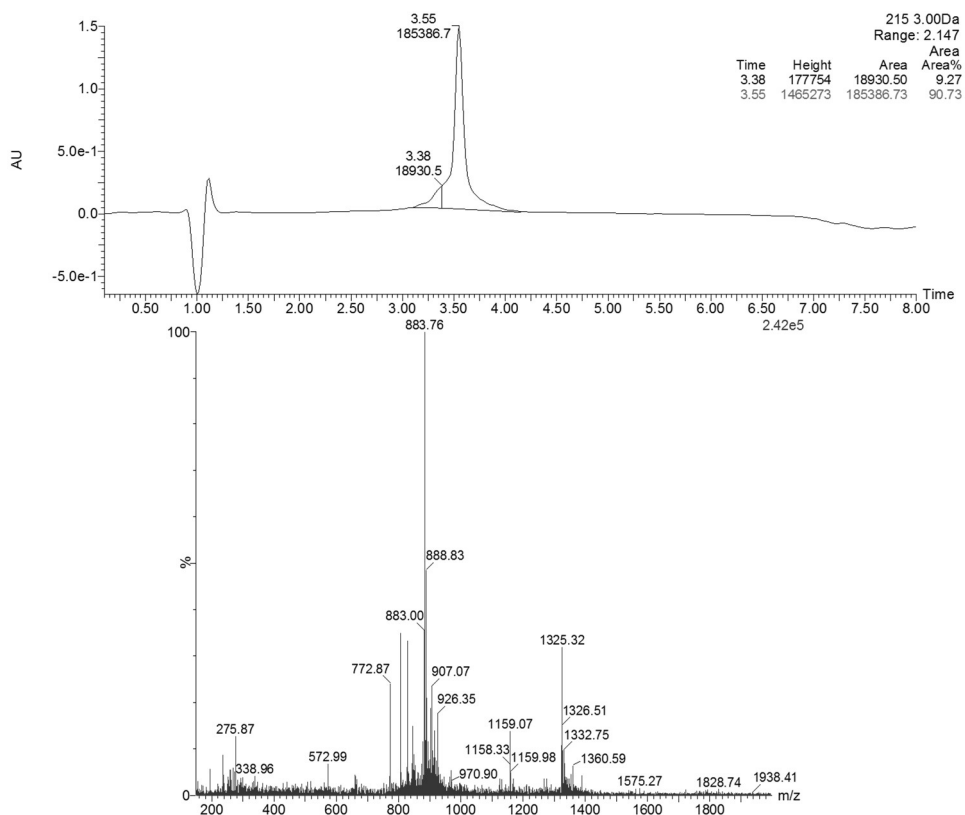
Figure R12. RP-HPLC trace of the Stapled peptide **IX**. BIOshell C18 column (Å160, 2,7 μm 3,0 x 100 mm), temperature 35°C; flow: 0,6 mL/min; λ 215 nm. Eluents: 0.1% (v/v) TFA in H_2O (A) and 0.1% (v/v) TFA in CH_3CN (B); gradient: 25-55% (v/v) B in A in 5 min. R_t 3.6 min: Stapled peptide **IX**. ESI-MS (m/z): [M+H]$^+$: 2647.4 (Calcd), [M+2H]$^{2+}$: 1325.3 (found), 1324.7 (Calcd), [M+3H]$^{3+}$: 833.8 (found), 833.1 (Calcd).

8. REFERENCES

[1] Sabatino, G.; D'Ercole, A.; Pacini, L.; Zini, M.; Ribecai, A.; Paio, A.; Rovero, P.; Papini, A.M. An Optimized Scalable Fully Automated Solid-Phase Microwave-Assisted cGMP-Ready Process for the Preparation of Eptifibatide. *Organic Process Research & Development* **2021**, *25* (3), 552–563.

[2] D'Ercole, A.; Sabatino, G.; Pacini, L.; Impresari, E.; Capecchi, I.; Papini, A.M.; Rovero, P. On‑resin microwave‑assisted copper‑catalyzed azide‑alkyne cycloaddition of H1‑relaxin B single chain 'stapled' analogues. *Peptide Science* **2020**, *112* (4), e24159.

[3] Zaman, M.; Abdel-Aal, A.-B. M.; Fujita, Y.; Ziora, Z. M.; Batzloff, M. R.; Good, M. F.; Toth, I. Structure–Activity Relationship for the Development of a Self-Adjuvanting Mucosally Active Lipopeptide Vaccine against Streptococcus Pyogenes. *Journal of Medicinal Chemistry* **2012**, *55* (19), 8515–8523.

[4] Zompra, A. A.; Galanis, A. S.; Werbitzky, O.; Albericio, F. Manufacturing Peptides as Active Pharmaceutical Ingredients. *Future Medicinal Chemistry* **2009**, *1* (2), 361–377.

[5] Joo, S.-H. Cyclic Peptides as Therapeutic Agents and Biochemical Tools. *Biomolecules and Therapeutics* **2012**, *20* (1), 19–26.

[6] Petersen J.; Purcell A.W.; Rossjohn J. Handbook of Biologically Active Peptides; Abba Kastin, **2013**; pp 580–589.

[7] Root Analysis business research & Consulting. Peptide Therapeutics Market by Type of Peptide (Small, Medium and Large), Route of Administration (Intravenous, Oral, Subcutaneous, Topical and Others), Key Geographical Regions (North America, Europe, Asia-Pacific and Rest of the World) and Key Therapeutic Area (Metabolic Diseases, Oncological Diseases, Endocrine Diseases, Digestive and Gastrointestinal Diseases and Others): Industry Trends and Global Forecasts, **2021-2030**.

[8] Kota, S. Peptide Manufacturing Methods and Challenges. *Peptide Therapeutics: Strategy and Tactics for Chemistry, Manufacturing, and Controls* **2019,** *72*, pp 111-150.

[9] Uhlig, T.; Kyprianou, T.; Martinelli, F. G.; Oppici, C. A.; Heiligers, D.; Hills, D.; Calvo, X. R.; Verhaert, P. The emergence of peptides in the pharmaceutical business: From exploration to exploitation. *EuPA Open Proteomics* **2014,** *4*, 58-69.

[10] Andersson, L.; Blomberg, L.; Flegel, M.; Lepsa, L.; Nilsson, B.; Verlander, M. Large-scale synthesis of peptides. *Biopolymers* **2000,** *55* (3), 227-250.

[11] Jad, Y. E.; Acosta, G. A.; Govender, T.; Kruger, H. G.; El-Faham, A.; de la Torre, B. G.; Albericio, F. Green solid-phase peptide synthesis 2. 2-Methyltetrahydrofuran and ethyl acetate for solid-phase peptide synthesis under green conditions. *ACS Sustainable Chemistry & Engineering* **2016,** *4* (12), 6809-6814.

[12] Jad, Y. E.; Govender, T.; Kruger, H. G.; El-Faham, A.; de la Torre, B. G.; Albericio, F. Green solid-phase peptide synthesis (GSPPS) 3. Green solvents for Fmoc removal in peptide chemistry. *Organic Process Research & Development* **2017,** *21* (3), 365-369.

[13] Jad, Y. E.; Kumar, A.; El-Faham, A.; de la Torre, B. G.; Albericio, F. Green Transformation of solid-phase peptide synthesis. *ACS Sustainable Chemistry & Engineering* **2019,** *7* (4), 3671-3683.

[14] Knauer, S.; Koch, N.; Uth, C.; Meusinger, R.; Avrutina, O.; Kolmar, H. Sustainable Peptide Synthesis Enabled by a Transient Protecting Group. *Angewandte Chemie International Edition* **2020,** 59 (31), 12984-12990.

[15] Kumar, A.; Jad, Y. E.; El-Faham, A.; de la Torre, B. G.; Albericio, F. Green Solid-Phase Peptide Synthesis 4. γ-Valerolactone and N -Formylmorpholine as Green Solvents for Solid Phase Peptide Synthesis. *Tetrahedron Letters*. **2017,** 58 (30), 2986–2988.

[16] Jad, Y. E.; Acosta, G. A.; Khattab, S. N.; de la Torre, B. G.; Govender, T.; Kruger, H. G.; El-Faham, A.; Albericio, F. 2-Methyltetrahydrofuran and Cyclopentyl Methyl Ether for Green Solid-Phase Peptide Synthesis. *Amino Acids.* **2016**, *48* (2), 419–426.

[17] Jad, Y. E.; Govender, T.; Kruger, H. G.; El-Faham, A.; de la Torre, B. G.; Albericio, F. Green Solid-Phase Peptide Synthesis (GSPPS) 3. Green Solvents for Fmoc Removal in Peptide Chemistry. *Organic Process Research & Development.* **2017**, 21 (3), 365–369.

[18] Mijalis, A. J.; Thomas, D. A.; Simon, M. D.; Adamo, A.; Beaumont, R.; Jensen, K. F.; Pentelute, B. L. A Fully Automated Flow-Based Approach for Accelerated Peptide Synthesis. *Nature Chemical Biology.* **2017**, *13* (5), 464–466.

[19] Sletten, E. T.; Nuño, M.; Guthrie, D.; Seeberger, P. H. Real-Time Monitoring of Solid-Phase Peptide Synthesis Using a Variable Bed Flow Reactor. *Chemical Communication.* **2019**, *55* (97), 14598–14601.

[20] Zorzi, A.; Deyle, K.; Heinis, C. Cyclic peptide therapeutics: past, present and future. *Current Opinion in Chemical Biology* **2017,** *38*, 24-29.

[21] Angeletti, R.H.; Bibbs, L.; Bonenwald, L.F.; et al. *Techniques in protein Chemistry VII*; Elsevier Science Publishing Co Inc: San Diego, United States, 1996, 553.

[22] Moroder, L.; Musiol, H.-J.; Schaschke, N.; Chen, L.; Hargittai, B. & Barany, G. *Protection of the thiol group. In: Synthesis of Peptides and Peptidomimetics*; Georg Thieme Verlag: Stuttgart, Germany, 2002, 384-424.

[23] Chen, L.; Annis, I.; Barany, G. Disulfide bond formation in peptides. *Current protocols in protein science* **2001,** *23* (1), 18-6.

[24] Hruby, Victor J. *Synthesis of cystine peptides. In: Synthesis of Peptides and Peptidomimetics. Houben-Weyl E22b:Methods of Organic Chemistry*; Georg ThiemeVerlag: Stuttgart, Germany, 2002; 101-141.

[25] Annis, I.; Balazs, H.; and Barany, G. Disulfide bond formation in peptides. *Methods in enzymology* **1997**, 289, 198-221.

[26] Moroder, L.; Besse, D.; Musiol, H. J.; Rudolph-Böhner, S.; Siedler, F. Oxidative folding of cystine-rich peptides vs regioselective cysteine pairing strategies. *Biopolymers* **1996,** *40* (2), 207-34.

[27] Darlak, K.; Wiegandt Long, D.; Czerwinski, A.; Darlak, M.; Valenzuela, F.; Spatola, A. F.; Barany, G. Facile preparation of disulfide-bridged peptides using the polymer-supported oxidant CLEAR-OX. *The Journal of Peptide Research* **2004,** *63* (3), 303-312.

[28] Yang, Y.; Hansen, L.; Badalassi, F. Investigation of Solid-phase Disulfide Formation for Large-scale Manufacturing of Cyclic Peptides: A Case Study. *Organic Process Research & Development* **2020**.

[29] Scarborough, R. M.; Naughton, M. A.; Teng, W.; Rose, J. W.; Phillips, D. R.; Nannizzi, L.; Arfsten, A.; Campbell, A. M.; Charo, I. F. Design of Potent and Specific Integrin Antagonists. Peptide Antagonists with High Specificity for Glycoprotein IIb-IIIa. *Journal of Biological Chemistry* **1993**, *268* (2), 1066–1073.

[30] Scarborough, R.M.; Wolf, D. L; Charo, I. F. Platelet Aggregation Inhibitors. EP0477295B1, January 2, 1997.

[31] *FDA, Integrilin (eptifibatide) Injection for Intravenous Administration NDA, Editor. 2011, USFDA: USA. p. 21.*

[32] Chong, B. H. Drug-Induced Thrombocytopenia: MIBS Trumps LIBS. *Blood* **2012**, *119* (26), 6177–6178.

[33] Scientific Discussion/human/000230/WC500034073. *EMA/document library/EPAR.* EMEA. **2004**, 1-22.

[34] Lax, R. The future of peptide development in the pharmaceutical industry. *PharManufacturing: The international peptide review* **2010,** *2*, 10-15.

[35] Yang, Y.; Hansen, L.; Badalassi, F. Investigation of Solid-phase Disulfide Formation for Large-scale Manufacturing of Cyclic Peptides: A Case Study. *Organic Process Research & Development* **2020**.

[36] Branch, S. K. Guidelines from the International Conference on Harmonisation (ICH). *Journal of pharmaceutical and biomedical analysis* **2005**, *38* (5), 798–805.

[37] Guideline, I. H. T. Impurities in New Drug Substances Q3A (R2); Citeseer, 2006; Vol. 25.

[38]US Food and Drug Administration. ANDAs for Certain Highly Purified Synthetic Peptide Drug Products That Refer to Listed Drugs of RDNA Origin, Guidance for Industry. *Silver Spring, MD: US Food and Drug Administration* **2017**.

[39] Charo, I. F; Scarborough, R. M; Wolf, D. L. Platelet aggregation inhibitors. WO9015620A1, December 27, 1990.

[40] Varray, S.; Werbitzky, O.; Zeiter, T. Solid-phase peptide cyclization. Patent EP1805203A2, 2011.

[41] Kota, S.; Tallapaneni, V.; Adibhatla, K. S.; Bhujanga, R.; Venkaiah, C. N. Improved Process For Preparation Of Eptifibatide By Fmoc Solid Phase Synthesis. Patent WO2009150657A1, 2009.

[42] Subha, N. V.; Ravindra B. B.; Venkata, S. K. I.; Seeta, R. G.; Venkata, S. R. R. K., Bala, Muralikrishna, M. Process for preparing eptifibatide. Patent US9156885B2, 2012.

[43] Han, Y.; Tong, G.; Wang, X.; Wen, Y., Zhu, C., Chengdu, S. Eptifibatide preparation method. Patent US9394341B2, 2016.

[44] Qin, L.; Yuan, J.; Li, H.; Ma, Y. Method for Preparing Eptifibatide with Solid Phase Method. CN 101538316 B, September 5, 2012.

[45] Wen, Y.; Zhu, C.; Wang, X.; Han, Y.; Tong, G. Eptifibatide Preparation Method. US 9394341B2, October 22, 2015.

[46] Varray, S., Werbitzky, O., Zeiter, T. Solid-phase peptide cyclization. Solid-phase peptide cyclization. Patent WO2006045483, 2008

[47] Kota, S., Tallapaneni, V., Adibhatla, K. S., Bhujanga, R.,Venkaiah, C. N. Improved Process For Preparation Of Eptifibatide By Fmoc Solid Phase Synthesis. Patent WO2009150657A1, 2009.

[48] Varray, S., Werbitzky, O., Zeiter, T. Solid-phase peptide cyclization. Patent EP1805203A2, 2011.

[49] Ho, G., Paone, A. D., Forni, L., Detollenaere, C. Processes for preparing eptifibatide and pertinent intermediate compounds. Patent EP2204383B1, 2011.

[50] Babu, B., Gorantla, S., Indukuri, V., Madivada, B., Ramakrishna, V., Velayudhan, S. N. Process for preparing eptifibatide. Patent US2014163203A1, 2014.

[51] Velayudhan, S. N., Babu, B., Indukuri, V., Gorantla, S., Kallam, V. S. R. R., Madivada, B. Process for preparing eptifibatide. Patent US009156885B2, 2015.

[52] Yongjun, W., Chuanbin, Z., Xiaoli, W., Yu, H., Guangbin, T. Eptifibatide preparation method. Patent US9394341B2, 2016.

[53] Varray, S.; Werbitzky, O.; Zeiter, T. Solid-phase Peptide Cyclization. WO2006045483A2, May 4, 2006.

[54] Muttenthaler, M.; King, G. F.; Adams, D. J.; Alewood, P. F. Trends in Peptide Drug Discovery. *Nature Reviews Drug Discovery* **2021**, *20* (4), 309–325.

[55] Bathgate, R.; Halls, M. L.; van der Westhuizen, E. T.; Callander, G.; Kocan, M.; Summers, R. J. Relaxin Family Peptides and Their Receptors. *Physiological reviews* **2013**, *93* (1), 405–480.

[56] Büllesbach, E. E.; Schwabe, C. The Trap-like Relaxin-Binding Site of the Leucine-Rich G-Protein-Coupled Receptor 7. *Journal of Biological Chemistry* **2005**, *280* (14), 14051–14056.

[57] Sedaghat, K.; Shen, P.-J.; Finkelstein, D.; Henderson, J.; Gundlach, A. Leucine-Rich Repeat-Containing G-Protein-Coupled Receptor 8 in the Rat Brain: Enrichment in Thalamic Neurons and Their Efferent Projections. *Neuroscience* **2008**, *156* (2), 319–333.

[58] Smith, C. M.; Ryan, P. J.; Hosken, I. T.; Ma, S.; Gundlach, A. L. Relaxin-3 Systems in the Brain—the First 10 Years. *Journal of chemical neuroanatomy* **2011**, *42* (4), 262–275.

[59] Ang, S. Y.; Evans, B. A.; Poole, D. P.; Bron, R.; DiCello, J. J.; Bathgate, R. A.; Kocan, M.; Hutchinson, D. S.; Summers, R. J. INSL5 Activates Multiple Signalling Pathways and Regulates GLP-1 Secretion in NCI-H716 Cells. *Journal of molecular endocrinology* **2018**, *60* (3), 213–224.

[60] Halls, M.; Bathgate, R.; Sutton, S.; Dschietzig, T.; Summers, R.; International Union of Basic and Clinical Pharmacology. XCV. Recent Advances in the Understanding of the Pharmacology and Biological Roles of Relaxin Family Peptide Receptors 1-4, the Receptors for Relaxin Family Peptides. *Pharmacological Reviews* **2015**, *67* (2), 389.

[61] Bani, D. Relaxin: A Pleiotropic Hormone. *General Pharmacology: The Vascular System* **1997**, *28* (1), 13–22.

[62] Dschietzig, T.; Bartsch, C.; Baumann, G.; Stangl, K. Relaxin—a Pleiotropic Hormone and Its Emerging Role for Experimental and Clinical Therapeutics. *Pharmacology & therapeutics* **2006**, *112* (1), 38–56.

[63] Kakouris, H.; Eddie, L. W.; Summers, R. J. Cardiac Effects of Relaxin in Rats. *The Lancet* **1992**, *339* (8801), 1076–1078.

[64] RELAX-AHF-2, ClinicalTrials.gov No. NCT01870778.

[65] Nistri, S.; Bigazzi, M.; Bani, D. Relaxin as a Cardiovascular Hormone: Physiology, Pathophysiology and Therapeutic Promises. *Cardiovascular & Hematological Agents in Medicinal Chemistry (Formerly Current*

Medicinal Chemistry-Cardiovascular & Hematological Agents) **2007**, *5* (2), 101–108.

[66] Du, X.-J.; Bathgate, R. A.; Samuel, C. S.; Dart, A. M.; Summers, R. J. Cardiovascular Effects of Relaxin: From Basic Science to Clinical Therapy. *Nature Reviews Cardiology* **2010**, *7* (1), 48–58.

[67] Samuel, C.; Royce, S.; Hewitson, T.; Denton, K.; Cooney, T.; Bennett, R. G. Anti□fibrotic Actions of Relaxin. *British journal of pharmacology* **2017**, *174* (10), 962–976.

[68] Sarwar, M.; Du, X.; Dschietzig, T. B.; Summers, R. J. The Actions of Relaxin on the Human Cardiovascular System. *British Journal of Pharmacology* **2017**, *174* (10), 933–949.

[69] Haugaard-Kedstrom, L. M.; Shabanpoor, F.; Hossain, M. A.; Clark, R. J.; Ryan, P. J.; Craik, D. J.; Gundlach, A. L.; Wade, J. D.; Bathgate, R. A.; Rosengren, K. J. Design, Synthesis, and Characterization of a Single-Chain Peptide Antagonist for the Relaxin-3 Receptor RXFP3. *Journal of the American Chemical Society* **2011**, *133* (13), 4965–4974.

[70] Tan, Y. Y.; Wade, J. D.; Tregear, G. W.; Summers, R. J. Comparison of Relaxin Receptors in Rat Isolated Atria and Uterus by Use of Synthetic and Native Relaxin Analogues. *British Journal of Pharmacology* **1998**, *123* (4), 762–770.

[71] Wade, J. D.; Lin, F.; Hossain, M. A.; Shabanpoor, F.; Zhang, S.; Tregear, G. W. The Chemical Synthesis of Relaxin and Related Peptides. *Annals of the New York Academy of Sciences* **2009**, *1160* (1), 11–15.

[72] Hossain, M. A.; Wade, J. D. Synthetic Relaxins. *Current opinion in chemical biology* **2014**, *22*, 47–55.

[73] Marglin, B.; Merrifield, R. The Synthesis of Bovine Insulin by the Solid Phase Method1. *Journal of the american chemical society* **1966**, *88* (21), 5051–5052.

[74] Wade, J.; Lin, F.; Salvatore, D.; Otvos, Jr. L.; Tregear, G. Synthesis and Characterization of Human Gene 1 Relaxin Peptides. *Biomedical peptides, proteins & nucleic acids: structure, synthesis & biological activity* **1996**, *2 (2)*, 27–32.

[75] Bullesbach, E.E.; Schwabe, C. Total synthesis of human relaxin and human relaxin derivatives by solid-phase peptide synthesis and site-directed chain combination. *Journal of Biological Chemistry* **1991**, *266 (17)*, 10754–10761.

[76] Hossain, M.A.; Belgi, A.; Lin, F.; Zhang, S.; Shabanpoor, F.; Chan, L.; Belyea, C.; Truong, H.-T.; Blair, A.R.; Andrikopoulos, S.; et al. Use of a Temporary "Solubilizing" Peptide Tag for the Fmoc Solid-Phase Synthesis of Human Insulin Glargine via Use of Regioselective Disulfide Bond Formation. *Bioconjugate Chemistry* **2009**, *20 (7)*, 1390–1396.

[77] Hossain, M.A.; Rosengren, K.J.; Samuel, C.S.; Shabanpoor, F.; Chan, L.J.; Bathgate, R.A.D.; Wade, J.D. The Minimal Active Structure of Human Relaxin-2. *Journal of Biological Chemistry* **2011**, *286 (43)*, 37555–37565.

[78] Li, H.; Aneja, R.; Chaiken, I. Click Chemistry in Peptide-Based Drug Design. *Molecules* **2013**, *18* (8), 9797–9817.

[79] Skowron, K. J.; Speltz, T. E.; Moore, T. W. Recent Structural Advances in Constrained Helical Peptides. *Medicinal Research Reviews* **2019**, *39* (2), 749–770.

[80] Del Borgo, M.P.; Hughes, R.A.; Wade, J.D. Conformationally constrained single-chain peptide mimics of relaxin B-chain secondary structure. *Journal of Peptide Science, Publications - European Peptide Society* **2005**, *11 (9)*, 564–571.

[81] Hojo, K.; Hossain, M.A.; Tailhades, J.; Shabanpoor, F.; Wong, L.L.L.; Ong-Palsson, E.E.K.; Kastman, H.E.; Ma, S.; Gundlach, A.L.; Rosengren, K.J.; et al. Development of a Single- Chain Peptide Agonist of the

Relaxin-3 Receptor Using Hydrocarbon Stapling. *Journal of Medicinal Chemistry* **2016**, *59 (16)*, 7445–7456.

[82] Jayakody, T.; Marwari, S.; Lakshminarayanan, R.; Tan, F.C.K.; Johannes, C.W.; Dymock, B.W.; Poulsen, A.; Herr, D.R.; Dawe, G.S. Hydrocarbon stapled B chain analogues of relaxin-3 retain biological activity. *Peptides* **2016**, *84*, 44–57.

[83] Li, H.; Aneja, R.; Chaiken, I. Click Chemistry in Peptide-Based Drug Design. *Molecules* **2013**, *18* (8), 9797–9817.

[84] Tron, G. C.; Pirali, T.; Billington, R. A.; Canonico, P. L.; Sorba, G.; Genazzani, A. A. Click Chemistry Reactions in Medicinal Chemistry: Applications of the 1,3-Dipolar Cycloaddition between Azides and Alkynes. *Medicinal Research Reviews* **2008**, *28* (2), 278–308.

[85] Hou, J.; Liu, X.; Shen, J.; Zhao, G.; Wang, P. G. The Impact of Click Chemistry in Medicinal Chemistry. *Expert Opinion on Drug Discovery* **2012**, *7* (6), 489–501.

[86] Kim, S.; Cho, M.; Lee, T.; Lee, S.; Min, H.-Y.; Lee, S. K. Design, Synthesis, and Preliminary Biological Evaluation of a Novel Triazole Analogue of Ceramide. *Bioorganic & Medicinal Chemistry Letters* **2007**, *17* (16), 4584–4587.

[87] Brik, A.; Alexandratos, J.; Lin, Y.-C.; Elder, J. H.; Olson, A. J.; Wlodawer, A.; Goodsell, D. S.; Wong, C.-H. 1,2,3-Triazole as a Peptide Surrogate in the Rapid Synthesis of HIV-1 Protease Inhibitors. *ChemBioChem* **2005**, *6* (7), 1167–1169.

[88] Angelo, N. G.; Arora, P. S. Nonpeptidic Foldamers from Amino Acids: Synthesis and Characterization of 1,3-Substituted Triazole Oligomers. *Journal of the American Chemical Society* **2005**, *127* (49), 17134–17135.

[89] Appendino, G.; Bacchiega, S.; Minassi, A.; Cascio, M. G.; De Petrocellis, L.; Di Marzo, V. The 1,2,3-Triazole Ring as a Peptido- and Olefinomimetic Element: Discovery of Click Vanilloids and

Cannabinoids. *Angewandte Chemie International Edition* **2007**, *119* (48), 9472–9475.

[90] Beierle, J. M.; Horne, W. S.; van Maarseveen, J. H.; Waser, B.; Reubi, J. C.; Ghadiri, M. R. Conformationally Homogeneous Heterocyclic Pseudotetrapeptides as Three-Dimensional Scaffolds for Rational Drug Design: Receptor-Selective Somatostatin Analogues *Angewandte Chemie International Edition* **2009**, *48* (26), 4725–4729.

[91] Angell, Y.; Burgess, K. Ring Closure to β-Turn Mimics via Copper-Catalyzed Azide/Alkyne Cycloadditions. *The Journal of Organic Chemistry* **2005**, *70* (23), 9595–9598.

[92] Van Maarseveen, J. H.; Horne, W. S.; Ghadiri, M. R. Efficient Route to *C*₂ Symmetric Heterocyclic Backbone Modified Cyclic Peptides. *Organic Letters* **2005**, *7* (20), 4503–4506.

[93] Pokorski, J. K.; Miller Jenkins, L. M.; Feng, H.; Durell, S. R.; Bai, Y.; Appella, D. H. Introduction of a Triazole Amino Acid into a Peptoid Oligomer Induces Turn Formation in Aqueous Solution. *Organic Letters* **2007**, *9* (12), 2381–2383.

[94] Tam, A.; Arnold, U.; Soellner, M. B.; Raines, R. T. Protein Prosthesis: 1,5-Disubstituted[1, 2, 3]Triazoles as *Cis*-Peptide Bond Surrogates. *Journal of the American Chemical Society* **2007**, *129* (42), 12670–12671.

[95] Hitotsuyanagi, Y.; Motegi, S.; Fukaya, H.; Takeya, K. A Cis Amide Bond Surrogate Incorporating 1,2,4-Triazole. *The Journal of Organic Chemistry* **2002**, *67* (10), 3266–3271.

[96] Kawamoto, S. A.; Coleska, A.; Ran, X.; Yi, H.; Yang, C.-Y.; Wang, S. Design of Triazole-Stapled BCL9 α-Helical Peptides to Target the β-Catenin/B-Cell CLL/Lymphoma 9 (BCL9) Protein–Protein Interaction. *Journal of Medicinal Chemistry* **2012**, *55* (3), 1137–1146.

[97] Le Chevalier Isaad, A.; Papini, A. M.; Chorev, M.; Rovero, P. Side Chain-to-Side Chain Cyclization by Click Reaction. *Journal of Peptide Science* **2009**, *15* (7), 451–454.

[98] Testa, C.; Scrima, M.; Grimaldi, M.; D'Ursi, A. M.; Dirain, M. L.; Lubin-Germain, N.; Singh, A.; Haskell-Luevano, C.; Chorev, M.; Rovero, P.; Papini, A. M. 1,4-Disubstituted-[1,2,3]Triazolyl-Containing Analogues of MT-II: Design, Synthesis, Conformational Analysis, and Biological Activity. *Journal of Medicinal Chemistry* **2014**, *57* (22), 9424–9434.

[99] Melacini, G.; Zhu, Q.; Goodman, M. Multiconformational NMR Analysis of Sandostatin (Octreotide): Equilibrium between β-Sheet and Partially Helical Structures ,. *Biochemistry* **1997**, *36* (6), 1233–1241.

[100] Testa, C.; D'Addona, D.; Scrima, M.; Tedeschi, A. M.; D'Ursi, A. M.; Bernhard, C.; Denat, F.; Bello, C.; Rovero, P.; Chorev, M.; Papini, A. M. Design, Synthesis, and Conformational Studies of [DOTA]□Octreotide Analogs Containing [1,2,3]Triazolyl as a Disulfide Mimetic. *Peptide Science* **2018**, *110* (5), e24071.

[101] Cantel, S.; Le Chevalier Isaad, A.; Scrima, M.; Levy, J. J.; DiMarchi, R. D.; Rovero, P.; Halperin, J. A.; D'Ursi, A. M.; Papini, A. M.; Chorev, M. Synthesis and Conformational Analysis of a Cyclic Peptide Obtained via *i* to *i* +4 Intramolecular Side-Chain to Side-Chain Azide−Alkyne 1,3-Dipolar Cycloaddition. *The Journal of Organic Chemistry* **2008**, *73* (15), 5663–5674.

[102] Testa, C.; D'Addona, D.; Scrima, M.; Tedeschi, A. M.; D'Ursi, A. M.; Bernhard, C.; Denat, F.; Bello, C.; Rovero, P.; Chorev, M.; Papini, A. M. Design, Synthesis, and Conformational Studies of [DOTA]□Octreotide Analogs Containing [1, 2, 3]Triazolyl as a Disulfide Mimetic. *Peptide Science* **2018**, *110* (5), e24071.

[103] Scrima, M.; Le Chevalier-Isaad, A.; Rovero, P.; Papini, A. M.; Chorev, M.; D'Ursi, A. M. CuI-Catalyzed Azide–Alkyne Intramolecular i-to-(I+4)
203

Side-Chain-to-Side-Chain Cyclization Promotes the Formation of Helix-Like Secondary Structures. *European Journal of Organic Chemistry* **2010**, *2010* (3), 446–457.

[104] Turner, R. A.; Oliver, A. G.; Lokey, R. S. Click Chemistry as a Macrocyclization Tool in the Solid-Phase Synthesis of Small Cyclic Peptides. *Organic Letters* **2007**, *9* (24), 5011–5014.

[105] Rostovtsev, V. V.; Green, L. G.; Fokin, V. V.; Sharpless, K. B. A Stepwise Huisgen Cycloaddition Process: Copper(I)-Catalyzed Regioselective "Ligation" of Azides and Terminal Alkynes *Angewandte Chemie International Edition* **2002**, *41* (14), 2596–2599.

[106] Pérez-Balderas, F.; Ortega-Muñoz, M.; Morales-Sanfrutos, J.; Hernández-Mateo, F.; Calvo-Flores, F. G.; Calvo-Asín, J. A.; Isac-García, J.; Santoyo-González, F. Multivalent Neoglycoconjugates by Regiospecific Cycloaddition of Alkynes and Azides Using Organic-Soluble Copper Catalysts. *Organic Letters* **2003**, *5* (11), 1951–1954.

[107] Lewis, W. G.; Magallon, F. G.; Fokin, V. V.; Finn, M. G. Discovery and Characterization of Catalysts for Azide−Alkyne Cycloaddition by Fluorescence Quenching. *Journal of the American Chemical Society* **2004**, *126* (30), 9152–9153.

[108] Hewitson, T. D.; Ho, W. Y.; Samuel, C. S. Antifibrotic Properties of Relaxin: In Vivo Mechanism of Action in Experimental Renal Tubulointerstitial Fibrosis. *Endocrinology* **2010**, *151* (10), 4938–4948.

[109] Guideline, Quality risk management, ICH Q9, European Medicines Agency. **2015**. London, UK.

[110] European Regulation (EC) n°1272/2008.

[111] Achyuthan, K. E.; Wheeler, D. R. Easy parallel screening of reagent stability, quality control, and metrology in solid phase peptide synthesis (SPPS) and peptide couplings for microarrays. *Journal of Peptide Science* **2015,** *21* (10), 751-757.

[112] Anderson, N. G.; Burdick, D. C.; Reeve, M. M. Current Practices of Process Validation for Drug Substances and Intermediates. *Organic Process Research & Development.* **2011**, *15* (1), 162–172.

[113] Martin, V.; Egelund, P. H. G.; Johansson, H.; Thordal Le Quement, S.; Wojcik, F.; Sejer Pedersen, D. Greening the Synthesis of Peptide Therapeutics: An Industrial Perspective. *RSC Advances* **2020**, *10* (69), 42457–42492.

[114] Specifications: Test Procedures and Acceptance Criteria for New Drug Substances and New Drug Products: Chemical Substances, ICH Q6A, European Medicines Agency. **2000**. London, UK.

[115] Buellesbach E. E.; Danho W.; Heilbig H. J.; Zahn H. *Side Reactions in Peptide Synthesis*. **1978**, Wroclaw: Wroclaw University Press. 1979, 643–646.

[116] Barany G.; Merrifield R. B. *The Peptides Analysis, Synthesis, Biology*. **1979**, New York: Academic Press. *2*, 1–298.

[117] Moroder, L.; Musiol, H. J.; Schaschke, N.; Chen, L.; Hargittai, B.; Barany, G. Protection of the Thiol Group. *Synthesis of Peptides and Peptidomimetics*. **2001**, Stuttgart, Germany. Georg Thieme, Verlag. *E22a*, 384–423.

[118] Yang, Y. Peptide Global Deprotection/Scavenger-Induced Side Reactions. *Side Reactions in Peptide Synthesis.* **2016**, Oxford, UK: Academic Press. *3*, 43–75.

[119] Al Musaimi, O.; Jad, Y. E.; Kumar, A.; El-Faham, A.; Collins, J. M.; Basso, A.; de la Torre, B. G.; Albericio, F. Greening the Solid-Phase Peptide Synthesis Process. 2-MeTHF for the Incorporation of the First Amino Acid and Precipitation of Peptides after Global Deprotection. *Organic Process Research & Development* **2018**, *22* (12), 1809–1816.

[120] Al Musaimi, O.; Jad, Y. E.; Kumar, A.; Collins, J. M.; Basso, A.; de la Torre, B. G.; Albericio, F. Investigating Green Ethers for the Precipitation

of Peptides after Global Deprotection in Solid-Phase Peptide Synthesis. *Current Opinion in Green and Sustainable Chemistry.* **2018**, *11*, 99–103.

[121] Alder, C. M.; Hayler, J. D.; Henderson, R. K.; Redman, A. M.; Shukla, L.; Shuster, L. E.; Sneddon, H. F. Updating and Further Expanding GSK's Solvent Sustainability Guide. *Green Chemistry.* **2016**, *18* (13), 3879–3890.

[122] Prat, D.; Pardigon, O.; Flemming, H. W.; Letestu, S.; Ducandas, V.; Isnard, P.; Guntrum, E.; Senac, T.; Ruisseau, S.; Cruciani, P. Sanofi's Solvent Selection Guide: A Step toward More Sustainable Processes. *Organic Process Research & Development* **2013**, *17* (12), 1517–1525.

[123] European Chemicals Agency Candidate List of substances of very high concern for Authorisation, http://echa.europa.eu/candidate-list-table.

[124] Prat, D.; Wells, A.; Hayler, J.; Sneddon, H.; McElroy, C. R.; Abou-Shehada, S.; Dunn, P. J. Correction: CHEM21 Selection Guide of Classical-and Less Classical-Solvents. *Green Chemistry* **2015**, *17* (10), 4848–4848.

[125] Sidorova, M.; Molokoedov, A.; Az'muko, A.; Kudryavtseva, E.; Krause, E.; Ovchinnikov, M.; Bespalova, Z. D. The Use of Hydrogen Peroxide for Closing Disulfide Bridges in Peptides. *Russian Journal of Bioorganic Chemistry* **2004**, *30* (2), 101–110.

[126] Calce, E.; Vitale, R. M.; Scaloni, A.; Amodeo, P.; De Luca, S. Air Oxidation Method Employed for the Disulfide Bond Formation of Natural and Synthetic Peptides. *Amino Acids* **2015**, *47* (8), 1507–1515.

[127] Tam, J. P.; Wu, C. R.; Liu, W.; Zhang, J. W. Disulfide Bond Formation in Peptides by Dimethyl Sulfoxide. Scope and Applications. *Journal of the American Chemical Society* **1991**, *113* (17), 6657–6662.

[128] Song, C.; Sun, J.; Zhao, X.; Huo, S.; Shen, S. A Study to Develop Platinum (Iv) Complex Chemistry for Peptide Disulfide Bond Formation. *Dalton Transactions* **2020**, *49* (6), 1736–1741.

[129] Calce, E.; Vitale, R. M.; Scaloni, A.; Amodeo, P.; De Luca, S. Air oxidation method employed for the disulfide bond formation of natural and synthetic peptides. *Amino Acids* **2015**, 47 (8), 1507-1515.

[130] Andreu, D.; Albericio, F.; Solé, N. A.; Munson, M. C.; Ferrer, M.; Barany, G. Formation of Disulfide Bonds in Synthetic Peptides and Proteins. *Peptide synthesis protocols* **1994**, 91–169.

[131] Sidorova, M.; Molokoedov, A.; Az'muko, A.; Kudryavtseva, E.; Krause, E.; Ovchinnikov, M.; Bespalova, Z. D. The Use of Hydrogen Peroxide for Closing Disulfide Bridges in Peptides. *Russian Journal of Bioorganic Chemistry* **2004**, *30* (2), 101–110.

[132] Calce, E.; Vitale, R. M.; Scaloni, A.; Amodeo, P.; De Luca, S. Air Oxidation Method Employed for the Disulfide Bond Formation of Natural and Synthetic Peptides. *Amino Acids* **2015**, *47* (8), 1507–1515.

[133] Tam, J. P.; Wu, C. R.; Liu, W.; Zhang, J. W. Disulfide Bond Formation in Peptides by Dimethyl Sulfoxide. Scope and Applications. *Journal of the American Chemical Society.* **1991**, *113* (17), 6657–6662.

[134] Song, C.; Sun, J.; Zhao, X.; Huo, S.; Shen, S. A Study to Develop Platinum (Iv) Complex Chemistry for Peptide Disulfide Bond Formation. *Dalton Transactions* **2020**, *49* (6), 1736–1741.

[135] Albericio, F.; Andreu, D.; Giralt, E.; Navalpotro, C.; Pedroso, E.; Ponsati, B.; Ruiz-Gayo, M. Use of the NPyS thiol protection in solid phase peptide synthesis. Application to direct peptide-protein conjugation through cysteine residues. *International Journal of Peptide and Protein Research* **1989,** *34* (2), 124-8.

[136] Galande, A. K.; Weissleder, R.; Tung, C.H. An effective method of solid-phase disulfide bond formation in peptides. *Journal of combinatorial chemistry* **2005,** *7* (2), 174-177.

[137] Fernandes, P. A.; Ramos, M. J. Theoretical insights into the mechanism for thiol/disulfide exchange. *Chemistry* **2004,** *10* (1), 257-66.

[138] Nagy, P. Kinetics and mechanisms of thiol–disulfide exchange covering direct substitution and thiol oxidation-mediated pathways. *Antioxidants & redox signaling* **2013,** *18* (13), 1623-1641.

[139] Postma, T. M.; Albericio, F. N-Chlorosuccinimide, an efficient reagent for solid-phase disulfide formation in solid-phase peptide synthesis. *Organic Letters* **2013,** *15* (3), 616-9.

[140] Alcaro, M. C.; Sabatino, G.; Uziel, J.; Chelli, M.; Ginanneschi, M.; Rovero, P.; Papini, A. M. Solid-phase head-to-tail cyclization of cyclotetrapeptides: Optimization of crucial parameters. *Journal of Peptide Science* **2004,** *10* (4), 218-228.

[141] Galanis, A.S.; Albericio, F.; Grøtli, M. Enhanced microwave□assisted method for on□bead disulfide bond formation: Synthesis of α□conotoxin MII. *Peptide Science: Original Research on Biomolecules*, **2009**, 92(1), 23-34.

[142] Keire, D. A.; Strauss, E.; Guo, W.; Noszal, B.; Rabenstein, D. L. Kinetics and equilibria of thiol/disulfide interchange reactions of selected biological thiols and related molecules with oxidized glutathione. *The Journal of Organic Chemistry* **1992**, 57(1), 123-127.

[143] Insuasty Cepeda, D. S.; Pineda Castañeda, H. M.; Rodríguez Mayor, A. V.; García Castañeda, J. E.; Maldonado Villamil, M.; Fierro Medina, R.; Rivera Monroy, Z. J. Synthetic Peptide Purification via Solid-Phase Extraction with Gradient Elution: A Simple, Economical, Fast, and Efficient Methodology. *Molecules.* **2019**, *24* (7), 1215.

[144] Bickler, B. How to choose between linear gradient and step gradients for flash chromatography. Biotage. https://selekt.biotage.com/blog/how-to-choose-between-linear-gradients-and-step-gradients-for-flash chromatography.

[145] Sikora, K.; Jaśkiewicz, M.; Neubauer, D.; Migoń, D.; Kamysz, W. The Role of Counter-Ions in Peptides—An Overview. *Pharmaceuticals* **2020**, *13* (12), 442.

[146] Keire, D. A., Strauss, E., Guo, W., Noszal, B., Rabenstein, D. L. Kinetics and equilibria of thiol/disulfide interchange reactions of selected biological thiols and related molecules with oxidized glutathione. *The Journal of Organic Chemistry* **1992,** 57(1), 123-127.

[147] Patil, N. A.; Rosengren, K. J.; Separovic, F.; Wade, J. D.; Bathgate, R. A. D.; Hossain, M. A. Relaxin Family Peptides: Structure–Activity Relationship Studies. *British Journal of Pharmacology* **2017**, *174* (10), 950–961.

[148] Appukkuttan, P.; Dehaen, W.; Fokin, V. V.; Van der Eycken, E. A Microwave-Assisted Click Chemistry Synthesis of 1,4-Disubstituted 1,2,3-Triazoles via a Copper(I)-Catalyzed Three-Component Reaction. *Organic Letters* **2004**, *6* (23), 4223–4225.

[149] Jlalia, I.; Meganem, F.; Herscovici, J.; Girard, C. "Flash" Solvent-Free Synthesis of Triazoles Using a Supported Catalyst. *Molecules* **2009**, *14* (1), 528–539.

[150] Stefanucci, A.; Lei, W.; Pieretti, S.; Novellino, E.; Dimmito, M. P.; Marzoli, F.; Streicher, J. M.; Mollica, A. On Resin Click-Chemistry-Mediated Synthesis of Novel Enkephalin Analogues with Potent Anti-Nociceptive Activity. *Scientific Reports* **2019**, *9* (1), 1–13.

[151] Lietard, J.; Meyer, A.; Vasseur, J.-J.; Morvan, F. New Strategies for Cyclization and Bicyclization of Oligonucleotides by Click Chemistry Assisted by Microwaves. *The Journal of Organic Chemistry* **2008**, *73* (1), 191–200.

[152] Rostovtsev, V. V.; Green, L. G.; Fokin, V. V.; Sharpless, K. B. A Stepwise Huisgen Cycloaddition Process: Copper(I)-Catalyzed

Regioselective "Ligation" of Azides and Terminal Alkynes. *Angewandte Chemie International Edition* **2002**, *41* (14), 2596–2599.

[153] Collins, J. M.; Leadbeater, N. E. Microwave Energy: A Versatile Tool for the Biosciences. *Organic & biomolecular chemistry* **2007**, *5* (8), 1141–1150.

[154] Tulumello, D. V.; Deber, C. M. SDS Micelles as a Membrane-Mimetic Environment for Transmembrane Segments. *Biochemistry* **2009**, *48* (51), 12096–12103.

[155] Hossain, M. A.; Rosengren, K. J.; Samuel, C. S.; Shabanpoor, F.; Chan, L. J.; Bathgate, R. A.; Wade, J. D. The Minimal Active Structure of Human Relaxin-2. *Journal of Biological Chemistry* **2011**, *286* (43), 37555–37565.

[156] Hewitson, T. D.; Ho, W. Y.; Samuel, C. S. Antifibrotic Properties of Relaxin: In Vivo Mechanism of Action in Experimental Renal Tubulointerstitial Fibrosis. *Endocrinology* **2010**, *151* (10), 4938–4948.

[157] Nguyen, B. T.; Yang, L.; Sanborn, B. M.; Dessauer, C. W. Phosphoinositide 3-Kinase Activity Is Required for Biphasic Stimulation of Cyclic Adenosine 3′, 5′-Monophosphate by Relaxin. *Molecular endocrinology* **2003**, *17* (6), 1075–1084.

[158] Bani, D.; Nistri, S.; Cinci, L.; Giannini, L.; Princivalle, M.; Elliott, L.; Bigazzi, M.; Masini, E. A Novel, Simple Bioactivity Assay for Relaxin Based on Inhibition of Platelet Aggregation. *Regulatory peptides* **2007**, *144* (1–3), 10–16.

[159] Halls, M. L.; Bond, C. P.; Sudo, S.; Kumagai, J.; Ferraro, T.; Layfield, S.; Bathgate, R. A. D.; Summers, R. J. Multiple Binding Sites Revealed by Interaction of Relaxin Family Peptides with Native and Chimeric Relaxin Family Peptide Receptors 1 and 2 (LGR7 and LGR8). *Journal of Pharmacology and Experimental Therapeutics* **2005**, *313* (2), 677–687.

[160]Sabatino, G.; D'Ercole, A.; Pacini, L.; Zini, M.; Ribecai, A.; Paio, A.; Rovero, P.; Papini, A. M. An Optimized Scalable Fully Automated Solid-Phase Microwave-Assisted CGMP-Ready Process for the Preparation of Eptifibatide. *Organic Process Research & Development* **2020**, *25* (3), 552-563.

[161] Vergote, V.; Burvenich, C.; Van de Wiele, C.; De Spiegeleer, B. Quality Specifications for Peptide Drugs: A Regulatory-Pharmaceutical Approach. *Journal of Peptide Science* **2009**, *15* (11), 697–710.

9. PUBLICATIONS

FULL PAPER

On-resin microwave-assisted copper-catalyzed azide-alkyne cycloaddition of H1-relaxin B single chain 'stapled' analogues

Annunziata D'Ercole[1,2] | Giuseppina Sabatino[1,3] | Lorenzo Pacini[2] |
Elisa Impresari[4] | Ilaria Capecchi[4] | Anna Maria Papini[1,3,5] | Paolo Rovero[3,4]

[1]Laboratory of Peptide and Protein Chemistry and Biology, Department of Chemistry 'Ugo Schiff', University of Florence, Sesto Fiorentino, Italy

[2]FIS Fabbrica Italiana Sintetici S.p.A, Vicenza, Italy

[3]CNR-IC Istituto di Cristallografia, Catania, Italy

[4]Laboratory of Peptide and Protein Chemistry and Biology, Department of Neurosciences, Psychology, Drug Research and Child Health—Section of Pharmaceutical Sciences and Nutraceutics, University of Florence, Sesto Fiorentino, Italy

[5]PeptLab@UCP and Laboratory of Chemical Biology EA4505, CY Cergy Paris University, Cergy-Pontoise, France

Correspondence

Paolo Rovero, Laboratory of Peptide and Protein Chemistry and Biology, Department of Neurosciences, Psychology, Drug Research and Child Health—Section of Pharmaceutical Sciences and Nutraceutics, University of Florence, Via Ugo Schiff 6, 50019 Sesto Fiorentino, Italy.
Email: paolo.rovero@unifi.it

Present address

Elisa Impresari, Department of Pharmaceutical Sciences, University of Milano, Milan, Italy

Funding information

Fondazione Ricerca Relaxina Firenze, Grant/Award Number: 05/2017; Ente Cassa di Risparmio di Firenze, Grant/Award Number: 2018/0306

Abstract

The development of conformationally constrained analogues of bioactive peptides is a relevant goal in peptide medicinal chemistry. Among the several classes of conformationally constrained peptides, the so-called stapled peptides, which bear a side-chain-to-side-chain bridge, are particularly interesting since they offer the possibility to stabilize specific conformational elements, such as α-helices or β-turns. We describe an efficient and reproducible microwave-assisted strategy to prepare side-chain-to-side-chain clicked peptides, performing the copper-catalyzed azide-alkyne cycloaddition on solid phase, using as a model peptide a portion of the H1-relaxin B chain, which contains the binding cassette motif of this important bioactive peptide. All the relevant parameters, that is, resin, solvent, catalytic system, microwave energy and reaction time were optimized using a systematic one-factor-at-a-time (OFAT) approach. This method will be useful for the preparation of libraries of conformationally constrained relaxin analogues.

KEYWORDS

H1-relaxin B chain, microwave-assisted click reaction, on-resin CuAAC, stapled peptides

1 | INTRODUCTION

The human relaxin peptide family is composed by seven peptides: H1-relaxin, H2-relaxin, H3-relaxin and the human insulin-like peptides INSL3, INSL4, INSL5 and INSL6,[1] characterized by a molecular weight up to 6000 Da.[2] They are formed by two peptide chains, termed A and B, presenting the same overall fold, and characterized by

two intermolecular disulfide bridges on four conserved cysteine residues and an additional intramolecular disulfide bridge located on two conserved cysteine residues in the A chain.

The three relaxins differ from the other peptides of the family for the presence, within the B chain, of the so-called 'Relaxin Binding Cassette', a specific amino acid motif (RXXXRXXI), essential for the high affinity binding of these peptides to the ectodomain of their

receptor,[3] while the A chain contains a low affinity binding motif.[4] Four human relaxin receptor subtypes, termed RXFP1-RXFP4 and belonging to the G-protein-coupled receptors (GPCRs) family, have been described[5,6] and H1-relaxin is considered the preferred ligand of the RXFP1 receptor. As far as physiological activity is concerned, relaxin peptides play a relevant role in both female and male fertility, they mediate the ability to remodel the uterus during pregnancy and the development of mammary nipple, but are also active on the cardiovascular system, in feeding behaviour and in the control of stress responses.[7] Even if the physiological role of H1-relaxin is not yet well known, Tan and co-workers[8] claimed that it could have biological properties comparable to that of the much better characterized H2-relaxin, due to their structural similarity. Interestingly, the putative bioactive conformation of the B chain is an α-helix, presenting on the same face the three residues characteristic of the Relaxin Binding Cassette, considered relevant for the interaction with the receptor, that is, Arg, Arg and Ile.[9]

A synthetic strategy to obtain the relaxin peptides by Fmoc/t-Bu solid-phase peptide synthesis (SPPS) was described in literature for the synthesis of the silkworm insulin-like peptide, bombixin IV.[10] This method features the sequential and regioselective formation of the three disulfide bridges of these peptides using three orthogonal protecting groups on the six involved cysteine residues. This strategy is troubled by a very low overall yield, due to the required multiple synthetic steps and, most importantly, to the need for intermediate purification steps, hampered by solubility problems.[11]

A relevant research effort was also devoted to the design and synthesis of relaxin partial sequences and simplified analogues, with the aim of obtaining important pharmacological data about possible minimal active sequence(s) of the native hormone, able to retain receptor affinity and/or to show selectivity toward different receptor subtypes. Comparing binding results of the so-called 'mini-relaxin 2' H2-(A4-24)(B7-24) and the native H2-relaxin in HEK-293 T cells expressing the RXFP2 receptor, Hossain et al. showed the advantage of the minimized structure, fully selective for RXFP1 over RXFP2.[12]

In 2016, Hossain et al. described the synthesis of a single chain H2-relaxin analogue, based on the B chain and therefore containing the Relaxin Binding Cassette.[13] Starting from the observation that the B-chain of H2-relaxin can be processed in vivo into three equally active isoforms (B1-29, B1-31 and B1-33, Table 1) and that the native H2 B-chain with 29 residues (B1-29) is insoluble in water and

functionally inactive, these authors produced an analogue based on the longer B1-33 sequence, removing six amino acid residues from the N-terminus, in order to obtain a sequence showing an overall positive charge (+5) and a less hydrophobic nature. Finally, the two Cys residues in positions 11 and 23 were replaced with isosteric serine residues, to prevent possible dimerization and aggregation due to cysteine oxidation (Table 1), thus obtaining the analogue [Ser[11], Ser[23]]H2 (B7-33), termed B7-33.[13] This peptide was reported to be freely soluble in water and able to bind RXFP1, despite a significant decrease in affinity and potency. Nevertheless, B7-33 was demonstrated to have an equipotent anti-fibrotic activity compared to native H2-relaxin.[7]

Prompted by these observations we focused our attention on the B chain of H1-relaxin, which has been the subject of very few studies, with the aim of stabilizing the putative bioactive conformation of the Relaxin Binding Cassette through the introduction of a conformational constraint based on side-chain-to-side-chain cyclisation. As the Relaxin Binding Cassette secondary structure appears to be crucial for the binding of these peptides to the cognate RXFP1 receptor ectodomain, attempts to stabilize this motif within the relaxin B chain have already been reported, either in the case of H2 relaxin, via lactam or disulfide bridges, with a i to i + 4 topology,[14] and in H3-relaxin, using the Ring Closure Metathesis (RCM) approach.[15,16] However, to the best of our knowledge, side-chain-to-side-chain conformational constraints based on a triazole bridge, obtained by copper (I)-catalyzed alkyne-azide cycloaddition (CuAAC), have never been introduced into the sequence of relaxins. Accordingly, the present study aims to develop an efficient and reproducible on-resin microwave assisted strategy for the introduction of a triazole bridge in a model peptide derived from the B chain of H1-relaxin. The method will be subsequently used for the preparation of a series of H1-relaxin single chain constrained analogues, in which the Relaxin Binding Cassette is stabilized by a i to i + 4 triazole bridge.

In order to develop an efficient, reproducible and fully on-resin microwave-assisted synthetic strategy, we selected the B chain of H1-relaxin (peptide I in Figure 1) as model peptide. We replaced Cys[10] and Cys[22] with Ser, as previously done also by Hossain et al.[7] and we used positions 14 and 18, which are not directly involved in receptor binding, to construct an i to i + 4 side-chain-to-side-chain

TABLE 1 H1 and H2 Single B-chain analogues

Single B chain analogues	Sequence
[Ser[11], Ser[23]]H2 (B7-33)	VIKLSGRELVRAQIAISGMSTWSKRSL
H2(B1-29)	DSWMEEVIKLCGRELVRAQIAICGMSTWS
H2(B1-31)	DSWMEEVIKLCGRELVRAQIAICGMSTWSKR
H2(B1-33)	DSWMEEVIKLCGRELVRAQIAICGMSTWSKRSL
H1(B1-28)	KWKDDVIKLCGRELVRAQIAICGMSTWS
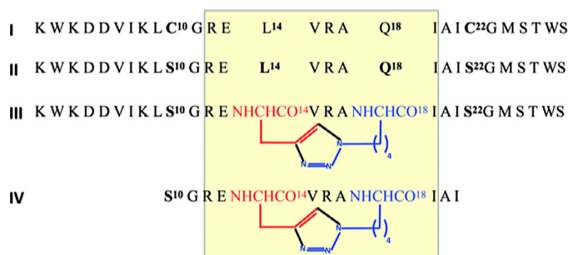
FIGURE 1 I, H1-Relaxin B chain; II, [Ser[10], Ser[22]] H1-Relaxin B; III, 14[3],18[6]-(1H-1,2,3-triazole-4,1-diyl) derivative of [Ser[10], Ala[14], Nle[18], Ser[22]] H1-Relaxin B chain; IV, 14[3],18[6]-(1H-1,2,3-triazole-4,1-diyl) derivative of [Ser[10], Ala[14], Nle[18]] H1-Relaxin B chain (10-21)

bridge, in order to introduce a conformational constraint stabilizing the α-helix conformation. In fact, we previously reported a direct correlation between the α-helix secondary structure formation and the *i*, *i* + 4 positions chosen for the insertion of the modified amino acids involved in cyclisation.[17,18] We also demonstrated that the substitution of an *i* to *i* + 5 disulfide bridge in Octreotide, an important bioactive peptide, with a [1,2,3]triazolyl ring led to the stabilization of the β-turn bioactive conformation,[19] establishing a dynamic equilibrium between β-turn and 3^{10} helix-like conformations.[20] Generally speaking, this information is commonly used to fix the secondary structure in the bioactive conformation in the so-called single and multiple triazole-stapled peptides.[21] Conformationally constraining these often leads to improved activity and/or receptor selectivity, as well as permeability and metabolic stability of peptide analogues.[22] Accordingly, Leu[14] was replaced by Pra and Gln[18] was replaced by Lys(N_3), obtaining the stapled cyclo-peptide **III** after CuAAC reaction. Moreover, we designed the minimal H1-relaxin cyclo-peptide **IV** containing the Relaxin Binding Cassette motif 'RXXXRXXI' and two more residues on C- and N-terminal.

2 | MATERIALS AND METHODS

2.1 | Materials

All Fmoc-protected amino acids, Fmoc-Ser-NovaSyn TGA resin (0.16 mmol/g, 90 μm beads), Fmoc-Ile-NovaSyn TGA (0.19 mmol/g, 90 μm beads), Fmoc-Ile-Wang resin (0.7 mmol/g, 100-200 μm beads), DIC, Oxyma, were purchased by Novabiochem (Merck KGaA, Darmstadt, Germany). DIPEA, 2,6-lutidine, DMSO, DCM and trifluoroacetic acid (TFA) were purchased by Sigma Aldrich (Milano, Italy). 2-(1H-benzotriazol-1-yl)-1,1,3,3-tetramethyluronium hexafluorophosphaten (HBTU) and 1-[Bis(dimethylamino)methylene]-1H-1,2,3-triazolo[4,5-b] pyridinium 3-oxide hexafluorophosphate (HATU) were purchased from Iris Biotech GmbH (Marktredwitz, Germany).

Peptide-synthesis grade N,N-dimethylformamide (DMF) was purchased from Scharlau (Barcelona, Spain); acetonitrile from Carlo Erba (Milano, Italy). The scavengers for cleavage of peptides from resin, Triisopropyl silane (TIS) and 1,2-Ethanedithiol (EDT), were purchased from Sigma Aldrich (Milano, Italy). Diisopropyl ether (iPr$_2$O), diethyl ether (Et$_2$O), Click reagent copper (I) bromide (CuBr), copper (II) sulfate pentahydrate (CuSO$_4$·5H$_2$O) and sodium L-ascorbate were purchased from Sigma Aldrich (Milano, Italy).

2.2 | Methods

2.2.1 | Microwave-assisted SPPS: general protocol

The peptide was synthesized with a CEM Liberty Blue automated peptide synthesizer, equipped with a CEM Discovery microwave reactor (Matthews, NC, USA) following the Fmoc/tBu strategy. Reaction temperatures were monitored by an internal fiberoptic sensor. The

Fmoc deprotections were performed with 20% piperidine in DMF (2 M). The couplings were performed by Fmoc-amino acids (5 equiv, 0.2 M), DIC (5 equiv, 0.5 M) and Oxyma Pure (5 equiv, 1 M). Both deprotection and coupling reactions were performed in a Teflon vessel with microwave energy and nitrogen bubbling.

2.2.2 | Small-scale analytical cleavage (In Process Control, IPC): general protocol

A sample of the resin (25 mg) bearing the clicked analogue has been washed as follows: 1) DMF (3 × 3 mL); 2) Fmoc-His-OH solution (to help the elimination of copper ions according to the well-known formation of Cu-Histidine complexes) in DMF:H$_2$O 1:1 (3 × 2 mL, 5 mM); 3) DCM (3 × 3 mL) and dry off. Peptide cleavage from the resin and deprotection of the amino acids side chains were carried out with TFA/TIS/H$_2$O (96:2:2: v/v/v/v, 1 mL) solution. The mixture was maintained for 30 min at 38 °C under magnetic stirring. The resins were washed with TFA (1 mL) and then filtered. The crude product was precipitated with ice-cold Et$_2$O (4 mL), collected by centrifugation, dissolved in H$_2$O (1 mL) and lyophilized by a 5Pascal LIO5PDGT lyophilizer.

2.2.3 | Cleavage: general protocol

Final cleavage from the resin with concomitant side-chains deprotection, was achieved by treatment of resin-bound peptide with a TFA/TIS/water solution (95:5:5, 1 mL mixture/100 mg of resin). The cleavage was carried out for approximately 3 h at room temperature. The resin was filtered, rinsed TFA (3 × 3 mL). The peptide solution was added to the washes and the product was precipitated from this solution by addition of ice-cold Et$_2$O (15 mL). The crude was washed with ice-cold Et$_2$O (3 × 3 mL) and dried under vacuum.

2.2.4 | RP-UHPLC-MS

The analysis by RP-UHPLC-MS were performed on a Thermo Scientific Ultimate 3000 equipped with a diode array detector, Thermo Scientific-MSQ PLUS, using a Waters Acquity UHPLC CSH C18 1.7 μm 2 × 100 mm Column at 0.5 mL/min. The solvent systems used were A (0.1% TFA in H$_2$O) and B (0.1% TFA in CH$_3$CN), λ 215 and 254 nm.

2.3 | Microwave-assisted SPPS of 14³,18⁶-(1*H*-1,2,3-triazole-4,1-diyl) derivative of [Ser[10], Ala[14], Nle[18], Ser[22]] H1-Relaxin B chain (III)

2.3.1 | C-terminal fragment IAISer²²GMSTWS-NovaSyn TGA resin

The peptide was synthesized on 0.1 mmol scale starting from Fmoc-Ser-NovaSyn TGA resin (0.16 mmol/g, 90 μm beads). The fragment

TABLE 2 Microwave cycle used for C-terminal fragment IAISer[22]GMSTWS

Step	Temperature (°C)	Power (W)	Hold Time (s)	Delta T (°C)
Deprotection	75	100	240	2
Coupling	22	0	600	5
	75	30	300	2

TABLE 3 Microwave cycle used for Fmoc-Lys(N₃)-OH

Step	Temperature (°C)	Power (W)	Hold time (s)	Delta T (°C)
Deprotection	50	90	240	2
Coupling	22	0	120	2
	25	50	10	2
	49	35	780	1

TABLE 4 On-resin microwave-assisted CuAAC of the fragment Pra[14]VRALys(N₃)[18]IAISer[22]GMSTWS-resin

Temperature (°C)	Power (W)	Hold time (s)	Delta T (°C)
75	100	30	2
80	60	600	1

was obtained through double coupling exposed to the microwave cycle described in Table 2.

2.3.2 | Stability study of Fmoc-Lys(N₃)-OH

A Fmoc-Lys(N₃)-OH (79 mg, 0.2 M) solution in DMF has been subjected to four microwave-assisted cycles described in the Table 3.

The study was followed by RP-UHPLC MS, samples were analyzed with the gradient 5%-95% B in 10 min, column at 45 °C, at λ 254 nm, mass range 50-1000 m/z.

2.3.3 | Elongation of the fragment Pra[14]VRALys(N₃)[18] and Microwave-assisted CuAAC

The elongation until Pra[14] was performed through a double coupling by a three steps microwave-method (Table 3). The on-resin microwave-assisted CuAAC (Table 4) was performed using CuSO₄·5H₂O (1.2 equiv), sodium ascorbate (1.5 equiv) in H₂O:t-BuOH: DCM 1:1:1 (3 mL).

2.3.4 | Elongation of the N-terminal fragment KWKDDVIKLS[10]GRE and cleavage

The remaining amino acid residues were coupled by a standard microwave-assisted protocol described in Table 5.

The crude peptide (III), obtained after cleavage (General Protocol modified using 94% TFA, 1% TIS, 2.5% EDT, 2.5% H₂O and ice-cold iPr₂O), has been lyophilized and purified by semi-preparative RP-HPLC (model 600, Waters, Milford, MA) on a Phenomenex Jupiter C18

(10 mm, 250 mm × 10 mm) column (Phenomenex, Castel Maggiore, Italy) at 4 mL/min. The solvent systems used were: 0.1% TFA in H₂O (A) and 0.1% TFA in CH₃CN (B) and the gradients used was 20%-60% B in 20 min. Characterization of the crude peptide (III) (see supporting information) was performed by analytical RP-HPLC (Waters Alliance model 2695) with UV detection at 215 nm, coupled with an ESI-MS detector (Micromass ZQ, Waters, Milford MA, USA) using a BIOshell A160 Peptide C18 (2.7 mm, 10 cm × 30 mm) column at 35 °C, at a flow rate of 0.6 mL/min. The solvent systems used were: 0.1% TFA in H₂O (A) and 0.1% TFA in CH₃CN (B). Data were acquired and processed using MassLynx software (Waters, Milford, MA, USA), with a gradient from 20% to 80% of B in 5 min. Expected peptide, R_t 4.02 min. ESI-MS (m/z): calcd for $C_{141}H_{228}N_{42}O_{40}S$, 3182.7; found 1062.4 $[M + 3H]^{3+}$; 797.6 $[M + 4H]^{4+}$; 637.3 $[M + 5H]^{5+}$.

2.4 | On-resin microwave-assisted CuAAC of the Fmoc-protected fragment Pra[14]VRALys(N₃)[18] IAI: One-factor-at-a-time (OFAT) approach

Following the microwave-assisted protocol used above (Table 3), we synthesized the Fmoc-protected fragment Pra[14]VRALys(N₃)[18]IAI on 0.1 mmol of Fmoc-Ile-NovaSyn TGA resin (0.19 mmol/g, 90 μm beads). Subsequencially, the resin was divided into four portions (0.025 mmol each) to perform the experiments **A-D** (as shown in Figure 4, section 3.2).

Experiment **A**. Peptide-resin (0.025 mmol), CuSO₄·5H₂O (1.2 equiv), sodium ascorbate (1.5 equiv) in H₂O:t-BuOH:DCM 1:1:1 (3 mL), microwave-assisted CuAAC in Table 4.

Experiment **B**. Peptide-resin (0.025 mmol), CuSO₄·5H₂O (1.2 equiv), sodium ascorbate (1.5 equiv) in H₂O:t-BuOH:DCM 1:1:1 (3 mL), microwave-assisted CuAAC in Table 6.

Experiment **C**. Peptide-resin (0.025 mmol), CuSO₄·5H₂O (1.2 equiv), sodium ascorbate (1.5 equiv) in H₂O:t-BuOH:DCM 1:1:1 (3 mL), microwave-assisted CuAAC in Table 7.

Experiment **D**. Peptide-resin (0.025 mmol); CuBr (2 mg, 1.2 equiv) and sodium ascorbate (6 mg, 1.5 equiv) diluted into a mixture of DMSO (1 mL) and DMF (2 mL), DIPEA (18 μL, 5 equiv) and 2,6-Lutidine (12 μL, 5 equiv), microwave-assisted CuAAC in Table 6.

TABLE 5 Standard microwave-assisted cycle

Step	Temperature (°C)	Power (W)	Hold time (s)	Delta T (°C)
Deprotection	80	200	30	2
	90	50	70	1
Coupling	75	170	15	2
	90	30	100	1

TABLE 6 Microwave-assisted CuAAC at 55 °C for 10 min

Temperature (°C)	Power (W)	Hold time (s)	Delta T (°C)
49	150	15	2
54	30	600	1

TABLE 7 Microwave-assisted CuAAC at 55 °C for 5 min

Temperature (°C)	Power (W)	Hold time (s)	Delta T (°C)
49	150	30	2
54	30	300	1

Two experiments (**E-F**) were carried out on aliquots of 0.02 mmol of Fmoc-Pra^{14}VRALys(N$_3$)^{18}IAI-Wang resin (0.7 mmol/g, 100-200 mesh) obtained by a manual Fmoc/tBu SPPS strategy. The resin was swollen for 40 min in DMF (1 mL/100 mg resin). Single couplings were carried out with a mixture of Fmoc-Xaa-OH (5 equiv), HBTU, (5 equiv) and DIPEA, (6 equiv) in DMF for 25 min. Single coupling of Fmoc-Lys(N$_3$)-OH and Fmoc-Pra-OH were performed with a mixture of Fmoc-Xaa-OH (2.50 equiv), HATU (2.75 equiv) and DIPEA (3.75 equiv) in DMF for 25 min. After each coupling, the resin was washed with DMF (3 × 5 mL) and DCM (2 × 5 mL).

Experiment **E**. Peptide-resin (0.02 mmol); CuSO$_4$·5H$_2$O (1.2 equiv), sodium ascorbate (1.5 equiv) in H$_2$O:t-BuOH:DCM 1:1:1 (3 mL), microwave-assisted CuAAC at 55 °C for 10 min (Table 6).

Experiment **F**. Peptide-resin (0.02 mmol), CuBr (2 mg, 1.2 equiv) and sodium ascorbate (6 mg, 1.5 equiv) diluted into a mixture of DMSO (1 mL) and DMF (2 mL), DIPEA (18 μL, 5 equiv) and 2,6-Lutidine (12 μL, 5 equiv), microwave-assisted CuAAC at 55 °C for 10 min (Table 6).

Each peptide portions was cleaved following the general cleavage protocol and analyzed by RP UHPLC-MS. Gradient 10%-80% B in 10 min. Column Waters Acquity UHPLC CSH C18 1.7 μm 2 × 100 mm at 0.5 mL/min, column at 65 °C. Solvent systems A (0.1% TFA in H$_2$O) and B (0.1% TFA in CH$_3$CN), λ 215 nm. Clicked peptide, R_t 3.8 min. ESI-MS (m/z): calcd for C$_{40}$H$_{70}$N$_{14}$O$_9$ 891.1, found 891.5 [M + H]$^+$. Unreacted linear peptide, R_t 4.6 min. ESI-MS (m/z): calcd for C$_{40}$H$_{70}$N$_{14}$O$_9$ 891.1, found 891.7 [M + H]$^+$. Dimer peptide, R_t 5.0 min. ESI-MS: ESI-MS (m/z): calcd for C$_{80}$H$_{140}$N$_{28}$O$_{18}$ 1782.2, found 891.8 [M + 2H]$^{2+}$, 595.1 [M + 3H]$^{3+}$.

2.5 | Microwave-assisted SPPS of 14^3,18^6-(1H-1,2,3-triazole-4,1-diyl) derivative of [Ser^{10},Ala^{14},Nle^{18}] H1-Relaxin B chain (10-21) (IV)

The linear peptide was synthesized on Fmoc-Ile-NovaSyn TGA resin (0.19 mmol/g, 90 μm beads) 0.02 mmol scale with the microwave-assisted method described in Table 3. The on-resin CuAAC was performed by CuBr (2 mg, 1.2 equiv) and sodium ascorbate (6 mg, 1.5 equiv) diluted into a mixture of DMSO (1 mL) and DMF (2 mL), DIPEA (18 μL, 5 equiv) and 2,6-Lutidine (12 μL, 5 equiv), microwave-assisted CuAAC at 55 °C for 10 min (Table 6). The peptide was cleaved following the general cleavage protocol and analyzed by RP-UHPLC-MS.

A microwave-assisted larger scale synthesis was performed on 0.1 mmol with the method described in Table 3. The cyclisation was performed by CuBr (17 mg, 1.2 equiv) and sodium ascorbate (30 mg, 1.5 equiv) diluted into a mixture of DMSO (6 mL) and DMF (12 mL), DIPEA (87 μL, 5 equiv) and 2,6-Lutidine (53 μL, 5 equiv), microwave-assisted CuAAC at 55 °C for 10 min (Table 8).

The peptide was cleaved following the general cleavage protocol and analyzed by RP-UHPLC-MS. The crude peptide (148 mg) was purified by a Flash chromatography system (Biotage Isolera One, Sweden) with UV Detector, equipped with a 30 g SNAP Ultra C$_{18}$ column, Column Volume (CV) 45 mL. The solvent systems used were: 0.1% TFA in H$_2$O (A) and 0.1% TFA in CH$_3$CN (B), the flow rate 25 mL/min and the gradient 3 CV A, 10 CV from 10% to 60% of B, 3CV B. After lyophilization we obtained 42.3 mg (yield 25.5%) of purified peptide **IV**.

The peptide was characterized by Thermo Scientific MSQ Plus spectrophotometer (ESI-MS) with analytic Ultimate 3000 UHPLC (Thermo Scientific) on Acquity UPLC Column CSH C18 1.7 μm 2.1 × 100 mm. The solvent systems used were: 0.1% TFA in H$_2$O (A) and 0.1% TFA in CH$_3$CN (B), the flow rate 0.5 mL/min, column at 45 °C, gradient from 10% to 60% of B in 10 min, λ 215 nm. R_t 4.9 min. Purity (HPLC): >95%. ESI-MS (m/z): calcd for C$_{56}$H$_{97}$N$_{21}$O$_{16}$, 1320.5; found 1321.1 [M + H]$^+$; 661.7 [M + 2H]$^{2+}$.

3 | RESULTS AND DISCUSSION

3.1 | Synthesis of 14^3,18^6-(1H-1,2,3-triazole-4,1-diyl) derivative of [Ser^{10}, Ala^{14}, Nle^{18}, Ser^{22}] H1-Relaxin B chain (III)

The on-resin strategy described in Figure 2 can be carried out in a fully automated mode by a suitable microwave-assisted peptide synthesizer and it is based on the following steps: (a) elongation of the C-terminal portion of the sequence; (b) introduction of the unnatural amino acids Pra and Lys(N$_3$); (c) on-resin formation of the triazole ring; (d) elongation of the N-terminal portion; (e) final cleavage from the resin. To prevent the formation of by-products from the on-resin click reaction, due to aggregation of the hydrophobic fragments and intermolecular cyclisation/dimerization, we selected a low loading PEG-PS-copolymer resin.

TABLE 8 On-resin microwave-assisted method for 0.1 mmol scale

Temperature (°C)	Power (W)	Hold time (s)	Delta T (°C)
51	150	30	2
54	40	600	1

X : Ile-Ala-Ile-Ser-Gly-Met-Ser-Thr-Trp-Ser

Y : Lys-Trp-Lys-Asp-Asp-Val-Ile-Lys-Leu-Ser-Gly-Arg-Glu

X^1 : Ile-Ala-Ile-Ser(tBu)-Gly-Met-Ser(tBu)-Thr(tBu)-Trp(Boc) Ser(tBu)

Y^1 : Lys(Boc)-Trp(Boc)-Lys(Boc)-Asp(OtBu)-Asp(OtBu)-Val⌐
 └Ile-Lys(Boc)-Leu-Ser(tBu)-Gly-Arg(Pbf)-Glu(OtBu)
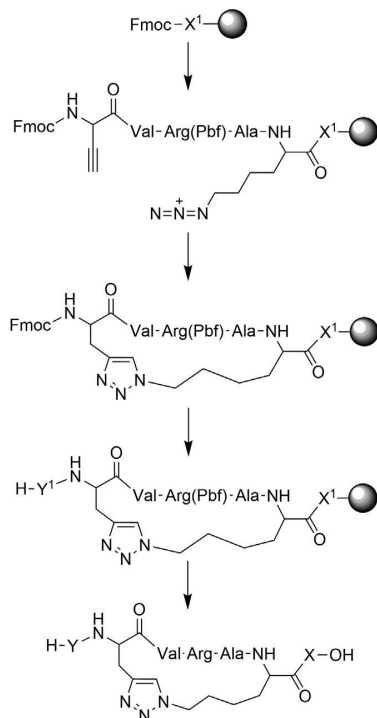
FIGURE 2 MW-SPPS of $14^3,18^6$-(1H-1,2,3-triazole-4,1-diyl) derivative of [Ser[10], Ala[14],Nle[18],Ser[22]] H1-Relaxin B chain (III)

The construction of the C-terminal portion [Ser[22]]H1-Relaxin B (19-28) did not show particular criticalities, but it was necessary to optimize the microwave protocol to avoid possible side reactions that could compromise the next steps. After using a standard microwave-assisted double coupling (Table 5), a small-scale cleavage performed as analytical In-Process Control (IPC), showed the presence of some impurities, probably due to the racemization of unidentified residue(s) during the microwave activation step at high temperature. In fact, a microwave protocol based on a lower temperature and a two steps activation strategy (Table 2) allowed to reduce considerably these side products.

Regarding the microwave incorporation of Pra and Lys(N_3), we initially planned a conventional coupling at room temperature to insert Lys(N_3) and we tried different coupling reagents (HBTU, HATU, PyBop), bases (DIPEA and NMM) and solvents (TFE, DCM, DMF), but all our attempts failed, probably because of the steric hindrance of the triplet IAI. As microwave energy is reported to disrupt secondary structures during peptide elongation,[23] we planned a mild microwave-assisted coupling (Table 3), after an appropriate stability study of this amino acid. With the aim of simulating the conditions of microwave-assisted deprotection and coupling cycles, we exposed a solution of Fmoc-Lys(N_3)-OH in DMF to the microwave irradiation, following by RP-UHPLC the stability of this residue. As shown in Figure 3, we did not observe degradation of the azido group side-chain, since we did not observe a peak overlapping with that of the Fmoc-Lys-OH reference standard. At variance, we observed an unknown peak at R_t 8.85 min, probably due to dibenzofulvene deriving from the partial deprotection of Fmoc in DMF solution by microwave irradiation. Our hypothesis is supported by the formation of the same unknown peak at R_t 8.85 min with different amino acid such as Fmoc-Gly-OH under the same conditions of microwave-assisted deprotection and coupling.

Therefore, using the optimized method reported in the Table 3 we successfully obtained an almost quantitative coupling of Lys(N_3), with the deletion sequence desLys(N_3) limited to 1.5%, and we applied this protocol to elongate the sequence until Pra[14], to obtain [Pra[14], Lys(N_3)[18], Ser[22]] H1-Relaxin B (14-28).

The on-resin formation of the triazole ring presents the following significant advantages, as compared to the solution approach: (a) pseudo-dilution effect of the solid support; (b) the possibility to easily wash-out the copper catalyst by filtration; (c) reduction of the number of synthetic steps and (d) no isolation of the azido-intermediate linear peptide. Moreover, this procedure enables the continuation of the elongation of the N-terminal fragment by a standard microwave protocol at high temperature, once the triazole ring is formed.

It has been reported that microwave irradiation in solution could radically increase the CuAAC reaction rate,[24] improving the yield and reducing reaction time. However, the laborious and time-consuming work-up in solution required for the elimination of copper residues from the final product leads to the development of heterogeneous CuAAC reactions.[25] Click reaction on solid phase represents the simplest strategy to perform an easy-cleanable CuAAC. Literature available until now reports CuAAC on solid phase performed at room temperature for up to 24 h, which can be unsuitable in the presence of unstable residues and would hardly be scalable to large-scale production.[26,27] Lietard et al. have demonstrated that the solid supported reaction led to better purity, thanks to the copper residue removal,[28] for the production of different kinds of cyclic oligonucleotides by microwave-assisted CuAAC, both in solution and on solid support. In this scenario, we aim to develop a robust synthetic strategy that enables the production of cyclic peptides by CuAAC assisted by microwave radiation.

To perform the cyclisation, two different catalytic systems are herein described: Cu(I) in situ formation through $CuSO_4 \cdot 5H_2O$
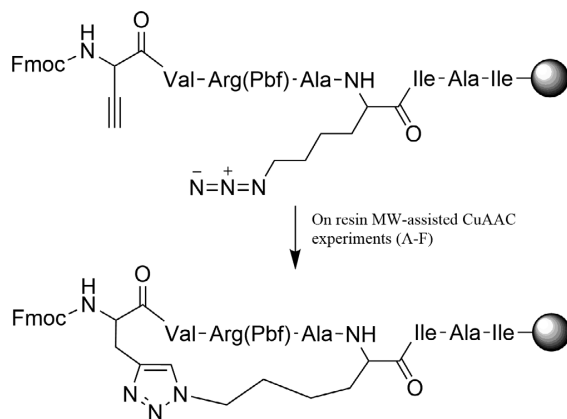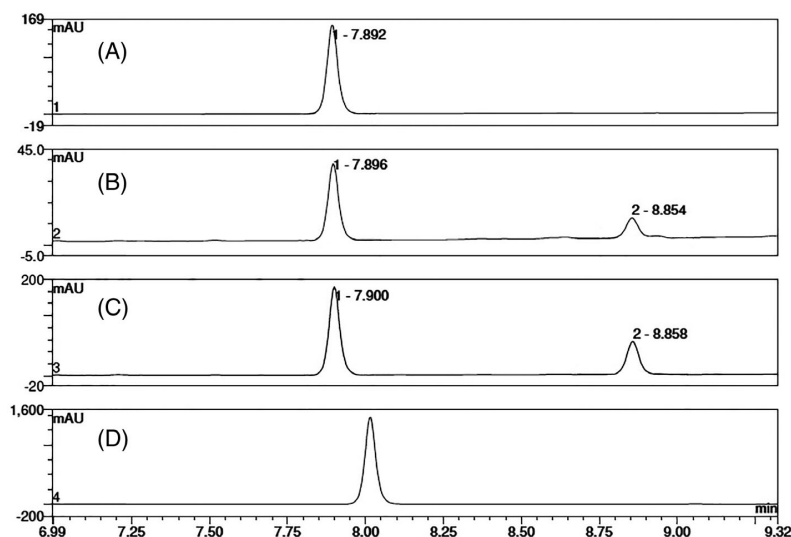
FIGURE 4   On-resin microwave-assisted CuAAC of the Fmoc-protected [Pra^{14}, Lys(N$_3$)^{18}] H1-Relaxin B (14-21)

reduction in the presence of sodium ascorbate in water/alcohol,[29] and the direct use of a Cu(I) salt, such as CuBr or CuI. Contrary to the first protocol, the latter requires an excess of base (DIPEA, 2,6-lutidine) to deprotonate the alkyne moiety to form the Cu(I)-acetylide intermediate.[29] We performed the on-resin microwave-assisted CuAAC of the Fmoc-protected [Pra^{14}, Lys(N$_3$)^{18}, Ser^{22}] H1-Relaxin B (14-28) by in situ Cu(I) formation via CuSO$_4$ and sodium ascorbate in presence of DCM, to increase solubility of hydrophobic reactants. During the sample solubilization in H$_2$O/CH$_3$CN (1:1) for the RP-HPLC-MS analysis, we interestingly observed that the crude peptide obtained from the IPC cleavage after the click reaction appeared more soluble than the linear fragment.

The successful on-resin microwave-assisted triazole ring formation allowed us to continue the synthesis of the remaining part of the sequence by standard microwave-assisted double coupling

(Table 5).[30] Moreover, we were able to cleave the peptide containing methionine with a thiol scavenger, which cannot be used in the presence of the azido moiety.

Therefore, this solid-phase microwave-assisted protocol enabled us to obtain the crude model cyclo-peptide 14^3,18^6-(1H-1,2,3-triazole-4,1-diyl) derivative of [Ser^{10}, Ala^{14}, Nle^{18}, Ser^{22}] H1-Relaxin B chain (**III**), although with low yield (0.2%) and limited purity (see supporting information). In view of these results, we decided to proceed with further optimization of the method in order to enable a viable preparation of several analogues with a yield and purity compatible with biological testing. For this reason, we designed a simplified stapled H1-Relaxin B model peptide for further synthetic optimization.

3.2 | Synthesis of the minimized stapled analogue 14^3,18^6-(1H-1,2,3-triazole-4,1-diyl) derivative of [Ser^{10}, Ala^{14},Nle^{18}] H1-Relaxin B chain (10-21) (IV)

On the basis of previous publications on linear and constrained derivatives of H2-relaxin,[12–14] we choose a H1-relaxin chain minimization approach based on the Relaxin Binding Cassette motif 'RXXXRXXI', extended by two residues on both C- and N-terminal ends (peptide **IV** in Figure 1). By the mild microwave-assisted protocol (Table 3) used for the longer stapled analogue **III**, we obtained the Fmoc-protected fragment Pra^{14}VRALys(N$_3$)^{18}IAI (Figure 4) that we used for a systematic optimization of the microwave-assisted on-resin CuACC.

We modulated the microwave energy and the reaction time in order to increase the cyclisation yield and concomitantly reduce the side reactions such as dimerization. Moreover, we compared CuSO$_4$/sodium ascorbate in H$_2$O/t-BuOH/DCM vs CuBr/sodium ascorbate in DMSO/DMF and a PEG-PS-copolymer resin vs a more commonly used and less expensive polystyrene resin. Following a One-Factor-

At-a-Time (OFAT) approach, we changed each critical factor (resin, solvent, catalytic system, microwave energy and reaction time) at a time. After each cyclisation experiment and the N-terminal Fmoc deprotection, the crude peptide $14^3,18^6$-(1H-1,2,3-triazole-4,1-diyl) derivative of [Ala[14], Nle[18]] H1-Relaxin B chain (14-21), fragment 14-21 of the peptide IV (**IV 14-21**), was cleaved from the resin and analyzed by RP-HPLC-MS in order to quantify the expected clicked product, the unreacted linear peptide and the by-product(s), for example, dimer peptide, as shown in Figure 5. The results are summarized in Table 9.

In the experiments **A-C** (Table 9), we held as constant the resin and the catalyst CuSO₄ while we changed the temperature and the reaction time. At 80 °C for 10 min (method in Table 4) we found the expected clicked peptide (37.7%) but we detected a side product, probably due to intermolecular dimerization (27.7%). Decreasing by half the microwave power (method Table 6), which led to achieve a lower final temperature (55 °C), we increased the clicked product

(46.2%) and we decreased the dimer (17.8%). Finally, reducing the reaction time to 5 min we found a high quantity of unreacted linear peptide (19.7%), while the dimer was still present (10%). Changing the copper system (CuBr), while maintaining the best temperature, reaction time and resin (entry **B**, Table 9), we successfully obtained the clicked peptide in a good purity (entry **D**, Table 9). Additionally, to asses also the role of the solid support, we fixed the best time of reaction and temperature (10 min at 55 °C) and we changed the resin. By these experiments performed on the polystyrene resin we confirmed that CuBr/sodium ascorbate in DMSO/DMF (entry **F**, Table 9) is better than CuSO₄/sodium ascorbate in H₂O/t-BuOH/DCM with which we surprisingly did not obtain the clicked peptide (entry **E**, Table 9 and Figure 5). Moreover, it was remarkable how using a high loading (0.7 mmol/g) polystyrene resin we found a high quantity of unreacted linear peptide, instead of the expected increase of the dimer. The quantity of dimer depended both on the temperature/microwave energy and on the exposure time to the microwave irradiation.

TABLE 9 On-resin microwave assisted CuAAC optimization study

Entry[a]	Analogue	Resin[b]	Catalytic system	Solvent	Temp max (°C)	Time (min)	Cyclo (a/a%)[c]	Linear (a/a%)	Dimer (a/a%)
A	IV 14–21	PEG-PS	CuSO₄ sodium ascorbate	H₂O: t-BuOH:DCM 1:1:1	80	10	37.7	1.2	27.7
B	IV 14–21	PEG-PS	CuSO₄ sodium ascorbate	H₂O: t-BuOH:DCM 1:1:1	55	10	46.2	2.6	17.8
C	IV 14–21	PEG-PS	CuSO₄ sodium ascorbate	H₂O: t-BuOH:DCM 1:1:1	55	5	27.1	19.7	10.0
D	IV 14–21	PEG-PS	CuBr sodium ascorbate	DMSO:DMF 1:2	55	10	64.1	0.9	5.5
E	IV 14–21	PS	CuSO₄ sodium ascorbate	H₂O: t-BuOH:DCM 1:1:1	55	10	-	68.3	1.0
F	IV 14–21	PS	CuBr sodium ascorbate	DMSO:DMF 1:2	55	10	19.7	21.4	6.8
G	IV	PEG-PS 0.02 mmol	CuBr sodium ascorbate	DMSO:DMF 1:2	55	10	55.8	5.8	3.7
H	IV	PEG-PS 0.1 mmol	CuBr sodium ascorbate	DMSO:DMF 1:2	55	10	69.1	-	6.5

[a]A-F: on-resin CuAAC of the Fmoc-protected fragment Pra[14]VRALys(N₃)[18]IAI; G-H: on-resin CuAAC of the fragment S[10]GREPra[14]VRALys(N₃)[18]IAI.
[b]Resin PEG-PS: Fmoc-Ile-NovaSyn TGA 0.2 mmol/g; Resin PS Fmoc-Ile-Wang: 0.7 mmol/g.
[c]a/a%: area of the peak of interest expressed as % of the total area of all the relevant peaks in the chromatogram.
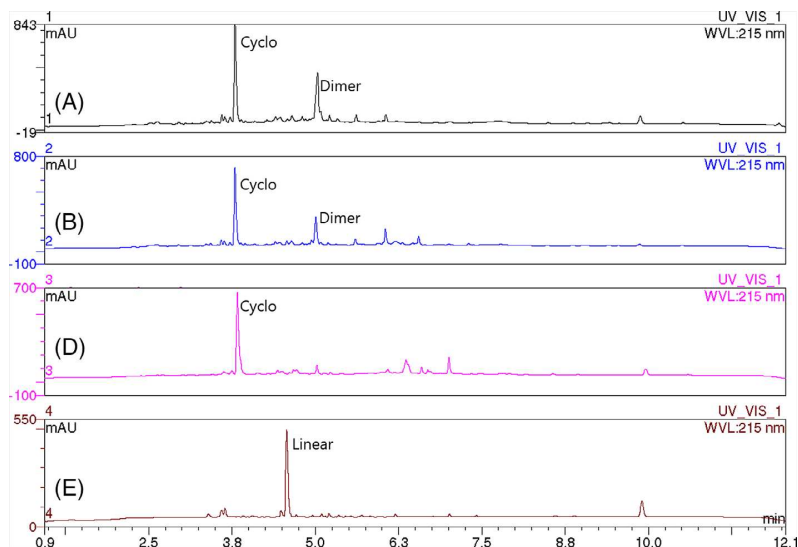
FIGURE 5 Comparison among different microwave-assisted CuAAC on Fmoc-protected [Pra[14], Lys(N₃)[18]] H1-Relaxin B (14-21). Experiments A, B and D were performed with NovaSyn TGA resin 0.2 mmol/g. A, CuSO₄/sodium ascorbate, 80 °C, 10 min; B, CuSO₄/ sodium ascorbate, 55 °C, 10 min; D, CuBr/sodium ascorbate 55 °C, 10 min. Experiment E was performed with Wang polystyrene resin 0.7 mmol/g, CuSO₄/ sodium ascorbate, 55 °C, 10 min

FIGURE 6 On-resin microwave-assisted synthesis of $14^3,18^6$-(1H-1,2,3-triazole-4,1-diyl) derivative of [Ser^{10}, Ala^{14}, Nle^{18}] H1-Relaxin B chain (10-21) (**IV**)
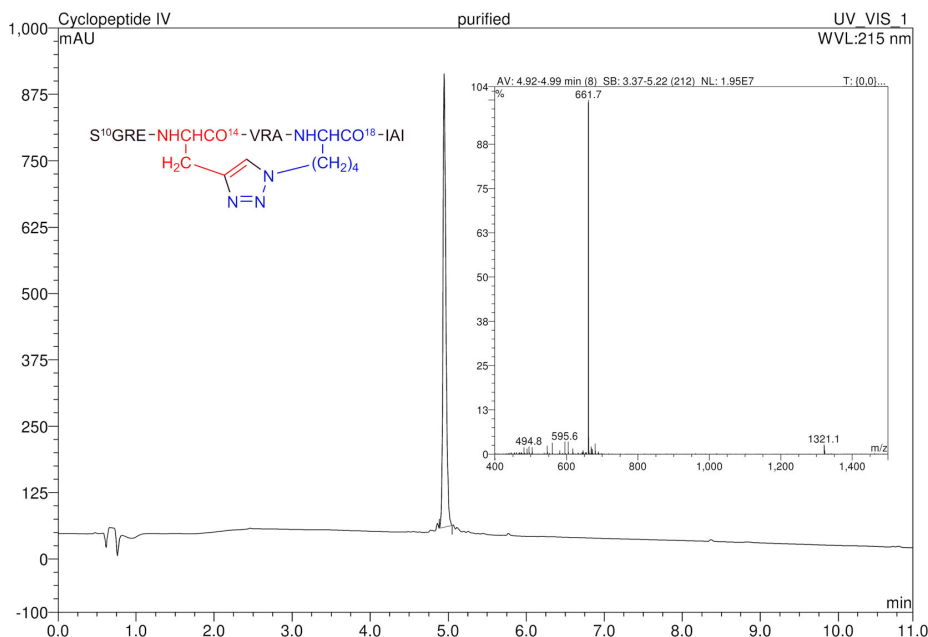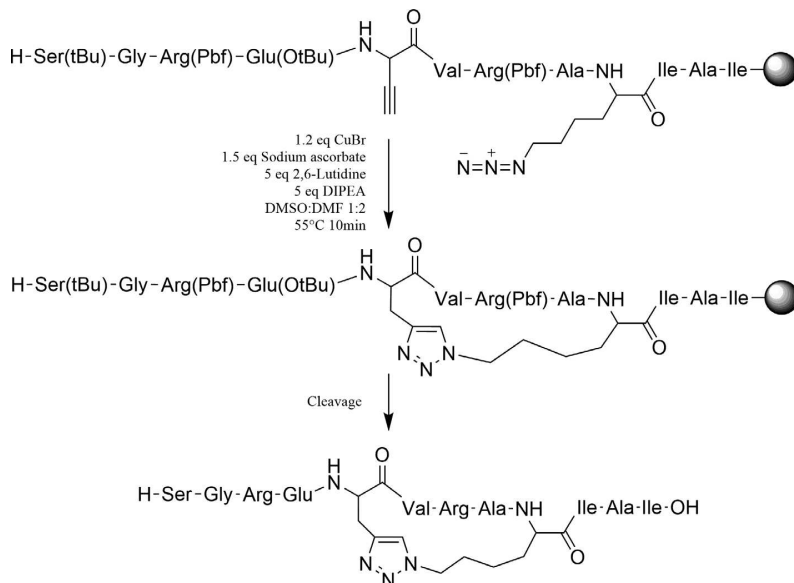
FIGURE 7 Analytical RP-UHPC-MS of the purified peptide $14^3,18^6$-(1H-1,2,3-triazole-4,1-diyl) derivative of [Ser^{10}, Ala^{14}, Nle^{18}] H1-Relaxin B chain (10-21) (**IV**) (Entry G, Table 9). UHPLC chromatogram of the expected peptide R_t = 4.95 min. Gradient 10%-60% B in 10 min. Column Waters Acquity UHPLC CSHTM C18 1.7 μm 2 × 100 mm at 0.5 mL/min. Solvent systems A (0.1% TFA in H$_2$O) and B (0.1% TFA in CH$_3$CN), λ 215. Inset: ESI-MS spectrum of the expected peptide [M + H]$^+$ 1321.1 (calcd 1321.5) [M + 2H]$^{2+}$ 661.7 (calcd 661.2)

Moreover, the use of CuBr increased the peak area % of the cyclo peptide in comparison with CuSO$_4$. In Figure 5, we report the RP-UHPLC traces of the crude products obtained from different on-resin MW-assisted CuAAC experiments on PEG-PS-copolymer resin (entries **A**, **B**, **D**, Table 9) and on Wang polystyrene resin (entries **E**, Table 9).

After the identification of all the critical factors, the protocol reported in Figure 6 enabled us to obtain the stapled minimized

analogue **IV** (entry **G**, Table 9) in a small scale (0.02 mmol), at high purity, in a short time and without isolation of the intermediates.

To demonstrate the robustness and the reproducibility of the MW-assisted CuAAC method, we repeated the click reaction at a five-fold larger scale (0.1 mmol) (Entry **H**, Table 9), with minor modifications to the microwave method (Table 8) because of the larger quantity of resin. The good result (42.3 mg, yield 25.5%, Figure 7) of this scale-up experiment provided a final crude product at the same purity level, as compared to the smaller scale (Entry **G**, Table 9), clearly indicating that the developed strategy is robust enough to be exploited to synthesize a library of stapled analogues. The chosen model sequence, $S^{10}GREPra^{14}VRALys(N_3)^{18}IAI$, can be considered a suitable starting point for the preparation of longer and different H1-relaxin sequences.

4 | CONCLUSIONS

We have developed an efficient and reproducible microwave-assisted strategy to prepare side-chain-to-side-chain clicked peptides, performing on solid phase the copper-catalyzed azide-alkyne cycloaddition, using as a model peptide a portion of the H1-relaxin B chain, containing the binding cassette motif of this bioactive peptide. All the relevant parameters, that is, resin, solvent, catalytic system, microwave energy and reaction time were optimized using a systematic one-factor-at-a-time approach. This method will be useful for the preparation of libraries of conformationally constrained analogues of the relaxins.

CONFLICT OF INTEREST

The authors declare no competing financial interest.

ORCID

Giuseppina Sabatino https://orcid.org/0000-0001-7737-7517
Anna Maria Papini https://orcid.org/0000-0002-2947-7107
Paolo Rovero https://orcid.org/0000-0001-9577-5228

REFERENCES

[1] T. N. Wilkinson, T. P. Speed, G. W. Tregear, R. A. Bathgate, *BMC Evol. Biol.* **2005**, *5*, 14.
[2] D. Bani, *Gen. Pharmacol.* **1997**, *28*, 13.
[3] E. E. Büllesbach, S. Yang, C. Schwabe, *J. Biol. Chem.* **1992**, *267*, 22957.
[4] M. P. Del Borgo, R. A. Hughes, R. A. D. Bathgate, F. Lin, K. Kawamura, J. D. Wade, *J. Biol. Chem.* **2006**, *281*, 13068.
[5] R. A. Bathgate, R. Ivell, B. M. Sanborn, O. D. Sherwood, R. J. Summers, *Pharmacol. Rev.* **2006**, *58*, 7.
[6] S. P. Alexander, A. P. Davenport, E. Kelly, N. Marrion, J. A. Peters, H. E. Benson, et al., *Br. J. Pharmacol.* **2015**, *172*, 5744.
[7] N. A. Patil, K. J. Rosengren, F. Separovic, J. D. Wade, R. A. D. Bathgate, M. A. Hossain, *Br. J. Pharmacol.* **2017**, *174*, 950.
[8] Y. Y. Tan, J. D. Wade, G. W. Tregear, R. J. Summers, *Br. J. Pharmacol.* **1998**, *123*, 762.
[9] E. E. Büllesbach, C. Schwabe, *J. Pept. Res.* **2001**, *57*, 77.
[10] K. Maruyama, K. Nagata, M. Tanaka, H. Nagasawa, A. Isogai, H. Ishizaki, et al., *J. Protein Chem.* **1992**, *11*, 1.
[11] M. A. Hossain, J. D. Wade, *Curr. Opin. Chem. Biol.* **2014**, *22*, 47.
[12] M. A. Hossain, K. J. Rosengren, C. S. Samuel, F. Shabanpoor, L. J. Chan, R. A. D. Bathgate, et al., *J. Biol. Chem.* **2011**, *286*, 37555.
[13] M. A. Hossain, M. Kocan, S. T. Yao, S. G. Royce, V. B. Nair, C. Siwek, et al., *Chem. Sci.* **2016**, *7*, 3805.
[14] M. P. Del Borgo, R. A. Hughes, J. D. Wade, *J. Pept. Sci.* **2005**, *11*, 564.
[15] K. Hojo, M. A. Hossain, J. Tailhades, F. Shabanpoor, L. L. L. Wong, E. E. K. Ong-Pålsson, et al., *J. Med. Chem.* **2016**, *59*, 7445.
[16] T. Jayakody, S. Marwari, R. Lakshminarayanan, F. C. K. Tan, C. W. Johannes, B. W. Dymock, et al., *Peptides* **2016**, *84*, 44.
[17] S. Cantel, A. Le Chevalier Isaad, M. Scrima, J. J. Levy, R. D. DiMarchi, P. Rovero, et al., *J. Org. Chem.* **2008**, *73*, 5663.
[18] M. Scrima, A. L. Chevalier-Isaad, P. Rovero, A. M. Papini, M. Chorev, A. M. D'Ursi, *Eur. J. Org. Chem.* **2010**, *2010*, 446.
[19] G. Melacini, Q. Zhu, M. Goodman, *Biochemistry* **1997**, *36*, 1233.
[20] C. Testa, A. M. Papini, M. Chorev, P. Rovero, *Curr. Top. Med. Chem.* **2018**, *18*, 591.
[21] S. A. Kawamoto, A. Coleska, X. Ran, H. Yi, C.-Y. Yang, S. Wang, *J. Med. Chem.* **2012**, *55*, 1137.
[22] V. Haridas, *Eur. J. Org. Chem.* **2009**, *2009*, 5112.
[23] J. M. Collins, N. E. Leadbeater, *Org. Biomol. Chem.* **2007**, *5*, 1141.
[24] P. Appukkuttan, W. Dehaen, V. V. Fokin, E. Van der Eycken, *Org. Lett.* **2004**, *6*, 4223.
[25] I. Jlalia, F. Meganem, J. Herscovici, C. Girard, *Molecules* **2009**, *14*, 528.
[26] A. Stefanucci, W. Lei, S. Pieretti, E. Novellino, M. P. Dimmito, F. Marzoli, et al., *Sci. Rep.* **2019**, *9*, 5771.
[27] Z.-M. Wu, S.-Z. Liu, X.-Z. Cheng, W.-Z. Ding, T. Zhu, B. Chen, *Chin. Chem. Lett.* **2016**, *27*, 1731.
[28] J. Lietard, A. Meyer, J.-J. Vasseur, F. Morvan, *J. Org. Chem.* **2008**, *73*, 191.
[29] V. V. Rostovtsev, L. G. Green, V. V. Fokin, K. B. Sharpless, *Angew. Chem. Int. Ed.* **2002**, *41*, 2596.
[30] A. S. Kumar, V. D. Ghule, S. Subrahmanyam, A. K. Sahoo, *Chem. Eur. J* **2013**, *19*, 509.

SUPPORTING INFORMATION

Additional supporting information may be found online in the Supporting Information section at the end of this article.

Article

An Optimized Scalable Fully Automated Solid-Phase Microwave-Assisted cGMP-Ready Process for the Preparation of Eptifibatide

Giuseppina Sabatino,[¶] Annunziata D'Ercole,[¶] Lorenzo Pacini,[¶] Matteo Zini, Arianna Ribecai, Alfredo Paio, Paolo Rovero, and Anna Maria Papini*

ACCESS | Metrics & More | Article Recommendations | SI Supporting Information

ABSTRACT: We investigated several strategies, based on the use of microwave-assisted solid-phase peptide synthesis (MW-SPPS) and scalable to kilogram-scale manufacturing, for the preparation of Eptifibatide, a disulfide-bridged cyclo-heptapeptide drug approved as an antithrombotic agent. Following the very fast microwave-assisted Fmoc/tBu synthesis of the linear precursor, we explored both the solution (off-resin) and the solid-phase (on-resin) disulfide formation. In order to optimize the oxidation in solution, we focused our attention on the mild disulfide formation procedure based on the use of air, observing some drawbacks, such as the formation of unwanted oxidation byproducts, such as dimers, or the use of large volumes of an environmentally unfriendly solvent (CH_3CN). In order to overcome these difficulties, we studied four different on-resin strategies, with the final aim to develop a fully automated, single reactor procedure, exploring different strategies to protect the thiol side-chain functional group on the C-terminal Cys residue and to form the Eptifibatide ring. The main difference among these strategies is represented by the final cyclization mode that was obtained either by direct formation of an S—S disulfide bridge or by head to MPA on cysteine side-chain amide bond formation. In conclusion, the optimization of the latter strategy enabled us to devise an optimized scalable fully automated solid-phase microwave-assisted cGMP-ready process to prepare Eptifibatide.

KEYWORDS: active pharmaceutical ingredient, peptide, scale-up, oxidation, automated on-resin disulfide bond formation, off-resin disulfide bond formation, single reactor solid-phase synthesis

■ INTRODUCTION

The need of new, specific, safe and well-tolerated medicines led several pharmaceutical companies to move toward peptide-based drugs.[1,2] In the past few years the U.S. Food and Drug Administration (FDA) approved 15 new peptides or peptide-containing drugs (7% of the total number of drugs).[3] Moreover, since many patents of peptide drugs are expiring, a large number of generic peptide drugs are also entering the market or are expected to do so in the near future. Accordingly, the few Contract Manufacturing Organizations (CMOs) specialized in production of peptides as Active Pharmaceutical Ingredients (APIs) constantly strive to meet an increasing need for large quantities of different new peptide APIs in compliance with current Good Manufacturing Practice (cGMP).[4]

Of the approximately 60 approved peptide APIs available on the market, roughly half are manufactured by 9-fluorenylmethyloxycarbonyl/*tert*-butyl (Fmoc/tBu) solid-phase peptide synthesis (SPPS),[5] although, generally speaking, solid-phase strategies are commonly used to prepare small volumes of short peptides, whereas hybrid technologies (combining solid-phase and solution methods) are applied to produce longer peptide sequences and/or higher volumes.[6]

The large-scale manufacturing of peptides as APIs, requiring full compliance with cGMP regulations,[7] leads pharmaceutical companies to face many challenges related to the complexity of peptide synthesis in terms of size, modifications, conjugation methods, stability, and purity. This requires on one hand the

development of robust manufacturing processes and on the other hand keeping production costs at a reasonable level.

An additional critical factor is the use of large quantities of nonaqueous hazardous organic solvents, such as dimethylformamide (DMF) and *N*-methyl-2-pyrrolidone (NMP), restricted under REACH (European Regulation on Registration, Evaluation, Authorization, and Restriction of Chemicals). For this reason, there is a growing research interest in Green Solid-Phase Peptide Synthesis (GSPPS), looking for an alternative to DMF, commonly employed for washings, couplings, and Fmoc-removal steps;[8–10] still, SPPS in water is a very demanding procedure.[11]

If the synthetic target is a cyclopeptide, further difficulties arise. Cyclization is typically used as a method to constrain structures and stabilize the putative bioactive peptide folding, thus enhancing selectivity toward the target receptor. Last but not least, cyclic peptides are less degraded by proteases, and therefore, they display an in vivo higher stability. Indeed on average, one new cyclopeptide drug is approved each year.[12]

Among the different and sometimes very unusual cyclization strategies available in the tool-box of the peptide medicinal

chemist, the first to be mentioned is the formation of disulfide bridge(s) by oxidation of suitably located cysteines and/or thiol-containing unnatural amino acid residues. Recently, an extensive review reported the most commonly used oxidation methods to form disulfide bridges by oxidation mediated by I_2, Tl(III) trifluoroacetate, potassium ferricyanide, dimethyl sulfoxide (DMSO), both in acidic and basic conditions and/or simply in air in basic conditions or in the presence of activated charcoal.[13−19] However, not all of these methods can be applied to the kilogram-scale production. In developing a robust, large-scale cGMPs-compliant chemical process, it is crucial to take into account and due consideration critical factors such as reactants toxicity, raw materials costs, and optimization of the oxidative conditions (concentration, pH, etc.).[20]

This paper reports a scalable cGMP-ready multigram synthesis of the disulfide-bridge containing cyclopeptide Eptifibatide as API, marketed in the United States under the trademark INTEGRILIN (Figure 1). This drug is used as an antithrombotic agent to treat patients with acute coronary syndrome such as unstable angina and/or acute myocardial infarction.
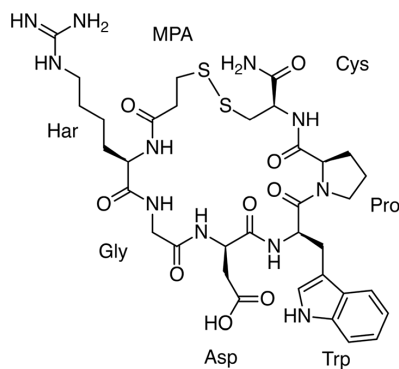
Figure 1. Eptifibatide: N^6-(aminoiminomethyl)-N^2-(3-mercapto-1-oxopropyl)-L-lysylglycyl-L-α-aspartyl-L-tryptophyl-L-prolyl-L-cysteinamide, cyclic (1 → 6)-disulfide.

This synthetic heterodetic cyclo-heptapeptide is characterized by the presence of the unnatural amino acid homoarginine (Har) and a single disulfide bridge between the C-terminal cysteinamide and the N-terminal deamino-cysteine residue, 3-mercaptopropionic acid (MPA). Eptifibatide is currently prepared on a large scale applying a hybrid strategy, based on SPPS combined with in-solution strategies.[21−24] All these procedures are generally designed to prevent the occurrence during the process of major side-reactions, such as racemization, deletion(s), Har deguanidylation, and dimer sequences formation. In particular, the latter undermines formation of the disulfide bridge, which is often the crucial and final step of the synthesis.

The aim of the present paper is to present an optimized and fast protocol for the synthesis of Eptifibatide at a satisfactory purity degree, suitable for an effective process transfer to kilogram-scale manufacturing in the pharmaceutical industry. In particular, we focused on production needs, investigating different Fmoc/tBu automated microwave-assisted solid-phase peptide synthesis (MW-SPPS) protocols, using the high-speed and high-efficiency CEM technology (Charlotte, NC, U.S.A.),

widely used for R&D, available for both gram-scale (Liberty Prime and Liberty Blue systems) and more recently for kilogram-scale synthesis thanks to the newly developed Liberty PRO, especially designed for cGMP compliance. Moreover, we compared the thiol-free off-resin disulfide bond formation in Eptifibatide production process with four novel and different on-resin approaches, in which ring closure was obtained both by disulfide bond and head to MPA on cysteine side-chain by a simple amide bond formation.

■ RESULTS AND DISCUSSION

The possibility of developing efficient and reliable scale-up processes is becoming more and more crucial for all pharmaceutical companies. Peptide manufacturers need to improve their processes both chemically and economically, that is, in terms of profitability: such remarkable advancement can be achieved being able to optimize the solid-phase synthesis of an active peptide as pharmaceutical ingredient on a laboratory scale and then to perform the same synthesis on the larger scale, up to hundreds of times, with the same efficiency in terms of peptide quality and impurities profile. This unique goal can be reached by automated microwave-assisted solid-phase peptide synthesis (MW-SPPS), as proven by several experimental evidence (Jon Collins' personal communications from CEM, U.S.A.). Therefore, once a synthetic protocol has been optimized at the laboratory scale (up to 5 mmol), the same quality (indeed higher, usually) can be achieved directly on a much bigger scale. Therefore, intermediate-scale peptide synthesis is no longer required and the optimized synthetic strategy can be directly scaled up from grams to multigrams/kilograms. With these considerations in mind, in the present paper we focused our interest to the scale-up from R&D multigram-scale of the active peptide ingredient Eptifibatide by the microwave-assisted solid-phase synthesizer (Liberty Blue CEM, Charlotte, NC, U.S.A.), affording and solving both technical and economic issues, to transfer the technology to an industrial kilogram-scale production plant based on the recently engineered Liberty PRO (CEM, Charlotte, NC, U.S.A.), allowing fully automated, production scale, microwave synthesis with full cGMP compatibility. Our strategy differs considerably from those previously reported in the literature, including patents (Table S1) in the management of the disulfide bridge formation critical step. This step was optimized not only in the most common solution conditions (off-resin), but mainly, in the interest of API producers, on-resin, by a fully automatic protocol, directly in the microwave solid-phase synthesizer.

Five-Millimolar Scale Synthesis of Eptifibatide by Fmoc/tBu MW-SPPS of the Linear Precursor and Off-Resin Disulfide Bridge Formation. First of all we optimized the microwave protocol for a 5 mmol scale fully automated Fmoc/tBu solid-phase synthesis of the linear Eptifibatide precursor MPA(Trt)-Har(Pbf)-Gly-Asp(OtBu)-Trp(Boc)-Pro-Cys(Trt)-Rink Amide AM resin (Table S2). The peptide was assembled via standard Fmoc/tBu MW-SPPS strategy (see Experimental Section), using as coupling reagents N,N'-diisopropylcarbodiimide (DIC) and Oxyma Pure, which is nonexplosive, compared with 1-hydroxybenzotriazole (HOBt), used for years for amide bond formation, but that is no more accepted at the industrial level.[25] The coupling system based on DIC/Oxyma, in addition to being safe and low cost, does not require the use of a base unlike the most popular onium coupling methods, such as 3-[bis(dimethylamino)-
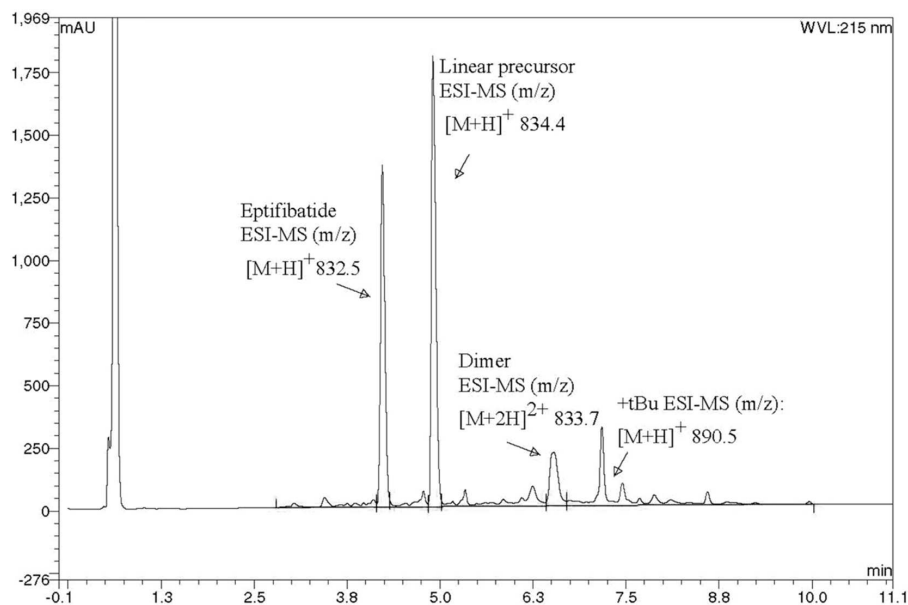
Figure 2. RP-UHPLC monitoring of Eptifibatide disulfide bridge formation by off-resin strategy (pH 8, H_2O/CH_3CN 2:1, 5.3 mM, 22 h at rt). RP-UHPLC-MS: C18 column Waters Acquity CSH (130 Å, 1.7 μm, 2.1 × 100 mm); temperature 45 °C; flow: 0.5 mL/min; eluent: 0.1% (v/v) TFA in H_2O (A) and 0.1% (v/v) TFA in CH_3CN (B), λ 215 nm, gradient: 12−45% B in 10 min.

methyliumyl]-3*H*-benzotriazol-1-oxide hexafluorophosphate (HBTU), requiring high base quantities (e.g., *N,N*-diisopropylethylamine, DIPEA). Moreover, DIC is convenient in terms of time and solvent consumption because it is stable at 90 °C (temperature reached in the microwave conditions) and requires lower DMF washing volumes because of its higher solubility. The acid-labile Trt group, protecting Cys and MPA thiol functions, was cleaved simultaneously after cleavage of the linear peptide precursor from the resin (Supporting Information). Then the disulfide bridge between MPA at position 1 and Cys at position 7 was formed in solution starting from the free thiol-containing linear precursor MPA-Har-Gly-Asp-Trp-Pro-Cys-NH$_2$ under very mild basic conditions in the presence of atmospheric oxygen. Air oxidation of unprotected linear peptides is accepted as the cleanest and safest strategy,[26] occurring in eco-friendly buffered aqueous solution. However, in these conditions peptides are prone to uncontrolled intermolecular disulfide arrangements, typically occurring in basic conditions. Therefore, high dilution conditions (0.1−1 mM) are generally used for selective air oxidation in 0.1 M NH$_4$HCO$_3$ aqueous solution at pH 7−8 for 24 h. However, these conditions require large solvent volumes, dramatically increasing the final industrial process costs. In our strategy, we successfully used 10 times higher concentration solutions (2.1−10.6 mM) limiting side-products formation, with clear cost−benefit advantages.[26] In particular, optimization of the air-oxidation conditions of the crude linear Eptifibatide precursor was accomplished by fine-tuning the following critical parameters: (i) buffer (NH$_4$HCO$_3$ vs NH$_4$OH); (ii) pH (7.5−9.5 range); (iii) concentration (2.1−10.6 mM); (iv) solvent (different ratio of H$_2$O/CH$_3$CN, considering the low solubility in water of both the linear precursor and Eptifibatide itself). Moreover, monitoring of the possible intermolecular disulfide bond side-products

formation was an essential part of the study. Therefore, we used HPLC-ESI-MS to monitor the formation of Eptifibatide (cyclic oxidized form) and the concomitant consumption of the precursor (linear reduced form), in order to determine the conversion rate at different conditions, paying particular attention to the appearance of additional chromatographic peaks, attributed to dimers and oligomers formed by interchain disulfide bridge(s), which however in our 5 mmol-scale procedure was limited (Figure 2, Figures S1 and S2).

We initially tested the different conditions fixing the reaction time at 22 h, as summarized in Table 1. It is clear that

Table 1. Evaluation of Reaction Parameters 1; Effect of pH and Concentration at a Fixed Reaction Time of 22 h on Off-Resin Disulfide Bond Formation in Eptifibatide

entry	concentration (mM)	pH	−SH to S−S conversion (%)	dimer (%)
1	10.6	7.5	12.0	4.7
2	5.5	8.0	40.2	8.0
3	3.2	8.5	57.5	4.9
4	2.1	9.5	85.0	4.6

simultaneously increasing the pH (from 7.5 to 9.5) and decreasing the concentration (from 10.6 to 2.1 mM) enabled us to obtain a complete conversion limiting interchain disulfide bridged side-products formation.

At pH 7.5, the oxidation reaction was slow: only 12% Eptifibatide was formed after 22 h. On the other hand, an increase of pH from 8 to 9.5 allowed obtaining 85% of crude Eptifibatide at the same reaction time. Therefore, efficiency of the oxidation reaction was tested at pH 9.5, focusing on the reaction rate and solution concentration. Data are reported in Figure 3.
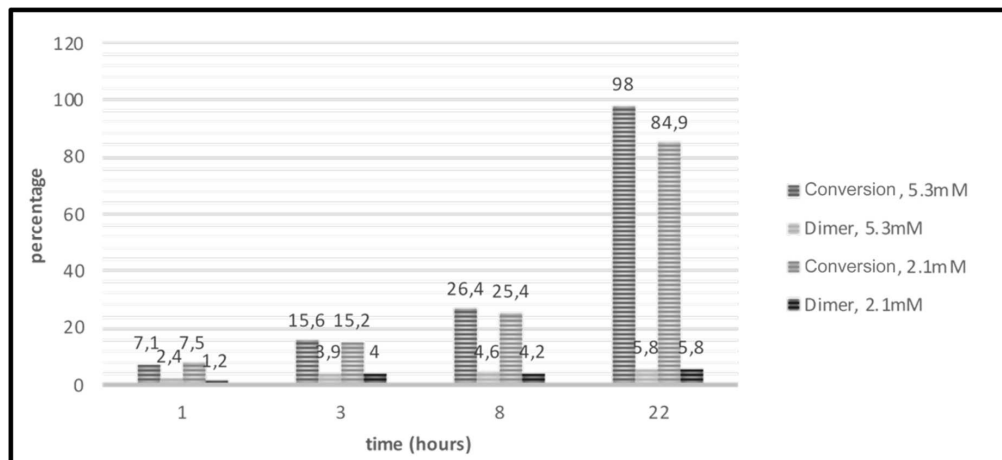
Figure 3. Evaluation of reaction parameters 2. Effect of reaction time and concentration at fixed pH 9.5 on off-resin disulfide bond formation in Eptifibatide.
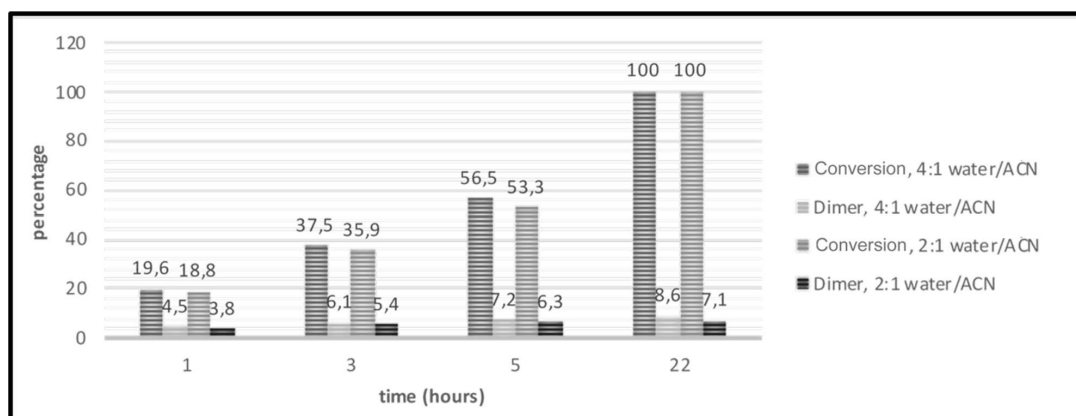
Figure 4. Evaluation of reaction parameters 3. Effect of solvent and reaction time at fixed pH 9.5 and concentration (5.3 mM) on off-resin disulfide bond formation in Eptifibatide.

Figure 5. RP-UHPLC-ESI-MS traces of Eptifibatide crude obtained by off-resin oxidation reaction (5.3 mM Eptifibatide linear precursor in H_2O/CH_3CN, 2:1; r.t.; pH 9.5; 22h). RP-UHPLC-ESI-MS: C18 column Waters Acquity CSH (130 Å, 1.7 μm, 2.1 × 100 mm); temperature 45 °C; flow: 0.5 mL/min; eluent: 0.1% (v/v) TFA in H_2O (A) and 0.1% (v/v) TFA in CH_3CN (B), λ 215 nm, gradient: 12−45% B in 10 min. Rt 4.196 min: Eptifibatide (Peak 1) and Rt 6.200 min: Dimer (Peak 2).

Scheme 1. Fully Automated Microwave-Assisted Synthesis of Eptifibatide Performing On-Resin Disulfide Bond Formation: Strategies A and B

At these pH conditions, maximum oxidation occurred in 22 h. Moreover, we observed that when the concentration was decreased (from 5.3 to 2.1 mM), the conversion at 22 h rate decreased without any advantage in terms of side-products formed. Generally speaking, the possibility to work at higher concentration (5.3 mM) is preferred because the volume to be handled is lower.

Moreover, no oxidation improvement was observed by changing the composition of the solvent mixture H_2O/CH_3CN from 4:1 to 2:1 (Figure 4).

In conclusion, optimal conditions to oxidize the linear Eptifibatide precursor by off-resin disulfide formation were estimated to be 5.3 mM concentration in H_2O/CH_3CN (2:1); pH 9.5; 22 h reaction time at room temperature. At these conditions, 98% conversion of the linear precursor was obtained, leading to crude Eptifibatide with an HPLC purity 61% (Figures 5 and S3a).

Selection of the less green and more expensive solvent mixture ratio H_2O/CH_3CN (2:1), compared with H_2O/CH_3CN (4:1), was forced by the lower dimer side-product formation in higher acetonitrile content mixture. In particular, in the higher water content mixture (4:1), a precipitate formation limited reaction monitoring and the putative side-product aggregate, sticking to the glass vessel, affected postsynthesis cleaning procedures. Moreover, off-resin disulfide bond formation suffers from the typical carbocation nucleophile reactivity, toward the free amino acid side chains

formed during the resin cleavage, affecting the final yield because of possible irreversible impurities (Figures S1, S2, and S3a).

Flash chromatography purification of 4.6 g crude Eptifibatide was carried out using Biotage Isolera One equipped with SNAP Ultra 120 g C18 column and H_2O/CH_3CN as eluent system. Eptifibatide (1.32 g, 1.88 mmol, 28.7% yield) showed a 99.2% RP-UHPLC purity, with 0.8% total impurities, and each impurity <0.5%, in agreement with cGMP requirements (Figure S3b).

Fully Automated Microwave-Assisted Synthesis of Eptifibatide: Comparison of Four Different On-Resin Disulfide Bond Formation Strategies. In order to overcome the above-described difficulties inherent to oxidation in solution of the Eptifibatide linear precursor, we deeply explored the possibility to develop a full on-resin, possibly single reactor process. With the idea in mind of developing a completely automatic synthetic procedure to be scaled in the Liberty PRO solid-phase peptide synthesizer, we investigated four on-resin different approaches (Strategies A−D) on a Liberty Blue instrumentation without isolating linear Eptifibatide precursor (Schemes 1 and 2).

The final aim of optimizing a fully automated synthesis of Eptifibatide is to provide a solid-phase single reactor process managing three-dimensional orthogonal protections on on-resin peptide residues involved in disulfide bridge formation (MPA1 and Cys7).

Scheme 2. Fully Automated Microwave-Assisted Synthesis of Eptifibatide Performing On-Resin Disulfide Bond Formation: Strategies C and D

Performing all steps in an automated instrument single reactor simplify the respect of cGMP compliances, cutting the financial and time costs related to multiple equipment qualification.

Moreover, a fully automated process is particularly appealing in the context of industrial production where limiting workforce and safety requirements are key challenges.

Strategies **A** and **B** (Scheme 1) require the Fmoc/tBu MW-assisted synthesis of the common peptide-resin fragment Fmoc-Har(Pbf)-Gly-Asp(OtBu)-Trp(Boc)-Pro-Cys(Mmt)-Rink Amide AM Resin.

The selection of the three-dimensional 4-methoxytrityl (Mmt) protecting group on Cys7 thiol side-chain was dictated both by its easy removal in mild acidic conditions and commercial availability of Fmoc-Cys(Mmt)-OH building block. The use of the most expensive Fmoc-Cys(Mmt)-OH, compared with Fmoc-Cys(Mtt)-OH, is justified by the milder acidic conditions required for its removal without affecting peptide stability to the Rink linker resin.

The possibility to use the same Mmt protecting group on thiol function in MPA is limited by commercial unavailability of MPA(Mmt). Therefore, we tested the efficiency of the commercially available MPA(PyS) in Strategy **A** and 3,3′-dithiodipropionic acid (DTDPA) in Strategy **B**, linked respectively to the N-terminal amino function on Har(Pbf)-Gly-Asp(OtBu)-Trp(Boc)-Pro-Cys(Mmt)-Rink Amide AM Resin, for further on-resin disulfide bridge formation (Scheme 1).

Strategy A. In particular in Strategy **A**, after coupling MPA(PyS) in the MW reactor to Har(Pbf)-Gly-Asp(OtBu)-Trp(Boc)-Pro-Cys(Mmt)-Rink Amide AM Resin, mild acidic conditions were used to cleave the Mmt protecting group on Cys and favoring the contemporary disulfide-exchange reaction between free thiol on Cys side-chain and the pyridyne-2-thiol group (PyS) on MPA.[27−29] This reaction occurring in 25 min at r.t., led to the desired disulfide bond in crude Eptifibatide that, after resin cleavage, was recovered in 60% yield with 34.9% HPLC purity (Figure S4). The main disadvantage of Strategy **A** is the high cost of the building blocks Fmoc-Cys(Mmt)-OH and MPA(PyS).

Strategy B. However, in Strategy **B**, after MW-assisted amide bond formation between DTDPA and the N-terminal amino function on Har(Pbf)-Gly-Asp(OtBu)-Trp(Boc)-Pro-Cys(Mmt)-Rink Amide AM Resin and DTT-mediated reduction of the S−S bond in DTDPA linked to the peptide-resin,[30] we took advantage of N-chlorosuccinimide (NCS) oxidative properties, leading to the disulfide bond formation by the highly reactive sulfenyl chloride formation toward thiol in Cys after Mmt removal with a rapid, clean, and efficient reaction. As previously demonstrated by Albericio et al.,[31] also in our experience, this reaction was strongly affected in terms of final crude purity, by the possible use of NCS reagent excess (data not shown). A more important drawback of Strategy **B** is the use of the harmful NCS reagent requiring management of the resin out of the microwave reactor of the synthesizer to avoid dramatic and unsafe instrument

contaminations, requiring cleaning procedures that will increase energy and water costs, a prime concern for manufacturers. Additionally, a big advantage (compared with the previously described Strategy **A**) is the use of the harmless, inexpensive, and greener DTDPA that is essentially the MPA S−S bridged dimer, that is, (MPA)$_2$ instead of the more expensive MPA(PyS) building block.

After resin cleavage, crude Eptifibatide was recovered in 82% yield with 42% HPLC purity (Figure S5).

Strategy C. The Strategy **C** starts from the same peptide-resin fragment above-described, i.e. Har(Pbf)-Gly-Asp(OtBu)-Trp(Boc)-Pro-Cys(Mmt)-Rink Amide AM Resin, used in Strategies **A** and **B**. After Mmt deprotection, S−S bond is formed on Cys7 free thiol function by MPA(PyS) mediated disulfide-exchange to obtain Cys(MPA). Then by PyBop/DIPEA activation (5:7 equiv) of the carboxylic function on Cys(MPA) at r.t. for 16 h,[32] the head to MPA on cysteine side-chain cyclization occurs by nucleophilic attack of the N-terminal Har on the peptide-resin (Scheme 2).

Optimization of Cys(MPA) formation on the resin was achieved performing the reaction directly in the MW reactor (90W, 50 °C, 30 min) as reported in Table S3, and as observed by IPC of Har-Gly-Asp-Trp-Pro-Cys(MPA)-NH$_2$ cleaved from the resin, using the protocol reported in the Supporting Information (Figure S6).

After resin cleavage, crude Eptifibatide was recovered in 61% yield with 56.5% HPLC purity (Figure S7). In conclusion, the peculiarity of Strategy **C** is the on-resin formation of S−S bond by disulfide-exchange between MPA(PyS) and thiol function in Mmt-cleaved cysteine. Then, the carboxylic function of MPA linked on cysteine by S−S bridge, that is, Cys(MPA), after appropriate activation could form the amide bond with the N-terminal amino function of Har(Pbf) on the peptide-resin. This strategy has the advantage that in the peptide industry, the formation of the amide bond is pivotal and among the more important transformations in the design of synthetic plants. Moreover, amide bond formation is optimized in solid-phase synthesis in particular in microwave-assisted peptide synthesizer.

Strategy D. The Strategy **D** (Scheme 2) takes advantage of the interesting step in Strategy **C** above-described (to form the disulfide bond directly on cysteine before closing the cyclopeptide by amide formation), using the less expensive building block Cys(StBu) compared with Cys(Mmt). Therefore, starting from the peptide-resin fragment Har(Pbf)-Gly-Asp(OtBu)-Trp(Boc)-Pro-Cys(StBu)-Rink Amide AM resin, the first issue of the Strategy **D** is to propose a greener, safer, and low-cost reducing agent for orthogonal deprotection conditions of Cys(StBu) at position 7.

DTT was immediately excluded because of its high cost in the industrialization process. Although DTT was widely reported in the literature as an efficient reducing agent also for functional groups in peptide sequences,[33,34] as well as demonstrated in the case of Strategy **B**.

Several assays with different reagents were performed with the aim to provide a scalable fully automated solid-phase microwave-assisted cGMP-ready process for Eptifibatide (see Supporting Information).

In particular, 20% (v/v) β-mercaptoethanol (βME) in basic conditions (0.1 M NMM or 0.05 M DIPEA) in DMF[33,34] allowed removing StBu at r.t., but it required a long reaction time. In the case of the starting peptide-resin used in Strategy **D**, quantitative reduction was reached with the same reaction cocktail, in 15 min in microwave conditions (75 °C, 45 W), (see Supporting Information).[33] However, the high toxicity and difficult cleaning procedures of the reaction vessel in the MW-synthesizer, make βME inconvenient for a kilogram-scale on-resin production.

Moreover, 10% (v/v) 2-aminoethane-1-thiol (2-MEA) in DMF at r.t. allowed quantitative reduction in 16 h. An increase of 2-MEA reagent up to 20% (v/v) did not correspond to an improved reaction rate, but to the on-resin formation of Har(Pbf)-Gly-Asp(OtBu)-Trp(Boc)-Pro-Cys(2-MEA)-Rink Amide AM resin as the result of a side-reaction involving the thiol functional group on Cys after StBu deprotection (IPC, Figure S8). Considering that MPA is the moiety that in Eptifibatide is linked by an amide bond to Har and that in biological systems has been reported to act as a reducing agent,[34] we used MPA for our optimized fully single reactor on-resin disulfide bond formation in Eptifibatide. To the best of our knowledge, we were the first to propose MPA to deprotect StBu on cysteine. In particular the peptide-resin Har(Pbf)-Gly-Asp(OtBu)-Trp(Boc)-Pro-Cys(StBu)-Rink Amide AM was treated with MPA/DIPEA (40:41 equiv) in DMF for 24 h at r.t. in the Liberty Blue instrument. We obtained an acceptable StBu deprotection with only 2.2% residual Cys(StBu) containing peptide but no disulfide-exchange on the free thiol on cysteine (IPC not shown). Therefore, the desired disulfide-exchange to link MPA on cysteine was successfully achieved treating the resin directly in the reaction vessel into the instrument, with a DMF solution of the MPA dimer (DTDPA) and DIPEA (40:1.2 equiv) at r.t. for 21 h. Then, the peptide-resin was finally ready for head to MPA on cysteine side-chain cyclization by amide bond formation between the carboxylic function of MPA on Cys and N-terminal Har, by MW-assisted coupling with DIC and Oxyma Pure (see Experimental section). After resin cleavage, crude Eptifibatide was recovered in 60% yield with 40.9% HPLC purity (Figure S9).

The relevance of Strategy **D** is essentially based on the selection of the StBu orthogonal protection on cysteine that is easily removed by MPA acting as a novel reducing agent for Cys(StBu) deprotection. Moreover, all Strategy **D** operations (amino acid couplings, orthogonal side-chain protecting groups removal, and final head to MPA on cysteine side-chain cyclization) can be really carried out in a single reactor on-resin condition. In fact, easy washings of MPA excess and removal of StBu deprotection byproduct compared with reagents and protecting groups used in the other strategies can be performed by fully automated process in the instrumentation.

To the best of our knowledge, this is a unique strategy performing all the processes including disulfide bond formation to prepare Eptifibatide in a single reactor.

■ CONCLUSIONS

We investigated several strategies for the preparation of Eptifibatide, scalable to kilogram-scale, having in common the use of the MW-SPPS procedure, which is now available not only at R&D level but also for the large-scale manufacturing of peptides. Following the very fast microwave-assisted Fmoc/tBu synthesis of the Eptifibatide linear precursor by a DIC/Oxyma Pure coupling protocol at 90 °C, we explored both the solution (off-resin) and the solid-phase (on-resin) disulfide bond formation.

Concerning the oxidation in solution, we focused our attention on the mild disulfide formation procedure based on the use of air and in particular, we studied the key factors (pH, concentration, reaction time, and solvent mixture composition) that affect the purity of the final product and the overall yield. In our hands, the best conditions for the off-resin oxidation of Eptifibatide linear precursor are the following: 5.3 mM concentration in H_2O/CH_3CN (2:1); pH 9.5; 22 h reaction time at room temperature. At these conditions, 98% conversion of the linear precursor was obtained on a 5 mmol scale, leading to crude Eptifibatide with a 61% HPLC purity. These overall satisfactory results are hampered in part by some drawbacks, particularly relevant for the large-scale production of this peptide, such as the formation of unwanted oxidation byproducts, mainly dimers, or the use of large volumes of an environmentally unfriendly solvent (CH_3CN).

In order to overcome these difficulties, we studied four different on-resin Strategies (**A**–**D**), with the final aim to develop a fully automated, single reactor procedure. To achieve the on-resin thiol deprotection we chose Mmt (**A**–**C**) or StBu (**D**) for the protection of the C-terminal Cys residue, while the N-terminal MPA moiety was introduced as activated SPyS (**A**) or as DTDPA, the MPA dimer (**B**). On the other hand, in Strategies **C**–**D**, the MPA moiety is introduced via S−S bond formation on cysteine after orthogonal deprotection. Therefore, the main difference among these strategies is the final cyclization step, obtained by direct formation of an S−S disulfide bridge (Strategies **A**–**B**) or via head to MPA on cysteine side-chain amide bond formation (Strategies **C**–**D**).

The need to select inexpensive raw material led us to perform a careful search for the most suitable reducing agent to deprotect StBu. We identified the βME (30 equiv in 20% v/v in DMF) in 0.05 M DIPEA with microwave assistance at 75 °C for 15 min as the best reduction condition. However, toxicity and difficult microwave-synthesizer cleaning from this thiol reagent makes its use not perfectly suitable for a kilogram-scale production. So, we switched to the safer 2-MEA (40 equiv in 10% v/v in DMF and 4 equiv NMM), obtaining complete StBu deprotection in 16 h at room temperature. Interestingly, we also investigated the use of MPA as a reducing reagent and the best oxidation condition identified has been 40 equiv of MPA and 41 equiv of DIPEA. MPA represents a simple replacement of the reducing agent with the advantage of using an unexpensive raw material of the moiety present in Eptifibatide.

In summary, Strategies **A**, **B**, and **C** lead us to identify a limit: repeated washes with weakly acid solution to remove Mmt can cleave part of the peptide from the resin, leading to a variable, but unacceptable loss of yield. This limit has been overcome replacing the Mmt protecting group with Cys-(StBu), as described in Strategy D, a method whose peculiarity is the use of MPA as reducing agent to perform at the same time the reduction of Cys(StBu) and its oxidation to Cys−S−S−MPA.

In conclusion, Strategy **D** represents an optimized scalable fully automated solid-phase microwave-assisted cGMP-ready process to prepare Eptifibatide.

■ EXPERIMENTAL SECTION

Materials. Peptide-grade *N,N*-dimethylformamide (DMF), all Fmoc protected amino acids (Fmoc-Gly-OH, Fmoc-Har(Pbf)-OH, Fmoc-Asp(OtBu)-OH, Fmoc-Cys(StBu)-OH, Fmoc-Cys(Trt)-OH, Fmoc-Cys(Mmt)-OH, Fmoc-Trp(Boc)-

OH, Fmoc-Pro-OH), 3-mercaptopropionic acid (MPA), and 3,3′-dithiodipropionic acid (DTDPA) were purchased from Sigma-Aldrich (Milan, Italy). Rink Amide AM resin was purchased from Sunresin New Materials Co. Ltd., Xi' AN (Shaanxi, China).

3-(2-Pyridinyldithio)propanoic acid MPA(PyS) was purchased from Carbosynth (Compton, U.K.).

Activators *N,N*′-diisopropylcarbodiimide (DIC), Oxyma Pure and (benzotriazol-1-yloxy)tripyrrolidinophosphonium hexafluorophosphate (PyBOP) were purchased from Sigma-Aldrich (Milan, Italy). *N*-Chlorosuccinimide (NCS), trifluoroacetic acid (TFA), triisopropylsilane (TIS), and 2,2′-(ethylenedioxy)diethanethiol (DODT), *N,N*-diisopropylethylamine (DIPEA), diisopropyl ether (iPr$_2$O), diethyl ether (Et$_2$O), 2-propanol, dichloromethane (DCM), and HPLC Plus Water were purchased from Sigma-Aldrich (Milan, Italy). HPLC-grade acetonitrile (CH_3CN) was purchased from Carlo Erba (Milan, Italy).

Fully Automated Synthetic Strategy of the Linear Precursor of Eptifibatide and Off-Resin Disulfide Bond Formation. *Preparation of the Linear Precursor of Eptifibatide by Fmoc/tBu MW-SPPS.* The fully protected linear precursor of Eptifibatide MPA(Trt)-Har(Pbf)-Gly-Asp-(OtBu)-Trp(Boc)-Pro-Cys(Trt)-Rink Amide AM resin was obtained starting from the Rink Amide AM resin (loading 0.93 mmol/g, 5.4 g, 5 mmol). Sequence elongation was performed on a microwave-assisted solid-phase peptide synthesizer Liberty Blue (CEM, Matthews, NC, U.S.A.) following the Fmoc/tBu strategy. Reaction temperatures were monitored by an internal fiber-optic sensor. Both deprotection and coupling reactions were performed in a Teflon vessel applying microwave energy under nitrogen bubbling. After the first Fmoc-deprotection, the following amino acids orthogonally protected were added automatically from C- to N-terminal: Fmoc-Cys(Trt)-OH, Fmoc-Pro-OH, Fmoc-Trp(Boc)-OH, Fmoc-Asp(OtBu)-OH, Fmoc-Gly-OH, Fmoc-Har(Pbf)-OH, MPA(Trt)-OH, in the presence of the coupling reagents DIC and Oxyma Pure. The Fmoc/tBu MW-SPPS cycle consisted in (1) swelling in DMF (50 mL) for 30 min; (2) Fmoc-deprotection by 30% (v/v) piperidine/DMF (40 equiv, 66 mL); (3) washings with DMF (3 × 50 mL); (4) coupling with the Fmoc-protected amino acids (2.5 equiv, 0.4 M in DMF), Oxyma Pure (2.5 equiv, 1 M in DMF), and DIC (2.5 equiv, 3 M in DMF); (5), washings with DMF (3 × 50 mL). Peptide elongation was performed by repeating the MW-SPPS cycle for each amino acid. Both deprotection and coupling reactions were performed reaching 90 °C except 50 °C for Cys coupling (Table S2).

After all amino acids were coupled, the resin was filtered, washed with DMF (3 × 50 mL) and 2-propanol (3 × 50 mL), and dried under vacuum to obtain 14.1 g of peptide-resin. The linear crude Eptifibatide precursor was cleaved from the resin following the procedure described in Supporting Information. The crude linear precursor of Eptifibatide (4.7 g, 5 mmol) was characterized with a 71% RP-UHPLC purity (yield 99%), R_t 4.9 min, gradient 12−45% B in 10 min. ESI-MS (*m/z*): [M + H]$^+$ 834.4 (found), 834.9 (calcd).

Optimized Synthetic Procedure for Off-Resin Disulfide Bond Formation in Eptifibatide. The crude linear Eptifibatide precursor (4.7 g, 5 mmol, HPLC purity 71%) was introduced in a 2 L round-bottom flask, and a mixture of water and CH_3CN (1:1, 630 mL) was added and then stirred for about 15 min. After complete dissolution, additional water (315 mL)

was added to the reaction mixture to obtain a final concentration of 5.3 mM. Initially the measured pH, being 2.5, was adjusted to 9.5 adding NH$_4$OH 7.5% (9.4 mL). After the mixture was mechanically stirred for 22 h at 350 rpm, at room temperature, the reaction was quenched by adding TFA (3.7 mL), adjusting the pH to 2.5. Then the reaction mixture was lyophilized without further evaporation.

The crude Eptifibatide was obtained with 61% HPLC purity (4.6 g, yield 98%). R$_t$ 4.2 min; ESI-MS (m/z): [M + H]$^+$ 832.5 (found); 831.96 (calcd) (Figure S3a).

The above-described procedure was optimized after performing the experiments in the conditions described in Table 1, Figure 3, and Figure 4, each one on 5 mmol of crude linear Eptifibatide precursor.

Fully Automated Synthetic Strategies of Eptifibatide Including on-Resin Disulfide Bond Formation (A−D). *Preparation of the Peptide-Resin Precursor Har(Pbf)-Gly-Asp(OtBu)-Trp(Boc)-Pro-Cys(Mmt)-Rink Amide AM Resin by Fmoc/tBu MW-SPPS (Strategies A, B, and C).* The fully protected linear precursor Har(Pbf)-Gly-Asp(OtBu)-Trp-(Boc)-Pro-Cys(Mmt)-Rink Amide AM resin was obtained starting from the Rink Amide AM resin (loading 0.93 mmol/g, 5.4 g, 5 mmol). Sequence elongation was performed on a microwave-assisted solid-phase peptide synthesizer Liberty Blue (CEM, Matthews, NC, U.S.A.) following the Fmoc/tBu strategy. Reaction temperatures were monitored by an internal fiber-optic sensor. Both deprotection and coupling reactions were performed in a Teflon vessel applying microwave energy under nitrogen bubbling. After the first Fmoc-deprotection, the following amino acids orthogonally protected were added automatically from C- to N-terminal: Fmoc-Cys(Mmt)-OH, Fmoc-Pro-OH, Fmoc-Trp(Boc)-OH, Fmoc-Asp(OtBu)-OH, Fmoc-Gly-OH, Fmoc-Har(Pbf)-OH, in the presence of the coupling reagents DIC and Oxyma Pure. The Fmoc/tBu MW-SPPS cycle consisted of (1) swelling in DMF (50 mL) for 30 min; (2) Fmoc-deprotection in 30% (v/v) piperidine/DMF (40 equiv, 66 mL); (3) washings with DMF (3 × 50 mL); (4) coupling with the Fmoc-protected amino acids (2.5 equiv, 0.4 M in DMF), Oxyma Pure (2.5 equiv, 1 M in DMF), and DIC (2.5 equiv, 3 M in DMF); (5), washings with DMF (3 × 50 mL). Peptide elongation was performed by repeating the MW cycle for each amino acid coupling and deprotections as reported in Table S2 of the Supporting Information. After all amino acids were coupled, the resin was filtered, washed with DMF (3 × 50 mL) and with 2-propanol (3 × 50 mL), and dried under vacuum to obtain 12.3 g of peptide-resin. The linear Eptifibatide precursor on the resin was divided into three aliquots for subsequent on-resin disulfide bond formation using Strategies A, B, and C.

Strategy A for On-Resin Disulfide Bond Formation in Eptifibatide. MPA(PyS) (216 mg, 10 equiv) was coupled to the on-resin protected linear peptide precursor Har(Pbf)-Gly-Asp(OtBu)-Trp(Boc)-Pro-Cys(Mmt)-Rink Amide AM resin (230 mg, 0.1 mmol, 0.43 mmol/g) by a microwave-assisted protocol (75 °C, 35 W, 5 min) using DIC (0.154 mL, 10 equiv) and Oxyma Pure (142 mg, 10 equiv) as coupling reagents in DMF (5 mL). Then, the peptide-resin was filtered and washed with DMF (3 × 2 mL) and DCM (3 × 2 mL). 4-Methoxytriphenylmethyl (Mmt) cysteine deprotection and contemporary formation of the disulfide bridge via disulfide-exchange reaction with the head terminal MPA(PyS) were achieved by treating the resin with a mixture of TFA/TIS/DCM (10 mL, 3:5:92) for 25 min at r.t. Following the cleavage

procedure described in the Supporting Information, we performed the final cleavage with the cocktail TFA/H$_2$O/TIS (10 mL, 95:2.5:2.5).

Crude Eptifibatide (50 mg, 60% yield) was obtained with a 34.9% HPLC purity (Figure S4).

Strategy B for On-Resin Disulfide Bond Formation in Eptifibatide. 3,3′-Dithiodipropionic acid (DTDPA) (2.63 g, 5 equiv) was coupled to the peptide-resin Har(Pbf)-Gly-Asp(OtBu)-Trp(Boc)-Pro-Cys(Mmt)-Rink Amide AM resin (2.5 mmol, 7.3 g, 0.34 mmol/g) by a microwave-assisted protocol at 75 °C (35 W, 5 min) using DIC (1.93 mL, 5 equiv) and Oxima Pure (1.77 g, 5 equiv) in DMF (40 mL). The coupling reaction was IPC monitored. The peptide-resin was filtered and washed with DMF (3 × 20 mL) and DCM (3 × 20 mL). DTDPA-Har(Pbf)-Gly-Asp(OtBu)-Trp(Boc)-Pro-Cys-(Mmt)-Rink Amide AM resin was treated with dithiothreitol (DTT, 3 g, 19 mmol) and 0.1 M 4-methylmorpholine (NMM) in DMF (60 mL) to reduce the S−S bond in DTDPA forming MPA. After 12 h, IPC monitoring confirmed 93% conversion (data not shown), the resin was washed with DMF (3 × 60 mL), Mmt deprotection was performed in a cocktail of TFA/TIS/DCM (8 × 20 mL, 2:5:93) until the yellow color disappeared and the deprotection solution turned colorless. Oxidation was performed treating the supported protected linear peptide MPA-Har(Pbf)-Gly-Asp(OtBu)-Trp(Boc)-Pro-Cys-Rink Amide AM resin (2.1 g, 0.75 mmol) with a solution of *N*-chlorosuccinimide (120 mg, 1.2 equiv) in DMF (24 mL) for 10 min at r.t. After washing the resin with DCM (3 × 25 mL), the cleavage was performed following the procedure described in Supporting Information using a mixture of TFA/H$_2$O/TIS (40 mL, 95:2.5:2.5).

Crude Eptifibatide (590 mg, 82% yield) was obtained with a 42.4% HPLC purity (Figure S5).

Strategy C for On-Resin Disulfide Bond Formation in Eptifibatide. The peptide-resin Har(Pbf)-Gly-Asp(OtBu)-Trp-(Boc)-Pro-Cys(Mmt)-Rink Amide AM resin (200 mg, 0.087 mmol) was treated with a cocktail of TFA/TIS/DCM (10 mL, 3:5:92) for 25 min at r.t. to deprotect the cysteine residue. On-resin disulfide-exchange between the activated MPA(PyS) (187 mg, 10 equiv) in DMF (5 mL) and DIPEA (45 μL, 3 equiv) and the free cysteine thiol function on the peptide-resin was performed in the microwave module of the Liberty Blue to form the disulfide bond (50 °C, 90 W, 30 min). The resin was filtered, washed with DMF (3 × 3 mL) and DCM (3 × 3 mL), and dried under vacuum. The IPC showed 82% of desired linear Eptifibatide derivative Har-Gly-Asp-Trp-Pro-Cys-(MPA)-NH$_2$ (Figure S6). The head to MPA on cysteine side-chain cyclization (required to obtain Eptifibatide), was achieved by PyBop (226 mg, 5 equiv) and DIPEA (105 μL, 7 equiv) in DMF (3 mL) at r.t. in 16 h. The final cleavage from the resin was performed following the procedure described in the Supporting Information using a cocktail of TFA/H$_2$O/TIS (5 mL, 95:2.5:2.5).

Crude Eptifibatide (50 mg, 61% yield) was obtained with a 56.5% HPLC purity (Figure S7).

Preparation of the Peptide-Resin Precursor Har(Pbf)-Gly-Asp(OtBu)-Trp(Boc)-Pro-Cys(StBu)-Rink Amide AM by Fmoc/tBu MW-SPPS (Strategy D). The fully protected linear precursor Har(Pbf)-Gly-Asp(OtBu)-Trp(Boc)-Pro-Cys-(StBu)-Rink Amide AM resin was obtained starting from the Rink Amide AM resin (loading 0.93 mmol/g, 1.1 g, 1 mmol). Sequence elongation was performed on a microwave-assisted solid-phase peptide synthesizer Liberty Blue (CEM, Matthews,

NC, U.S.A.) following the Fmoc/tBu strategy. Reaction temperatures were monitored by an internal fiber-optic sensor. Both deprotection and coupling reactions were performed in a Teflon vessel applying microwave energy under nitrogen bubbling. After the first Fmoc-deprotection, the following amino acids orthogonally protected were added automatically from C- to N-terminal: Fmoc-Cys(StBu)-OH, Fmoc-Pro-OH, Fmoc-Trp(Boc)-OH, Fmoc-Asp(OtBu)-OH, Fmoc-Gly-OH, Fmoc-Har(Pbf)-OH, in the presence of the coupling reagents DIC and Oxyma Pure. The Fmoc/tBu MW-SPPS cycle consisted of: (1) swelling in DMF (15 mL) for 30 min; (2) Fmoc-deprotection by 30% (v/v) piperidine/DMF (20 mL, 60 equiv); (3) washings with DMF (3 × 15 mL); (4) coupling with the Fmoc-protected amino acids (5 equiv, 0.4 M in DMF), Oxyma Pure (5 equiv, 1 M in DMF), and DIC (5 equiv, 3 M in DMF); (5), washings with DMF (3 × 15 mL). Peptide elongation was performed by repeating the MW cycle for each amino acid coupling and deprotections as reported in Table S2 of the Supporting Information. After all amino acids were coupled, the resin was filtered, washed with DMF (3 × 15 mL) and with 2-propanol (3 × 15 mL), and dried under vacuum to obtain 2.5 g of peptide-resin Har(Pbf)-Gly-Asp(OtBu)-Trp(Boc)-Pro-Cys(StBu)-Rink Amide AM.

Strategy D for Optimized Fully Single Reactor On-Resin Disulfide Bond Formation in Eptifibatide. The StBu protecting group was removed from cysteine on the linear peptide-resin Har(Pbf)-Gly-Asp(OtBu)-Trp(Boc)-Pro-Cys-(StBu)-Rink Amide AM (loading 0.43 mmol/g, 1.6 g, 0.7 mmol), treating the resin with a solution of MPA (2.44 mL, 40 equiv) and DIPEA (5 mL, 41 equiv) in DMF (25 mL). After 24 h at r.t. (without removing the resin from the Liberty Blue instrument), the IPC monitoring the reaction progress in solid-phase, showed an almost complete cysteine deprotection. The resin was filtered, washed with DMF (3 × 25 mL) and DCM (3 × 25 mL), and added with a solution of DTDPA (5.9 g, 40 equiv) and DIPEA (146.3 μL, 1.2 equiv) in DMF (25 mL), and maintained for 21 h at r.t. under N_2 bubbling in the instrument. The IPC showed that Cys(MPA) was correctly formed on the peptide-resin by disulfide-exchange (data not shown). Therefore, after filtration and washings with DMF (3 × 25 mL), the peptide-resin was added with DIC (130 μL, 1.2 equiv) and Oxyma Pure (120 mg, 1.2 equiv) under two consecutive MW cycles, refreshing the solution of the reagents (70 °C, 150 W in 30 s and then 90 °C, 30 W in 10 min) to form the head to MPA on cysteine side-chain amide-bond cyclization including the disulfide bridge of Eptifibatide. Finally, the resin was filtered and washed with DMF (3 × 25 mL) and DCM (3 × 25 mL), then dried under vacuum. The final cleavage was performed following the procedure described in the Supporting Information using the cocktail TFA/H_2O/TIS (20 mL, 95:2.5:2.5).

Crude Eptifibatide (400 mg, 60% yield) was obtained with a 40% HPLC purity (Figure S9).

ASSOCIATED CONTENT

ⓈI Supporting Information

The Supporting Information is available free of charge at https://pubs.acs.org/doi/10.1021/acs.oprd.0c00490.

> Table of patent landscape, microwave methods, and RP-UHPLC/MS analyses (PDF)

AUTHOR INFORMATION

Corresponding Author

Anna Maria Papini − MoD&LS Laboratory and Interdepartmental Research Unit of Peptide and Protein Chemistry and Biology, Department of Chemistry "Ugo Schiff", University of Florence, 50019 Sesto Fiorentino, Italy; CNR-IC Istituto di Cristallografia, 95126 Catania, Italy; PeptLab@UCP Platform of Peptide and Protein Chemistry and Biology, Neuville Campus, CY Cergy Paris Université, 95031 Cergy-Pontoise Cedex, France; ⓞ orcid.org/0000-0002-2947-7107; Email: annamaria.papini@unifi.it

Authors

Giuseppina Sabatino − MoD&LS Laboratory and Interdepartmental Research Unit of Peptide and Protein Chemistry and Biology, Department of Chemistry "Ugo Schiff", University of Florence, 50019 Sesto Fiorentino, Italy; CNR-IC Istituto di Cristallografia, 95126 Catania, Italy; ⓞ orcid.org/0000-0001-7737-7517

Annunziata D'Ercole − MoD&LS Laboratory and Interdepartmental Research Unit of Peptide and Protein Chemistry and Biology, Department of Chemistry "Ugo Schiff", University of Florence, 50019 Sesto Fiorentino, Italy; FIS - Fabbrica Italiana Sintetici S.p.A., 36075 Montecchio Maggiore, Vicenza, Italy

Lorenzo Pacini − MoD&LS Laboratory and Interdepartmental Research Unit of Peptide and Protein Chemistry and Biology, Department of Neurosciences, Psychology, Drug Research and Child Health, Section of Pharmaceutical Sciences and Nutraceutics, University of Florence, 50019 Sesto Fiorentino, Italy; FIS - Fabbrica Italiana Sintetici S.p.A., 36075 Montecchio Maggiore, Vicenza, Italy

Matteo Zini − FIS - Fabbrica Italiana Sintetici S.p.A., 36075 Montecchio Maggiore, Vicenza, Italy

Arianna Ribecai − MoD&LS Laboratory, University of Florence, 50019 Sesto Fiorentino, Italy; FIS - Fabbrica Italiana Sintetici S.p.A., 36075 Montecchio Maggiore, Vicenza, Italy

Alfredo Paio − MoD&LS Laboratory, University of Florence, 50019 Sesto Fiorentino, Italy; FIS - Fabbrica Italiana Sintetici S.p.A., 36075 Montecchio Maggiore, Vicenza, Italy

Paolo Rovero − MoD&LS Laboratory and Interdepartmental Research Unit of Peptide and Protein Chemistry and Biology, Department of Neurosciences, Psychology, Drug Research and Child Health, Section of Pharmaceutical Sciences and Nutraceutics, University of Florence, 50019 Sesto Fiorentino, Italy; CNR-IC Istituto di Cristallografia, 95126 Catania, Italy

Complete contact information is available at:
https://pubs.acs.org/10.1021/acs.oprd.0c00490

Author Contributions

¶G.S., A.D., and L.P. equally contributed to the optimization of Eptifibatide process in the context of PeptFarm, University of Florence.

Notes

The authors declare no competing financial interest.

ACKNOWLEDGMENTS

■ DEDICATION

Dedicated to Prof. Dr. Luis Moroder on the occasion of his 80th birthday.

■ ABBREVIATIONS

CMOs = contract manufacturing organizations; MW-SPPS = microwave -assisted solid-phase peptide synthesis; R&D = research and development; APIs = active pharmaceutical ingredients; cGMP = current good manufacturing practice; SPPS = solid-phase peptide synthesis; Fmoc = 9-fluorenylmethyloxycarbonyl; tBu = tert-butyl; FDA = Food and Drug Administration; NMP = N-methyl-2-pyrrolidone; REACH = European Regulation on Registration, Evaluation, Authorization, and Restriction of Chemicals; GSPPS = green solid-phase peptide synthesis; DMSO = dimethilsulfoxide; MPA = 3-mercaptopropionic acid; HOBt = 1-hydroxybenzotriazole; HBTU = 3-[bis(dimethylamino)methyliumyl]-3H-benzotriazol-1-oxide hexafluorophosphate; MW = microwave; MTBE = methyl-tert-butyl ether; CPME = cyclopentyl methyl ether; DMF = N,N-dimethylformamide; DTDPA or MPA$_2$ = 3,3′-dithiodipropionic acid; MPA(PyS) = 3-(pyridyne-2-thiol)-propanoic acid; DIC = N,N′-diisopropylcarbodiimide; PyBOP = (benzotriazol-1-yloxy) tripyrrolidinophosphonium hexafluorophosphate; NCS = N-Chlorosuccinimide; TFA = trifluoroacetic acid; TIS = triisopropylsilane; DODT = 2,2′-(ethylenedioxy)diethanethiol; DIPEA = N,N-diisopropylethylamine; iPr$_2$O = diisopropyl ether; Et$_2$O = diethyl ether; DCM = dichloromethane; CH$_3$CN = acetonitrile; NMM = 4-methylmorpholine; βME = β-mercaptoethanol; 2-MEA = 2-aminoethane-1-thiol; NPyS = 3-nitro-2-pyridynesulfenyl; Mmt = 4-methoxytrityl; PyS = pyridine-2-thiol; IPC = in process control; R$_t$ = retention time; calcd = calculated; ESI-MS = electrospray ionization mass spectrometry; RP-UHPLC-MS = reversed-phase ultrahigh performance liquid chromatography mass spectrometry; DTT = 1,4-dithiothreitol; NH$_4$OH = ammonium hydroxide; NH$_4$HCO$_3$ = Ammonium bicarbonate; StBu = S-tert-butylthio; Trt = triphenylmethyl; Pbf = 2,2,4,6,7-pentamethyldihydrobenzofuran-5-sulfonyl; Boc = tert-butyloxycarbonyl

■ REFERENCES

(1) Craik, D. J.; Fairlie, D. P.; Liras, S.; Price, D. The future of peptide-based drugs. *Chem. Biol. Drug Des.* **2013**, *81* (1), 136−147.

(2) Lau, J. L.; Dunn, M. K. Therapeutic peptides: Historical perspectives, current development trends, and future directions. *Bioorg. Med. Chem.* **2018**, *26* (10), 2700−2707.

(3) de la Torre, B. G.; Albericio, F. Peptide Therapeutics 2.0. *Molecules* **2020**, *25* (10), 2293.

(4) Lax, R. The future of peptide development in the pharmaceutical industry. *PharManufacturing: The international peptide review* **2010**, *2*, 10−15.

(5) Kota, S. Peptide Manufacturing Methods and Challenges. *Peptide Therapeutics: Strategy and Tactics for Chemistry, Manufacturing, and Controls* **2019**, *72*, 111−150.

(6) Uhlig, T.; Kyprianou, T.; Martinelli, F. G.; Oppici, C. A.; Heiligers, D.; Hills, D.; Calvo, X. R.; Verhaert, P. The emergence of

(7) Andersson, L.; Blomberg, L.; Flegel, M.; Lepsa, L.; Nilsson, B.; Verlander, M. Large-scale synthesis of peptides. *Biopolymers* **2000**, *55* (3), 227−250.

(8) Jad, Y. E.; Acosta, G. A.; Govender, T.; Kruger, H. G.; El-Faham, A.; de la Torre, B. G.; Albericio, F. Green solid-phase peptide synthesis 2. 2-Methyltetrahydrofuran and ethyl acetate for solid-phase peptide synthesis under green conditions. *ACS Sustainable Chem. Eng.* **2016**, *4* (12), 6809−6814.

(9) Jad, Y. E.; Govender, T.; Kruger, H. G.; El-Faham, A.; de la Torre, B. G.; Albericio, F. Green solid-phase peptide synthesis (GSPPS) 3. Green solvents for Fmoc removal in peptide chemistry. *Org. Process Res. Dev.* **2017**, *21* (3), 365−369.

(10) Jad, Y. E.; Kumar, A.; El-Faham, A.; de la Torre, B. G.; Albericio, F. Green Transformation of solid-phase peptide synthesis. *ACS Sustainable Chem. Eng.* **2019**, *7* (4), 3671−3683.

(11) Knauer, S.; Koch, N.; Uth, C.; Meusinger, R.; Avrutina, O.; Kolmar, H. Sustainable Peptide Synthesis Enabled by a Transient Protecting Group. *Angew. Chem., Int. Ed.* **2020**, *59* (31), 12984−12990.

(12) Zorzi, A.; Deyle, K.; Heinis, C. Cyclic peptide therapeutics: past, present and future. *Curr. Opin. Chem. Biol.* **2017**, *38*, 24−29.

(13) Angeletti, R. H.; Bibbs, L.; Bonenwald, L. F.; Fields, G. B.; McMurray, J. S.; Moore, W. T.; Stults, J. T. Formation of a disulfide bond in an octreotide-like peptide: a multicenter study. In *Techniques in Protein Chemistry*, Vol. 7; Marshak, D. R., Ed.; Academic Press: Cambridge, MA, 1996; pp 261−274.

(14) Moroder, L.; Musiol, H.-J.; Schaschke, N.; Chen, L.; Hargittai, B.; Barany, G. *Protection of the thiol group. In: Synthesis of Peptides and Peptidomimetics*; Georg Thieme Verlag: Stuttgart, Germany, 2002; pp 384−424.

(15) Chen, L.; Annis, I.; Barany, G. Disulfide bond formation in peptides. *Current protocols in protein science* **2001**, *23* (1), 18−6.

(16) Hruby, Victor J. *Synthesis of cystine peptides. In: Synthesis of Peptides and Peptidomimetics. Houben-Weyl E22b:Methods of Organic Chemistry*; Georg ThiemeVerlag: Stuttgart, Germany, 2002; pp 101−141.

(17) Annis, I.; Hargittai, B.; Barany, G. Disulfide bond formation in peptides. *Methods Enzymol.* **1997**, *289*, 198−221.

(18) Moroder, L.; Besse, D.; Musiol, H. J.; Rudolph-Böhner, S.; Siedler, F. Oxidative folding of cystine-rich peptides vs regioselective cysteine pairing strategies. *Biopolymers* **1996**, *40* (2), 207−34.

(19) Darlak, K.; Wiegandt Long, D.; Czerwinski, A.; Darlak, M.; Valenzuela, F.; Spatola, A. F.; Barany, G. Facile preparation of disulfide-bridged peptides using the polymer-supported oxidant CLEAR-OX. *J. Pept. Res.* **2004**, *63* (3), 303−312.

(20) Yang, Y.; Hansen, L.; Badalassi, F. Investigation of On-resin Disulfide Formation for Large-scale Manufacturing of Cyclic Peptides: A Case Study. *Org. Process Res. Dev.* **2020**, *24*, 1281.

(21) Varray, S.; Werbitzky, O.; Zeiter, T. On-resin peptide cyclization. Patent EP1805203A2, 2011.

(22) Kota, S.; Tallapaneni, V.; Adibhatla, K. S.; Bhujanga, R.; Venkaiah, C. N. Improved Process For Preparation Of Eptifibatide By Fmoc Solid Phase Synthesis. Patent WO2009150657A1, 2009.

(23) Subha, N. V.; Ravindra, B. B.; Venkata, S. K. I.; Seeta, R. G.; Venkata, S. R. R. K.; Bala, Muralikrishna, M. Process for preparing eptifibatide. Patent US9156885B2, 2012.

(24) Han, Y.; Tong, G.; Wang, X.; Wen, Y.; Zhu, C.; Chengdu, S. Eptifibatide preparation method. Patent US9394341B2, 2016.

(25) Subirós-Funosas, R.; Prohens, R.; Barbas, R.; El-Faham, A.; Albericio, F. Oxyma: An Efficient Additive for Peptide Synthesis to Replace the Benzotriazole-Based HOBt and HOAt with a Lower Risk of Explosion. *Chem. - Eur. J.* **2009**, *15*, 9394−9403.

(26) Calce, E.; Vitale, R. M.; Scaloni, A.; Amodeo, P.; De Luca, S. Air oxidation method employed for the disulfide bond formation of natural and synthetic peptides. *Amino Acids* **2015**, *47* (8), 1507−1515.

(27) Albericio, F.; Andreu, D.; Giralt, E.; Navalpotro, C.; Pedroso, E.; Ponsati, B.; Ruiz-Gayo, M. Use of the NPyS thiol protection in

solid phase peptide synthesis. Application to direct peptide-protein conjugation through cysteine residues. *Int. J. Pept. Protein Res.* **1989**, *34* (2), 124−8.

(28) Galande, A. K.; Weissleder, R.; Tung, C. H. An effective method of on-resin disulfide bond formation in peptides. *J. Comb. Chem.* **2005**, *7* (2), 174−177.

(29) Fernandes, P. A.; Ramos, M. J. Theoretical insights into the mechanism for thiol/disulfide exchange. *Chem. - Eur. J.* **2004**, *10* (1), 257−66.

(30) Nagy, P. Kinetics and mechanisms of thiol−disulfide exchange covering direct substitution and thiol oxidation-mediated pathways. *Antioxid. Redox Signaling* **2013**, *18* (13), 1623−1641.

(31) Postma, T. M.; Albericio, F. N-Chlorosuccinimide, an efficient reagent for on-resin disulfide formation in solid-phase peptide synthesis. *Org. Lett.* **2013**, *15* (3), 616−9.

(32) Alcaro, M. C.; Sabatino, G.; Uziel, J.; Chelli, M.; Ginanneschi, M.; Rovero, P.; Papini, A. M. On-resin head-to-tail cyclization of cyclotetrapeptides: Optimization of crucial parameters. *J. Pept. Sci.* **2004**, *10* (4), 218−228.

(33) Galanis, A. S.; Albericio, F.; Grøtli, M. Enhanced microwave-assisted method for on-bead disulfide bond formation: Synthesis of α-conotoxin MII. *Biopolymers* **2009**, *92* (1), 23−34.

(34) Keire, D. A.; Strauss, E.; Guo, W.; Noszal, B.; Rabenstein, D. L. Kinetics and equilibria of thiol/disulfide interchange reactions of selected biological thiols and related molecules with oxidized glutathione. *J. Org. Chem.* **1992**, *57* (1), 123−127.

Article

An Optimized Safe Process from Bench to Pilot cGMP Production of API Eptifibatide Using a Multigram-Scale Microwave-Assisted Solid-Phase Peptide Synthesizer

Published as part of the Organic Process Research & Development joint virtual special issue "Process Safety from Bench to Pilot to Plant" in collaboration with ACS Chemical Health & Safety and Journal of Loss Prevention in the Process Industries.

Annunziata D'Ercole,[∇] Lorenzo Pacini,[∇] Giuseppina Sabatino, Matteo Zini, Francesca Nuti, Arianna Ribecai, Alfredo Paio, Paolo Rovero, and Anna Maria Papini*

Cite This: https://doi.org/10.1021/acs.oprd.1c00368

Read Online

ACCESS | Metrics & More | Article Recommendations | Supporting Information

ABSTRACT: A growing industrial interest toward the peptide drug market fueled the need for the development of effective and cGMP compliant manufacturing methods for these complex molecules. Solid-phase strategies are considered methods of election for medium-length peptide syntheses not only on the research scale but for multigram-scale production, as well. The possibility to use microwave-assisted technology on the multigram scale, recently introduced, prompted us to evaluate the possibility to conveniently set up a safe and fully cGMP-compliant pilot process to produce eptifibatide, a generic peptide active pharmaceutical ingredient. Accordingly, we developed an optimized process on the laboratory scale (1−5 mmol), which was subsequently successfully scaled up to 70 mmol, obtaining all the information required by regulatory agencies to validate the process and qualify the pilot scale plant. The process consists of 5 steps: (1) automated microwave-assisted solid-phase synthesis of eptifibatide linear precursor; (2) cleavage from the resin with concomitant amino acid side-chains deprotection; (3) disulfide-bond formation in solution; (4) purification by flash column chromatography; (5) ion-exchange solid-phase extraction. Since the direct scale-up of a multigram-scale cGMP compliant peptide API production procedure is a challenge that requires an accurate understanding of each involved step, we initially performed a quality management risk assessment, which enabled a smooth and effective achievement of a successful final result.

KEYWORDS: *generic peptide drug, peptide production scale-up, multigram-scale microwave-assisted peptide synthesis, technology transfer, peptide production pilot plant*

■ INTRODUCTION

According to the latest "Transparency Market Research" report, the global peptide therapeutics market was valued in 2018 at ca. 25 billion USD, and it is anticipated to expand until 2027 at a Compound Annual Growth Rate (CAGR) of 7.9%.[1] Moreover, a recent report by Roots Analysis, Business Research and Consulting, expects that the peptide therapeutics market following industry trends and global forecast 2021−2030, will be directly associated with increasing investments in R&D activities, in search of new drug substances for treating infectious diseases, metabolic disorders, diabetes, cancer, and other diseases.[1] Additionally, companies are moving toward the generic peptide drug market that appears to offer a relatively easy and lucrative option, also because of several patents expiring.

Industries that produce generic peptide drugs following cGMP requirements have to cooperate with regulatory authorities, such as the European Medicines Agency (EMA) and US Food and Drug Administration (FDA), to harmonize guidelines on therapeutics production.[2] In this frame, a potential application for EMA and/or FDA approval of a synthetic peptide drug, referred to as a previously approved one, shall be submitted as an Abbreviated New Drug Application (ANDA) of the Federal Food, Drug, and Cosmetic Act (FD&C Act). According to this document, ANDA application is mandatory to demonstrate that the active pharmaceutical ingredient (API) is equivalent to the reference listed drug (RLD). ANDA approval strictly depends on the impurity profile. In particular, a proposed generic synthetic peptide drug cannot contain more than 0.5% of each new specified peptide-related impurity that has to be characterized and demonstrated not affecting safety and effectiveness of the drug.[3−5] Therefore, methods validation and facilities qualification become part and parcel of this demonstrative process, to ensure and preserve the identity, quality, effectiveness, and purity of the generic peptide drug candidate.

Solid-phase strategies are considered methods of election for medium-length peptide syntheses not only on the research scale but more and more also for multigram-scale production. Since large quantities of hazardous solvents such as DMF, NMP, and/or CH_2Cl_2 are required to perform reactions and washings in this multistep process, innovative synthetic technologies and purification protocols have been proposed with the primary goal to identify greener solvents and procedures. Albericio and co-workers proposed as green solvents 2-MeTHF and Gamma-Valerolactone (GVL), demonstrating good swelling capacity of the solid support (2-chlorotrityl chloride and Wang resins), solubilization capability, and reactivity of amino acid building blocks and coupling reagents, even if demonstrated only on the small scale.[6−8]

Another aspect investigated to improve the efficiency of solid-phase peptide synthesis (SPPS), also from the instrument engineering perspective, is temperature control of the reaction. Pentelute and co-workers reported the development of an automated fast-flow instrument to synthesize up to 164-amino-acid peptide chains via 327 reaction steps, with coupling cycles of 40 s at 90 °C.[9] However, "a potentially limiting factor for the setup is synthesis scale".[10] In fact, the capacity of the reactor currently available allows hosting only 200 mg of resin with a loading of ca. 0.5 mmol/g. To the best of our knowledge, multigram-scale equipment is available only for conventional synthetic approaches in the solid-phase at room temperature (CS-Bio, Gyros).

Consistent with new frontiers of synthesis automation and control engineering is the variable bed flow reactor (VBFR) developed by Seeberger and co-workers. VBFR-SPPS allows monitoring of on-resin aggregation, secondary structure formation, as well as deprotection and coupling reactions that may lead to variation of resin swelling, resulting into decreased coupling efficiency. Although thorough real-time monitoring is pivotal to guaranteeing reproducibility for multigram-scale production, to the best of our knowledge, larger equipment compatible with this technology is still not available.[11]

A different perspective is offered by microwave (MW) technology, which has been demonstrated to overcome possible drawbacks of multigram-scale solid-phase synthesis. As reported by Collins et al., MW irradiation significantly decreases reaction time, increasing crude purity.[12−14] Therefore, MW-SPPS is now considered one of the most important strategies to obtain synthetic peptides. Indeed, among all the innovative technologies above-described, MW irradiation is the unique one currently exploited in a commercially available synthesizer for multigram-scale production. CEM Corporation (Charlotte, NC, U.S.A.) provides three microwave-assisted solid-phase synthesizers allowing the scale-up of a MW-SPPS optimized process.[15] These instruments can perform syntheses from 0.005 to 5 mmol scale (Liberty Prime and Liberty Blue systems) and from 5 to 800 mmol scale (Liberty Pro system). The latter was used within the work reported herein for a cGMP compliant industrial production of a 70 mmol pilot-scale peptide active pharmaceutical ingredient to be commercialized as a generic drug.

Several patents claiming synthetic processes to produce the disulfide-bridged cycloheptapeptide eptifibatide include strategies based on SPPS, liquid-phase peptide-synthesis (LPPS), and hybrid approaches. Among the most remarkable SPPS strategies, Qin et al. disclosed the synthesis of a linear

eptifibatide precursor on Sieber resin. Acetamidomethyl (Acm) was used as an orthogonal protecting group of the thiol function both of cysteine and mercaptopropionic acid (MPA). Contemporary Acm removal and disulfide bond formation led to the desired cyclopeptide eptifibatide.[16] Despite the method appearing easy, poor handling of the resin makes it less exploitable, with low yield as an output. On the other hand, Wen et al. proposed the use of different solid supports, such as Rink Amide, Rink Amide AM, and Rink Amide MBHA resins. However, each strategy requires several intermediate steps before isolation of the desired cyclopeptide.[17]

Concerning the strategies used for multigram-scale disulfide bond formation, most of the methods reported in the literature are based on oxidation in solution, after cleavage of the corresponding linear precursor from the resin. Strong oxidizing reagents (such as H_2O_2, DMSO, I_2) are proposed for off-resin oxidation.[18] However, disulfide bridge formation under basic conditions requires accurate reaction optimization conditions, and in particular pH, concentration, and the solvent mixture must be carefully controlled. As recently described, automated MW-assisted solid-phase synthesis significantly decreased production times and waste volumes to obtain up to 5 mmol eptifibatide (Figure 1).[15]
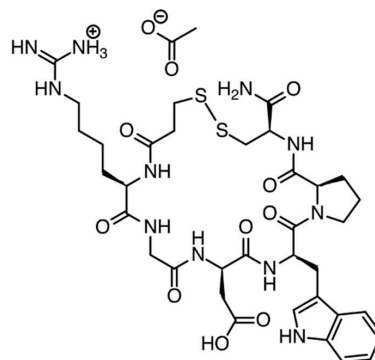
Figure 1. Eptifibatide acetate: N^6-(aminoiminomethyl)-N^2-(3-mercapto-1-oxopropyl)-L-lysylglycyl-L-α-aspartyl-L-tryptophyl-L-prolyl-L-cysteinamide, cyclic (1→6)-disulfide acetate.

■ RESULTS AND DISCUSSION

Final aim of the present work is to provide a proof-of-concept that industrial manufacturing of peptide APIs can take advantage from the performances of MW-assisted solid-phase synthesizers available on the market. This approach can be strategic for the scale-up of the synthetic process, particularly for those manufacturers entering the market of peptide generic drugs and requiring scientific knowledge transfer and support in overcoming possible unforeseen events in peptide chemistry.

We report herein the laboratory process optimization (1−5 mmol) of the heterodetic cyclopeptide API eptifibatide acetate (Figure 1) in five steps: (1) eptifibatide linear precursor automated MW-assisted solid-phase synthesis (Liberty Blue, CEM, Charlotte, NC, U.S.A, step 1); (2) cleavage from the resin and amino acid side-chain deprotection (step 2); (3) in solution disulfide-bond formation (step 3); (4) purification by flash column chromatography (step 4), followed by (5) ion-exchange solid-phase extraction (step 5). Different steps are

Scheme 1. Synthetic Scheme of Eptifibatide Acetate Production

Figure 2. Ishikawa diagram for the development of the cGMP eptifibatide acetate production process. Critical process parameters (CPPs) are reported in **bold**.

defined in Scheme 1. We also demonstrated the scalability of this protocol to an industrial cGMP compliant robust manufacturing process to produce 70 mmol peptide API. To the best of our knowledge, this is the first time that the automated MW-assisted solid-phase multigram-scale peptide synthesizer Liberty Pro (CEM, Charlotte, NC, U.S.A) was used for cGMP production of a peptide API.

In addition, since industrial process optimization shall consider specific requirements such as safety, economic, and, most importantly, regulatory aspects, we examined in depth all those features that we considered critical during the technology transfer from lab- to pilot-scale. These aspects are described in specific paragraphs, titled "scale-up activities", after the description of each step lab-scale optimization.

Finally, since the direct scale-up of a kilogram-scale, cGMP compliant peptide API production procedure is a challenge that requires an accurate understanding of each involved step, we initially performed a quality management risk assessment, as described in the following paragraph.

Quality Risk Management: Identification of Critical Quality Attributes and Critical Process Parameters to Be Optimized. Implementation of Abbreviated New Drug Application (ANDA) for eptifibatide approval by regulatory agencies (as for any other peptide generic drug) required a systematic approach to preliminarily define Critical Quality Attributes (CQAs) and understanding the process to follow, identifying critical material attributes (CMAs) and critical process parameters (CPPs). This allowed the establishment of the functional relationships linking CMAs/CPPs to CQAs, according to the International Conference of Harmonization document Q8 (ICH Q8). In this process, profound knowledge of peptide science and therefore of the organic chemistry of the molecule to be produced is pivotal.

In this framework, the Ishikawa diagram was selected to plot the list of the parameters involved in the eptifibatide acetate manufacturing process to identify the critical parameters that have been considered into the optimization process on 1−5 mmol lab-scale (Figure 2).

The present work does not claim to be a detailed description of GMP requirements, rather it would show an example of process optimization and pioneering pilot scale transfer according to cGMP requirements.

We followed the principles of quality risk management to establish a suitably controlled cGMP compliant manufacturing process of an eptifibatide acetate pilot batch across the product life cycle. In particular, we evaluated the risk to quality (thanks to the scientific knowledge of peptide chemistry), and we provided formalities and documentations of the performed experiments commensurate with the level of risk, integrated with facilities, equipment, utilities qualification, materials management, laboratory control, and stability testing.[19] The identification of hazards and the analysis and evaluation of risks associated with exposure to those hazards is a relevant part of risk assessment (EUH019, hazard statement in Classification, Labeling & Packaging regulation).[20]

Step 1. Optimization and Scale-up of Solid-Phase Synthesis of on-Resin Eptifibatide Linear Precursor by Automated MW-Assisted Synthesizers. At the industrial level, cost flow in process costing requires evaluation of direct material costs from the beginning of the process, i.e., reagents and solvents to be used for peptide synthesis, isolation, and purification, including ion-exchange solid-phase extraction. Solid-phase synthesis through stepwise assembly of building blocks on a solid support usually requires large excesses of reagents essential to overcoming limitations due to reactions in the heterogeneous phase. However, this practice strongly affects the cost of the final product.

In this framework, automation is fundamental to getting continuous cycle manufacturing, minimizing intermediates isolation, and preserving both safety and reproducibility.

On-resin fully protected linear eptifibatide precursor MPA-(Trt)-Har(Pbf)-Gly-Asp(OtBu)-Trp(Boc)-Pro-Cys(Trt)-Rink Amide AM resin was built via a standard Fmoc/tBu MW-SPPS strategy (see Experimental Section). The coupling system based on N,N′-diisopropylcarbodiimide (DIC) and Oxyma Pure is considered safe, has a low cost, and is suitable for MW-SPPS because of its stability at 90 °C (temperature reached in

the MW conditions) and requires lower DMF washing volumes, due to its higher solubility, as compared to more classic coupling reagents.

We describe herein the successful scale-up to 70 mmol of fully protected on-resin eptifibatide linear precursor in 1 day by an automated MW-assisted process, using the Liberty Pro synthesizer, after having optimized the synthesis on a 5 mmol scale on the Liberty Blue synthesizer. The aim is to demonstrate that the MW-assisted process dramatically decreases the time of production, compared to conventional room temperature solid-phase synthesis, usually requiring at least 1 week to obtain similar length peptides. Consequently, labor price, the most relevant cost for industrial manufacturers, will be decreased.

Evaluation of the Minimal Quantity of the High-Cost Building Block Fmoc-L-Har(Pbf)-OH. As underlined above, a careful analysis of the purity profile is pivotal to producing a generic API compliant with cGMP requirements. The on-resin synthesis of the linear eptifibatide precursor requires use of the high cost building block Fmoc-L-Har(Pbf)-OH.

Therefore, optimization of its coupling conditions, minimizing cost flow in process costing, is a challenge. First, we explored the scalability from a 1 to 5 mmol scale investigating (1) single vs double coupling; (2) the use of lower reagents excess; and (3) an increase of coupling time, maintaining the temperature at 90 °C and adapting MW-power to the different scale.

We demonstrated that the first coupling should not be performed with <2.5 equiv of Fmoc-L-Har(Pbf)-OH (Table S1, entries 1−3). This is fundamental to limiting Des-Har[2]-linear precursor impurity formation that was observed (Figure S1) possibly because of the high hindrance of the Pbf protecting group and/or δ-lactam formation from the activated Fmoc-Har(Pbf)-OH building block, affecting coupling efficiency.[21] A large excess of activated building blocks or double couplings may overcome this problem. However, in our case, double coupling did not appear to be advantageous in terms of limiting Des-Har[2]-linear precursor impurity formation. We succeeded in optimizing the coupling conditions of Fmoc-Har(Pbf)-OH on a 5 mmol scale in 15 min, using 1 × 2.5 equiv, at 90 °C and 17−26 W, obtaining only a 0.6% Des-Har[2]-linear eptifibatide impurity (Table S1, entry 5), compared with the 1 mmol scale (Table S1, entry 4). Interestingly, the scale-up to 70 mmol (1 × 2.5 equiv of Fmoc-Har(Pbf)-OH at 90 °C and 1800−800 W, Table S4) did lead in only 40 min to <0.1% of the Des-Har[2]-linear eptifibatide impurity (see Experimental Section: IPC by resin cleavage). Therefore, no further investigation was performed of possible δ-lactam formation from the activated Fmoc-Har(Pbf)-OH building block, as recently reported in the case of Fmoc-Arg(Pbf)-OH by de la Torre et al., who observed large quantities of Des-Arg peptides once the temperature was not maintained at <55 °C but without microwaves.[22]

Scaling-up the coupling step from 5 mmol on Liberty Blue to 70 mmol on Liberty Pro (characterized by an optimized dual-mode mixing with overhead mechanical stirring and N₂ bubbling, homogeneously heating resin and diffusing solvents) required a proportional increase of MW power and reaction time to guarantee optimal performances of the synthesis. Increasing the time of coupling was possible because of the stability and the efficiency of the DIC/Oxyma pure coupling system under MW conditions. Reproducibility of the MW-

SPPS on the pilot-scale was unequivocally demonstrated (Tables S2, S3, and S4).

Quality Check of Solvents and Reagents in Compliance with Critical Material Attributes (CMAs). Industrial raw materials (RMs) are generally stored in large tanks in the manufacturer's warehouse department and withdrawn as needed.[23,24] The industrial grade material attributes must be demonstrated to be compliant with the analytical ones. Consequently, before starting the 70 mmol pilot scale production, industrial-grade DMF and Oxyma pure quality were tested (use test). First of all, we demonstrated that the reagents were compliant with suppliers' certificate of analysis (CoA). Moreover, their performances were compared on a 5 mmol scale synthesis with a second synthesis performed under the same conditions using analytical-grade reagents. As the UHPLC purity (after cleavage) of the eptifibatide linear precursor crude and Des-Har²-linear precursor impurity amount resulted as comparable, we considered it acceptable to use industrial-grade DMF and Oxyma pure reagent, decreasing the production cost (Table S5).

Step 2. Cleavage from the Resin and Amino Acid Side-Chains Deprotection to Obtain the Crude Eptifibatide Linear Precursor. The cleavage step, which consists of the concomitant cleavage of the peptide from the resin and side-chain deprotection, can potentially generate impurities that must be precisely characterized to fulfill cGMP requirements for the final regulatory approval.

Identification of the critical quality attributes (CQAs) of the API and critical processing parameters (CPPs) are pivotal to the release of the final peptide batch.[25] Cleavage conditions have to be considered CPPs because of their direct connection to the final purity profile (Figure 2). Deviations and being out of specification (OOS) from the expected behavior may affect the safety and efficacy of the final product, invalidating final approval for human use marketing. Consequently, further investigations to demonstrate the causes, followed by time-consuming corrective actions, are required.

Investigation on the Cleavage Scavenger Mixture Effect on Crude Purity. The mixture TFA/TIS/DODT/H$_2$O 92.5:2.5:2.5:2.5 (v/v/v/v) was tested first to cleave the eptifibatide linear precursor from the resin (Figures S2 and S3). After cleavage, UHPLC/ESI-MS analysis of the crude product obtained after precipitation in ether showed three main side products: R_t = 5.154 min, $[M + H]^+$ m/z = 890.39 (Imp a); R_t = 5.333 min, $[M + H]^+$ m/z = 890.39 (Imp b), both deviating +56 m/z; R_t = 4.258 min, $[M + H]^+$ m/z = 878.32 (Imp c), deviating +44 m/z, from the calculated mass value $[M + H]^+$ m/z = 834.33 (R_t = 4.333 min) of the eptifibatide linear precursor, respectively (Figures S4, S5, S6, and S7).

Reactions to cleave tBoc and tBu protecting groups from Trp and Asp side chains, respectively, generate *tert*-butyl carbocation species. This highly reactive electrophilic species shall be quenched *in situ* by appropriate nucleophiles added to the TFA cleavage cocktail, i.e., scavengers, in order to prevent reattachment or modification of the deprotected nucleophilic side chains, such as thiol function on cysteine.[26,27]

In the specific case of the eptifibatide linear precursor, cysteine and MPA thiol functions represent possible electrophilic attack acceptors. In this framework, MS/MS analysis of the peak at R_t = 5.154 min revealed the fragment $[M + H]^+$ m/z = 487.3 corresponding to the b$_4$ fragment with *tert*-butyl carbocation reattachment on MPA thiol function. Therefore,

we demonstrated that Imp a is the *tert*-butyl derivative of the eptifibatide linear precursor (Figure S5). Consequently, we can hypothesize that R_t = 5.333 min (Imp b) corresponds to the impurity of the *tert*-butyl derivative on cysteine thiol function.

Cysteine and MPA thiol functions in the crude could be both deprotected from the newly formed StBu-peptide side product only using hazardous reagents, requiring expensive strong acid-resistant equipment. However, since Imp a and Imp b cleaning from the eptifibatide TFA salt after purification (step 4) led to residual amounts compliant with international regulatory standards, we did not consider strong acid treatments.

The best crude UHPLC purity was achieved performing the cleavage in two steps. In the first 30 min, two different cleavage cocktails were tested at 2 mmol, and the data are shown in Table 1. In the second step, a further 230 mL of TFA were

Table 1. Cleavage Cocktails Tested to Obtain the Highest UHPLC Crude Purity

| entry	1st step cleavage mixture volume ratio	UHPLC crude purity,[a] %	Imp a [a] % / Imp b [a] %
1	TFA/H$_2$O/TIS/DODT (72:7:7:14)	61.5	4.1 / 1.8
2	TFA/H$_2$O/TIS/DODT (60:10:10:20)	57.1	3.6 / 1.0

[a]Method used to isolate eptifibatide linear precursor crude: Et$_2$O (80 mL/g resin), r.t., 30 min stirring; 0 °C and 60 min stirring.

added and maintained under stirring for 2.5 h at r.t. to maximize eptifibatide linear precursor crude recovery. Both cleavage conditions led to comparable impurities (Table 1). However, the best crude UHPLC purity was achieved using entry 1 mixture. Therefore, in the final cleavage mixture selected for the multigram-scale synthesis, the TFA/H$_2$O/TIS/DODT ratio was 91:2.3:2.3:4.4 (v/v/v/v), which corresponds to 0.11 M TIS, 0.33 M DODT, and 1.3 M H$_2$O.

Moreover, Imp c was hypothesized to correspond to the intermediate of the eptifibatide linear precursor containing Trp-carbamic acid ($[M + H]^+$ m/z = 878.32).[28,29] In fact, deprotection of the tBoc protecting group from Trp indolyl side-chain occurs via a stepwise pattern of tBu carbocation formation followed by acidolysis of the Trp-carbamic acid intermediate derivative. Interestingly, slow decarboxylation kinetics are distinctly beneficial to avoiding additional impurity formation by electrophilic attack of the tBu carbocation to the indolyl side chain, otherwise favored in the presence of unprotected Trp.

Our hypothesis was demonstrated treating an isolated IPC of the eptifibatide linear precursor crude with 0.1% (v/v) TFA in H$_2$O/CH$_3$CN 2:1 (v/v) mixture and analytically monitoring the disappearance of the peak at R_t = 4.258 (completed in 60 min, Figure 3). Therefore, a simple, longer deprotection step should be sufficient for the disappearance of Imp c.

Evaluation of the Optimal Antisolvent to Precipitate Eptifibatide Linear Precursor Crude. Eptifibatide linear precursor crude was precipitated after filtering off the resin from cleavage solution using an antisolvent. Diethyl ether (Et$_2$O), diisopropyl ether (iPr$_2$O), methyl-*tert*-butyl ether (MTBE), and cyclopentyl-methyl ether (CPME) were tested, also considering toxicity and safety (Table 2). The high-cost CPME, recently introduced by Albericio and co-workers as a
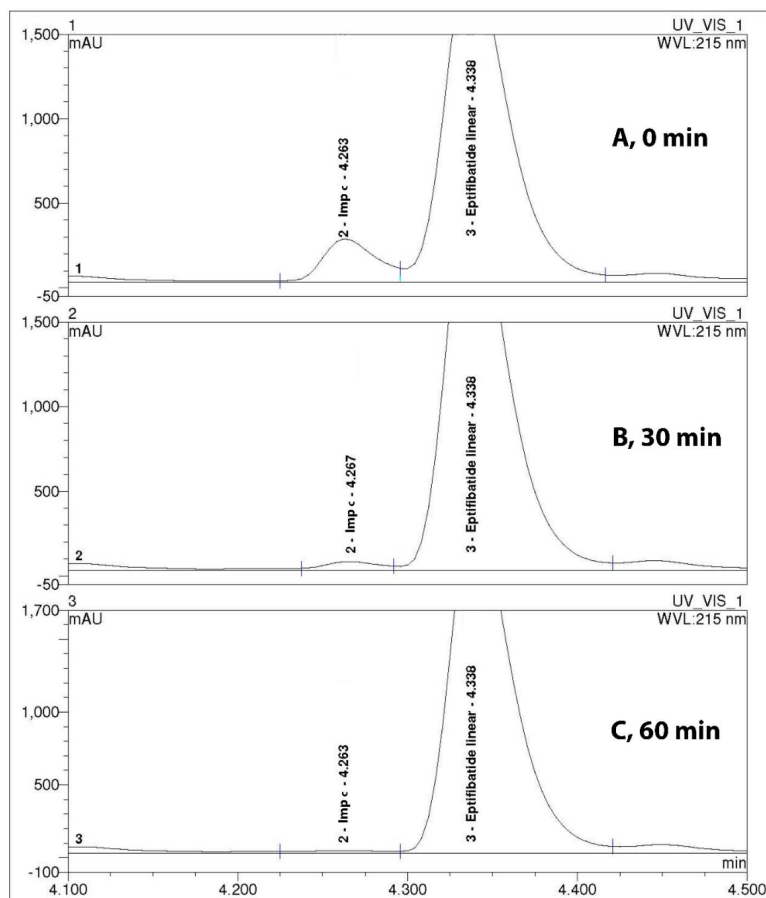
Figure 3. RP-UHPLC traces of eptifibatide linear precursor crude monitoring Trp(Boc) deprotection at different reaction times (zoom 4.1–4.5 min). Panel A, 0 min; panel B, 30 min; panel C, 60 min. C18 column Waters Acquity CSH (130 Å, 1.7 μm, 2.1 × 100 mm); temperature 45 °C; flow, 0.5 mL/min; eluent, 0.1% (v/v) TFA in H$_2$O (A) and 0.1% (v/v) TFA in CH$_3$CN (B); λ, 215 nm, gradient, 12–45% B in 10 min. R_t = 4.26 ± 0.015 min: Imp c. R_t 4.34 ± 0.01 min: linear eptifibatide precursor.

Table 2. UHPLC Purity Profile, Yield, and Cost of Eptifibatide Linear Precursor Crude Obtained after Resin Cleavage and Precipitation Using Different Solvents

entry	synthesis scale, mmol	antisolvent	UHPLC crude purity,[a] %	Imp a[a]% Imp b[a]%	crude yield,[b] %	cost,[c] €/L
1	0.18	Et$_2$O	57.0	7.24 2.57	52.3	40−100
2		iPr$_2$O	58.8	6.85 2.57	73.4	40−50
3		MTBE	55.4	7.18 2.67	73.9	46−65
4		CPME	66.4	4.60 1.63	62.8	100−200
5	1.80	iPr$_2$O	60.7	6.45 1.05	73.5	40−50

[a]Resin cleavage cocktail: TFA/H$_2$O/TIS/DODT 92.5:2.5:2.5:2.5 (v/v/v/v), 20 mL/g resin, stirring 3 h at r.t. Method used to isolate eptifibatide linear precursor crude: 80 mL solvent/g resin; r.t., 30 min stirring; 0 °C, 150 min stirring. [b]Yield (%) = $\frac{\text{found weight} \times \left(\frac{\text{peptide content}}{100}\right)}{\text{calcd weight}} \times 100$ (UV average peptide content: 72.0%). [c]Analytical-grade solvent costs for lab-scale production.

"green alternative to the hazardous Et$_2$O and MTBE", did not fulfill industrial needs.[30,31]

Despite the good performances in terms of cost (46−65 €/L), crude precipitate yield (73.9%), and UHPLC purity (55.4%), the antisolvent MTBE (usually considered as an industrial alternative to Et$_2$O, typically used in lab-scale) has the disadvantage of being classified in the list of substances of very high concern (SVHC) drafted by the European Chemicals Agency (ECHA) as hazardous chemicals for both the environment and human health.[32−34] After evaluation of all factors, iPr$_2$O was selected as an antisolvent because of low volatility, facilitating large volume management (crude yield 73.4% and UHPLC purity 58.8%) with a competitive cost (40−50 €/L). Moreover, the 10-fold scale-up of crude precipitation conditions maintained the same performance (Table 2, entries 2 and 5).

Scale-up Activities of Cleavage Step (Step 2). The cleavage step process on both the 5 and 70 mmol scale shows that the scale-up produced extremely comparable UHPLC crude purities (5 mmol, 74.1%; 70 mmol, 73.7%) and yields (5 mmol, 84.6%; 70 mmol, 82.2%) as reported in Table 3.

Table 3. Cleavage Step Comparative Analysis at 5 mmol vs 70 mmol Scale, to Obtain Eptifibatide Linear Precursor: UHPLC Crude Purity Profile and Yield

step 2 output[a,b]		70 mmol	5 mmol
eptifibatide linear precursor crude	UHPLC purity (%)	73.7	74.1
	yield[c] (%)	82.2	84.6
impurities	Imp a (%)	5.5	5.3
	Imp b (%)	3.5	2.1

[a]Loading of Rink amide AM resin: 0.97 mmol/g. Coupling conditions: single coupling 1 × 2.5 equiv building block (0.4 M), 1 × 2.5 equiv DIC (3 M), and 1 × 2.5 equiv Oxyma pure (1 M). All reagents were dissolved in DMF. Final resin washing: 9.3 mL/g resin (3 × iPrOH). [b]Resin cleavage cocktail: TFA/H$_2$O/TIS/DODT 72:7:7:14 (v/v/v/v); 7 mL/g resin, stirring 30 min, r.t.; further addition of 15 mL TFA/g resin, stirring 2.5 h, r.t. Procedure used to isolate eptifibatide linear precursor crude: 80 mL iPr$_2$O/g resin, 2 h, 0 °C. [c]Yield (%) = $\frac{\text{found weight} \times \left(\frac{\text{peptide content}}{100}\right)}{\text{calcd weight}} \times 100$ (UV average peptide content: 79.0%).
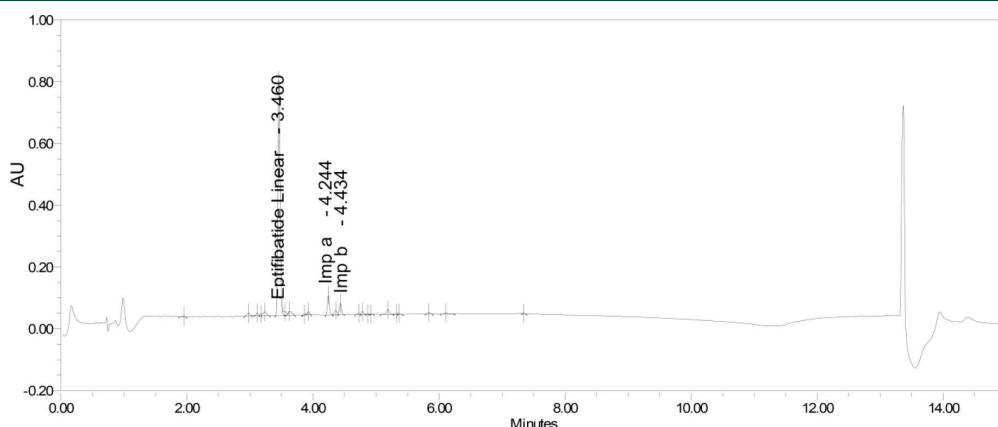
Moreover, both impurity profiles on the 5 mmol scale (Figure S8) and 70 mmol scale show the following: Imp a, ca. 5%; Imp b, ca. 3% (Table 3, Figure 4). Interestingly, no new impurities were detected in the 70 mmol scale crude analysis, demonstrating the successful direct scale-up process (Table S6).

Evaluation of Quality and Risk Assessment of Resin Cleavage Materials: Risk Analysis Associated with Exposure to Volatile Ethers and Peroxide Content, Exothermic Hazard, and TFA Quality (Use Test). Ethers volatility and peroxide-forming tendency are directly related to the fire and explosion propensity. Therefore, peroxide content in iPr$_2$O was identified as a hazard in risk assessment.[35] Moreover, peroxides can contribute to uncontrolled oxidation of amino acid side chains (such as Cys, Trp), dramatically affecting purity outcomes. Three different industrial-grade iPr$_2$O with different peroxide content (0, 350, >1000 ppm) were compared with an analytical-grade peroxide-free iPr$_2$O (Merck KGaA, Darmstadt, Germany; Table S7). A peroxide content of >1000 ppm dramatically affected the purity (32.5% vs >60%) of the crude displaying high retention time broad peaks in the UHPLC profile (oligomer formation). A slight decrease in purity was obtained with iPr$_2$O containing 350 ppm peroxides. However, undoubtedly, careful control of iPr$_2$O peroxide content (<350 ppm, ideally peroxide-free) must be performed before precipitation of the eptifibatide linear precursor crude for both safety and purity.

Precipitation of a crude eptifibatide linear precursor from TFA cleavage solution by adding iPr$_2$O was considered in the risk assessment management because of the exothermic effect during addition. In particular, lab-scale preliminary tests for hazard evaluation to quantitatively assess heat development during the process is fundamental for the final scale-up.[17]

Lab-scale precipitation from the TFA cleavage solution was performed following the optimized conditions described above. The temperature was maintained at <35 °C by ice-bath cooling to limit the temperature increase of the TFA solution during the exothermic addition of iPr$_2$O at 4 °C. In the 70 mmol pilot scale process, the temperature of the mixture was maintained at <35 °C using a thermostated jacketed reactor under stirring to manage the temperature increase developed during the exothermic iPr$_2$O addition. This procedure allowed both to

Figure 4. RP-HPLC trace of eptifibatide linear precursor crude (step 2 at 70 mmol scale). R_t = 3.46 min eptifibatide linear precursor; R_t = 4.24 min, Imp a; R_t = 4.43, Imp b (procedure S1).

G

Scheme 2. Industrial Plant Scheme Designed for Resin Cleavage, Side-Chains Deprotection, and Isolation of Crude Eptifibatide Linear Precursor TFA Salt (Table S9)
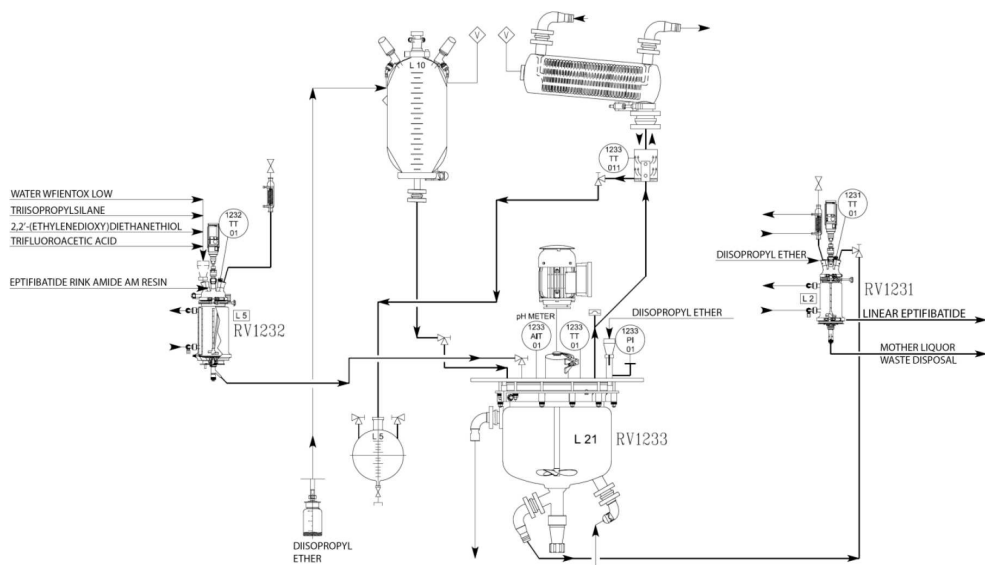
mitigate workplace safety risks and to guarantee eptifibatide linear precursor crude quality (data not shown).

TFA Quality Check (Use Test). Industrial-grade TFA specifications declared by the supplier (appearance: clear, colorless liquid, free of particulate matter; purity: ≥99.5%; water content: ≤0.1%; UV absorbance λ, 280 nm: ≤0.002; λ, 254 nm: ≤0.005; λ, 230 nm: ≤0.090) were confirmed before use, by the Quality Control Laboratory in FIS - Fabbrica Italiana Sintetici S.p.A. Industrial-grade TFA withdrawn from a storage tank was tested in a cleavage reaction performed on a resin batch obtained on the 5 mmol scale and compared with a second cleavage reaction performed under the same conditions using analytical-grade TFA (Aldrich-grade). Since the UHPLC purity of both eptifibatide linear precursor crudes were comparable (data not shown), the use of industrial-grade TFA was considered acceptable, decreasing the process cost.

Identification of Hold Points in the Scale-up Process. Our industrial production system was organized in batches. The adopted multistep process would need to be stopped before the term to manage any technical unforeseen events or inspection and test plan process (hold points). In particular, during the pilot-scale MW-SPPS (step 1), hold points were identified only after each coupling cycle (including washings and draining), before Fmoc-deprotection of the last building block on the resin. This was to avoid leaving reactive free amino functions on the resin in the reactor.

In addition, resin cleavage and side-chain deprotection under TFA harsh acidic conditions should be performed without delay to preserve purity and yield. The filtered solution containing the peptide crude in TFA was held at room temperature. After 24 h, the crude was precipitated in iPr$_2$O at 0 °C for 1 h. UHPLC crude purity dramatically decreased compared with the one obtained after immediate precipitation (data not shown). Therefore, the hold point to consider was the precipitation phase. A stability study of eptifibatide linear precursor crude was performed maintaining the suspension

after precipitation in iPr$_2$O at 0 °C for 1, 3, and 24 h. Monitoring UHPLC purity demonstrated crude stability up to 24 h (Table S8). Therefore, we established a TFA cleavage/deprotection treatment time of 0–1 h and a waiting time in the presence of iPr$_2$O at 0 °C of 3–24 h.

cGMP Equipment and Facilities for the 70 mmol Scale MW-SPPS (Step 1) and Resin Cleavage (Step 2). cGMP peptide API production requires the qualification of manufacturing equipment, proving the suitability of the system. The qualification process consists of four main actions: design, installation, operational, and performance qualifications. The design has to consider final product features, minimizing external contaminations, which could affect product quality. The plant was designed to include a walk-in fume hood (4 m^2) hosting the Liberty Pro MW-assisted synthesizer (CEM, Charlotte, NC, U.S.A) and to allow easy-cleaning procedures both before and after solid-phase peptide manufacturing (step 1). The equipment to perform step 2 was designed to limit both air exposition and operator's handling (Scheme 2).

The amount of starting material and reagents used for both cleavage and side-chain deprotection (step 2) are reported in Table 4.

After the drying session under N$_2$ inside the Liberty Pro reaction vessel, the linear precursor-resin was transferred into

Table 4. Starting Material and Reagents Used for Both Cleavage and Side-Chain Deprotection (Step 2)

chemical	vol (L)	amount (kg)
eptifibatide linear precursor-resin		0.170
H$_2$O low endotoxin	0.5	0.085
TIS	0.5	0.066
DODT	1	0.190
TFA	5 (Initial wash) + 22	6.90
iPr$_2$O	11.8 (Initial wash) + 92	12.68

the 5 L jacketed glass filter reactor (RV1232), thermostated at 20 °C. The cleavage cocktail was added from the top of the reactor, and the reaction was carried out under constant stirring. Then, the peptide-cleavage cocktail solution was transferred into the 21 L jacketed glass reactor (RV1233) through the filter on the bottom of the 5 L reactor (RV1232). The transfer to the receiving reactor was performed under vacuum conditions. Furthermore, the 5 L reactor bottom was linked to the head of the 21 L reactor (RV1233) by an inert Teflon tube. The 21 L reactor (RV1233) was thermostated at 0 °C and equipped with two thermometers (one inside the reactor and one immediately before the condenser) and one pHmeter (switched off during this step). The head of the 21 L reactor is linked to a 10 L glass reservoir by an inert Teflon tube and to a double-coil glass condenser (water-cooled) that is linked to a 5 L glass collection flask. Ether addition to the peptide-cleavage cocktail solution was performed while monitoring that the temperature was maintained at <35 °C.

After crude precipitation, the suspension was transferred under vacuum conditions to the 2 L jacketed glass filter reactor (RV1231) by an inert Teflon tube connecting the bottom of the 21 L reactor (RV1233) to the head of the 2 L reactor (RV1231). Final crude filtration was performed at 0 °C. Both transfer of the suspension from the 21 L reactor (RV1233) and eptifibatide linear precursor crude filtration were performed under vacuum conditions. Finally, after a drying session under N_2, the filtering bottom was disassembled from the rest of the 2 L reactor (RV1231), and the crude product was recovered.

Step 3. Disulfide Bond Formation in Solution to Obtain Crude Eptifibatide TFA Salt. Disulfide bond formation in the eptifibatide linear precursor is usually performed by an oxidant reagent. Intramolecular and undesired intermolecular reactions (dimerization/oligomerization) can affect final purity profile if crucial parameters such as, peptide concentration, pH, and type of oxidant reagent are not optimized.

We previously reported a detailed investigation on eptifibatide disulfide bond formation on the 5 mmol scale both in solution (5.3 mM peptide concentration, pH 9.5, in H_2O/CH_3CN, 2:1 (v/v)) by air oxidation over 22 h (98% conversion, 61% purity, and 6.6% dimer) and in the solid-phase. This solid-phase strategy had the advantage of synthesizing and cyclizing eptifibatide in the same reactor.[15] However, in the multigram-scale process developed herein, the use of the less expensive building-block Fmoc-Cys(Trt)-OH (compared to Fmoc-Cys(StBu)-OH used in the previously reported strategy) and the increased HPLC purity yield of eptifibatide crude obtained by air oxidation in solution (65% vs 40.9%) let us further investigate solution disulfide bond formation. Therefore, several oxidants and reaction conditions were tested,[36−40] in order to obtain the highest eptifibatide HPLC crude purity (data not shown). Disulfide bond formation in H_2O_2 aqueous solution was considered a balanced compromise in terms of efficacy, costs, sustainability, and postcleaning procedure of the equipment.

Despite of a fast conversion (<15 min) of the eptifibatide linear precursor (5.3 mM in H_2O/CH_3CN 2:1 v/v) on the 0.5 mmol scale, after the addition of 0.8 equiv of H_2O_2 in one shot at time 0, at pH 9.5 (NH_4OH), a substantial formation of a dimer impurity (>10%) was observed (Figures S9, S10, and S11). Therefore, different reaction conditions were investigated to obtain complete conversion with the highest eptifibatide TFA purity and lowest dimer impurity formation.

In particular, the same equivalents of H_2O_2 (0.8 equiv) were added in two or four portions (Table S10), and then the linear precursor concentration was decreased (Table S11). Two additions of 0.44 equiv of H_2O_2 (at 0 and 60 min, respectively, panel 1, Table 5) compared to 4 × 0.22 equiv

Table 5. Disulfide Bond Formation Comparative Analysis at 5 mmol vs 70 mmol Scale to Obtain Eptifibatide TFA: UHPLC Crude Purity Profile and Yield

	step 3 output[a]	70 mmol[c]	5 mmol
eptifibatide crude	UHPLC purity (%)	66.4	67.4
	yield (%)[b]	98.3	90.7
impurities	dimer (%)	5.3	5.9

[a]Conditions for disulfide bond formation (70 and 5 mmol): Eptifibatide linear precursor crude (2.1 mM in $H_2O:CH_3CN$ 2:1 v/v) was oxidized adding H_2O_2, pH 9.5 (NH_4OH), 2 h, r.t. [b]

$$\text{Yield (\%)} = \frac{\text{Eptifibotide crude weight} \times \left(\frac{\text{peptide contnet}}{100}\right)}{\text{Eptifibotide linear crude weight} \times \left(\frac{\text{peptide content}}{100}\right)} \times 100.$$ UV eptifibatide crude average peptide content: 71.0%. UV eptifibatide linear precursor crude average peptide content: 79.0%. [c]The procedure was repeated five times on the 10 mmol scale on cGMP compliant glassware.

(at 0, 30, 60, and 90 min, panel 2, Table 5) did not influence either the eptifibatide TFA yield or the dimer impurity formation. However, in the scale-up process, the possibility of four sequential additions of a lower number of H_2O_2 equiv/time allowed a more accurate in process control of the oxidation reaction (Figure 5).

Therefore, two different concentrations of linear eptifibatide precursor crude (2.1 mM and 1.6 mM) with the addition of 4 × 0.22 H_2O_2 were tested on the 0.5 mmol scale (Figure 6). Lowering the linear precursor concentration from 5.3 mM (entry 2, Table S10) to 1.6 mM (entry 2, Table S11) led to a dramatic decrease of dimer impurity formation (from 8.0% to 3.9%) and an increase in UHPLC purity of eptifibatide TFA (up to 67%).

In conclusion, the identified optimized conditions (eptifibatide linear precursor crude 1.6 mM in H_2O/CH_3CN 2:1 (v/v), pH 9.5 (NH_4OH), 4 × 0.22 equiv H_2O_2 additions at 0, 30, 60, and 90 min) allowed a decrease in reaction time from 22 to 2 h (Figures 5 and 6).

Scale-up Activities of Oxidation in Solution. The above-described optimized conditions for disulfide bond formation were tested on the 10 mmol scale and repeated twice in cGMP compliant glassware. In particular, a comparative analysis of the step 3 process (Table 5) shows that the scale-up produced extremely comparable UHPLC crude purities (5 mmol, 67.4%; 70 mmol, 66.4%) and increased yield (5 mmol, 90.7%; 70 mmol, 98.3%). Moreover, scale-up in process control demonstrates that dimer impurity formation was limited to <6% (Figures S12, S13, and Figure 7).

Concerning step 3 scale-up, a specific cGMP compliant industrial plant was designed both for off-resin disulfide bond formation and isolation of crude eptifibatide TFA salt by freeze-drying (Scheme 3). The amount of starting material and reagents used for pilot disulfide bond formation (step 3) are reported in Table 6.

A 21 L jacketed glass reactor (RV1233) was thermostated at 20 °C. After loading from the top of the reactor, the eptifibatide linear precursor crude was solubilized in the mixture WFI/CH_3CN 2:1 (v/v) previously prepared in a 10 L
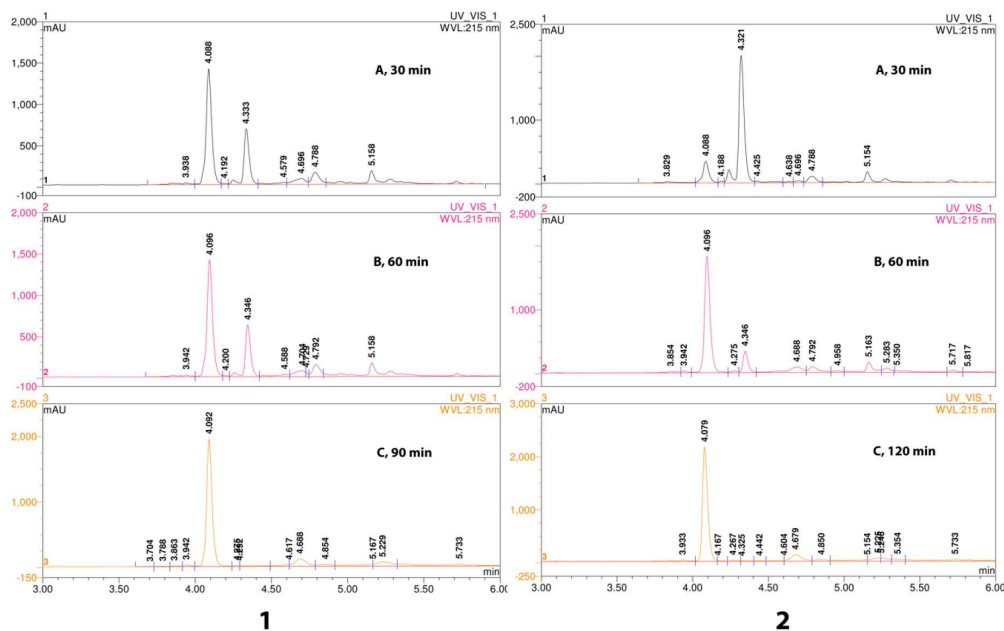
Figure 5. In process control of off-resin disulfide bond formation (0.5 mmol scale): RP-UHPLC traces of eptifibatide crude obtained by eptifibatide linear precursor crude in H$_2$O/CH$_3$CN 2:1 (v/v); 5.3 mM, with two (panel 1; entry 1, Table S10) and four (panel 2; entry 2, Table S10) additions of H$_2$O$_2$ at different times (A−C) and with pH 9.5, r.t. RP-UHPLC: C18 column Waters Acquity CSH (130 Å, 1.7 μm, 2.1 × 100 mm); temperature, 45 °C; flow, 0.5 mL/min; eluent, 0.1% (v/v) TFA in H$_2$O (A) and 0.1% (v/v) TFA in CH$_3$CN (B); λ, 215 nm; gradient, 5−95% B in 10 min. R_t = 4.085 ± 0.015 min, eptifibatide TFA; R_t = 4.33 ± 0.01 min, eptifibatide linear precursor; R_t = 4.77 ± 0.015 min, dimer impurity.
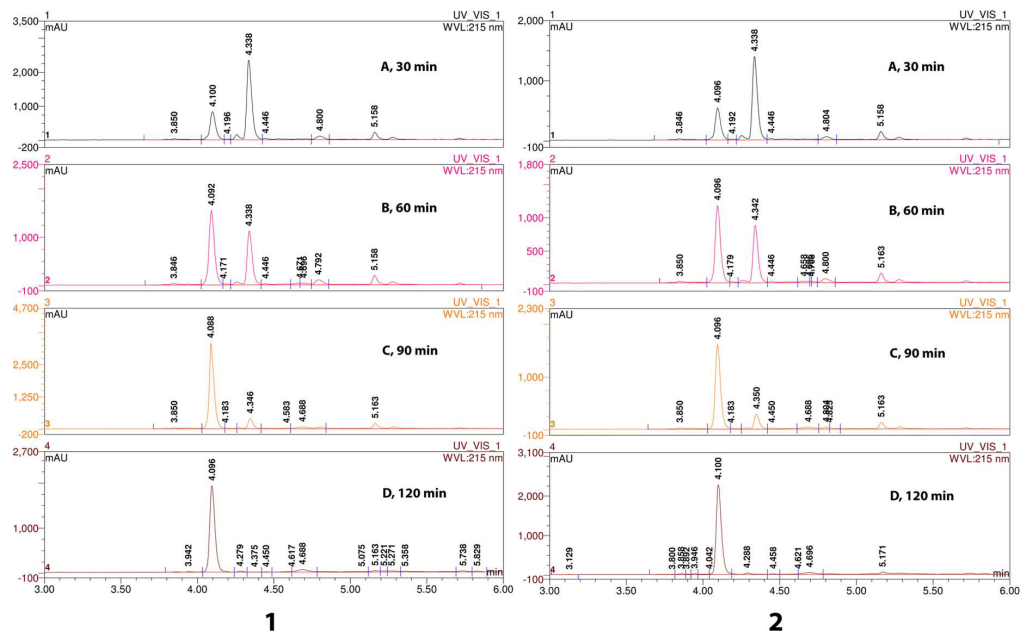
Figure 6. In process control of off-resin disulfide bond formation (0.5 mmol scale): RP-UHPLC traces of eptifibatide crude obtained by eptifibatide linear precursor crude in H$_2$O/CH$_3$CN 2:1 (v/v) at concentrations 1 (2.1 mM) and 2 (1.6 mM), with 4 × 0.22 equiv H$_2$O$_2$ additions at 0, 30, 60, and 90 min (Table S11); pH 9.5; r.t. RP-UHPLC: C18 column Waters Acquity CSH (130 Å, 1.7 μm, 2.1 × 100 mm); temperature, 45 °C; flow, 0.5 mL/min; eluent, 0.1% (v/v) TFA in H$_2$O (A) and 0.1% (v/v) TFA in CH$_3$CN (B); λ, 215 nm; gradient, 5−95% B in 10 min. R_t = 4.09 ± 0.015 min, eptifibatide TFA; R_t = 4.33 ± 0.01 min, eptifibatide linear precursor; R_t = 4.79 ± 0.015, dimer impurity.
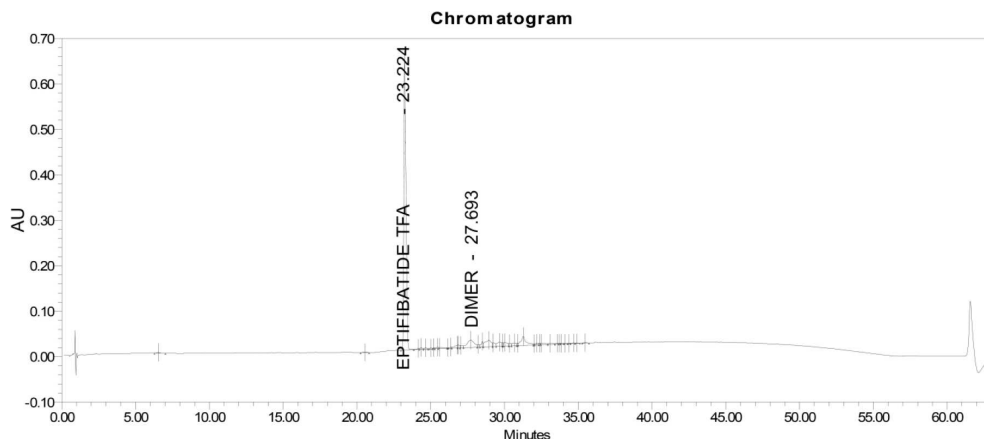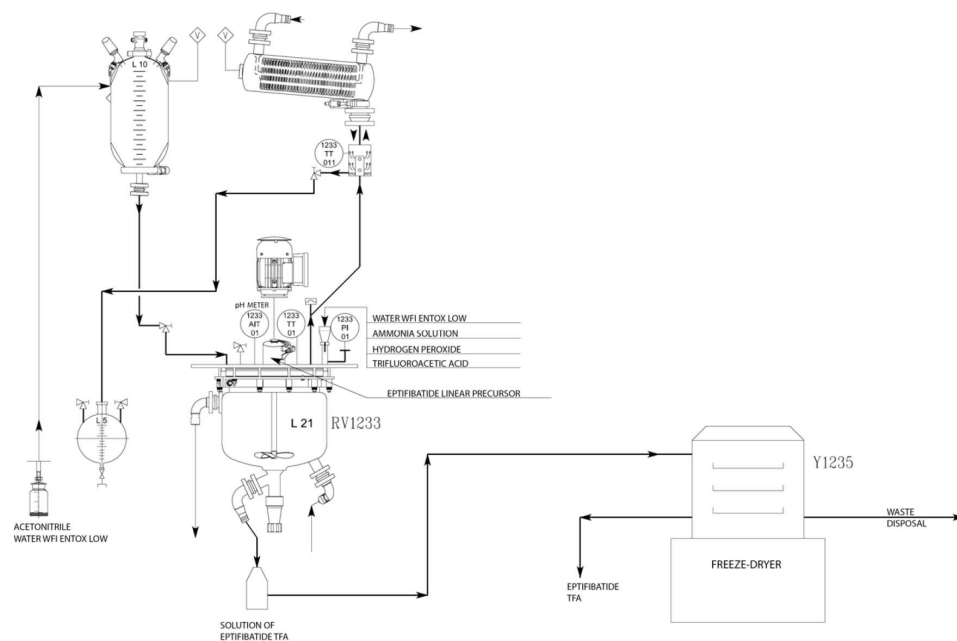
Figure 7. RP-UHPLC trace of eptifibatide TFA (step 3 at 70 mmol scale). R_t = 23.2 min, eptifibatide TFA; R_t = 27.7 min, dimer impurity (procedure S3).

Scheme 3. Industrial Plant Scheme Designed for off-Resin Disulfide Bond Formation to Obtain Crude Eptifibatide TFA Salt (Table S9)

Table 6. Starting Material and Reagents Used for Disulfide Bond Formation (Step 3)

chemical	vol (mL)	amount (g)
eptifibatide linear precursor crude		10.0
CH$_3$CN	1500.0	1173.0
H$_2$O low endotoxins	3485.0	3485.0
NH$_4$OH	0.5	0.45
H$_2$O$_2$	3 × 0.2	3 × 0.3
formic acid	15.0	18.3

glass reservoir connected to the head of the reactor by an inert Teflon tube. The pH was adjusted to 9.5 adding dropwise

NH$_4$OH (0.25 M in H$_2$O) and monitoring by a pHmeter inside the reactor (AIT1233).

The reaction mixture was recovered from the bottom of the reactor and transferred to steel plates into the freeze-dryer after monitoring the complete conversion by IPC via RP-UHPLC. Lyophilization consisted of three phases: reaction mixture freezing (P atm, −60 °C), freeze-drying (0.9 mbar, −60 °C to r.t.), and room temperature drying (0.9 mbar, r.t.). The process continued until water content and residual solvents satisfied critical quality attributes (Table S6).

Step 4. Purification of Crude Eptifibatide: Flash Column Chromatography. RP-UHPLC ESI-MS analysis of crude eptifibatide TFA salt, obtained by off-resin disulfide

bond formation in step 3 (Figures S13 and Figure 7), shown on both 5 and 70 mmol scale that the main impurity (5.3% and 5.9%, respectively) was in agreement with the formation of dimers (Table 5). A careful investigation of purification conditions by medium pressure chromatography was performed. In particular, flash reverse-phase chromatography (RPC) was selected as a versatile technology based on an automatic, low-cost, easy-handling purification both for laboratory and pilot scales, such as Isolera One (Biotage, Uppsala, Sweden) equipped with the HP-Sphere C18 column characterized by 25 μm spherical silica particles.[41,42]

The goal was to obtain eptifibatide TFA purity at >98.5%, limiting both eluents consumption and the volume of eluted fractions to freeze-dry. Several parameters were considered: flow rate, eluents composition, column performance, and column cleaning procedure. Moreover, elution mode (linear or step gradient), column loading, and volume to be lyophilized after pooling homogeneous fractions were evaluated. Linear gradient is characterized by an automated gradual increase of strong solvent percentage over time, ensuring result reproducibility and minimizing the possibility of error. Compared to the step gradient method, no elution band broadening occurs. Consequently, fraction volumes to be lyophilized and related costs are decreased.

Starting from 5% eptifibatide TFA crude column loading, two linear gradients were tested: 5−30% (v/v) B in A vs 10−37% (v/v) B in A, both eluted in 12 column volumes (A, 0.1% (v/v) TFA in H_2O; B, 0.1% (v/v) TFA in CH_3CN). While a 5−30% (v/v) B in A linear gradient required 0.8 L of B and 2.4 L of A (Figure S14), the 10−37% (v/v) linear gradient required a slightly lower amount of eluents (0.7 L B and 2.2 L A, Figure S15). On the other hand, yield increased from 24.7% to 34.3% producing the same eluted volume (165 mL, Table 7). We demonstrated that crude loading should be maintained <5% to achieve the highest purity and recovery yield. Despite 8% loading requiring a lower number of purification batches, lower yield was observed (Table 7, 18.1% yield, Figure S16).

Table 7. Recovery, Yield, and Eluate Volume from Eptifibatide TFA Flash Column Chromatography Purification (Step 4)

entry	gradient B in A,[a] %	column loading, %	purity range, %	recovery, g	yield,[b] %	eluate, mL
1	5−30	5	>98.5	1.3	24.7	165
			95−98	1.0		180
			90−92	1.3		405
2	10−37	5	>98.5	1.8	34.3	165
			95−98	0.8		150
			90−92	0.523		300
3	10−37	8	>98.5	1.45	18.1	150
			95−98	1.23		195
			90−92	1.24		390

[a]Flash column chromatography conditions: eptifibatide TFA crude was purified with Biotage Isolera One equipped with a SNAP Ultra C18 120g column (volume 164 mL). Eluents: 0.1% (v/v) TFA in H_2O (A), 0.1% (v/v) TFA in CH_3CN (B); 12 column volumes linear gradients; flow rate, 50 mL/min; λ, 215 nm. [b]

$$\text{Yield (\%)} = \frac{\text{Eptifibatide purified weight} \times \left(\frac{\text{peptide content}}{100}\right)}{\text{Eptifibatide crude weight} \times \left(\frac{\text{peptide content}}{100}\right)} \times 100.$$ UV Eptifibatide

TFA average peptide content: 85%. UV Eptifibatide TFA crude average peptide content: 71%.

Fractions containing eptifibatide TFA with 90−98.5% purity (recovery) were collected for further purification to reach the required purity, increasing the final yield (data not shown).

Scale-up Activities of the Flash Column Chromatography Purification. Purification experimental conditions of eptifibatide TFA salt (linear gradient 10−37% (v/v) B in A in 12 column volumes (A, 0.1% (v/v) TFA in H_2O; B, 0.1% (v/v) TFA in CH_3CN; crude loading ≤ 5%) were successfully confirmed at 5 mmol and scaled-up to 10 mmol scale to be repeated five times on cGMP compliant equipment (HPLC purity 5 mmol, 99.2%; 70 mmol, 99.3%; yield 5 mmol, 40.5%; 70 mmol, 41.6%). All the impurities identified in previous steps were observed to be <0.5% after flash column chromatography purification (Table 8, Figure 8, and Figures S17−S19), in agreement with ANDA requirements for eptifibatide, obtained following the cGMP process described herein.

Table 8. Flash Column Chromatography Purification Comparative Analysis at 5 mmol vs 70 mmol Scale, to Obtain Eptifibatide TFA: HPLC Purity Profile and Yield

step 4 output[a]		70 mmol[c]	5 mmol
eptifibatide TFA	HPLC purity (%)	99.3	99.2
	yield[b] (%)	41.6	40.5
impurities	Imp a (%)	<0.1	<0.1
	Imp b (%)	<0.1	<0.1
	Des-Har[2]-eptifibatide (%)	<0.1	<0.1
	dimer (%)	<0.1	<0.1
	unknown (%)	<0.5	<0.5

[a]Flash column chromatography conditions: eptifibatide TFA crude was dissolved in H_2O/CH_3CN 1:1(v/v) 0.35M. Column loading: 4% (5 mmol), 2.5% (70 mmol). Eluents: 0.1% (v/v) TFA in H_2O (A) and 0.1% (v/v) TFA in CH_3CN (B). Gradient: 10−37% (v/v) B in A linear gradient in 12 column volumes. [b]

$$\text{Yield (\%)} = \frac{\text{Eptifibatide purified weight} \times \left(\frac{\text{peptide content}}{100}\right)}{\text{Eptifibatide crude weight} \times \left(\frac{\text{peptide content}}{100}\right)} \times 100.$$ UV peptide

content of purified eptifibatide, 85%; UV peptide content of eptifibatide crude, 71%. [c]The procedure was repeated five times on the 10 mmol scale on cGMP compliant equipment.

Step 5. Counterion Exchange to Obtain Eptifibatide Acetate Salt. Eptifibatide commercialized under the trade name INTEGRILIN has been approved by the FDA as an acetate salt.[43] Considering that resin cleavage, side-chain deprotection, quenching of the reaction to form a disulfide bond, and final purification, performed in steps 2−4, required the use of harmful trifluoroacetic acid (pK_a = 0), complete counterion exchange of TFA with an acetate anion (pK_a = 4.5) was necessary. Therefore, we performed an SPE on the same equipment used for step 4 (Biotage Isolera, Uppsala, Sweden). In particular, eptifibatide TFA salt presents a charge-to-charge interaction between the carboxylate in TFA and the cation on the homoarginine side chain, the guanidinium group with a pK_a ca. 12.5. However, at pH >8, degradation of the disulfide bond in the drug was observed as previously described.[44] Therefore, the solution of purified eptifibatide TFA salt (output of step 4) in pure H_2O (2.6 mM) at r.t. was adjusted at pH 8 adding an NH_4OH solution (1.5% (v/v) in H_2O). Under these conditions, the peptide was completely soluble, and the resulting disulfide bond was stable (data not shown). Thus, the mixture was loaded on a C18 column. Two isocratic elutions, consisting of (a) 100% H_2O (3 column volumes) and (b) 100% of 0.5% (v/v) AcOH in H_2O (3 column volumes),
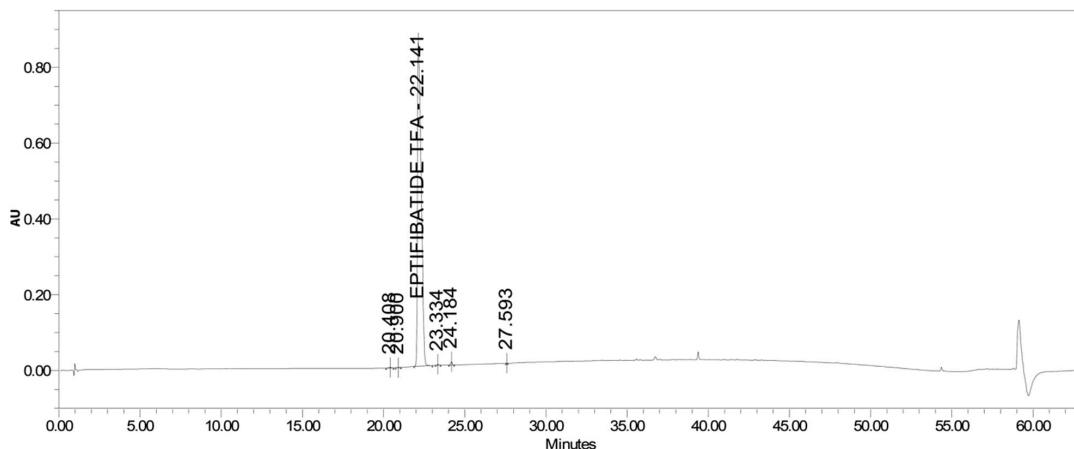
Figure 8. RP-HPLC trace of pure eptifibatide TFA (step 4 at 70 mmol scale). R_t = 22.1 min, pure eptifibatide TFA (procedure S3).

completely removed ammonium trifluoroacetate salt. Finally, the desired eptifibatide acetate solution was eluted with 0.5% (v/v) AcOH in 4:1 H_2O/CH_3CN (v/v); three column volumes. The resulting homogeneous fractions were pooled and freeze-dried to recover eptifibatide acetate.

Scale-up Activities of the Ion Exchange Step. The above-described TFA/acetate counterion exchange strategy was successfully scaled-up from 5 to 70 mmol scale (10 mmol scale repeated 5 times on cGMP compliant equipment) obtaining exactly the same 99.6% HPLC purity and slightly increased yield (5 mmol, 64.6%; 70 mmol, 65.8%, Table 9,

Table 9. Ion Exchange Comparative Analysis at 5 mmol vs 70 mmol Scale, to Obtain Eptifibatide Acetate: HPLC Crude Purity Profile and Yield

	step 5[a] output	70 mmol[c]	5 mmol
eptifibatide	HPLC purity (%)	99.6	99.6
	yield[b] (%)	65.8	64.6
counter Ion	acetate (% w/w)	3.9	4.6
	TFA (ppm)	230	335

[a]Ion exchange conditions: purified eptifibatide TFA was dissolved in H_2O (2.6 mM), column loading 0.8%, pH 8.0 (NH_4OH). Eluents: 0.5% (v/v) AcOH in H_2O (A), 0.5% (v/v) AcOH in CH_3CN (B), H_2O (C), and CH_3CN (D). Elution: a) 100% C, 3 column volumes; b) 100% A, 3 column volumes; c) 20% B in A, 3 column volumes; d) 100% D, 2 column volumes. [b]

$$\text{Yield (\%)} = \frac{\text{eptifibatide acetate weight} \times \left(\frac{\text{peptide content}}{100}\right)}{\text{eptifibatide purified TFA weight} \times \left(\frac{\text{peptide content}}{100}\right)} \times 100. \text{ UV eptifiba-}$$

tide acetate peptide content: 87%. UV eptifibatide purified TFA peptide content: 85%. [c]The procedure was repeated seven times at 10 mmol scale on cGMP compliant equipment.

Figure S20, and Figure 9). Since TFA residual content is considered a critical quality attribute (CQA) affecting the safety of preclinical and clinical applications, the above-described TFA/acetate exchange procedure was evaluated for its TFA residual content that was demonstrated to be significantly below the cGMP specification limit (5000 ppm). Moreover, acetate content resulted in a 4−10% specification range (Table 9).

Considering the yield of each step (steps 1−5; Tables 3, 5, 8, and 9), the final total yield of the eptifibatide acetate for the entire production process is 22.1%. All the listed quality attributes (Table 10) that are in agreement with the targets established in module 3 of the Common Technical Document for the Registration of Pharmaceuticals for Human Use (ICH *M4: Common Technical Document*) demonstrate that the above-described production process of eptifibatide acetate allows the release of the final cGMP compliant batch.

Quality attributes of process intermediates and a list of the equipment used to obtain cGMP compliant eptifibatide are summarized in Table S6 and Table 10. This information is required by regulatory agencies to validate the process and qualify the pilot scale plant above-described, to produce cGMP compliant eptifibatide acetate. This is, to the best of our knowledge, the first proof-of-concept of a cGMP compliant generic peptide drug synthesized by a MW-assisted solid-phase synthesizer, on the 70 mmol scale.

CONCLUSIONS

The successful transfer of the lab-scale process (5 mmol) to 70 mmol scale demonstrated the assessment of the quality risk management followed to establish an appropriate controlled manufacturing process of the cGMP eptifibatide acetate pilot batch. Critical attributes that were within CQA limits allowed the batch release of cGMP eptifibatide acetate to receive regulatory agencies' approval (Table 10). The key benefits of the new automated multigram-scale microwave solid-phase peptide synthesizer resulted in rapid production times and the ability to incorporate green chemistry protocols based on MW-SPPS improving peptide purity and minimizing excess reagents. The pilot plant equipped with this technology was qualified by F.I.S.—Fabbrica Italiana Sintetici S.p.A. for cGMP peptide production.

Our results definitely demonstrate that the strong collaboration between an academic facility and a contract development manufacturing organization, for small molecule APIs and intermediate industrial GMP production, is a powerful example of a joint laboratory satisfying the needs of a market entry strategy into peptide API production.
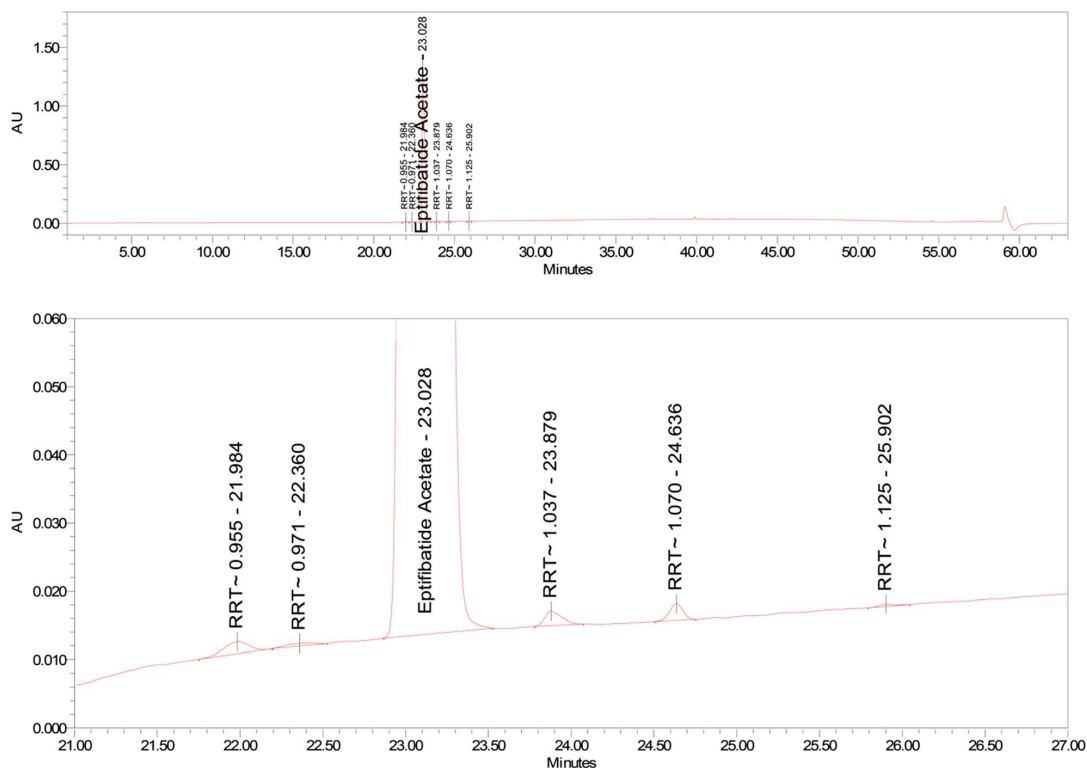
Figure 9. RP-HPLC trace of eptifibatide acetate (step 5 at 70 mmol scale). Top: full chromatogram. Bottom: zoom 21−27 min. R_t = 23.0 min: eptifibatide acetate (procedure S3).

■ EXPERIMENTAL SECTION

Materials. Peptide grade *N,N*-dimethylformamide (DMF), all Fmoc-protected amino acids (Fmoc-Gly-OH, Fmoc-Har-(Pbf)-OH, Fmoc-Asp(OtBu)-OH, Fmoc-Cys(Trt)-OH, Fmoc-Trp(Boc)-OH, Fmoc-Pro-OH), aand 3-mercaptopropionic acid (MPA) were purchased from Sigma-Aldrich (Milan, Italy). Rink Amide AM resin was purchased from Sunresin New Materials Co. Ltd., Xi' AN (Shaanxi, China).

Activators *N,N*′-diisopropylcarbodiimide (DIC) and Oxima pure were purchased from Sigma-Aldrich (Milan, Italy). Trifluoroacetic acid (TFA), triisopropyl silane (TIS), 2,2′-(ethylenedioxy)diethanethiol (DODT), *N,N*-diisopropylethylamine (DIPEA), diisopropyl ether (iPr$_2$O), diethyl ether (Et$_2$O), 2-methoxy-2-methylpropane (MTBE), methoxycyclopentane (CPME), 2-propanol, dichloromethane (DCM), acetic acid (99−100%), and HPLC-grade H$_2$O were purchased from Sigma-Aldrich (Milan, Italy). HPLC-grade acetonitrile (CH$_3$CN) was purchased from Carlo Erba (Milan, Italy).

Preparation of Eptifibatide Linear Precursor by Fmoc/tBu MW-SPPS. The fully protected eptifibatide linear precursor MPA(Trt)-Har(Pbf)-Gly-Asp(OtBu)-Trp(Boc)-Pro-Cys(Trt)-Rink Amide AM resin was obtained starting from Rink Amide AM resin (loading 0.93 mmol/g, 5.4 g, 5 mmol). Sequence elongation was performed on a microwave-assisted solid-phase peptide synthesizer (Liberty Blue, CEM, Matthews, NC, U.S.A.) following the Fmoc/tBu strategy. Reaction temperatures were monitored by an internal fiber-optic sensor. Both deprotection and coupling reactions were

performed in a Teflon vessel applying microwave energy under nitrogen bubbling. After the first Fmoc-deprotection, the following orthogonally protected amino acids were added from C- to N-terminal: Fmoc-Cys(Trt)-OH, Fmoc-Pro-OH, Fmoc-Trp(Boc)-OH, Fmoc-Asp(OtBu)-OH, Fmoc-Gly-OH, Fmoc-Har(Pbf)-OH, and MPA(Trt)-OH, in the presence of the coupling reagents DIC and Oxyma Pure. The Fmoc/tBu MW-SPPS cycle consisted of (1) swelling in DMF (50 mL) for 30 min; (2) Fmoc-deprotection by 30% (v/v) piperidine/DMF (40 equiv, 66 mL); (3) washings with DMF (3 × 50 mL); (4) coupling of Fmoc-protected amino acids (2.5 equiv, 0.4 M in DMF), Oxyma pure (2.5 equiv, 1 M in DMF), and DIC (2.5 equiv, 3 M in DMF); and (5) washings with DMF (3 × 50 mL). Peptide elongation was performed by repeating the MW-SPPS cycle for each amino acid. Both deprotection and coupling reactions were performed reaching 90 °C except 55 °C for cysteine coupling.

After all amino acids were coupled, the resin was filtered, washed with DMF (3 × 50 mL) and 2-propanol (3 × 50 mL), and dried under a vacuum to obtain 15.2 g of MPA(Trt)-Har(Pbf)-Gly-Asp(OtBu)-Trp(Boc)-Pro-Cys(Trt)-Rink Amide AM resin.

In Process Control (IPC) Monitoring of the Solid-Phase Reaction Progress. A sample of peptide-resin (25 mg) was washed with DMF (3 × 3 mL) and DCM (3 × 3 mL) and dried under vacuum. Peptide cleavage from the resin and concomitant deprotection of the acid sensitive amino-acid side chains were carried out with the cocktail TFA/TIS/H$_2$O (1 mL, 96:2:2 (v/v/v/v)). The mixture was maintained for 30

Table 10. Eptifibatide Acetate Quality Attributes for cGMP Compliant Batch Release

intermediate/ step	quality attribute	output found	target
eptifibatide acetate step 5	appearance	white powder	white to pink white powder
	HPLC identity[a]	compliant	standard-compliant R_t
	HPLC purity[a]	99.6%	≥98.5%
	HPLC assay[a]	91.2% (w/w)	n.a. reference value
	HPLC total impurities[a]	0.4%	<1.5%
	HPLC single largest impurity[a]	0.1%	<0.5%
	weight	2 g	1–4 g
	water content[b]	6.6% (w/w)	<10%
	acetonitrile content[c]	105 ppm	<410 ppm
	TFA content[d]	230 ppm	5000 ppm
	acetate content[d]	3.9%	<10%
	$[\alpha]_D^{20e}$	−85.0°	−94.0 to −79.0°
	MS identification[f]	compliant	$[M + H]^+$ 832.3[f]
	bacterial endotoxins[g]	<1.25 EU/mg	<20 ppm
	Cd[h]	<0.25 ppm	<2 ppm
	Co[h]	<0.25 ppm	<2 ppm
	As[h]	<1 ppm	<10 ppm
	Sb[h]	<1 ppm	<20 ppm
	Ni[h]	<0.5%	<20 ppm
	Cu[h]	15 ppm	<20 ppm
	V[h]	<1 ppm	<10 ppm
	Li[h]	<0.25 ppm	<20 ppm
	Hg[h]	2 ppm	<2 ppm

[a]HPLC analytical methods are described in the Supporting Information (procedures S2, S3, and S5). [b]Water content was quantified by Karl Fisher volumetric titration (USP 921, EP 2.5.12). [c]Acetonitrile content was quantified by headspace gas-chromatography (HS-GC); analytical method is described in the Supporting Information (procedure S7). [d]Ion exchange chromatography (IC); the analytical method is described in the Supporting Information (procedure S8). [e]Specific optical rotation $[\alpha]_D^{20}$ (USP 781, EP 2.2.7). [f]Mass found detected by ESI-MS; the analytical method is described in the Supporting Information (procedure S4). [g]Bacterial endotoxins were quantified by microbiological tests (USP 85, EP 2.6.14). [h]Heavy metals were quantified by inductively coupled plasma mass spectroscopy (ICP-MS, ICH Q3D; USP232, 233, 730; EP 2.4.20).

min at 38 °C under magnetic stirring. The resin was washed with TFA (1 mL) and filtered. The crude product was precipitated with ice-cold Et$_2$O (4 mL), collected after centrifugation, dissolved in H$_2$O (1 mL), freeze-dried by a LIO5P DGT lyophilizer (5 Pascal), and analyzed by RP-UHPLC-MS on a Thermo Scientific Ultimate 3000 equipped with a variable wavelength detector and a Thermo Scientific MSQ PLUS, using a C18 Waters Acquity CSH (130 Å, 1.7 μm, 2.1 × 100 mm; temperature, 45 °C; flow, 0.5 mL/min; eluents, 0.1% (v/v) TFA in H$_2$O (A) and 0.1% (v/v) TFA in CH$_3$CN (B); λ, 215 nm).[15]

Cleavage Step. The cleavage, with concomitant deprotection of acid sensitive amino-acid side chains was performed by treating MPA(Trt)-Har(Pbf)-Gly-Asp(OtBu)-Trp(Boc)-Pro-Cys(Trt)-Rink Amide AM resin (15.2 g, 5 mmol) with the cocktail TFA/TIS/H$_2$O/DODT 107 mL, 72:7:7:14 (v/v/v/v) for 30 min at room temperature under mechanical stirring (150 rpm). Then, the mixture was diluted with TFA (230 mL)

and stirred mechanically for 2.5 h. The resin was filtered and rinsed with fresh TFA (3 × 30 mL). The cleavage reaction mixture was transferred into a clean round-bottom flask, and the peptide was precipitated by the addition of ice-cold iPr$_2$O (1216 mL) in 30 min, keeping the temperature below 35 °C. The suspension was stirred for 1 h at 0 °C. The solid crude was filtered, washed with ice-cold iPr$_2$O (4 × 150 mL), and dried under vacuum. Characterization of the filtered eptifibatide TFA linear precursor crude was performed by analytical RP-HPLC-ESI-MS (Procedures S1, S2, and S4).

The eptifibatide TFA linear precursor crude (5.137 g, 5 mmol) showed 74.1% RP-UHPLC purity (yield 84.6%), R_t 4.3 min, ESI-MS (m/z): $[M + H]^+$ 834.4 (found), 834.9 (calcd; Figures S3 and S8).

Optimized Procedure for off-Resin Disulfide Bond Formation. Eptifibatide TFA linear precursor crude (2.5 g, 2.44 mmol, UHPLC purity 74.1%) was introduced in a 2 L round-bottom flask, dissolved in H$_2$O/CH$_3$CN (1:1 (v/v), 750 mL) solution, and maintained under stirring. After 15 min, H$_2$O (500 mL) was added to the reaction mixture to obtain a final concentration of 5.3 mM. The initial pH of 2.5 was adjusted to 9.5, adding 7.5% NH$_4$OH (v/v) in H$_2$O; 5.0 mL. The first aliquot of H$_2$O$_2$ (0.05 mL, 0.22 equiv) was added, and the reaction mixture was stirred for 30 min at r.t. Then, HPLC in process control (IPC) was performed to monitor the disulfide bond formation (procedure S6). This addition was repeated every 30 min until complete oxidation. A total of four additions in 2 h was necessary to complete the disulfide bond formation. The reaction was quenched adding TFA 99.9% (v/v); 5 mL, adjusting pH to 2.5. Then, the reaction mixture was lyophilized without further evaporation.

The recovered crude was characterized by analytical RP-UHPLC-ESI-MS (procedures S2, S3, and S4). Crude eptifibatide TFA salt (5.2 g, yield 90.7%) showed 67.4% UHPLC purity, R_t = 4.1 min; ESI-MS (m/z): $[M + H]^+$ 832.5 (found); 831.96 (calcd) (Figures S11 and S13).

Flash Column Chromatography Purification Procedure. Obtained crude eptifibatide TFA salt (4.90 g, 5.2 mmol, UHPLC purity 67.4%), dissolved in H$_2$O/CH$_3$CN (1:1 (v/v), 15 mL), was loaded on a SNAP Ultra C18 120g column (Biotage Isolera One, Uppsala, Sweden). Eluents: 0.1% (v/v) TFA in H$_2$O (A), 0.1% (v/v) TFA in CH$_3$CN (B). Flow rate: 25 mL/min. λ, 215 nm. Elution method: (a) 100% (v/v) A, 5 column volumes, (b) 10–37% (v/v) B in A gradient, 12 column volumes, (c) 100% (v/v) B, two column volumes. Fractions of 18 mL volume were collected and analyzed by RP-UHPLC-ESI-MS (Procedures S2, S3, and S4). Fractions corresponding to R_t = 4.1 min and UHPLC purity >98.5% were collected, obtaining a total volume of 198 mL that was lyophilized.

Eptifibatide TFA salt (1.69 g, yield 40.5%) was characterized by 99.2% UHPLC purity, R_t = 4.1 min (Figure S19). ESI-MS (m/z): $[M + H]^+$ 832.5 (found); 831.96 (calcd).

Exchange Strategy. Purified eptifibatide TFA salt (4.74 g, 5.0 mmol, UHPLC purity 99.2%) was introduced into a 3 L round-bottom flask and dissolved with pure H$_2$O (1923 mL, 2.6 mM), and the pH was adjusted to 8 with 1.5% NH$_4$OH (v/v); 9.6 mL under mechanical stirring (150 rpm). The solution was loaded on a SNAP Ultra C18 120 g column (Biotage Isolera One, Uppsala, Sweden). Eluents: 0.5% (v/v) AcOH in H$_2$O (A), 0.5% (v/v) AcOH in CH$_3$CN (B). Elution method: (a) 100% (v/v) H$_2$O, three column volumes; (b) 100% (v/v) A, three column volumes; (c) 20% (v/v) B in A, three column

volumes; (d) 100% (v/v) CH_3CN, two column volumes. Flow rate: 50 mL/min; λ, 215 nm. Fractions of 20 mL volume were collected and analyzed by RP-UHPLC-ESI-MS (procedures S2, S3, and S4). Fractions corresponding to R_t = 4.0 min and UHPLC purity >98.5% were collected, obtaining a total volume of 60 mL that was lyophilized.

Obtained eptifibatide acetate was analyzed by RP-UHPLC-ESI-MS (procedure S2, S3, S4, and S5). TFA and acetate content were quantified by ion exchange chromatography (procedure S8).

Eptifibatide acetate (2.99 g, yield 64.6%) characterized by 99.6% UHPLC purity, R_t = 4.0 min (Figure S20). ESI-MS (m/z): $[M + H]^+$ 832.5 (found); 831.96 (calcd). TFA residual content, 335 ppm; acetate content, 4.6% (w/w).

Overview of Eptifibatide Acetate cGMP Production at 70 mmol Scale. The procedures optimized for each step on a 5 mmol scale (steps 1–5) were scaled up to the pilot scale (70 mmol). MPA(Trt)-Har(Pbf)-Gly-Asp(OtBu)-Trp(Boc)-Pro-Cys(Trt)-Rink Amide AM resin was produced in a multi-gram-scale cGMP qualified MW-assisted solid-phase peptide synthesizer (Liberty Blue, CEM, Matthews, NC, U.S.A.), obtaining 196 g in a single batch. Cleavage from the resin was performed in a single batch, obtaining 51 g of eptifibatide TFA linear precursor crude showing 73.7% of HPLC purity (yield = 82.2%). A disulfide bond in the eptifibatide TFA linear precursor crude was formed in 5 × 10 g batch, obtaining 50 g total of eptifibatide TFA crude with a purity of 66.4% (yield = 98.3%). Eptifibatide TFA crude was purified by flash chromatography in five batches. Fractions with HPLC purity >98.5% (R_t = 23.0 min, Table S12) obtained after purification of each batch were collected, leading to 4 g/batch of pure eptifibatide TFA (99.2% HPLC purity, yield = 41.6%). Each batch of pure eptifibatide TFA salt (4 g) was treated as described in the above-described "exchange strategy" obtaining 2 g/batch of the eptifibatide acetate active pharmaceutical ingredient (API) with a purity of 99.6% (yield = 65.8%). The total yield of the eptifibatide acetate cGMP production process was 22.1%.

Glassware was cleaned following the standard operating procedures (SOP) before and after the manufacturing operations. Moreover, all the personnel involved in the cGMP process was adequately trained in technical operations, safety behavior, personal hygiene, and technical clothing in accordance with the cGMP requirements. The construction criteria of the pilot-scale facility followed the cGMP structural requirements (e.g., air-lock, system air shower, etc.). Monitoring of microbial contamination was duly scheduled as well as facility sanitizations.

■ ASSOCIATED CONTENT

Ⓢ Supporting Information

The Supporting Information is available free of charge at https://pubs.acs.org/doi/10.1021/acs.oprd.1c00368.

Microwave methods, RP-UHPLC/MS analyses, analytical procedures for 70 mmol scale (PDF)

■ AUTHOR INFORMATION

Corresponding Author

Anna Maria Papini − *MoD&LS Laboratory, University of Florence, 50019 Sesto Fiorentino, Italy; Interdepartmental Research Unit of Peptide and Protein Chemistry and Biology, Department of Chemistry "Ugo Schiff", University of Florence, 50019 Sesto Fiorentino, Italy; CNR-IC Istituto di Cristallografia, 95126 Catania, Italy; PeptLab@UCP Platform of Peptide and Protein Chemistry and Biology, Neuville Campus, CY Cergy Paris Université, 95031 Cergy-Pontoise Cedex, France;* ⓞ orcid.org/0000-0002-2947-7107; Email: annamaria.papini@unifi.it

Authors

Annunziata D'Ercole − *MoD&LS Laboratory, University of Florence, 50019 Sesto Fiorentino, Italy; Interdepartmental Research Unit of Peptide and Protein Chemistry and Biology, Department of Chemistry "Ugo Schiff", University of Florence, 50019 Sesto Fiorentino, Italy; F.I.S.- Fabbrica Italiana Sintetici S.p.A., 36075 Montecchio Maggiore, Vicenza, Italy*

Lorenzo Pacini − *MoD&LS Laboratory, University of Florence, 50019 Sesto Fiorentino, Italy; Interdepartmental Research Unit of Peptide and Protein Chemistry and Biology, Department of Chemistry "Ugo Schiff", University of Florence, 50019 Sesto Fiorentino, Italy; F.I.S.- Fabbrica Italiana Sintetici S.p.A., 36075 Montecchio Maggiore, Vicenza, Italy*

Giuseppina Sabatino − *MoD&LS Laboratory, University of Florence, 50019 Sesto Fiorentino, Italy; Interdepartmental Research Unit of Peptide and Protein Chemistry and Biology, Department of Chemistry "Ugo Schiff", University of Florence, 50019 Sesto Fiorentino, Italy; CNR-IC Istituto di Cristallografia, 95126 Catania, Italy*

Matteo Zini − *F.I.S.- Fabbrica Italiana Sintetici S.p.A., 36075 Montecchio Maggiore, Vicenza, Italy*

Francesca Nuti − *MoD&LS Laboratory, University of Florence, 50019 Sesto Fiorentino, Italy; Interdepartmental Research Unit of Peptide and Protein Chemistry and Biology, Department of Chemistry "Ugo Schiff", University of Florence, 50019 Sesto Fiorentino, Italy*

Arianna Ribecai − *MoD&LS Laboratory, University of Florence, 50019 Sesto Fiorentino, Italy; F.I.S.- Fabbrica Italiana Sintetici S.p.A., 36075 Montecchio Maggiore, Vicenza, Italy*

Alfredo Paio − *MoD&LS Laboratory, University of Florence, 50019 Sesto Fiorentino, Italy; F.I.S.- Fabbrica Italiana Sintetici S.p.A., 36075 Montecchio Maggiore, Vicenza, Italy*

Paolo Rovero − *MoD&LS Laboratory, University of Florence, 50019 Sesto Fiorentino, Italy; CNR-IC Istituto di Cristallografia, 95126 Catania, Italy; Interdepartmental Research Unit of Peptide and Protein Chemistry and Biology, Department of Neurosciences, Psychology, Drug Research and Child Health—Section of Pharmaceutical Sciences and Nutraceutics, University of Florence, 50019 Sesto Fiorentino, Italy;* ⓞ orcid.org/0000-0001-9577-5228

Complete contact information is available at:
https://pubs.acs.org/10.1021/acs.oprd.1c00368

Author Contributions

[∇]A.D. and L.P. equally contributed to the scale-up of the cGMP production process of eptifibatide and its transfer from PeptFarm University of Florence to FIS—Fabbrica Italiana Sintetici S.p.A.

Notes

The authors declare no competing financial interest.

■ ACKNOWLEDGMENTS

■ DEDICATION

This paper is dedicated to the memory of Hans-Jürgen Musiol (June 5, 1942 to July 9, 2021), who contributed to building several generations of peptide chemists at the Max-Planck Institute of Biochemistry, Martinsried (Germany).

■ ABBREVIATIONS

Aa, amino acid; Acm, acetamidomethyl; AcOH, acetic acid; ANDA, abbreviated new drug application; API, active pharmaceutical ingredient; Arg, arginine; Boc, *tert*-butyoxycarbonyl; CAGR, compound annual growth rate; CDMO, contract development manufacturing organization; cGMP, current good manufactoring practices; CH_2Cl_2, dichloromethane; CH_3CN, ACN acetonitrile; CH_3COONH_4, ammonium acetate; CLP, classification labeling and packaging; CPME, methoxycyclopentane; CPP, critical processing parameter; CQA, critical quality attribute; Cys, cysteine; DIC, *N,N′*-diisopropylcarbodiimide; Oxyma pure, ethyl cyanohydroxyiminoacetate; DMF, dimethylformamide; DMSO, dimethyl sulfoxide; DODT, 2,2′-(ethylenedioxy)diethanethiol; ECHA, European Chemicals Agency; EMA, European Medicines Agency; Et_2O, ethoxyethane; FA, formic acid; FC, flash chromatography; FD&C, Federal Food, Drug, and Cosmetic Act; FDA, Food and Drug Administration; Fmoc, fluorenylmethyloxycarbonyl; FY, financial year; HS-GC, headspace gas chromatography; GDUFA, generic drug user fee act; GVL, 5-methyloxolan-2-one; SPPS, solid-phase peptide synthesis; H_2O_2, hydrogen peroxide; Har, homoarginine; HCl, hydrochrloric acid; HP, high pressure/performance; HPLC, high performance liquid chromatography; IC, ion exchange chromatography; ICP-MS, inductively coupled plasma mass spectroscopy; IEC, ion exchange chromatography; iPr_2O, 2-[(Propan-2-yl)oxy]propane; iPrOH, isopropyl alcohol; KOH, potassium hydroxide; Leu, leucine; LPPS, liquid phase peptide synthesis; MBHA, 4-methylbenzhydrylamine; Met, methionine; MeTHF, 2-methyltetrahydrofuran; Mpa, 3-mercaptopropionic acid; MTBE, 2-methoxy-2-methylpropane; MW, microwave; MW-SPS, microwave solid-phase synthesis; MW-SPPS, microwave solid-phase peptide synthesis; NH_4OH, ammonium hydroxide; NMP, *N*-methyl-2-pyrrolidone dichloromethane; OOS, out of specification; Pbf, 2,2,4,6,7-pentamethyldihydrobenzofuran-5-sulfonyl; PS−PEG, polystyrene−polyethylene glycol; R&D, research and development; RLD, reference listed drug; RM, raw material; RP-HPLC, reverse-phase high performance liquid chromatography; RPC, reverse-phase chromatography; SPE, solid-phase extraction; SVHC, substances of very high concern; tBu, *tert*-butyl; TFA, trifluoroacetic acid; TIS, triisopropylsilane; Trp, tryptophan; USD, United States dollars; VBFR, variable bed flow reactor; WFI, water for injection

■ REFERENCES

(1) *Peptide Therapeutics Market by Type of Peptide (Small, Medium and Large), Route of Administration (Intravenous, Oral, Subcutaneous, Topical and Others), Key Geographical Regions (North America, Europe, Asia-Pacific and Rest of the World) and Key Therapeutic Area (Metabolic Diseases, Oncological Diseases, Endocrine Diseases, Digestive and Gastrointestinal Diseases and Others): Industry Trends and Global Forecasts*; Root Analysis Business Research & Consulting, 2021−2030.

(2) Teixeira, T.; Kweder, S. L.; Saint-Raymond, A. Are European Medicines Agency, US Food and Drug Administration, and Other International Regulators Talking to Each Other? *Clin. Pharmacol. Ther.* **2020**, *107* (3), 507−513.

(3) Branch, S. K. Guidelines from the International Conference on Harmonisation (ICH). *J. Pharm. Biomed. Anal.* **2005**, *38* (5), 798−805.

(4) *Guideline, I. H. T. Impurities in New Drug Substances, ICH Q3A (R2)*; European Medicines Agency: Geneva, Switzerland, 2006; p 25.

(5) *ANDAs for Certain Highly Purified Synthetic Peptide Drug Products That Refer to Listed Drugs of RDNA Origin, Guidance for Industry*; US Food and Drug Administration: Silver Spring, MD, 2017.

(6) Kumar, A.; Jad, Y. E.; El-Faham, A.; de la Torre, B. G.; Albericio, F. Green Solid-Phase Peptide Synthesis 4. γ-Valerolactone and N-Formylmorpholine as Green Solvents for Solid-Phase Peptide Synthesis. *Tetrahedron Lett.* **2017**, *58* (30), 2986−2988.

(7) Jad, Y. E.; Acosta, G. A.; Khattab, S. N.; de la Torre, B. G.; Govender, T.; Kruger, H. G.; El-Faham, A.; Albericio, F. 2-Methyltetrahydrofuran and Cyclopentyl Methyl Ether for Green Solid-Phase Peptide Synthesis. *Amino Acids* **2016**, *48* (2), 419−426.

(8) Jad, Y. E.; Govender, T.; Kruger, H. G.; El-Faham, A.; de la Torre, B. G.; Albericio, F. Green Solid-Phase Peptide Synthesis (GSPPS) 3. Green Solvents for Fmoc Removal in Peptide Chemistry. *Org. Process Res. Dev.* **2017**, *21* (3), 365−369.

(9) Hartrampf, N.; Saebi, A.; Poskus, M.; Gates, Z. P.; Callahan, A. J.; Cowfer, A. E.; Hanna, S.; Antilla, S.; Schissel, C. K.; Quartararo, A. J.; Ye, X.; Mijalis, A. J.; Simon, M. D.; Loas, A.; Liu, S.; Jessen, C.; Nielsen, T. E.; Pentelute, B. L. Synthesis of Proteins by Automated Flow Chemistry. *Science* **2020**, *368* (6494), 980−987.

(10) Mijalis, A. J.; Thomas, D. A.; Simon, M. D.; Adamo, A.; Beaumont, R.; Jensen, K. F.; Pentelute, B. L. A Fully Automated Flow-Based Approach for Accelerated Peptide Synthesis. *Nat. Chem. Biol.* **2017**, *13* (5), 464−466.

(11) Sletten, E. T.; Nuño, M.; Guthrie, D.; Seeberger, P. H. Real-Time Monitoring of Solid-Phase Peptide Synthesis Using a Variable Bed Flow Reactor. *Chem. Commun.* **2019**, *55* (97), 14598−14601.

(12) Collins, J. M.; Singh, S. K.; Vanier, G. S. Microwave Technology for Solid-Phase Peptide Synthesis. *Chem. Today.* **2012**, *30* (2), 26−29.

(13) Carpino, L. A.; Krause, E.; Sferdean, C. D.; Schümann, M.; Fabian, H.; Bienert, M.; Beyermann, M. Synthesis of 'Difficult' Peptide Sequences: Application of a Depsipeptide Technique to the Jung−Redemann 10- and 26-Mers and the Amyloid Peptide Aβ(1−42). *Tetrahedron Lett.* **2004**, *45* (40), 7519−7523.

(14) McNamara, J. F.; Lombardo, H.; Pillai, S. K.; Jensen, I.; Albericio, F.; Kates, S. A. An Efficient Solid-Phase Strategy for the Construction of Chemokines. *J. Pept. Sci.* **2000**, *6* (10), 512−518.

(15) Sabatino, G.; D'Ercole, A.; Pacini, L.; Zini, M.; Ribecai, A.; Paio, A.; Rovero, P.; Papini, A. M. An Optimized Scalable Fully Automated Solid-Phase Microwave-Assisted CGMP-Ready Process for the Preparation of Eptifibatide. *Org. Process Res. Dev.* **2021**, *25* (3), 552−563.

(16) Qin, L.; Yuan, J.; Li, H.; Ma, Y. Method for Preparing Eptifibatide with Solid-Phase Method. CN 101538316 B, September 5, 2012.

(17) Wen, Y.; Zhu, C.; Wang, X.; Han, Y.; Tong, G. Eptifibatide Preparation Method. US 9394341B2, October 22, 2015.

(18) Varray, S.; Werbitzky, O.; Zeiter, T. On-Resin Peptide Cyclization. WO2006045483A2, May 4, 2006.

(19) *Guideline, Quality risk management, ICH Q9*; European Medicines Agency: London, UK, 2015; p 303,

(20) European Regulation (EC) no. 1272/2008.

(21) Cezari, M. H.; Juliano, L. Studies on lactam formation during coupling procedures of N alpha-N omega-protected arginine derivatives. *Peptide Res.* **1996**, *9* (2), 88−91.

(22) De la Torre, B. G.; Kumar, A.; Alhassan, M.; Bucher, C.; Albericio, F.; Lopez, J. Successful development of a method for the incorporation of Fmoc-Arg (Pbf)-OH in solid-phase peptide synthesis using N-butylpyrrolidinone (NBP) as solvent. *Green Chem.* **2020**, *22* (10), 3162−3169.

(23) Anderson, N. G.; Burdick, D. C.; Reeve, M. M. Current Practices of Process Validation for Drug Substances and Intermediates. *Org. Process Res. Dev.* **2011**, *15* (1), 162−172.

(24) Martin, V.; Egelund, P. H. G.; Johansson, H.; Thordal Le Quement, S.; Wojcik, F.; Sejer Pedersen, D. Greening the Synthesis of Peptide Therapeutics: An Industrial Perspective. *RSC Adv.* **2020**, *10* (69), 42457−42492.

(25) *Specifications: Test Procedures and Acceptance Criteria for New Drug Substances and New Drug Products: Chemical Substances, ICH Q6A*; European Medicines Agency: London, UK, 2000.

(26) Buellesbach, E. E.; Danho, W.; Heilbig, H. J.; Zahn, H. *Side Reactions in Peptide Synthesis*; Wroclaw University Press: Wroclaw, 1979; pp 643−646.

(27) Barany, G.; Merrifield, R. B. *The Peptides Analysis, Synthesis, Biology*; Academic Press: New York, 1979; vol 2, pp 1−298.

(28) Moroder, L.; Musiol, H. J.; Schaschke, N.; Chen, L.; Hargittai, B.; Barany, G. Protection of the Thiol Group. *Synthesis of Peptides and Peptidomimetics*; Georg Thieme, Verlag: Stuttgart, Germany, 2001; vol E22a; pp 384−423.

(29) Yang, Y. Peptide Global Deprotection/Scavenger-Induced Side Reactions *Side Reactions in Peptide Synthesis*; Academic Press: Oxford, UK, 2016; vol 3, pp 43−75.

(30) Al Musaimi, O.; Jad, Y. E.; Kumar, A.; El-Faham, A.; Collins, J. M.; Basso, A.; de la Torre, B. G.; Albericio, F. Greening the Solid-Phase Peptide Synthesis Process. 2-MeTHF for the Incorporation of the First Amino Acid and Precipitation of Peptides after Global Deprotection. *Org. Process Res. Dev.* **2018**, *22* (12), 1809−1816.

(31) Al Musaimi, O.; Jad, Y. E.; Kumar, A.; Collins, J. M.; Basso, A.; de la Torre, B. G.; Albericio, F. Investigating Green Ethers for the Precipitation of Peptides after Global Deprotection in Solid-Phase Peptide Synthesis. *Current Opinion in Green and Sustainable Chemistry.* **2018**, *11*, 99−103.

(32) Alder, C. M.; Hayler, J. D.; Henderson, R. K.; Redman, A. M.; Shukla, L.; Shuster, L. E.; Sneddon, H. F. Updating and Further Expanding GSK's Solvent Sustainability Guide. *Green Chem.* **2016**, *18* (13), 3879−3890.

(33) Prat, D.; Pardigon, O.; Flemming, H.-W.; Letestu, S.; Ducandas, V.; Isnard, P.; Guntrum, E.; Senac, T.; Ruisseau, S.; Cruciani, P.; Hosek, P. Sanofi's Solvent Selection Guide: A Step toward More Sustainable Processes. *Org. Process Res. Dev.* **2013**, *17* (12), 1517−1525.

(34) European Chemicals Agency Candidate List of substances of very high concern for Authorisation. http://echa.europa.eu/candidate-list-table.

(35) Prat, D.; Wells, A.; Hayler, J.; Sneddon, H.; McElroy, C. R.; Abou-Shehada, S.; Dunn, P. J. Correction: CHEM21 Selection Guide of Classical-and Less Classical-Solvents. *Green Chem.* **2015**, *17* (10), 4848−4848.

(36) Andreu, D.; Albericio, F.; Solé, N. A.; Munson, M. C.; Ferrer, M.; Barany, G. Formation of Disulfide Bonds in Synthetic Peptides and Proteins. *Peptide synthesis protocols.* **1994**, *35*, 91−169.

(37) Sidorova, M.; Molokoedov, A.; Az'muko, A.; Kudryavtseva, E.; Krause, E.; Ovchinnikov, M.; Bespalova, Z. D. The Use of Hydrogen Peroxide for Closing Disulfide Bridges in Peptides. *Russ. J. Bioorg. Chem.* **2004**, *30* (2), 101−110.

(38) Calce, E.; Vitale, R. M.; Scaloni, A.; Amodeo, P.; De Luca, S. Air Oxidation Method Employed for the Disulfide Bond Formation of Natural and Synthetic Peptides. *Amino Acids* **2015**, *47* (8), 1507−1515.

(39) Tam, J. P.; Wu, C. R.; Liu, W.; Zhang, J. W. Disulfide Bond Formation in Peptides by Dimethyl Sulfoxide. Scope and Applications. *J. Am. Chem. Soc.* **1991**, *113* (17), 6657−6662.

(40) Song, C.; Sun, J.; Zhao, X.; Huo, S.; Shen, S. A Study to Develop Platinum (Iv) Complex Chemistry for Peptide Disulfide Bond Formation. *Dalton Transactions.* **2020**, *49* (6), 1736−1741.

(41) Insuasty Cepeda, D. S.; Pineda Castañeda, H. M.; Rodríguez Mayor, A. V.; García Castañeda, J. E.; Maldonado Villamil, M.; Fierro Medina, R.; Rivera Monroy, Z. J. Synthetic Peptide Purification via Solid-Phase Extraction with Gradient Elution: A Simple, Economical, Fast, and Efficient Methodology. *Molecules* **2019**, *24* (7), 1215.

(42) Bickler, B. How to choose between linear gradient and step gradients for flash chromatography. Biotage. https://selekt.biotage.com/blog/how-to-choose-between-linear-gradients-and-step-gradients-for-flash-chromatography.

(43) Sikora, K.; Jaśkiewicz, M.; Neubauer, D.; Migoń, D.; Kamysz, W. The Role of Counter-Ions in Peptides—An Overview. *Pharmaceuticals* **2020**, *13* (12), 442−1−29.

(44) Keire, D. A.; Strauss, E.; Guo, W.; Noszal, B.; Rabenstein, D. L. Kinetics and equilibria of thiol/disulfide interchange reactions of selected biological thiols and related molecules with oxidized glutathione. *J. Org. Chem.* **1992**, *57* (1), 123−127.